Universidad Autónoma de Madrid

Facultad de Ciencias

Departamento de Biología Molecular

Mechanistic insights into the role of secondary mutations of HIV-1 reverse transcriptase in the acquisition of antiretroviral drug resistance

Tesis doctoral

Gilberto José Betancor Quintana

Madrid, 2013

Memoria presentada por el Ldo. Gilberto José Betancor Quintana para optar al grado de Doctor en Ciencias por la Universidad Autónoma de Madrid.

Madrid, Noviembre, 2013

Research presented in this Thesis has been carried out at the Centro de Biología Molecular "Severo Ochoa" (Madrid, Spain) under the supervision of Dr. Luis Menéndez-Arias, and was supported in part by grants of the Spanish Ministery of Health, Social Services and Equality (grant no. EC11-025) and the Fundación para la Investigación y Prevención del SIDA en España (FIPSE) (grant no. 36771/08). Gilberto Betancor was a recipient of a predoctoral fellowship of the Spanish Government (FPU AP2008-01747).

Abbreviations

3TC	2´, 3´-dideoxy-3´-thiacytidine
3TCMP	2´, 3´-dideoxy-3´-thiacytidine monophosphate
3TCTP	2´, 3´-dideoxy-3´-thiacytidine triphosphate
AMP	Adenosine monophosphate
APOBEC	Apolipoprotein B mRNA editing enzyme
AZT	3´-azido-2´, 3´-dideoxythymidine
AZTMP	3´-azido-2´, 3´-dideoxythymidine monophosphate
AZTp$_4$A	3´azido-3´-deoxythymidine-(5´)-tetraphospho-(5´)-adenosine
AZTTP	3´-azido-2´, 3´-dideoxythymidine triphosphate
CA	Capsid protein (p24)
CBV	2-amino-9-[(1R, 4S)-4-(hydroxymethyl)cyclopent-2-en-1-yl]-9H-purin-6-ol
CBVMP	2-amino-9-[(1R,4S)-4-(hydroxymethyl)cyclopent-2-en-1-yl]-9H-purin-6-ol monophosphate
CBVTP	2-amino-9-[(1R,4S)-4-(hydroxymethyl)cyclopent-2-en-1-yl]-9H-purin-6-ol triphosphate
CCD	Central catalytic domain
CTD	C-terminal domain
CypA	Cyclophilin A
d4T	2´, 3´-didehydro-2´, 3´-dideoythymidine
d4TMP	2´, 3´-didehydro-2´, 3´-dideoythymidine monophosphate
d4TTP	2´, 3´-didehydro-2´, 3´-dideoythymidine triphosphate
ddA	2´, 3´-dideoxyanosine
ddAMP	2´, 3´-dideoxyanosine monophosphate
ddATP	2´, 3´-dideoxyanosine triphosphate
ddC	2´-3´-dideoxycytidine
ddCTP	2´-3´-dideoxycytidine triphosphate

DEC	Dead-end-complex
DLV	Delavirdine
dsDNA	Double-stranded DNA
EFV	Efavirenz
ETR	Etravirine
FTC	(-)-β-L-3´-thia-2´, 3´-dideoxy-5-fluorocytidine
FTCMP	(-)-β-L-3´-thia-2´, 3´-dideoxy-5-fluorocytidine monophosphate
FTCTP	(-)-β-L-3´-thia-2´, 3´-dideoxy-5-fluorocytidine triphosphate
HAART	Highly active antiretroviral tratment
HIV-1	Human immunodeficiency virus type 1
HIV-2	Human immunodeficiency virus type 2
IN	Integrase
IPTG	Isopropyl β-D-1-thiogalactopyranoside
ITP	Inosine triphosphate
k_{cat}	Steady-state catalytic rate
K_d	Dissociation equilibrium constant
K_i	Inhibition constant
k_{obs}	Pre-steady-state catalytic rate
k_{off}	Dissociation rate constant
k_{pol}	Nucleotide incorporation rate
LEDGF/p75	Lens epithelium-derived growth factor
LTR	Long terminal repeats
MA	Matrix protein (p17)
NC	Nucleocapsid protein (p6)
NNRTI	Non-nucleoside RT inhibitor
NRTI	Nucleoside RT inhibitor
NTD	N-terminal domain
NVP	Nevirapine

N-site	Nucleotide binding site
PBS	Primer binding site
PFV	Prototype foamy virus
PIC	Pre-integration complex
PPi	Pyrophosphate
PPT	Polypurine tract
PR	Protease
P-site	Priming site
RPV	Rilpivirine
RT	Reverse transcriptase
SAMHD1	Sterile α motif domain and histidine-aspartic domain-containing protein 1
SIV	Simian immunodeficiency virus
ssDNA	Single-stranded DNA
SU	Surface protein (gp120)
TAM	Thymidine analogue mutation
TAM-1	Thymidine analogue mutation pathway 1
TAM-2	Thymidine analogue mutation pathway 2
Tenofovir-DF	[(R)-9-(2-phosphonylmethoxypropyl)adenine] disoproxil fumarate
Tenofovir-DP	[(R)-9-(2-phosphonylmethoxypropyl)adenine] diphosphate
TM	Trans-membrane protein (gp41)
TRIM5α	Tripartite motif-containing protein 5
T/P	Template/primer
U3	Unique 3´-region
U5	Unique 5´-region
(w/v)	(weight/volume)

One and three letters code for amino acids

A (Ala) Alanine
C (Cys) Cysteine
D (Asp) Aspartic acid
E (Glu) Glutamic acid
F (Phe) Phenylalanine
G (Gly) Glycine
H (His) Histidine
I (Ile) Isoleucine
K (Lys) Lysine
L (Leu) Leucine
M (Met) Methionine
N (Asn) Asparagine
P (Pro) Proline
Q (Gln) Glutamine
R (Arg) Arginine
S (Ser) Serine
T (Thr) Threonine
V (Val) Valine
W (Trp) Tryptophan
Y (Tyr) Tyrosine

Index

Summary

The human immunodeficiency virus (HIV) is the causative agent of the acquired immunodeficiency syndrome (AIDS). Highly active antiretroviral therapy (HAART) has resulted in substantial improvements of the health of HIV-infected patients. However, the emergence of drug-resistant viral strains is still one of the major factors hampering effective response to antiretroviral therapy. HIV type 1 (HIV-1) reverse transcriptase (RT) is a multifunctional enzyme with RNA- and DNA-dependent DNA polymerase and RNase H activities. Due to its essential role in virus replication, RT is a key drug target. Thymidine analogue resistance mutations (TAMs) are frequently found in patients treated with nucleoside RT inhibitors (NRTIs). TAMs can be classified in two groups: TAM-1 (composed of mutations M41L, L210W and T215Y) and TAM-2 (including mutations D67N, K70R, K219E or Q and sometimes T215F). Combinations of those mutations confer different levels of resistance to almost all NRTIs currently used in the treatment of HIV-1 infection, although the largest effects are observed with zidovudine (AZT), stavudine (d4T) and tenofovir. Prolonged exposure to those drugs has led to emergence of resistant HIV-1 strains containing TAMs plus accessory mutations that facilitate their selection *in vivo*.

In this Thesis project we have determined the molecular mechanisms that facilitate the selection of mutations associated with TAMs during treatment with antiretroviral drugs. Thus, in the presence of TAMs, H208Y improves rescue efficiency of primers terminated with NRTIs, particularly with AZT, by increasing the ATP-dependent excision activity of the RT. These results are consistent with molecular dynamics simulations that predict that Tyr-208 influences the conformation of Trp-212 and this effect results in altered stacking interactions between Tyr-215 and the adenine ring of ATP. Mutations in the RT thumb subdomain influence NRTI resistance of TAM-containing enzymes through different mechanisms. While polymorphisms Pro-272/Arg-277/Thr-286 increase the affinity of the RT for RNA/DNA complexes, the amino acid substitution R284K improves the ability of the RT to incorporate nucleotides and therefore to extend growing DNA primers. The RT thumb subdomain plays an important role in the interaction with the nucleic acid substrate, and amino acid substitutions associated with TAMs and studied in this work could be affecting the proper positioning of the template/primer complex.

Recent studies have shown that RT connection subdomain mutations could influence resistance to non-nucleoside RT inhibitors (NNRTIs). Studies carried out during this Thesis project demonstrate that the combination of the connection subdomain mutations N348I/T369I impairs the RNase H activity of the RT. Interestingly, these effects are particularly relevant for the release of the polypurine tract (PPT) that acts as a primer in reverse transcription during (+) strand DNA synthesis. In the presence of NNRTIs, the PPT becomes susceptible to cleavage by the RNase H activity of the wild-type RT, although the double-mutant N348I/T369I RT is unable to cleave the PPT primer, thereby protecting it from unwanted degradation. These results predict that in the presence of NNRTIs, fitness differences between virus carrying the wild-type enzyme and the double-mutant N348I/T369I should be reduced. Finally, we have also studied the interaction between the RT and HIV-1 integrase (IN) protein and its effects on the RT's RNase H activity. Our results indicate that the viral IN facilitates the release of the PPT primer, without affecting the hydrolysis of heteropolymeric template/primer complexes.

Resumen

El virus de la inmunodeficiencia humana (VIH) es el agente causante del síndrome de inmunodeficiencia adquirida (SIDA). La terapia antirretroviral de gran actividad (HAART) ha producido una mejora sustancial en la salud de los pacientes infectados por el VIH. No obstante, la aparición de cepas resistentes del virus sigue siendo uno de los mayores inconvenientes que dificultan la adecuada respuesta a la terapia antirretroviral. La retrotranscriptasa (RT) del VIH de tipo 1 (VIH-1) es una enzima multifuncional con actividad ADN polimerasa dependiente de ARN y ADN y actividad RNasa H. Debido a que juega un papel fundamental durante la replicación del virus, la RT es una diana terapéutica de gran importancia. Las mutaciones de resistencia a análogos a timidina (TAMs) aparecen frecuentemente en pacientes tratados con inhibidores de la RT análogos a nucleósido (NRTIs). Las TAMs se clasifican en dos grupos: TAM-1 (formado por las mutaciones M41L, L210W y T215Y) y TAM-2 (que engloba las mutaciones D67N, K70R, K219E o Q y en ocasiones T215F). Combinaciones de estas mutaciones confieren distintos niveles de resistencia a casi todos los NRTIs usados actualmente en el tratamiento de la infección por VIH-1, aunque los niveles de resistencia más altos se han observado con zidovudina (AZT), estavudina (d4T) y tenofovir. La exposición prolongada a estos fármacos ha provocado la aparición de cepas resistentes del virus portadoras de TAMs junto con mutaciones accesorias que facilitan su selección *in vivo*.

En este proyecto de Tesis hemos determinado los mecanismos moleculares que facilitan la selección de mutaciones asociadas a TAMs durante el tratamiento con fármacos antirretrovirales. De esta manera, en presencia de TAMs, H208Y mejora la eficacia de rescate de iniciadores terminados con NRTIs, en especial con AZT, aumentando la actividad de escisión dependiente de ATP de la RT. Estos resultados son apoyados por simulaciones de dinámica molecular, las cuales predicen que la Tyr-208 afecta a la conformación del Trp-212 y como resultado de ello se produce una alteración en las interacciones de apilamiento entre la Tyr-215 y el anillo de adenina del ATP. Las mutaciones en el subdominio “thumb” de la RT afectan a la resistencia de RTs portadoras de TAMs mediante distintos mecanismos. Mientras que los polimorfismos Pro-272/Arg-277/Thr-286 aumentan la afinidad de la RT por complejos ARN/ADN, el cambio de aminoácido R284K mejora la capacidad de la RT para incorporar nucleótidos y por tanto para extender cadenas de ADN. El subdominio “thumb” de la RT juega un importante papel en la interacción con el ácido nucleico y las sustituciones de aminoácido asociadas con TAMs y que se estudian en este trabajo podrían estar afectando al posicionamiento correcto del complejo molde/iniciador.

Estudios recientes han puesto de manifiesto que mutaciones del subdominio “connection” de la RT podrían afectar a la resistencia de la RT a inhibidores no análogos a nucleósido (NNRTIs). Los estudios desarrollados durante este proyecto de Tesis demuestran que la combinación de mutaciones del subdominio “connection” N348I/T369I disminuye la actividad RNasa H de la RT. Estos efectos son especialmente relevantes durante la eliminación de la secuencia de purinas (PPT) que actúa como iniciadora durante la síntesis de la cadena de ADN de polaridad positiva en el proceso de retrotranscripción. En presencia de NNRTIs, el PPT es susceptible al corte por la RNasa H de la RT de genotipo silvestre, mientras que la RT N348I/T369I es incapaz de cortar el iniciador PPT, protegiéndolo así de una degradación no deseada. Estos resultados predicen que en presencia de NNRTIs las diferencias de capacidad replicativa entre los virus portadores de las enzimas de genotipo silvestre y del mutante N348I/T369I deberían ser menores que las observadas en ausencia de fármacos. Por último, también hemos estudiado la interacción entre la RT y la integrasa (IN) del VIH-1 y su efecto sobre la actividad RNasa H de la RT. Nuestros resultados indican que la IN facilita la liberación del iniciador PPT, sin afectar a la hidrólisis de complejos molde/iniciador heteropoliméricos.

1.Introduction

1. Introduction

1.1 Human Immunodeficiency Virus (HIV)

In 1983 a group from the Pasteur Institute led by Luc Montagnier isolated a new retrovirus (Barré-Sinoussi *et al.*, 1983). This retrovirus, referred formerly as lymphadenopathy-associated virus (LAV) (Barré-Sinoussi *et al.*, 1983) or human T-lymphotropic virus III (HTLV-III) (Gallo *et al.*, 1984; Popovic *et al.*, 1984) was finally named human immunodeficiency virus (HIV), and is the etiological agent of the acquired immunodeficiency syndrome (AIDS).

HIV belongs to the *Lentivirus* genus, *Lentivirinae* subfamily, included in the *Retroviridae* family. HIV is classified into two different types, HIV-1 and HIV-2. HIV-2 infection courses with less morbidity and mortality (reviewed in de Silva *et al.*, 2008). Both viruses originate from different zoonotic events from non-human primates. HIV-1 group M, N and O comes from a simian immunodeficiency virus (SIV) that infects chimpanzees (SIVcpz), while HIV-1 group P viruses come from a SIV that infects gorillas (SIVgor) (Sharp & Hahn, 2011). HIV-2 was transmitted from sooty mangabeys (SIVsm). The origin of HIV-1, calculated by molecular clock dating techniques, set the origin of the infection in early 1900s (Zhu *et al.*, 1998, Korber *et al.*, 2000, Keele *et al.*, 2006, Wertheim *et al.*, 2009; reviewed in Hemelaar, 2012).

The HIV-1 virion (the free form of the virus) contains a lipid bilayer derived from the infected cell (Fig 1A). The gp41 (TM) protein is embedded in the viral envelope and is also anchored to the trimeric complex of surface protein gp120 (SU). The matrix (MA, p17) protein is associated with the inner leaflet of the viral membrane, forming a sort of protein layer. The viral core consists of a conical shell composed of roughly 250 capsid protein (CA, p24) hexamers and 12 CA pentamers. This core contains the virus genome (composed of two RNA copies) that is stabilized by interactions with the nucleocapsid (NC, p6) protein. Inside the viral capsid, there are three pivotal enzymes in the retroviral life cycle: (i) the reverse transcriptase (RT), responsible for converting the viral RNA into a double-stranded DNA (dsDNA); (ii) the integrase (IN), that carries out the insertion of the virus dsDNA (proviral DNA) in the host cell DNA; and (iii) the protease (PR) that catalyzes the proteolytic processing of precursor polyproteins yielding the mature proteins that form the virion. In addition, the HIV-1 genome codifies for 6 viral accessory and regulatory proteins Vpu, Vpr, Tat, Rev, Nef and Vif. These proteins are dispensable for a productive infection, but improve viral fitness. Only Vpr, Vif and Nef seem to be found in the virion, while the other three are produced upon infection of the host cell (reviewed in Turner & Summers, 1999; Adamson & Freed, 2007; Ganser-Pornillos, *et al.*, 2012).

The HIV-1 genome has approximately 9.8 kb and contains 9 different open reading frames (ORFs). Three of these ORFs codify the three structural genes: *gag*, *pol* and *env*, three codify regulatory genes *nef*, *tat* and *rev*, and the last three codify the accessory and regulatory genes *vpu*, *vpr*, and *vif* (Fig 1B). The HIV-1 genome is flanked in both extremes by long terminal repeats

(LTRs). Both LTRs are composed of three subregions designated U3 (unique 3´ region, located at the 5´-end of each LTR), R (repeated sequence, in the central region of each LTR) and U5 (unique 5´ sequence, located at the 3´-end of the LTRs) (Gallo *et al.*, 1988).

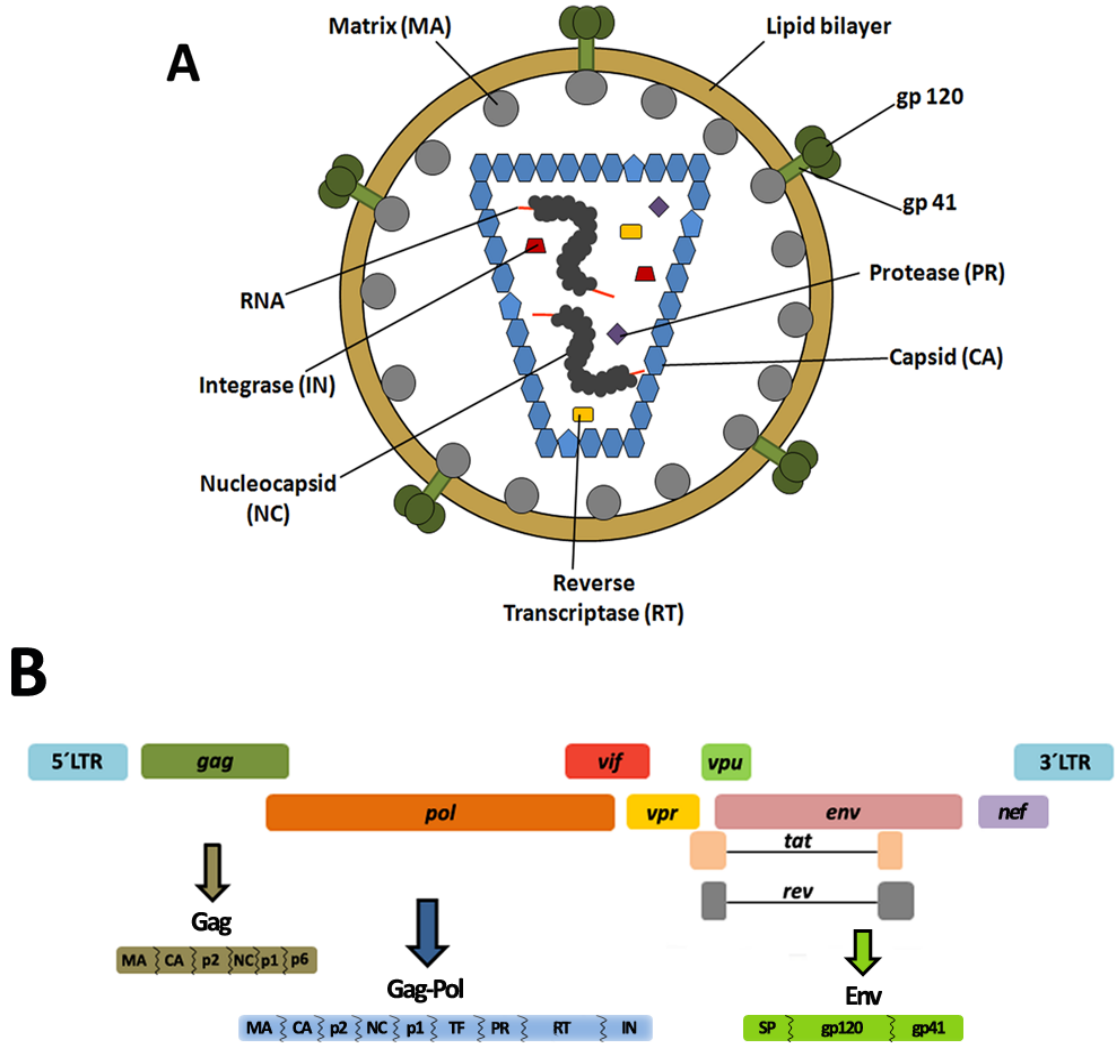

Fig 1. HIV-1 virion and genome organization. (A) Schematic representation of the viral particle. (B) Viral genome, showing the two long terminal repeats, as well as the genes codifying the principal and the accessory proteins. Major polyproteins derived from genes *gag*, *pol* and *env* are shown. Specific protease cleavage sites are represented as jagged lines.

HIV-1 transcription is a complex process where viral and cellular factors are implicated (reviewed in Colin & Van Lint, 2009; Ott *et al.*, 2011). Transcription starts at the 5´ LTR generating a 9 kb transcript that is processed by the cellular splicing machinery into several spliced transcripts. After translation, these transcripts originate Tat, Rev and Nef. Tat binds the TAR (transactivation response) element, located at the U5 region of the LTR, increasing the level of viral RNA transcription. On the other hand, Rev accumulates in the cell and binds the Rev response element (RRE) located in the *env* gene. The bound Rev facilitates the transport of unspliced and singly spliced RNA molecules from the nucleus to the cytoplasm (Fig 2). The uncleaved forms have the potential to be packaged and serve as genomic RNA. In addition they are expressed to produce the

Gag and Gag-Pol polyproteins. Gag-Pol is generated by a ribosomal frameshift occurring at the 3´-end of the *gag* gene. The frequency of this frameshift is approximately 5%. Gag and Gag-Pol polyproteins are substrates of the viral PR, that after cleavage yield the viral proteins MA, CA, p2, NC, p1, p6, PR (free form), RT and IN (reviewed in Ganser-Pornillos *et al.*, 2008; Lee *et al.*, 2012). Singly-spliced forms of viral RNA yield the Env polyprotein, separated in signal peptide (SP), gp120 and gp41 after cleavage by a cellular protease known as furin. Finally, different spliced forms of the viral RNA result in the expression of accessory and regulatory proteins (*i.e.* Vif, Vpr, Vpu and Nef) (Fig 1B) (reviewed in Krogstad 2003; Nielsen *et al.*, 2005).

HIV-1 primarily infects $CD4^+$ T cells and macrophages (reviewed in Carter & Ehrlich, 2008; Koppensteiner *et al.*, 2012). Viral infection initiates with the interaction between gp120 and the cellular surface receptor CD4, which produces a conformational change that allows the virus to interact with a second receptor (coreceptor), usually a chemokine receptor such as CCR5 or CXCR4 (Fig 2). The attachment of the virus triggers rearrangements of the gp41 protein, leading to the fusion of cell membrane and the viral envelope, and thereby to viral uncoating. This phenomenon delivers the viral core into the cytoplasm. In addition, several host factors, such as the actin microtubules and cyclophilin A (CypA), are likely to play a role during this step, forming a structure known as the reverse transcription complex (Hottiger *et al.*, 1995; reviewed in Nisole & Saïb, 2004; Gomez & Hope, 2005; Fassati, 2012). The maturation of this complex results in the pre-integration complex (PIC). HIV PICs are composed of dsDNA associated with several viral proteins (at least RT, MA, Vpr and IN), as well as host proteins (CypA and others). PICs travel to the nuclear membrane, where they associate with nuclear pore complexes. After docking to the nuclear pores, several cellular factors help the PIC to break into the nucleus (reviewed in Nisole & Saïb, 2004; Gomez & Hope, 2005; Fassati, 2012). Viral dsDNA integration is catalyzed by the viral IN. The integration of viral DNA normally takes place within cellular genes (Schroder *et al.* 2002; Han *et al.*, 2004).

HIV-1 can remain as a provirus for long periods of time. However, under certain conditions not well understood, HIV-1 "wakes up" and initiates the transcription process described above (reviewed in Colin & Van Lint, 2009; Siliciano & Greene, 2011). The process leading to the formation of the provirus starts with the association of Gag and Gag-Pol precursor polyproteins. Initially just a few Gag molecules bind two copies of the viral RNA genome and bind into assembly sites in the plasma membrane (Fig 2). This membrane binding event is facilitated by a post-translationally modification of the N-terminal domain of Gag (corresponding to the MA region) that contains a myristic acid (a fatty acid chain). Then, more Gag molecules are recruited and the interactions between the CA regions of different Gag proteins form a shell of Gag hexamers just beneath the viral envelope. Also, Env polyproteins are incorporated in the nascent virus during this step. This is thought to happen through the interaction of Env with the MA region of Gag (reviewed in Briggs & Kraüsslich, 2011; Ganser-Pornillos *et al.*, 2012). While the immature viral capsid is being formed, virus budding occurs. This process is facilitated by the endosomal sorting complexes required for transport (ESCRT) machinery (reviewed in Weiss & Göttlinger, 2011).

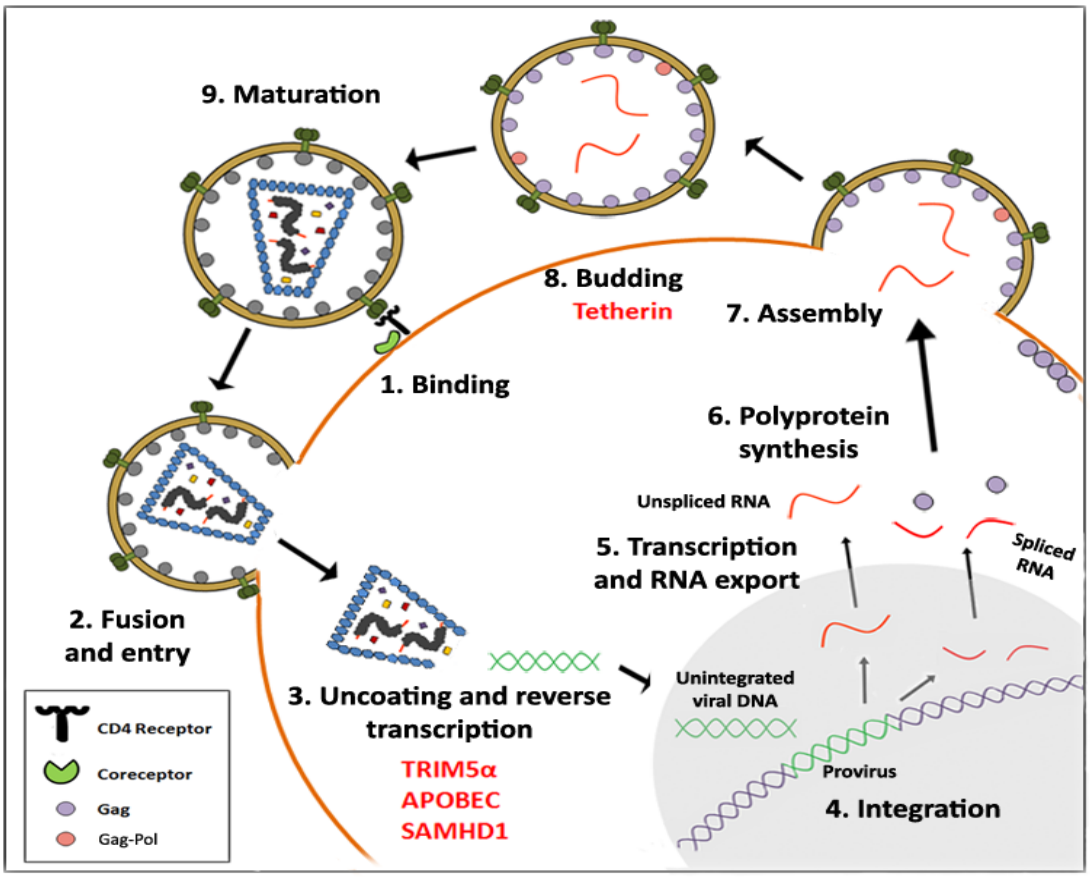

Fig 2. HIV-1 viral life cycle. Representation of the different stages of the HIV-1 life cycle. Cellular receptors and immature viral polyproteins are indicated in the boxed legend. Cell cytoplasm is shown in white, while the nucleus is a gray circle with chromosomal DNA in light purple. Cellular restriction factors are highlighted in red at the specific step where they act.

As mentioned above, Gag-Pol precursors represent only 5% of total Gag products. It is believed that retroviral maturation requires the dimerization of two PR regions of Gag-Pol polyproteins to form an active protease that then initiates the proteolytic processing of the Gag and Gag-Pol polyproteins. This process results in the formation of the structural proteins MA, CA and NC. CA hexamers are rearranged to form the mature conical capsid of the virus, which is stabilized by the presence of 12 CA pentamers (Fig 1A). The NC proteins cover the two RNA strands, adopting a stable structure, while MA proteins remain attached to the inner surface of the virion lipid bilayer (reviewed in Ganser-Pornillos *et al.*, 2008; Briggs & Kraüslich, 2011; Ganser-Pornillos *et al.*, 2012; Lee *et al.*, 2012).

An overwhelming number of cellular factors involved in HIV infection have been identified (Brass *et al.*, 2008; König *et al.*, 2008; reviewed in Friedrich *et al.*, 2011). A few of them have been described as restriction factors (Fig 2). APOBEC is a family of proteins that catalyze DNA C-to-U deamination. APOBEC3G is the principal enzyme of the family and shows anti-HIV activity, driving the virus towards lethal mutagenesis, because it has the ability to be incorporated in the nascent virion, and then influence the reverse transcription of genomic RNA (Bishop *et al.*, 2008). The viral Vif protein mediates the ubiquitinitation of the APOBEC family by promoting their degradation by cellular proteasomes (reviewed in Malim & Emerman, 2008; Harris *et al.*, 2012). TRIM5α is another

restriction factor that acts by accelerating viral uncoating and therefore leads to abortive reverse transcription. Although the human TRIM5α is unable to inhibit HIV-1 infection, TRIM5α from Old World monkeys generally can (reviewed in Malim & Bieniasz, 2012). Tetherin is a membrane protein which acts as an anchor that traps the virion while it attempts to bud from the cell. HIV-1 Vpu counteracts the effect of tetherin by reducing its level in the cell surface, either by retarding its progress through the secretory pathway or by causing its internalization (reviewed in Harris *et al.*, 2012; Malim & Bieniasz, 2012). Finally, SAMHD1 is a deoxynucleotide triphosphate (dNTP) hydrolase able to reduce the dNTPs levels to a point that abort viral reverse transcription (Hrecka *et al.*, 2011; Laguette *et al.*, 2011). Vpx proteins from HIV-2 and several SIVs, but not HIV-1 Vpr protein, can direct SAMHD1 to a proteasome pathway, rescuing viral infectivity (Goldstone *et al.*, 2011; Laguette *et al.*, 2011; Powell *et al.*, 2011; Lahouassa, *et al.*, 2012; reviewed in Harris *et al.*, 2012; Laguette and Benkirane, 2012).

1.2 HIV-1 integrase

HIV-1 IN is a 32-KDa protein containing 288 amino acids (Fig 3). It is composed of three domains including an N-terminal domain (NTD) (residues 1-49), that carries an HHCC motif, important on protein multimerization, a catalytic or central domain (CCD) (residues 50-212) implicated in the binding of viral DNA extremes and that bears a conserved (D, D-35, E) motif, responsible for the catalytic activity of the enzyme, and a C-terminal domain (CTD) (residues 213-288), mainly implicated on DNA and protein binding (Krishnan & Engelman, 2012). The catalytic competent form of IN *in vivo* is called intasome, and in its minimal form it involves a tetramer (dimer of dimers) of IN proteins attached to viral DNA. In this conformation the inner IN subunits of each dimer establish extensive dimer-dimer contacts through their catalytic domains. These domains are responsible for all interactions with viral DNA and the IN catalytic activity. The outer IN subunits do not have interactions within proteins, nor with DNA and likely play a supporting role (Fig 3) (Hare *et al.*, 2010a,b; Maertens *et al.*, 2010; reviewed in Cherepanov *et al.*, 2011).

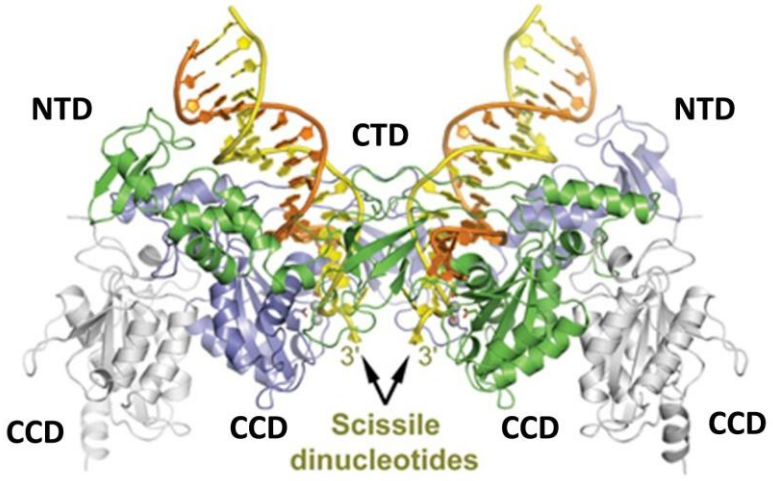

Fig 3. Intasome structure. Ribbon representation of prototype foamy virus (PFV) intasome prior to 3´-end processing. Inner subunits are colored blue and green, and outer chains in gray. The reactive and nonreactive viral DNA strands are depicted as yellow and orange cartoons, respectively. Visible subdomains are indicated (figure extracted from Hare *et al.*, 2012).

IN is a multifunctional enzyme with three different activities: 3´-end processing, strand transfer and disintegration (Fig 4). During the course of viral infection, the first activity carried out by the IN is 3´-end processing of viral DNA. Although an IN dimer is able to carry out this reaction *in vitro*, the *in vivo* process seems to involve the complete intasome (reviewed in Delelis *et al.*, 2008; Krishnan & Engelman, 2012). Through this reaction IN cleaves the conserved C-A dinucleotides from both viral ends, creating the reactive ends needed in the subsequent strand-transfer reaction. Structural data of pre- and post-3´-end processed intasome of the related PFV allow a mechanistic interpretation of the process (Hare *et al.*, 2012; reviewed in Cherepanov *et al.*, 2011), showing a endonucleolytic reaction, involving two divalent cations (Mn^{2+} or Mg^{2+}). The strand-transfer reaction involves simultaneously binding of processed viral ends and target (chromosomal) DNA. In this configuration the target DNA suffers a severe deformation, leading to a great expansion of its major groove. This phenomenon implies the insertion of the scissile phosphodiesters into the intasome binding site. Afterwards, a nucleophilic attack of the 3´-OH recessed viral ends on target DNA creates a gap of five nucleotides where viral DNA integrates. Therefore HIV-1 integration produces a duplication of five nucleotides at each provirus end (Hare *et al.*, 2010b, 2012; reviewed in Krishnan & Engelman, 2012). Finally the chromosomal nicks created by IN are corrected by the cellular DNA repairing machinery (reviewed in Skalka & Katz, 2005). Although a disintegration activity has been described *in vitro* (Chow *et al.*, 1992), its occurrence *in vivo* is unlikely (reviewed in Delelis *et al.*, 2008). The disintegration process is the strand transfer reaction run in reverse and only needs the central catalytic domain of IN to proceed (Chow *et al.*, 1992).

Inside the cell, IN interacts with the cellular lens epithelium-derived growth factor (LEDGF/p75) protein. LEDGF/p75 is a protein with chromatin binding properties that assists IN in several ways: promotes tetramerization of IN monomers, increases IN-DNA affinity, aids to integrate viral DNA on regions of active transcription, increases strand transfer activity and could also avoid IN degradation by cellular proteasomes (Kessl *et al.*, 2011; reviewed in Poeschla, 2008).

Additionally, IN-RT interaction has been reported using pull-down, yeast-two hybrid and dot blot far Western assays (Wu *et al.*, 1999; Tasara *et al.*, 2001; Hehl *et al.*, 2004; Zhu *et al.*, 2004; Wilkinson *et al.*, 2009). This interaction has been mapped to occur between the C-terminal domain of IN, implicating the region between residues 220-270 (Hehl *et al.*, 2004; Zhu *et al.*, 2004; Wilkinson *et al.*, 2009), and two regions of RT: one located within residues 1-242 and the other between residues 387-422 (Hehl *et al.*, 2004). The significance of this interaction is controversial. While some authors found that RT inhibits all IN activities (Tasara *et al.*, 2001; Oz *et al.*, 2002), others found that RT inhibits IN 3´-end processing but fosters the strand transfer activity (Hehl *et al.*, 2004). In the case of RT activities, some reports found that the presence of IN had no effect on DNA polymerase or RNase H activities of the RT (Oz *et al.*, 2002; Hehl *et al.*, 2004), while others found significant inhibition of the DNA-dependent DNA polymerase activity (Tasara *et al.*, 2001). Notably, two studies have reported an enhancer effect of IN on RT-DNA polymerase activity during initiation of reverse transcription (Dobard *et al.*, 2007; Nishitsuji *et al.*, 2009). This stimulating effect of IN on

RT activity could be mediated by another IN partner, the cellular protein Gemin2, by improving IN oligomerization, IN binding to the reverse transcription complex and by aiding RT association with the RNA (Hamamoto *et al.*, 2006; Nishitsuji *et al.*, 2009).

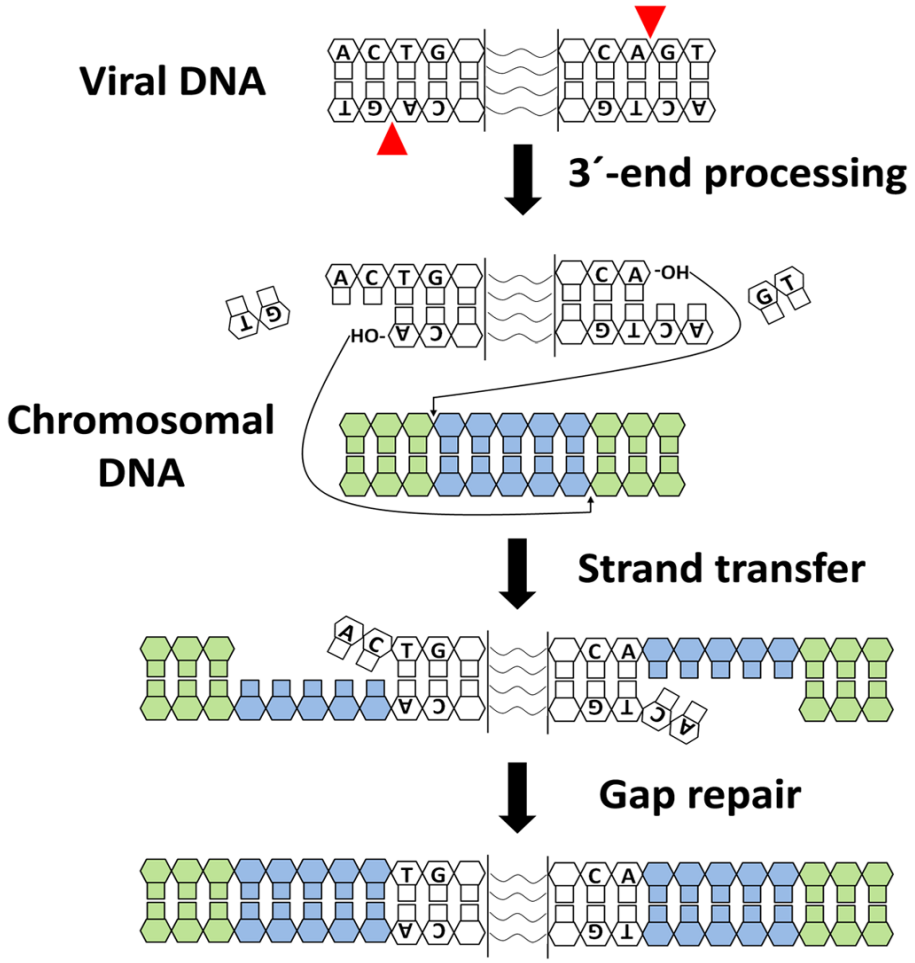

Fig 4. HIV-1 integration. Schematic representation of the integration process, with important sequence features of both viral ends indicated. IN cleavages are indicated with red triangles. The chromosomal DNA is shown in green and the five nucleotides where IN creates the gap are represented in blue. Insertion of viral DNA leads to the duplication of these five nucleotides at both viral ends.

1.3 HIV-1 RT

The RT is the enzyme responsible of the conversion of the viral single stranded RNA genome into a dsDNA complex in a process called reverse transcription.

1.3.1 Reverse transcription

Although not well understood, the initiation of reverse transcription seems to be modulated by the exposition of the viral complex to a high dNTP concentration inside the cell, and by specific rearrangements in the viral RNA (Cobrinik *et al.*, 1988; reviewed in Abbink & Berkhout, 2008). Reverse transcription is initiated from a tRNA primer, a feature common to all retroviruses. In HIV-1

the $tRNA^{Lys,\ 3}$ used is present in the viral particle and is incorporated together with the lysyl-tRNA synthetase protein (LysRS) from a previously infected cell (reviewed in Abbink & Berkhout, 2008; Levin *et al.*, 2010). This $tRNA^{Lys,\ 3}$ binds to the primer binding site (PBS), located downstream of the 5´-end of genomic RNA (reviewed in Levin *et al.*, 2010).

A representation of the different steps of reverse transcription is shown in Fig 5. Upon $tRNA^{Lys,\ 3}$ binding, combined DNA polymerase and RNase H activities of the RT copy and degrade the 5´-end of the viral (+) RNA, generating the minus-strong-stop DNA ((-)ssDNA). By taking advantage of the sequence homology between both viral RNA ends, the newly copied DNA binds the 3´-end, in a process called (-) strand transfer. Then, the complete (-) strand DNA is synthesized, and the viral RNA is simultaneously degraded. However, the 3´- and central-polypurine tracts (PPTs) remain unaffected by the RNase H activity. Furthermore, these ribonucleotide segments serve as primers for the synthesis of the (+) strand DNA. The use of the central-PPT involves discontinuous DNA synthesis, generating a DNA flap, called central flap (later eliminated by cellular endonucleases), and the plus-strong-stop DNA ((+) ssDNA) product. The presence of the PBS sequence in the 3´-end of the (-) strand DNA supports the second or (+) strand transfer, therefore facilitating the annealing of both PBS segments. Finally, the elongation of the (+) and (-) strands of DNA leads to the synthesis of the complete double-stranded viral DNA, that is longer than the RNA genome and that contains the same U3-R-U5 sequence at each end (reviewed in Abbink & Berkhout, 2008, Matamoros et al., 2011; Hu and Hughes, 2012; Le Grice, 2012).

Reverse transcription takes place in the cytoplasm of the infected cell. After entry, the viral core reorganizes and forms the reverse transcription complex. The cornerstones of this complex are the RT and the RNA genome. However, accumulating evidence reveals the contribution of additional viral and host factors. Among the viral factors, it has been shown that NC plays different roles during reverse transcription. For example, fostering the annealing of the tRNA and the PBS sequence, or facilitating (-) strand transfer (reviewed in Levin *et al.*, 2010). Nef and Tat also interact with the RT and increase the efficiency of reverse transcription (Fournier *et al.*, 2002; Apolloni *et al.*, 2007). As discussed above, IN is also associated with the reverse transcription complex, stimulating the synthesis of reverse transcription products (Wu *et al.*, 1999; Dobard *et al.*, 2007). Other viral factors, such as MA, CA, Vif and Vpr, also constitute part of the reverse transcription complex, where they probably help to create a more favorable environment and/or recruit host factors (reviewed in Warrilow *et al.*, 2009; Fassati *et al.*, 2012).

A number of cellular factors have been implicated in reverse transcription. Examples are specific proteins, such as AKAP149, HuR, Top1 and Gemin2, although their precise role is not clear (Hamamoto *et al.*, 2006; Lemay *et al.*, 2008a,b; Ahn *et al.*, 2010; reviewed in Warren *et al.*, 2009). In addition, mammalian cell lysates as well as purified fractions stimulate also reverse transcription (Warrilow *et al.*, 2008, 2010).

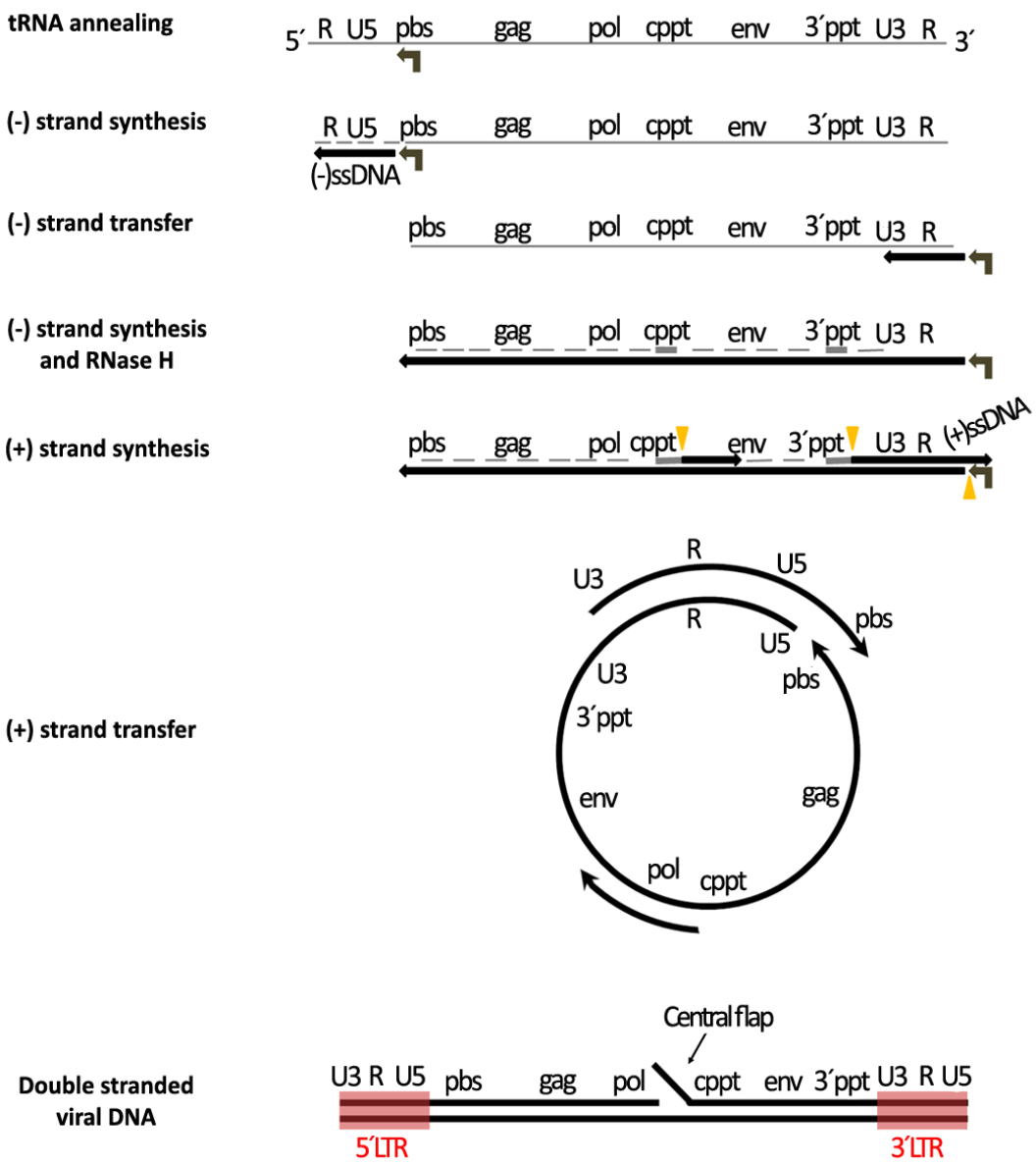

Fig 5. Reverse transcription process. The viral RNA is shown with a gray thin line. The $tRNA^{Lys,3}$ is represented by a ocher bended arrow. The newly synthesized DNA is shown as a black thick line. RNase H-degraded RNA is shown with dashed lines, and specific RNase H cleavage sites that produce PPT primers and eliminate the $tRNA^{Lys,3}$ are represented by yellow triangles.

1.3.2 HIV-1 RT structure

HIV-1 RT is a heterodimer composed of two subunits designated as p66 (560 amino acids) and p51 (440 amino acids) (Di Marzo Veronese *et al.*, 1986). Only p66 has catalytic activity, and is composed of a DNA polymerase and a RNase H domain. The DNA polymerase domain is divided into four subdomains termed fingers (residues 1-85 and 118-155), palm (residues 86-117 and 156-236), thumb (237-318) and connection (319-426). As all the other DNA polymerases, the RT DNA polymerase domain has a structure resembling a right hand (Fig 6A). The p51 subunit lacks the RNase H domain, is catalytically inactive and plays a pivotal role in stabilizing the heterodimer

(Chung *et al.*, 2013). In both p66 and p51 the four polymerase subdomains fold similarly (Kohlstaedt *et al.*, 1992; Jacobo-Molina *et al.*, 1993). However, the spatial organization of the subdomains in p51 differs from p66.

The HIV-1 RT heterodimer contains a nucleic acid binding-cleft, where the thumb of p51 and the connection of both subunits form the "floor". In addition, the fingers, palm and thumb subdomains of p66 establish lateral and apical interactions with the nucleic acid (Jacobo-Molina *et al.*, 1993; Rodgers *et al.*, 1995; Hsiou *et al.*, 1996). Interestingly, in the absence of a nucleic acid substrate, the thumb subdomain of p66 is folded down resulting in a partial occlusion of the nucleic acid binding cleft (Rodgers *et al.*, 1995; Hsiou *et al.*, 1996) (Fig 6B).

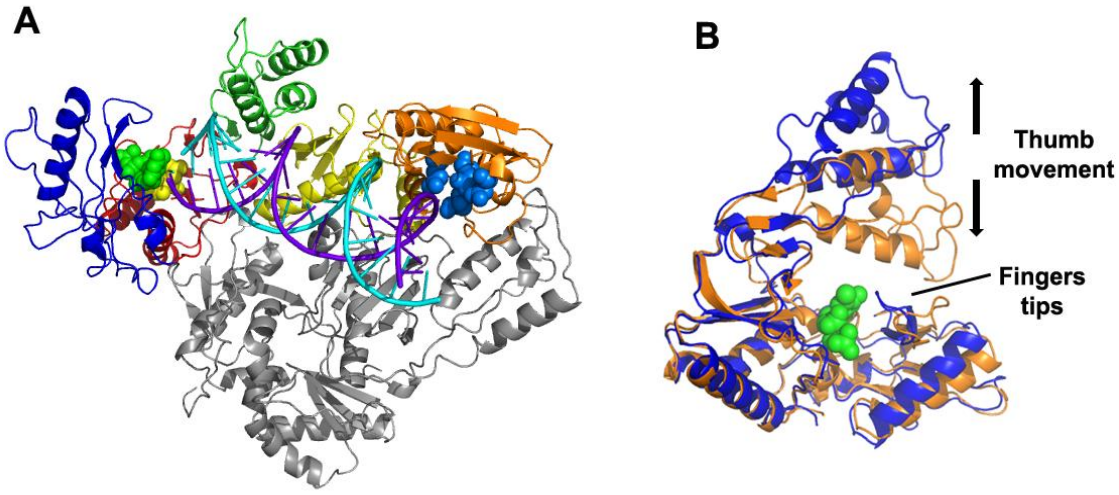

Fig 6. HIV-1 RT structure and effects of template/primer and dNTP binding. (A) Ribbon representation of the structure of the HIV-1 RT bound to DNA/DNA and dNTP showing the fingers, palm and thumb subdomains of p66 in blue, red and green, respectively, the connection subdomain in yellow, the RNase H domain in orange, and p51 in grey. The template strand is shown in purple, the primer strand in cyan and the incoming dNTP as green spheres. Catalytic residues of the DNA polymerase active site (Asp-110, Asp-185 and Asp-186), as well as those of the RNase H active site (Asp-443, Glu-478, Asp-498 and Asp-549) are shown with yellow and blue spheres, respectively. (B) Superposition of p66 thumb subdomains of RT bound to DNA/DNA (blue) and an unliganded RT (orange) showing the movement of the thumb subdomain upon nucleic acid binding. In addition, the closure of the fingers tips on the bound dNTP (represented as green spheres) is also shown. Coordinates of RT bound to DNA/DNA and the dNTP, and unliganded RT were taken from PDB files 1RTD and 1DLO, respectively. Structures were obtained with the PyMOL Molecular Graphics System (DeLano Scientific) software.

The catalytic residues of the polymerase activity (Asp-110, Asp-185 and Asp-186) are located in the palm subdomain of the p66 subunit (Fig 6A), facing the nucleic acid binding cleft (Smerdon *et al.*, 1994). In addition to this catalytic triad, there are other important motifs implicated in RT activity, indicated in Table 1.

Structures of RT bound to double-stranded nucleic acids (Jacobo-Molina *et al.*, 1993; Ding *et al.*, 1998; Sarafianos *et al.*, 2001) showed that the nucleic acid binding cleft can accommodate 17-18 nucleotides between the polymerase and the RNase H catalytic sites. The most pronounced conformational change undertaken by the RT upon nucleic acid binding involves the movement of the p66 thumb to an extended conformation, away from the fingers subdomain, creating a space that

is filled by the nucleic acid (Fig 6B) (Jacobo-Molina *et al.*, 1993; Rodgers *et al.*, 1995). There are no big differences in the way RT binds DNA/DNA and RNA/DNA complexes. In both DNA/DNA and RNA/DNA complexes, nucleic acids undertake a transition from an A-type to a B-type conformation near the p66 thumb subdomain. In addition, a second bend of approximately 20º-30º entering the RNase H domain produces an increase in the width of the major groove of the RNA/DNA duplex (Lapkouski *et al.*, 2013). Recent studies have pointed out that nucleic acid-RT interactions could be more complex, due to the ability of RT to "flip" on the nucleic acid substrate (Abbondanzieri *et al.*, 2008; Liu *et al.*, 2008, 2010).

Table 1. HIV-1 RT motifs and residues participating in nucleic acid interaction

Motif name	Subdomain	Residues	Role in RT function
Primer grip	p66 palm (β12-β13)	227-235	Helps to position the primer 3´-OH in the priming site
DNA polymerase catalytic site	p66 palm	Asp-110, Asp-185, Asp-186	Nucleotide incorporation catalytic residues
Helix clamp	p66 thumb (αH-αI)	255-268 (αH)/278-286 (αI)	Acts as a nucleic acid clamp
RNase H primer grip	p51 connection, p66 connection, p66 RNase H	358-361 (p66 connection), 395-396 (p51 connection), 473-476, 501, 505 (p66 RNase H)	Closely associated with the primer strand
Template grip	p66 fingers, p66 palm (β4, αB, β5, β8-αE)	73-77 (β4), 78-83 (αE), 86-90 (β5), 141-174 (β8-αE)	Closely associated with the template strand
RNase H catalytic site	RNase H	Asp-443, Glu-478, Asp-498, Asp-549	RNA hydrolysis catalytic residues
β3-β4 hairpin loop	p66 fingers (β3-β4)	63-73	Implicated in nucleotide incorporation, fidelity and processivity
YMDD	p66 palm	183-186	Implicated in nucleotide incorporation

Binding of a dNTP (or a nucleotide analog) produces further conformational changes. The most important is the closure of the fingers tips (β3-β4 strands) over the palm subdomain creating a dNTP binding site (or N site) just in front of the primer 3´-OH site (or P site) (Fig 6B) (Huang *et al.*, 1998; Tuske *et al.*, 2004; Das *et al.*, 2009, 2012; reviewed in Sarafianos *et al.*, 2009). In the dNTP binding pocket, the nucleotide is stabilized by interactions with residues Lys-65, Arg-72, Asp-113, Ala-114 and Gln-151. Tyr-115 acts as a "steric gate" discriminating between dNTPs and rNTPs (Martín-Hernández *et al.*, 1996; Cases-González *et al.*, 2000). Nucleotide incorporation also requires the proper positioning of the primer 3´-OH, stabilized by the side-chains of Tyr-183 and Met-184 (part of the YMDD motif) (Huang *et al.*, 1998). The nucleophilic attack of the 3´-OH of the primer terminus on the α phosphate of the dNTP renders an elongated primer and a PPi molecule, which is released with one of the Mg^{2+} ions that participates in the catalysis (Huang *et al.*, 1998; Mendieta *et al.*, 2008). Upon dNMP incorporation, the RT should translocate to continue the polymerization, positioning the primer terminus in the P-site and leaving the N-site free for the incorporation of a new dNTP. Structural data show that the YMDD motif (formed by Tyr-183, Met-184, Asp-185 and Asp-186) acts as a "springboard" supplying some of the energy required for translocation (Sarafianos *et al.*, 2002; reviewed in Singh *et al.*, 2010).

1.3.3 HIV-1 RT activities

The RT is a multifunctional enzyme with DNA- and RNA-dependent DNA polymerization activities, as well as RNase H activity.

1.3.3.1 DNA polymerase activity

Early biochemical work using pre-steady state kinetics showed that nucleotide incorporation is a two-phase reaction including a rapid burst phase followed by a linear phase (Kati *et al.*, 1992; Reardon *et al.*, 1992; Wöhrl *et al.*, 1999), a behaviour shared by other DNA polymerases (Patel *et al.*, 1991). The rate limiting step in the reaction was identified as the fingers movement needed to properly position the dNTP prior to the nucleophilic attack (Sarafianos *et al.*, 2009). However, the dissociation of the RT from the template/primer is the rate limiting step of the overall reaction when performed under steady-state conditions (Reardon & Miller, 1990; Kati *et al.*, 1992; Jaju *et al.*, 1995).

The RT is able to use RNA/DNA, DNA/DNA and even RNA/RNA (during the initiation of reverse transcription) as substrates for nucleotide incorporation. However, RNA/DNA duplexes are more efficient substrates, as the dNTP dissociation constant (K_d) is lower on RNA/DNA than on DNA/DNA, and the nucleotide incorporation rate (k_{pol}) is also slightly increased when RNA/DNA complexes are used (Kati *et al.*, 1992). The processivity of the enzyme is also enhanced with RNA/DNA template/primers (Reardon & Miller, 1990). In addition, the RT affinity for nucleic acid complexes is higher for RNA/DNA complexes than for DNA/DNA duplexes, due to their lower dissociation rate (k_{off}) (DeStefano *et al.*, 1993a).

1.3.3.2 RNase H activity

RNase H activity is critical to accomplish productive infection since RNase H-deficient viruses are non-infectious (Schatz *et al.*, 1989). The RNase H domain acts as an endonuclease that hydrolyzes the RNA strand in (and only in) RNA/DNA heteroduplexes. The catalytic active site is composed of four acid residues: Asp-443, Glu-478, Asp-498 and Asp-549 (Fig 6A). Those amino acids coordinate two divalent metal cations (most probably Mg^{2+}) required for the phosphodiester-bond cleavage (Nowotny *et al.*, 2007; reviewed in Schultz & Champoux, 2008; Champoux & Schultz, 2009; Sarafianos *et al.*, 2009; Herschhorn & Hizi, 2010; LeGrice, 2012). Several residues from the thumb subdomain of the p51 subunit, especially Gln-294, are important modulators of the RNase H activity, probably through contacts with the RNase H domain (Sevilya *et al.*, 2001, 2003). Also, some residues from the connection subdomain have an impact on the RNase H activity. For example, the amino acid substitution A361H impairs RNA cleavage (Julias *et al.*, 2003) while the RNase H mutation Q509L also reduces the enzyme´s activity (Brehm *et al.*, 2008). Substitutions P52G, P55G and S156A at the palm and fingers subdomains also impair RNase H activity (Gao *et al.*, 1998).

Depending on the position of the DNA polymerase and RNase H domains of the RT in relation to the RNA/DNA ends, three different types of RNase H cleavages have been reported (Fig 7).

1) DNA 3´-end directed: In this type of cleavage, the DNA polymerase domain is positioned on the 3´-end of the DNA strand, annealed to a longer RNA template (Liu *et al.*, 2008). Biochemical evidences show that the RT is able to cleave the RNA between 15-20 nucleotides away from the recessed end (Furfine & Reardon, 1991; Schultz *et al.*, 2009).
2) RNA 5´-end directed cleavage: Here the polymerase domain of the RT is associated with an RNA 5´-end of a recessed RNA annealed to a DNA strand. The DNA polymerase domain is located towards the RNA 5´-end, and therefore the RNase H domain binds the RNA strand 13-19 nucleotides away (DeStefano *et al.*, 1993b; reviewed in Schultz & Champoux, 2008). This type of cleavage is predominant when RNA strands are used as primers on RNA/DNA heteroduplexes (Fuentes *et al.*, 1995; Schultz *et al.*, 2003).
3) Internal cleavage: In this type of cleavage there is no strand-end recognition by the RT (Fuentes *et al.*, 1995), and the most important determinant is the nucleotide sequence (Schultz *et al.*, 2004).

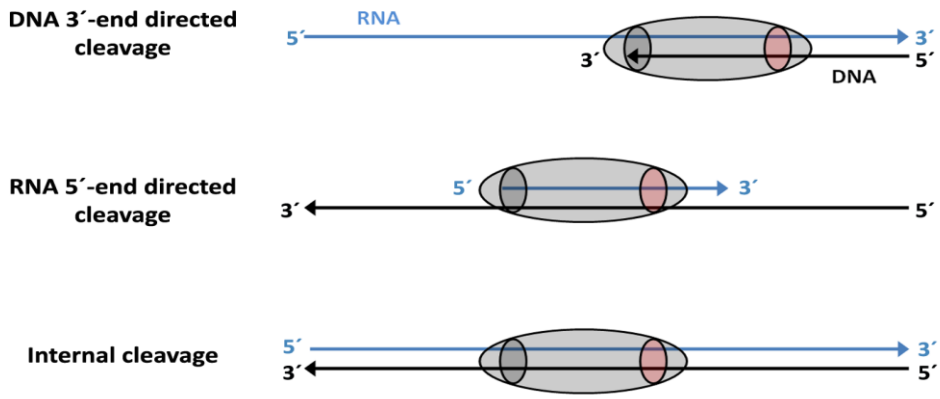

Fig 7. RT RNase H cleavage modes. Schematic representation of the three modes of RT-associated RNase H cleavage. In all modes of association, heteroduplex substrates contain an RNA strand (blue) and a DNA strand (black). The 3´-termini are indicated by arrowheads. The RT is represented by an oval, indicating the DNA polymerase (gray circle) and RNase H (pink circle) active sites.

The PPT sequence (Fig 8) is resistant to RNase H cleavage (Huber & Richardson, 1990). The PPT structure has a U tract at its 5´-end, a central A tract (interrupted by a single G) and a run of Gs at its 3´-end. The RT carries out three specific cleavages in the PPT (Fig 8) (reviewed in Rausch & LeGrice, 2004). The first two cleavages take place during (-) strand DNA synthesis. One of them occurs at the 5´-end of the PPT, normally 15, 17 or 19 nucleotides away from the PPT-U3 junction, defining the length of the PPT primer (Huber & Richardson, 1990; Julias *et al.*, 2002; Rausch & LeGrice, 2007). The other (-) strand DNA synthesis cleavage releases the viral genomic RNA at the PPT-U3 junction. The third specific cleavage takes place at the RNA-DNA junction during (+) strand DNA synthesis and results in the production of the U3 end of the viral DNA. Evidence obtained from *in vitro* and *in vivo* experiments have shown that the specific sequences of both PPT ends are the

most important determinants for RT cleavage. The central A tract has a stronger effect on the efficiency of the PPT-U3 cleavage relative to the PPT 5´-end cleavage (Huber & Richardson, 1990; Dash *et al.*, 2004; McWilliams *et al.*, 2003, 2006, 2008; Julias *et al.*, 2004; Jones & Hughes, 2007).

Although RNA primers are not efficiently extended by the RT (Fuentes *et al.*, 1995), the PPT primer is an exception. This special property has been associated with the presence of a consensus 3´-end G tract (Fig 8) (Huber & Richardson, 1990; Powell & Levin, 1996; Götte *et al.*, 1999; Schultz *et al.*, 2003; Rausch & LeGrice, 2007).

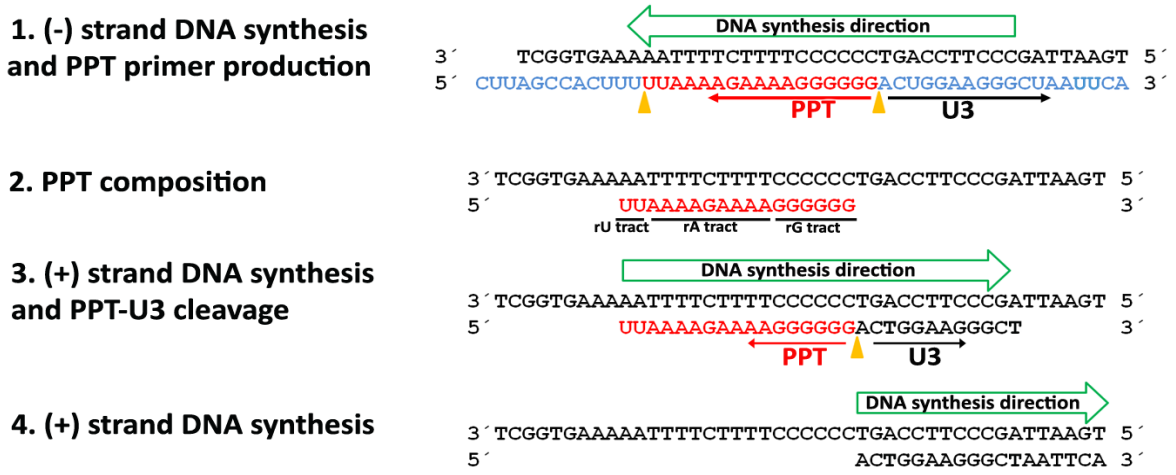

Fig 8. PPT usage. Representation of specific cleavages on the PPT. RNA and DNA strands are shown in blue and black, respectively, with the PPT sequence highlighted in red. Specific RNase H cleavages are represented by yellow triangles and the DNA polymerization direction is indicated by an arrow.

Finally, some thumb subdomain and RNase H primer grip residues have been shown to affect PPT usage (Powell *et al.*, 1999; Julias *et al.*, 2004; McWilliams *et al.*, 2006; reviewed in Rausch & LeGrice, 2004).

1.4 Antiretroviral treatment

RT inhibitors play a major role in current antiretroviral therapy. Licensed RT inhibitors are classified into two major groups, depending on their inhibitory mechanism: nucleos(t)ide reverse transcriptase inhibitors (NRTIs) and non nucleoside reverse transcriptase inhibitors (NNRTIs) (Fig 9).

During the first years of the AIDS epidemic, the treatment of HIV-1 infection was limited to very few drugs and the appearance of resistance strains leading to treatment failure was a major problem in the clinical management of the disease (Larder *et al.*, 1989; St Clair *et al.*, 1991; Shirasaka *et al.*, 1993; Lin *et al.*, 1994; Shafer *et al.*, 1994). The emergence of resistance was facilitated by the high replication capacity of the virus and its high rates of mutation and recombination (reviewed in Menéndez-Arias, 2002, 2009).

However, in the mid 90´s, with the introduction of protease inhibitors, the use of combinations of three or more drugs has greatly reduced the morbidity and mortality of HIV-1 infection (reviewed in De Clercq, 2009a,b; Arts & Hazuda, 2012). These cocktails are referred to as HAART (highly active antiretroviral therapy). An example of this approach is represented by Atripla®, a pill containing tenofovir, emtricitabine and efavirenz, commonly used in developed countries.

1.4.1 Nucleos(t)ides analogues (NRTIs)

At present, there are eight NRTIs approved for clinical use (Fig 9A). All NRTIs lack a 3´-OH group and use a common mechanism of inhibition, first described for AZT in 1986 (Furman *et al.*, 1986). This mechanism involves the competition between the NRTI and the natural substrate and the subsequent interruption of DNA synthesis due to the incorporation of the NRTI in the growing DNA strand. The absence of the 3´-OH group blocks the formation of new phosphodiester bonds with incoming nucleotides (Fig 10). Based on this mechanism, NRTIs are also defined as chain-terminators (Menéndez-Arias, 2008; De Clercq, 2009b).

However, before their use by the RT, the effectiveness of NRTIs depends on several factors such as their entry efficiency inside the cells or their half-life (Cihlar & Ray, 2010). Nonetheless, the most important step required by a NRTI is its phosphorylation to an active triphosphate form: AZT triphosphate (AZTTP), d4T triphosphate (d4TTP), ddA (ddA is the active metabolite of ddI) triphosphate (ddATP), ddC triphosphate (ddCTP), 3TC triphosphate (3TCTP), FTC triphosphate (FTCTP), carbovir (carbovir is the active metabolite of abacavir) triphosphate (CBVTP) and tenofovir diphosphate (tenofovir-DP). NRTI phosphorylation is carried out by cellular kinases (De Clercq, 2009a,b; Cihlar & Ray, 2010).

Prolonged use of NRTIs may produce toxic side effects, like lactic acidosis, myopathy or pancreatitis. These toxic effects mainly include the inhibition of mitochondrial DNA polymerase γ, due to the inability of this enzyme to discriminate between NRTIs and natural dNTPs (Feng *et al.*, 2004; Anderson, 2010; reviewed in Lewis *et al.*, 2003; Akanbi *et al.*, 2012).

However, the main problem associated with the use of NRTIs is the development of resistance mutations. Classically, the mutations rendering resistant RTs are divided in two groups, depending if the decreased susceptibility relies on a discriminatory ability to distinguish between the NRTI and the natural dNTP, or on the excision of the NRTI from the blocked DNA strand.

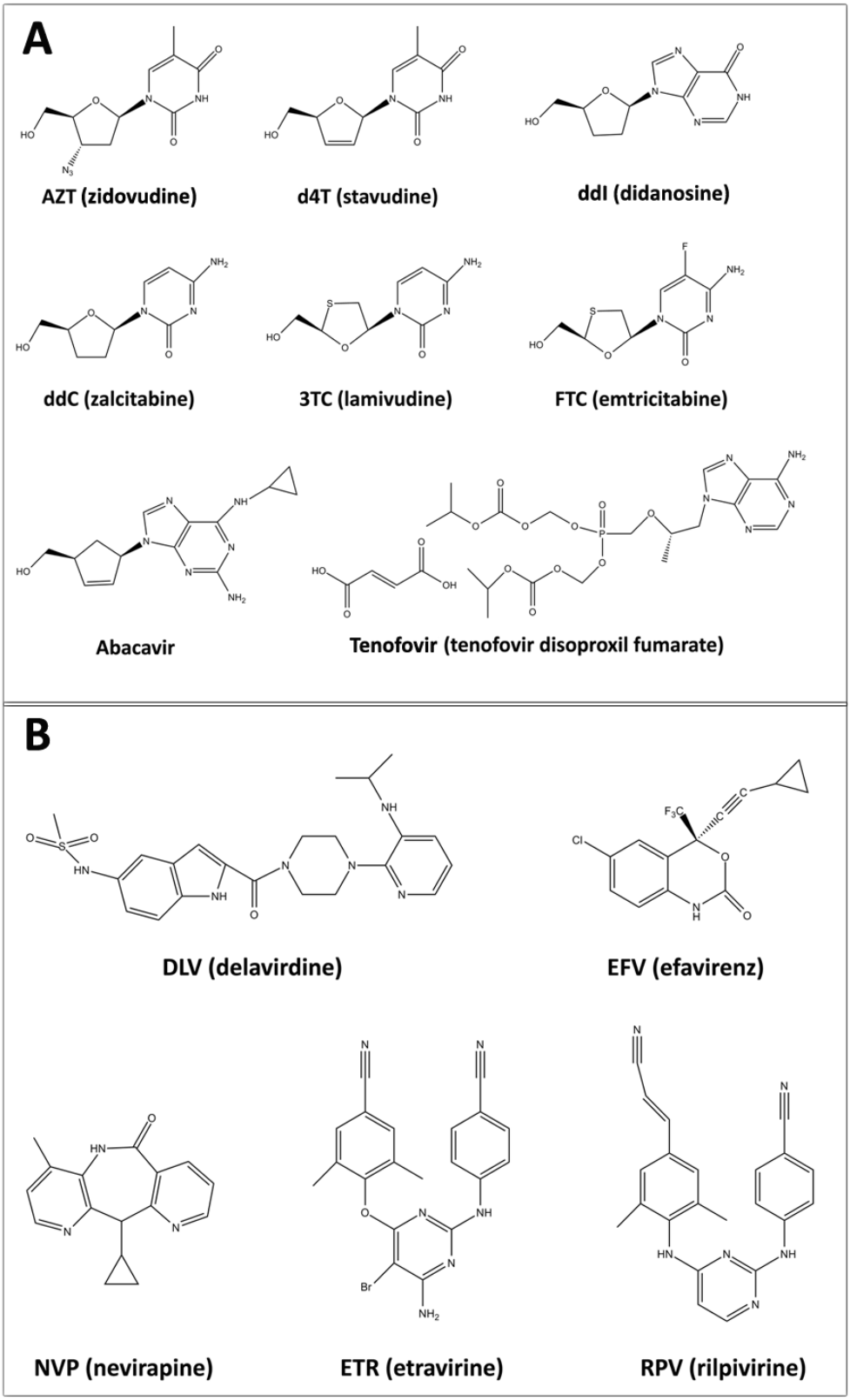

Fig 9. NRTIs and NNRTIs currently approved for clinical use. (A) NRTIs are 3´-azido-2´,3´-dideoxythymidine (**AZT**); 2´,3´-didehydro-2´,3´-dideoythymidine (**d4T**); didanosine, 2´,3´-dideoxyinosine (**ddI**); (1*S*,4*R*)-4-[2-amino-6-(cyclopropylamino)-9*H*-purine-9-yl]-2cyclopentene-1-methanol (**ABC**); 2´-3´-dideoxycytidine (**ddC**); 2´,3´-dideoxy-3´-thiacytidine (**3TC**); (-)-β-L-3´-thia-2´,3´-dideoxy-5-fluorocytidine (**FTC**) and [(R)-9-(2-phosphonylmethoxypropyl)adenine] disoproxil fumarate (**tenofovir**). (B) NNRTIs.

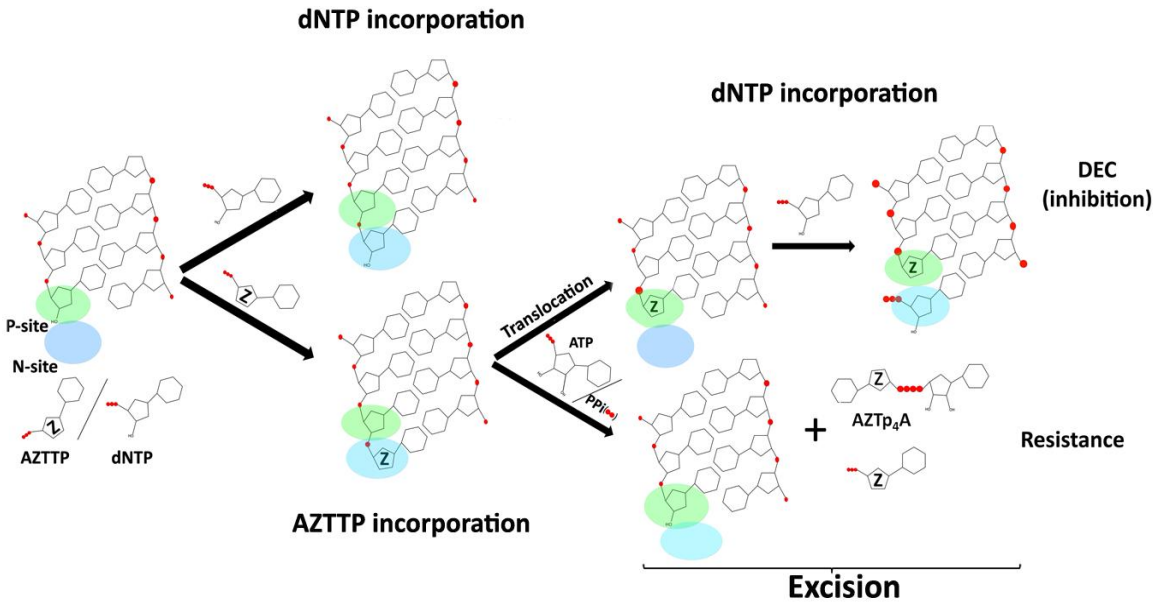

Fig 10. Chain termination and excision mechanism. Schematic representation of dNTP or AZTTP incorporation. The RT nucleotide binding site (N-site) and the priming site (P-site) are represented by blue and green circles, respectively. In the presence of dTTP and AZTTP, the RT can incorporate the natural substrate and the DNA synthesis continues. However, upon AZTMP incorporation, the RT can use a PPi donor (ATP and a PPi molecule are represented) to excise the AZTMP molecule. This process produces a free 3´-OH end to resume DNA synthesis and leads to the formation of $AZTp_4A$ (when ATP is the donor) or AZTTP (when PPi is the donor) molecule. The ATP-dependent excision reaction is favored when TAMs are present. However, the RT can also translocate along the blocked- T/P, positioning the 3´-inhibitor in the P-site. In this configuration the excision of the chain-terminator cannot take place. If RT further binds the next correct dNTP, a stable complex referred to as "dead-end-complex" (DEC) is formed. If such a thing happens, the RT is blocked in this position and therefore the DNA synthesis is abrogated.

1.4.1.1 Resistance to NRTIs by a discriminatory mechanism

Through this mechanism the RT is able to favor the incorporation of the correct dNTP instead of the triphosphorylated NRTI. All of the mutations acting through this pathway exert a direct effect on the nucleotide/inhibitor incorporation step. Many mutations acting through this mechanism impair the viral replication capacity (reviewed in Menéndez-Arias *et al.*, 2003).

Apart from major mutations described in Table 2, there are other less frequent mutations that also act through a discriminatory mechanism. For example, mutations K70E/Q, V75T, V118I, Y181I and the deletion at codon 69 (Δ69) have been found to enhance the discriminatory ability of the RT (Hertogs *et al.*, 2000; Selmi *et al.*, 2001; Blanca *et al.*, 2003; Girouard *et al.*, 2003; Sluis-Cremer *et al.*, 2007; Kisic *et al.*, 2008, 2011; Hachiya *et al.*, 2011).

1.4.1.2 Resistance to NRTIs by an excision mechanism:

Mutations at positions 41 (M41L), 67 (D67N), 70 (K70R), 210 (L210W), 215 (T215F/Y) and 219 (K219Q/E) were soon identified in patients failing treatment with AZT (Larder *et al.*, 1989; St Clair *et al.*, 1991; Kellam *et al.*, 1992; Harrigan *et al.*, 1996; Hooker *et al.*, 1996). The resistance mechanism involved in the selection of these mutations was not related with discrimination between

AZTTP and dTTP (Reardon & Miller, 1990; Lacey *et al.*, 1992; Carroll *et al.*, 1994). A moderate enhancement of processivity and binding affinity for AZTMP-terminated primers had been invoked to explain the effect of AZT-resistance-associated mutations (Caliendo *et al.*, 1996; Canard *et al.*, 1998). However, two different groups showed that the most relevant difference between wild-type and AZT-resistant RTs was the increased ability of the latter to excise 3´-terminal chain-terminator inhibitors from blocked DNA primers through phosphorolysis mediated by PPi or a PPi-donor (Arion *et al.*, 1998; Meyer *et al.*, 1998). The pyrophosphorolysis reaction results in the removal of AZTMP from the end of the primer and the production of a polyphosphate product containing the AZTMP molecule linked to the PPi donor substrate (Fig 10). Chemically, PPi-dependent excision process is the same that the nucleotide incorporation reaction, but run in reverse.

Table 2. Major mutations that increase the RT´s ability to discriminate between NRTIs and dNTPs

Mutation	Enzyme resistant to	Residue role on nucleotide incorporation	Resistance mechanism	Comments	References
K65R	CBVTP, 3TCTP, tenofovir-DP	Interacts with the incoming nucleotide	Reduces k_{pol}	Most frequently selected in subtype C viruses. The side-chain of Arg-65 stacks against the side-chain of Arg-72, increasing the discriminatory ability of the RT	1-23
L74V	CBVTP, ddGTP, ddATP	Stabilizes the template nucleoside	Reduces k_{pol}	Diminished RT capacity to synthesize early reverse-transcribed viral DNA	5, 24-31
Q151M	All NRTIs except 3TCTP and FTCTP	Interacts with the incoming nucleotide	Reduces k_{pol}	Preferred AZT resistance mutation in HIV-2. Frequently found associated with other mutations in the cluster A62V/V75I/F77L/F116V/Q151M, also known as the Q151M complex	3, 28, 29, 32-41
M184I/V	3TCTP, FTCTP	Interacts with primer 3´-OH	Increases K_d	Part of the YMDD motif. M184I/V causes a steric hindrance with the β-L-oxathialone ring of 3TCTP	7, 28, 29, 39, 42-48

References correspond to (1) Srinivas & Fridland, 1998, (2) Wainberg *et al.*, 1999, (3) Ray *et al.*, 2002, (4) White *et al.*, 2002, (5) Deval *et al.*, 2004, (6) Miller *et al.*, 2004, (7) Stone *et al.*, 2004, (8) Tuske *et al.*, 2004, (9) White *et al.*, 2005, (10) Wirden *et al.*, 2005, (11) Brenner *et al.*, 2006, (12) Doualla-Bell *et al.*, 2006, (13) Margot *et al.*, 2006, (14) Parikh *et al.*, 2006, (15) Parikh *et al.*, 2007, (16) Sluis-Cremer *et al.*, 2007, (17) Murray *et al.*, 2008, (18) von Wyl *et al.*, 2008, (19) Brenner & Coutsinos 2009, (20) Coutsinos *et al.*, 2009, (21) Das *et al.*, 2009, (22) Invernizzi *et al.*, 2009, (23) Das & Arnold, 2013, (24) St Clair *et al.*, 1991, (25) Larder. 1992, (26) Martin *et al.*, 1993, (27) Lacey *et al.*, 1994, (28) Ueno & Mitsuya, 1997, (29) Huang *et al.*, 1998, (30) Ren *et al.*, 1998, (31) Frankel *et al.*, 2005, (32) Shafer *et al.*, 1994, (33) Shirasaka *et al.*, 1995, (34) Ueno *et al.*, 1995, (35) Iversen *et al.*, 1996, (36) Kosalaraska *et al.*, 1999, (37) Deval *et al.*, 2002, (38) Deval *et al.*, 2005, (39) Reid *et al.*, 2005, (40) Boyer *et al.*, 2006, (41) Frangeul *et al.*, 2008, (42) Wainberg *et al.*, 1996, (43) Wilson *et al.*, 1996, (44) Sarafianos *et al.*, 1999, (45) Chamberlain *et al.*, 2002, (46) Stoeckli *et al.*, 2002, (47) Whitcomb *et al.*, 2003, (48) Ly *et al.*, 2007.

The same mutations selected under AZT therapy are also found in virus isolated from patients treated with d4T (Coakley *et al.*, 2000; Cozzi-Lepri *et al.*, 2009). For this reason, these mutations are commonly referred as TAMs (thymidine analogue resistance mutations). TAMs appear usually in two different clusters known as TAM-1, composed of mutations M41L, L210W and T215Y and TAM-2, including D67N, K70R, K219Q, and sometimes T215F (Yahi *et al.*, 1999; Cozzi-Lepri *et al.*, 2005, 2009; Svicher *et al.*, 2006). The TAM-1 cluster is more frequent and confers higher levels of resistance to AZT (Japour *et al.*, 1995; reviewed in Menéndez-Arias, 2010). The selection of either TAM-1 or the TAM-2 pathway probably depends on the emergence of the K70R or T215Y as the first mutations selected under therapy (Cozzi-Lepri *et al.*, 2009; Brehm *et al.*, 2012). Individually,

those mutations confer low-level resistance to AZT (Lacey *et al.*, 1994; Boyer *et al.*, 2001; Radzio *et al.*, 2010).

AZTMP, d4TMP and tenofovir are the best substrates of the excision reaction, while cytidine analogues are resistant to ATP-mediated excision (Isel *et al.*, 2001; Naeger *et al.*, 2002; Ray *et al.*, 2003; Boyer *et al.*, 2004; White *et al.*, 2004, 2005; Marchand *et al.*, 2007; Parikh *et al.*, 2007; Iyidogan & Anderson, 2012; reviewed in Goldschmidt *et al.*, 2004). Purines are generally better substrates than pyrimidines as shown with 3´-azidopyrimidines and 3´-azidopurines (Sluis-Cremer *et al.*, 2005; Meteer *et al.*, 2011). Although WT and mutant RTs are equally efficient in PPi-dependent excision reactions, the use of bi- and tri-phosphorylated molecules as PPi donors (e.g nucleoside triphosphates (NTPs), nucleoside diphosphates (NDPs), dNTPs, etc) is favored by the presence of TAMs in the RT coding sequence. However, NTPs are the most efficient PPi donors of the reaction (Meyer *et al.*, 1998, 1999, 2000; Boyer *et al.*, 2001; reviewed in Sluis-Cremer *et al.*, 2000). Use of PPi or a PPi donor depends on their relative concentration inside the cell, which is also regulated by the cellular activation state (Barshop *et al.*, 1991; De la Rosa *et al.*, 1991; Gribble *et al.*, 2000; Smith *et al.*, 2005; reviewed in Smith & Scott, 2006). Among all nucleoside-triphosphates, ATP is the only one with intracellular concentrations high enough to be readily use as PPi donor and therefore it is widely accepted that this is the relevant PPi donor *in vivo*.

A recent study determining the structure of wild-type and mutant M41L/D67N/K70R/T215Y/K219Q RTs bound to a dsDNA and a 3´-azido-3´-deoxythymidine-(5´)-tetraphospho-(5´)-adenosine ($AZTp_4A$) molecule provided a rational explanation for the role of TAMs in NRTI excision (Tu *et al.*, 2010). $AZTp_4A$ is a product of the ATP-dependent excision reaction of primers terminated with AZTMP (Fig 10, 11). Tu and colleagues demonstrated that "primary" TAMs K70R and/or T215Y create a new ATP binding-site by interacting with the AMP (adenosine monophosphate) moiety of the molecule, while the other TAMs help to stabilize the molecule in its binding to the RT through hydrogen bonds (Fig 11). The new ATP binding-site facilitates the proper alignment of the molecule for the nucleophilic attack, producing the excision of the blocking inhibitor, rather than increasing the affinity for ATP (Ray *et al.*, 2003; Selmi *et al.*, 2003). Interestingly, this $AZTp_4A$ product, as well as other polyphosphate molecules, such as dinucleoside tetraphosphates, can be more efficiently used as nucleotide analogues by RTs containing TAMs than by the wild-type enzyme (Meyer *et al.*, 2006; Dharmasena *et al.*, 2007; reviewed in Acosta-Hoyos & Scott, 2010; Das & Arnold, 2013).

A number of factors have been shown to affect the excision reaction rate. For example, the RNA/DNA or DNA/DNA nature of the template/primer, the specific nucleic acid sequence or the Mg^{2+} concentration (Isel *et al.*, 2001; Rigourd *et al.*, 2002; Ray *et al.*, 2003; Meyer *et al.*, 2004; Goldschmidt *et al.*, 2006; Iyidogan & Anderson, 2012; reviewed in Smith & Scott, 2006). However, the most important factor *in vivo* is the RT susceptibility to the next complementary nucleotide. Binding of the RT to the template/primer defines two different sites, *i.e.*, the nucleotide binding site

(N-site) and the priming site (P-site) (Fig 10) (Boyer *et al.*, 2001; Marchand & Götte, 2003). For excision to occur, the inhibitor incorporated at the 3´-end should be located at the N-site, and forms a pre-translocation complex. However, movement of the RT along the template strand leaves the chain-terminator at the P-site, forming a post-translocation complex (Boyer *et al.*, 2001; Sarafianos *et al.*, 2002). This complex leaves a free N-site which can be occupied by the incoming nucleotide. In this case, the ternary RT-T/P-NRTI complex forms a stable aggregate known as the "dead-end-complex" (DEC) which is resistant to the excision reaction (Tong *et al.*, 1997; Meyer *et al.*, 1999) (Fig 10).

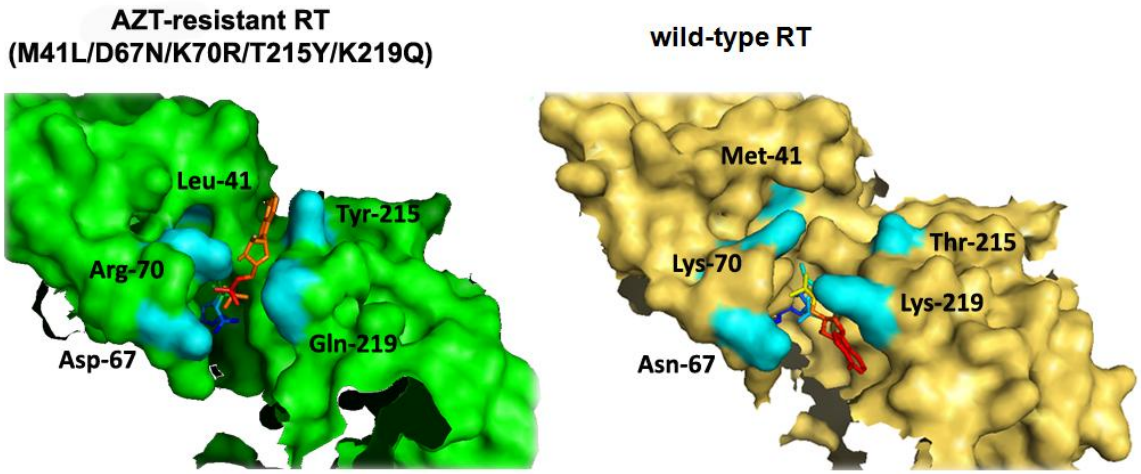

Fig 11. ATP-binding site. Surface representation of an AZT-resistant RT bearing mutations M41L/D67N/K70R/T215Y/K219Q (left, in green), and the WT RT (right, in wheat). TAM mutations are shown in cyan and the $AZTp_4A$ molecule is represented with sticks. The AMP moiety of the $AZTp_4A$ molecule (in orange) adopts a conformation that favors excision in the AZT-resistant RT, stabilized by the side-chains amino acid residues Leu-41, Asp-67, Arg-70, Tyr-215 and Gln-219. In the WT RT structure, the AMP moiety (in red) is in a less favorable configuration for the excision reaction. Coordinates of the AZT-resistant and WT RTs were obtained from PDB files 3KLF and 3KLE, respectively. Structures were generated with the PyMOL Molecular Graphics System (DeLano Scientific) software.

TAMs facilitate the excision of the inhibitor from the 3´-end of the primer, while favoring the formation of pre-translocated complexes (Meyer *et al.*, 1999, 2000; Mas *et al.*, 2002; Marchand & Götte, 2003; Selmi *et al.*, 2003; White *et al.*, 2004). Different NRTIs show different propensities to generate these complexes. Thus, excision of d4TMP or tenofovir is highly susceptible to inhibition by low concentrations of the next correct nucleotide (*i.e.*, between 0.5 and 25 μM) (Meyer *et al.*, 1999, 2000; Ray *et al.*, 2003; Marchand *et al*, 2007; Matamoros *et al.*, 2009, reviewed in Smith & Scott, 2006). On the other hand, the high volume of the azido group impairs the incorporation of a subsequent nucleotide, facilitating AZTMP excision even in the presence of high concentrations of dNTP (*e.g.*, > 200 μM) (Boyer *et al.*, 2001).

Clinical, virological and biochemical data have shown that certain mutations impair TAM function (Table 3). However, the analysis of a large number of viral sequences has also allowed the identification of a number TAM-associated mutations that improve fitness of TAM-containing HIV-1 strains (Table 4).

Table 3. Mutations that antagonize the effect of TAMs on ATP- or PPi-dependent excision

Group	Mutation	Comments	References
NRTI resistance mutations involved in dNTP discrimination	K65R	Primary mutation involved in tenofovir resistance	1-7
	L74V	ddI resistance mutation	8-11
	V75I	Part of the Q151M complex	12
	M184V	3TC and FTC resistance mutation	5,10,11,13,14
Foscarnet (phosphonoformic acid)	W88G/S, E89K, L92I, S156A, Q161L	Rarely found in patients, since foscarnet is not currently prescribed for HIV-1 treatment	15-18
NNRTI resistance mutations	I132M	Rare nevirapine and delavirdine resistance mutation. Reduces RT´s ability to discriminate between NRTIs and dNTPs	19,20
	Y181C	Nevirapine resistance mutation	9, 21
Others	R172K	Impairs NRTI and NNRTI resistance in different sequence contexts	22, 23

References correspond to (1) Parikh *et al.*, 2006, (2) Ly *et al.*, 2007, (3) Parikh *et al.*, 2007, (4) Sluis-Cremer *et al.*, 2007, (5) Zelina *et al.*, 2008, (6) Das *et al.*, 2009, (7) Xu *et al.*, 2009, (8) St Clair *et al.*, 1991, (9) Larder, 1992, (10) Frankel *et al.*, 2005, (11) Miranda *et al.*, 2005, (12) Matamoros *et al.*, 2009, (13) Boyer *et al.*, 2002a, (14) von Wyl *et al.*, 2010, (15) Mellors *et al.*, 1995, (16) Tachedjian *et al.*, 1996, (17) Tramontano *et al.*, 1998, (18) Meyer *et al.*, 2003a, (19) Nissley *et al.*, 2007, (20) Ambrose *et al.*, 2009, (21) Selmi *et al.*, 2003, (22) Hachiya *et al.*, 2012, (23) Menéndez-Arias, 2013.

In addition, several connection and RNase H mutations have been associated with antiretroviral treatment failure: E312Q (Nikolenko *et al.*, 2007; Hachiya *et al.*, 2009), G333E (Hachiya *et al.*, 2009), G335C/D (Nikolenko *et al.*, 2007; Delviks-Frankenberry *et al.*, 2008, 2013; Hachiya *et al.*, 2009), N348I (Nikolenko *et al.*, 2007; Yap *et al.*, 2007; Delviks-Frankenberry *et al.*, 2008, 2013; Ehteshami *et al.*, 2008; Hachiya *et al.*, 2008; Gupta *et al.*, 2010; Radzio *et al.*, 2010; Sluis-Cremer *et al.*, 2010; Von Wyl *et al.*, 2010; Lengruber *et al.*, 2011; Radzio & Sluis-Cremer, 2011), A360I/V/T (Nikolenko *et al.*, 2007; Delviks-Frankenberry *et al.*, 2008; Ehteshami *et al.*, 2008; Brehm *et al.*, 2012), V365I (Nikolenko *et al.*, 2007; Delviks-Frankenberry *et al.*, 2008; Hachiya *et al.*, 2009), A371V (Hachiya *et al.*, 2009; Lengruber *et al.*, 2011; Delviks-Frankenberry *et al.*, 2013), A376S (Nikolenko *et al.*, 2007; Delviks-Frankenberry *et al.*, 2008, 2013; Hachiya *et al.*, 2009), A400T (Von Wyl *et al.*, 2010; Delviks-Frankenberry *et al.*, 2009; 2013) and Q509L (Brehm *et al.*, 2008). Although not all of these mutations have been mechanistically characterized, several of them are thought to act by reducing the RNase H activity of the enzyme, giving RT more time to remove the chain-terminator inhibitor before RNA degradation (reviewed in Götte, 2007; Ehteshami & Götte, 2008; Delviks-Frankenberry *et al.*, 2010) (Fig 12). Biochemical data have shown that mutations N348I, Q509L and the combination N348I/A360V reduced RT RNase H activity while increasing AZTMP excision on RNA/DNA complexes, but not on DNA/DNA complexes (Nikolenko *et al.*, 2007; Yap *et al.*, 2007; Brehm *et al.*, 2008; Delviks-Frankenberry *et al.*, 2008; Ehteshami *et al.*, 2008; Hachiya *et al.*, 2008; Radzio *et al.*, 2010). These mutations impair RNase H activity, especially the secondary cleavages responsible for the generation of RNA oligonucleotides of less than 13 bases, a length insufficient to serve as excisable substrate if blocked with an NRTI at their 3´-end (Brehm *et al.*, 2008; Radzio & Sluis-Cremer 2008).

Table 4. TAMs associated mutations located in the fingers, palm and thumb subdomains of HIV-1 RT

Mutation/s	Comments	References
E40F	When combined with M41L/T215Y, this substitution increases AZT resistance in phenotypic assays. It also reduces viral fitness	1
K43E	Although this mutation does not affect viral AZT resistance, addition of K43E to E40F/M41L/T215Y mutations restores viral replication capacity	1
E44D	Addition of E44D mutation improves 3TCMP excision efficiency of the mutant M41L/D67N/L210W/T215Y enzyme	2
V118I	When combined with T215Y it increases by 2-fold the IC_{50} for d4T. In enzymatic assays the presence of V118I alone or combined with different TAMs increases AZT, 3TC and ddA resistance by reducing NRTI incorporation. V118I reduces AZTMP and 3TCMP excision both on a wild-type and on mutated M41L/E44D/D67N/L210W/T215Y background	2, 3
Q207D	Virus carrying M41L/D67N/K70R/Q207D/H208Y/T215Y/K219Q has an IC_{50} for AZT that is 2.7-fold higher than the IC_{50} for the mutant virus M41L/D67N/K70R/H208Y/T215Y/K219Q	4
H208Y	When combined with T215Y it increases by 2-fold the IC_{50} for d4T while decreasing viral fitness. Further addition of V118I increases the IC_{50} by 3.3-fold	3
F214L	Polymorphism negatively associated with the TAM-1 pathway but positively associated with TAM-2 mutations	5, 6

References correspond to (1) Huigen *et al.*, (2008), (2) Girouard *et al.*, (2003), (3) Clark *et al.*, (2006), (4) Lu *et al.*, (2005), (5) Svicher *et al.*, 2006, (6) Puertas *et al.*, 2009. Additional clinical and epidemiological data supporting the association of these mutations with antiretroviral treatment and/or TAMs can be found in Garriga *et al.*, 2009 (H208Y), Chen *et al.*, 2004 (V118I), Ceccherini-Silberstein *et al.*, 2005 (K43E, E44D, V118I, H208Y), Cane *et al.*, 2007 (K43E, H208Y), von Wyl *et al.*, 2010 (K43E, E44D, V118I, H208Y), Saracino *et al.*, 2006 (K43E, H208Y), Stürmer *et al.*, 2003 (H208Y), Romano *et al.*, 2002 (K43E, E44D, V118I, H208Y), Svicher *et al.*, 2006 (K43E, H208Y), Nebbia *et al.*, 2007 (H208Y), Shulman *et al.*, 2004 (found V118I and H208Y associated with NNRTI hypersusceptibility), Stoeckli *et al.*, 2002 (E44D, V118I, Q207D, H208Y), Masquelier *et al.*, 2004 (E44D, V118I), Melikian *et al.*, 2012 (E40F, K43E, V118I, H208Y). Finally, Gonzales *et al.*, 2003 found mutations at positions 43, 44, 118 and 208 associated with increased exposure to NRTIs.

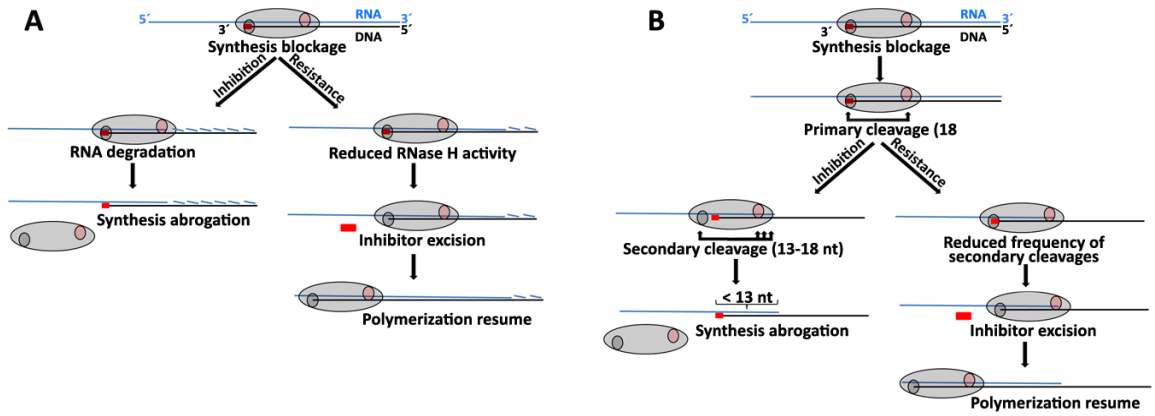

Fig 12. Mechanisms proposed to explain enhanced NRTIs resistance mediated by connection subdomain mutations. (A) Reduced RNase H activity gives RT more time to excise the 3´-end inhibitor before synthesis abrogation. RNA and DNA strands are blue and dark, respectively and the 3´-end inhibitor is represented by a red square. RT (grey oval) posses a RNase H and a DNA polymerase active sites, illustrated by red and grey circles, respectively. (B) Similarly, reduced ability to produce secondary cleavages rendering RNA/DNA duplexes less than 13 nucleotides long, limits the amount of non-excisable substrates.

Interestingly, another connection subdomain mutation, G333D has been found to compensate for the excision impairment produced by the presence of the M184V mutation together with TAMs (Kemp *et al.*, 1998). Addition of G333D on a background of M41L/M184V/L210W/T215Y mutations compensates AZTMP excision by increasing the affinity of the RT for the blocked complex (Zelina *et al.*, 2008).

Finally, associated with the presence of TAMs, a number of changes in the β3-β4 hairpin loop of RT fingers subdomain, including dipeptide insertions between codons 69-70 (sometimes

accompanied by mutations T69S and A62V), and the deletion of codon 67 (together with mutations T69G and K70R) (*i.e.*, the Δ67 complex), have been described as enhancers of the excision reaction (Mas *et al.*, 2000, 2002; Boyer *et al.*, 2002b; Meyer *et al.*, 2003b; Matamoros *et al.*, 2004; White *et al.*, 2004; Cases-González *et al.*, 2007; Kisic *et al.*, 2011; reviewed in Menéndez-Arias *et al.*, 2006).

1.4.2 Resistant to non-nucleoside RT inhibitors (NNRTIs)

There are five NNRTIs currently approved for clinical use: the dipyrodiazepinone nevirapine (NVP), the bis(heteroaryl)piperazine (BHAP) derivative delavirdine (DLV), the benzoxazinone efavirenz (EFV) and the most recently approved diarylpyrimide (DAPY) analogues etravirine (ETR, formerly known as TMC125) and rilpivirine (RPV, formerly known as TMC278) (Fig 9B). Unlike NRTIs, NNRTIs do not need further modifications inside the cell to be active. In addition, all approved NNRTIs share the same inhibitory mechanism. All act as allosteric inhibitors binding to a pocket situated approximately 10 Å away from the dNTP binding site (Fig 13A) (Kohlstaedt *et al.*, 1992; Smeardon *et al.*, 1994). This pocket is formed upon NNRTI binding and involves the movement of the side-chains of Tyr-181 and Tyr-188 from a down configuration (as observed in the unliganded RT) to an upper configuration (Rodgers *et al.*, 1995; Hsiou *et al.*, 1996; reviewed in Ren & Stammers, 2008; Singh *et al.*, 2010). Inside the binding pocket, NNRTIs establish a number of stacking interactions that could vary depending on the specific inhibitor (Fig 14).

NNRTI binding produces a number of rearragments in the RT structure (Fig 13B, C), including the hyperextension of the thumb subdomain, which coupled with a movement of the 3´-end of the primer strand, relocate the 3´-end in a non-catallytically position. In addition, there is a change in the conformation of the β3-β4 structure of the fingers subdomain, that impairs the productive binding of the dNTP (Fig 13C) (Das *et al.*, 2012). Kinetic studies have shown that NNRTIs inhibit the chemical step of dNTP incorporation, but not the conformational change (Spence *et al.*, 1995, 1996). Furthermore, NNRTI binding enhances the RT affinity for dNTPs in a metal-dependent way (Xia *et al.*, 2007). In addition, apart from the polymerase inhibitory effect, NNRTIs also impact the RNase H activity, producing an enhancement of the hydrolytic activity (Palaniappan *et al.*, 1995; Shaw-Reid *et al.*, 2005; Hang *et al.*, 2007; Radzio & Sluis-Cremer 2008; Biondi *et al.*, 2010; reviewed in Sluis-Cremer & Tachedjian, 2008).

Studies from different groups have shown that efavirenz, etravirine and in a lesser extend nevirapine promote RT dimerization (Tachedjian *et al.*, 2001; Figueiredo *et al.*, 2006; Braz *et al.*, 2010a,b; reviewed in Sluis-Cremer & Tachedjian, 2008). This behavior can be explained by the strong tendency of NNRTIs to bind the p66 monomer. Interestingly, binding of EFV to the RT structure in the Gag and Gag-Pol precursos may lead to the formation of RT dimers, but also protease dimers, producing the premature cleavage of the Gag and Gag-Pol polyproteins (Figueiredo *et al.*, 2006; Chiang *et al.*, 2009; Sudo *et al.*, 2013; reviewed in Sluis-Cremer & Tachedjian, 2008).

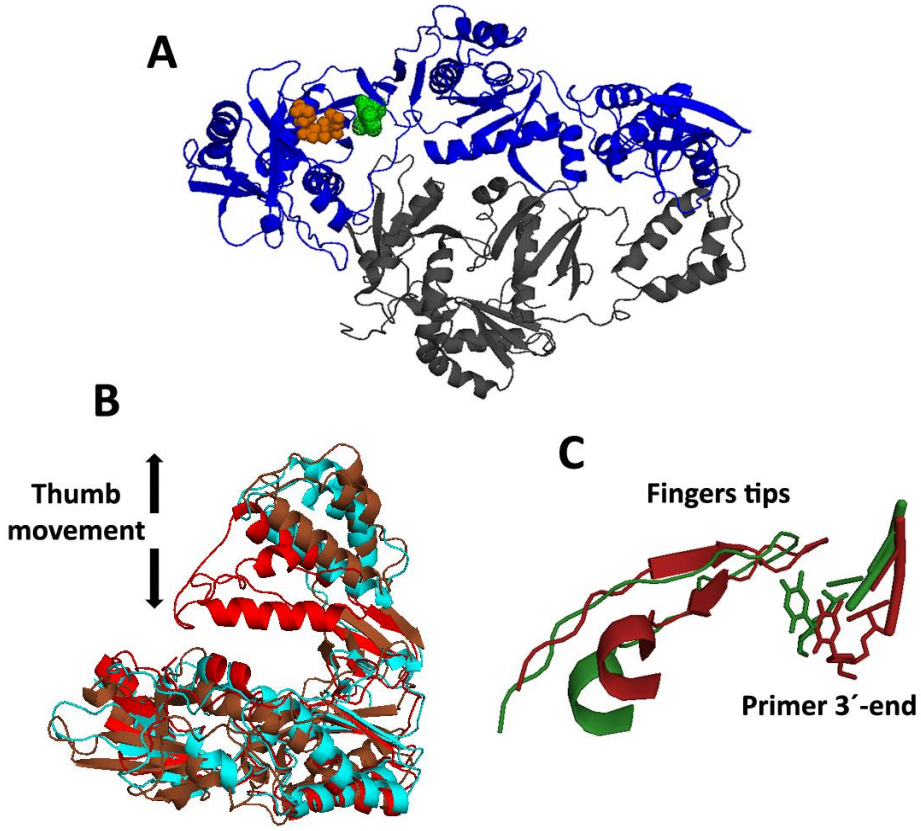

Fig 13. Effects of NNRTI binding on RT structure. (A) Ribbon representation of the RT bound to NVP (PDB code 3HVT). Structure showing the p66 and p51 subunits in blue and gray, respectively. NVP is shown as green dots, and polymerase catalytic aspartic acids Asp-110, Asp-185, Asp-186 are shown as orange spheres. (B) Comparison of the conformation of the thumb subdomain in the unliganded RT (PDB file 1HMV), in red, RT bound to DNA/DNA (PDB file 2HMI), in cyan, and RT-NVP binary complex (PDB file 3HVT), in brown. (C) Superposition of RT-DNA/DNA-NVP (PDB file 3V81) and RT-DNA/DNA-AZTTP (PDB file 3V4I) complexes, in green and red, respectively. The primer 3´-end of each structure is shown in the same color code. NVP binding produces a relocation of the primer 3´-end as well as the movement of fingers tip β3-β4 loop. Structures were obtained with the PyMOL Molecular Graphics System (DeLano Scientific) software.

NNRTI resistance mutations (Fig 15) are classified in three groups according with their mechanism of resistance. Thus, mutations such as Y181C/I or Y188C/L eliminate specific stacking interactions between the NNRTI and the RT (Kohlstaedt *et al.*, 1992; Smeardon *et al.*, 1994; Ren *et al.*, 2001; Das *et al.*, 2007). Other mutations, such as L100I and G190A/S introduce a steric hindrance, decreasing the space available for the NNRTI to bind the RT (Hsiou *et al.*, 1998; Ren *et al.*, 2004; Das *et al.*, 2008). Finally, mutations such as K101E and K103N prevent the entry of the NNRTI by altering hydrogen bond interactions in the NNRTI binding site (Maga *et al.*, 1997; Hsiou *et al.*, 2001; Ren *et al.*, 2006). Interestingly, combinations of at least two of these classical NNRTI resistance mutations are needed to show phenotypic resistance to the newly developed NNRTIs etravirine and rilpivirine (Ghosn *et al.*, 2009; Alcaro *et al.*, 2011). These drugs were designed to have high flexibility, to facilitate their accommodation inside the binding pocket. Structural studies have shown the ability of these drugs to reorient and reposition into the pocket through conformational changes designated as "wiggling" and "jiggling" (Das *et al.*, 2004, 2008; Lansdon *et al.*, 2010). Although etravirine and rilpivirine were expected to have a higher genetic barrier to resistance (*i.e.*,

required 2 or 3 amino acid substitutions for high-level resistance), epidemiological and virological studies have reported the quick appearance of the E138K substitution in patients treated with those drugs (Tambuyzer *et al.*, 2009; Asahchop *et al.*, 2011; Hu & Kuritzkes 2011; Xu *et al.*, 2011, 2012, 2013; Singh *et al.*, 2012).

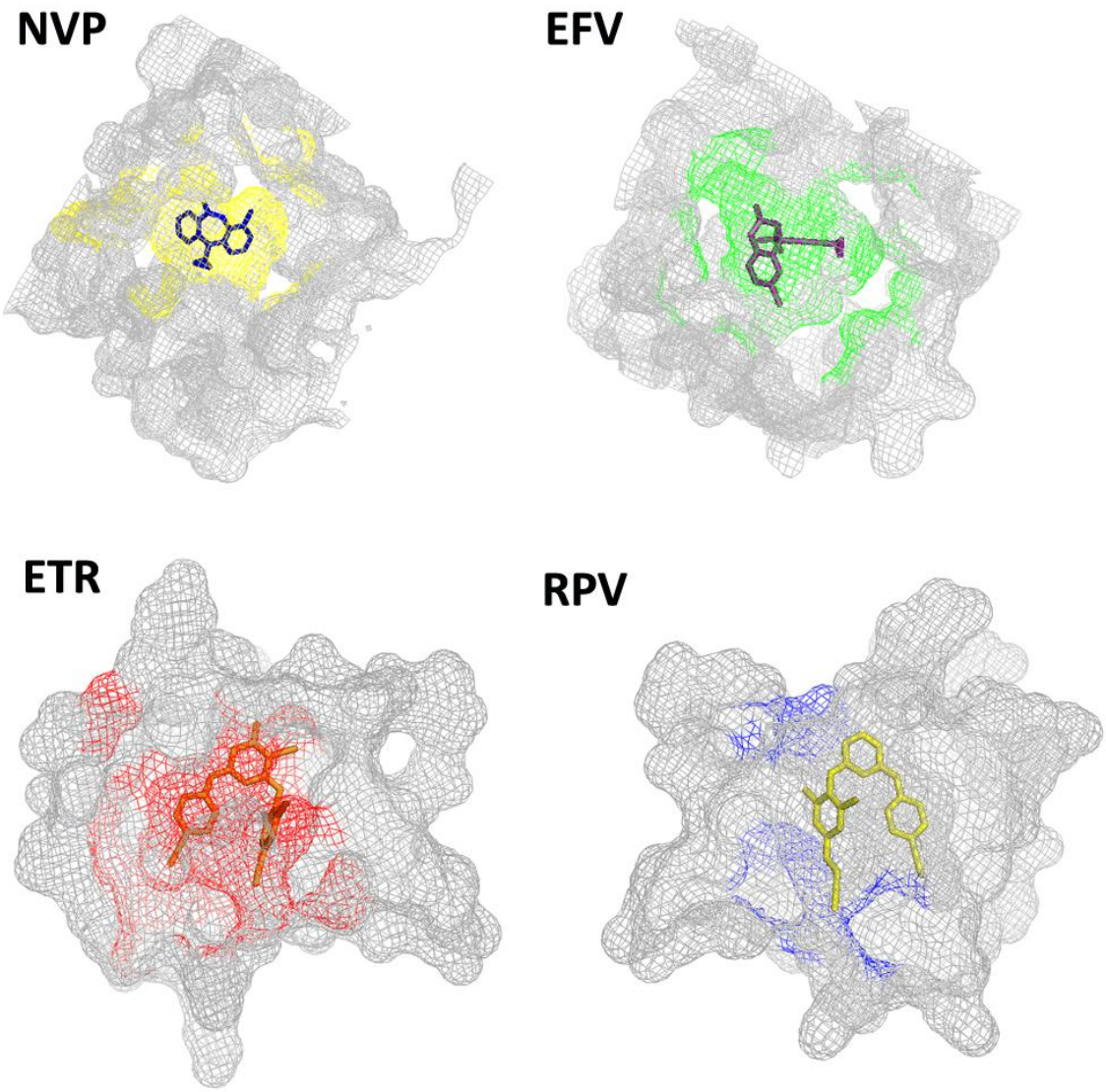

Fig 14. Structure of nevirapine, efavirenz, etravirine and rilpivirine binding pockets and resistance-associated mutations. Panels show the binding pockets of four inhibitors, using a mesh representation. NNRTIs are represented with blue, purple, orange and yellow sticks for nevirapine, efavirenz, etravirine and rilpivirine, respectively. Major interactions for each NNRTI are indicated. For nevirapine, residues Leu-100, Lys-103, Val-106, Tyr-181, Tyr-188, Gly-190, Phe-227, Trp-229, Leu-234, Pro-236 and Tyr-318 are shown in yellow. For efavirenz, residues Leu-100, Lys-101, Lys-103, Val-106, Val-179, Tyr-181, Tyr-188, Phe-227, Trp-229 and Tyr-318 are shown in green. In etravirine and rilpivirine complexes, residues Leu-100, Val-106, Val-179, Tyr-188, Pro-225, Phe-227, Trp-229, Leu-234, Pro-236 and Tyr-318 (in red) and residues Phe-227, Trp-229 and the p51 residue Glu-138 (in blue), respectively, are highlighted. Coordinates were taken from PDB files 3HVT (NVP), 1FK9 (EFV), 3MEC (ETR) and 3MEE (RPV). Structures were obtained with the PyMOL Molecular Graphics System (DeLano Scientific) software.

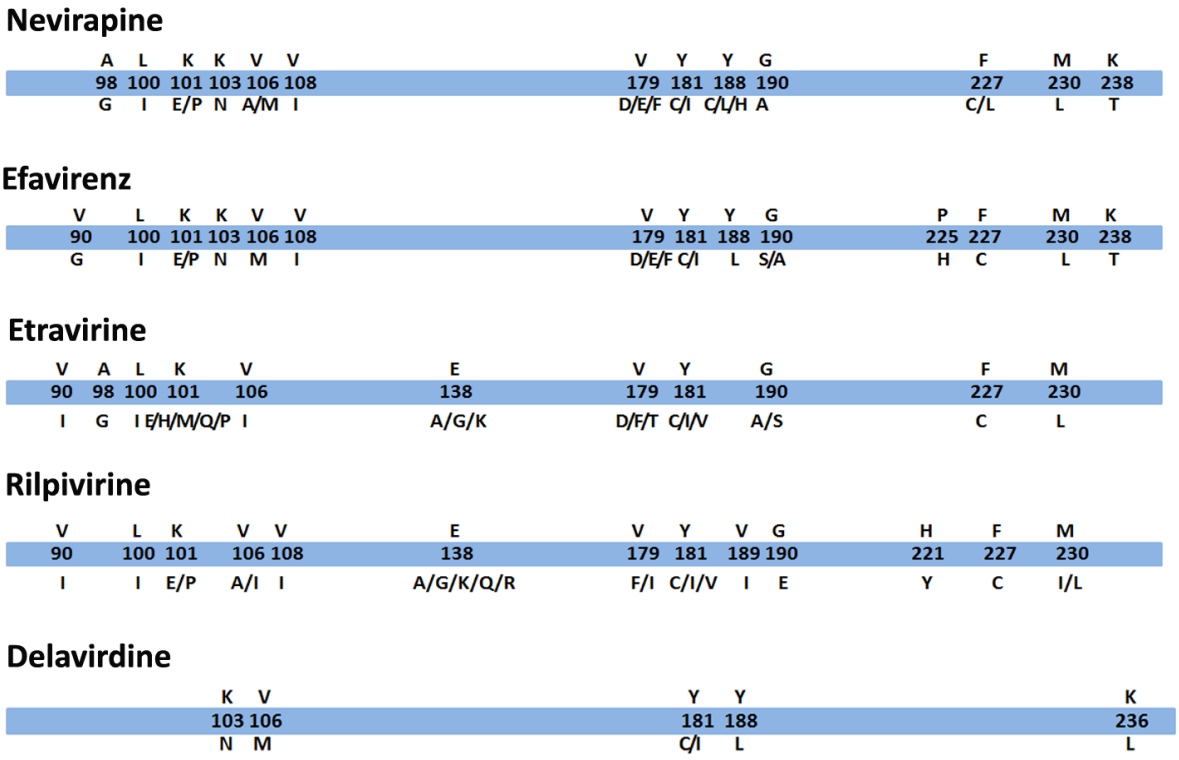

Fig 15. **NNRTI resistance-associated mutations.**

In addition, connection subdomain mutations E312Q, Y318F, G333D/E, G335C, N348I, K358R, G359S, A360I/V, V365I, T369I/V, A371V, I375V, A376S, T377M, T386A, I393L and E399D, as well as the RNase H domain mutation Q509L have been found associated with NNRTI resistance (Pelemans *et al.*, 1998; Harrigan *et al.*, 2002; Vingerhoets *et al.*, 2005; Yap *et al.*, 2007; Zhang *et al.*, 2007; Hachiya *et al.*, 2008, 2009; Gupta *et al.*, 2010, 2011; Sluis-Cremer *et al.*, 2010; Lengruber *et al.*, 2011; McCormick *et al.*, 2011; Paredes *et al.*, 2011; Delviks-Frankenberry *et al.*, 2013; reviewed in Menéndez-Arias *et al.*, 2011). Biochemical studies carried out with RTs bearing the mutation Y318F or Y318W, showed that they conferred resistance to DLV (Y318F) and NVP (Y318W) (Pelemans *et al.*, 1998). It has been shown that the A376S mutation alone confers 3.8-fold resistance to NVP, due to a reduced NVP binding affinity and an improved affinity for DNA/DNA complexes (Paredes *et al.*, 2011). However, for the most studied mutation (N348I), four different mechanism have been proposed to explain the observed phenotypic resistance to NVP. Thus, this mutation could act by (i) reducing NVP binding to the inhibitor binding pocket, (ii) decreasing the affinity of the RT for the template/primer in the presence of the NNRTI, (iii) diminishing the RT RNase H activity, and (iv) affecting the orientation of the RT relative to the nucleic acid substrate, a property relevant for PPT-RNA primer removal during (+) strand DNA synthesis (Fig 16) (Yap *et al.*, 2007; Biondi *et al.*, 2010; Nikolenko *et al.*, 2010; Schuckmann *et al.*, 2010; Radzio & Sluis-Cremer 2011; reviewed in Menéndez-Arias *et al.*, 2011). Interestingly, while the N348I substitution in the p51 subunit is the responsible for the reduced RNase H activity (Schuckmann *et al.*, 2010; Radzio & Sluis-Cremer, 2011), the reduced NVP affinity conferred by this amino acid substitution seems to rely on the presence of N348I in the p66 subunit (Schuckmann *et al.*, 2010).

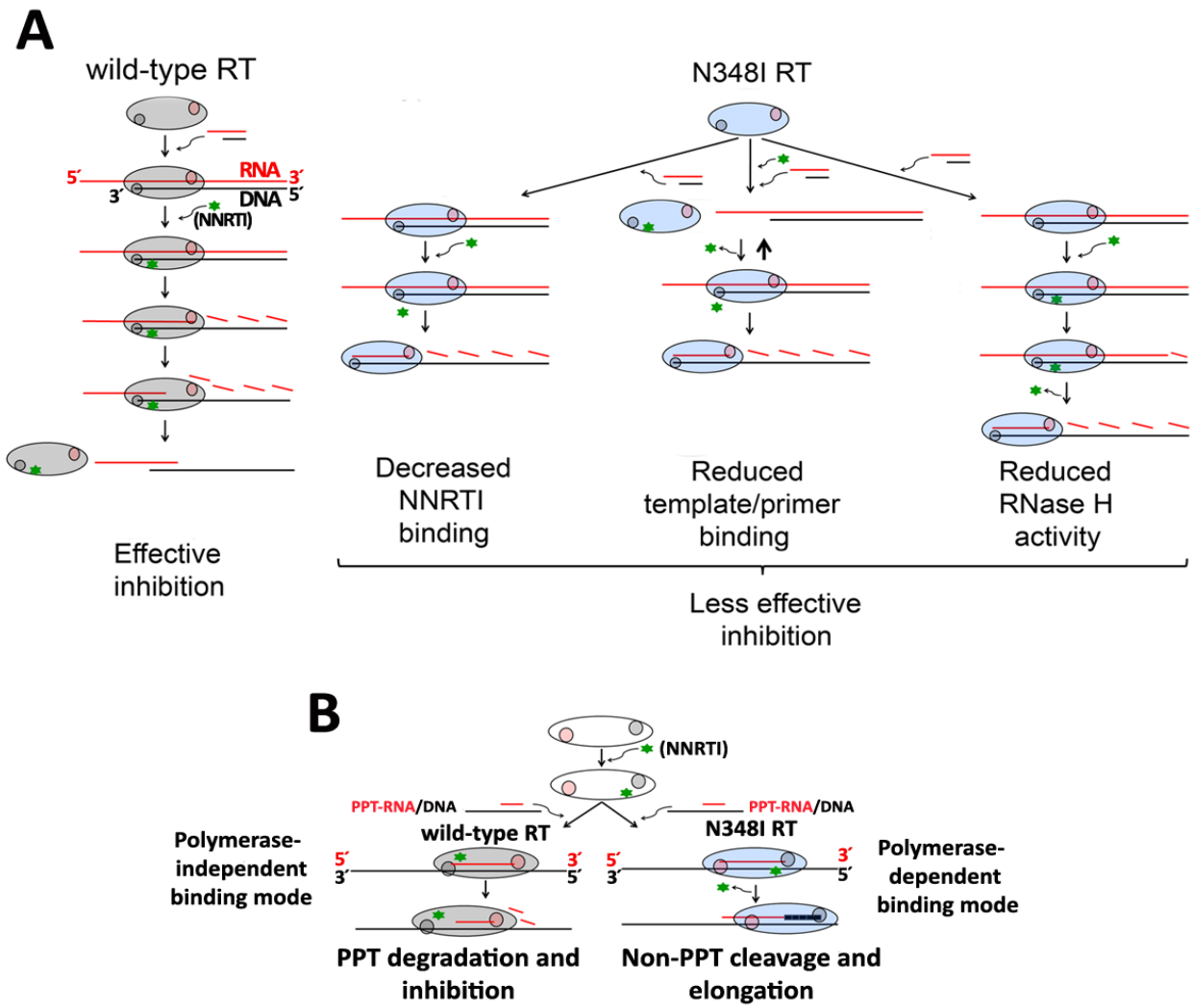

Fig 16. Potential mechanisms to explain NNRTI resistance mediated by N348I. (A) Behavior of wild-type and N348I mutant RTs with a heteropolymeric RNA/DNA. RT mutation can affect interactions with the NNRTI and the RNA/DNA template/primer and therefore, the balance between the RNA-dependent DNA polymerase and RNase H activities of the enzyme during DNA elongation. (B) Proposed effect of the N348I mutation on initiation of (+) strand DNA synthesis is based on the reduced tendency of N348I RT to bind on an RNase H-dependent orientation. Therefore, the PPT-RNA primer is not degraded and gives RT more time to dissociate from the NNRTI and resume the synthesis.

Finally, simultaneous usage of NRTIs and NNRTIs produces a synergistic action, where NNRTIs antagonize the effects of TAMs on NRTI excision from blocked template/primers (Basavapathruni *et al.*, 2004, 2006; Radzio & Sluis-Cremer, 2008).

2.Objectives

2. Objectives

1. To determine the role of RT thumb subdomain polymorphisms Pro-272, Arg-277 and Thr-286 associated with thymidine analogue resistance mutations (TAMs) in resistance to nucleoside analogues inhibitors.
2. To characterize the molecular mechanism underlying the selection of the RT thumb subdomain substitution R284K under treatment with NRTIs, in the presence of TAM-1 pathway mutations (*i.e.*, M41L, L210W and T215Y).
3. To study the mechanism by wich H208Y contributes to the selection of NRTI-resistant strains containing mutations of the TAM-1 pathway.
4. To determine the effects of different RT connection subdomain mutations in resistance to nevirapine and other non-nucleoside RT inhibitors and to analyze their contribution to PPT removal in reverse transcription during (+) strand DNA synthesis
5. To determine the effect of HIV-1 integrase in the RNase H activity of the RT in the processing of the PPT during reverse transcription and in the hydrolysis of heteropolymeric RNA/DNA complexes.

3.Materials & Methods

3. Materials & Methods

3.1 Site-directed mutagenesis

In this work several RTs bearing different combination of amino acids substitutions have been used. To obtain these mutant enzymes the "QuickChange™ Site-Directed Mutagenesis Kit" of Stratagene was used according to the manufacturer's instructions.

Plasmid pRT66B (Fig 17) contains the sequence of the RT-coding region from the HIV-1 wild-type BH10 strain (group M, subtype B). This plasmid was used as template to introduce mutations M41L, H208Y, T215Y, P272A, R277K, R284K, T286A, N348I, M357T, T369I, T369V and T376S. Additionally, a derivative of the pRT66B plasmid containing the mutations M41L/T215Y ($pRT66B_{LY}$) and obtained during this project, was used to introduce mutations P272A/R277K/T286A, H208Y and L210W. In addition, the $pRT66B_{LWY}$ plasmid, containing mutations M41L/L210W/T215Y was used to introduce mutations H208Y, R284K and M357T. Another variant of the pRT66B plasmid containing the sequence of a mutated RT bearing a Ser-Ser insertion between codons 69 and 70 and mutations M41L, A62V, T69S, K70R, and T215Y was also used (Matamoros *et al.*, 2004).

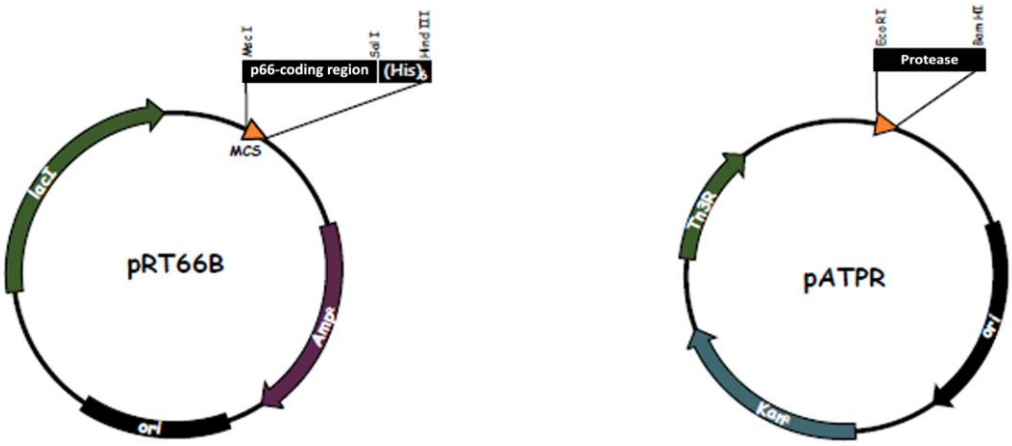

Fig 17. Plasmids used in RT purification. Left, plasmid pRT66B (Boretto *et al.*, 2001). This plasmid codifies the p66 subunit of RT and derives from plasmid pTcr99A (Amersham Bioscience). The plasmid pTcr99A was modified by introducing the p66 coding sequence and a six-histidine tag in sites generated by MscI and HindIII endonucleases. Right, plasmid pATPR, codifying HIV-1 protease. The plasmid pATPR (Boretto *et al.*, 2001) derived from pAT contained an ATG codon followed by the protease coding sequence in the ribosome binding site (RBS) of T7g10, flanked by EcoRI and BamHI endonuclease restriction sites. pRT66B and pATPR are expressed simultaneously to produce p66/p51 heterodimers resulting from cleavage of p66 by the viral protease.

Mutagenesis reactions were carried out using plasmids pRT66B, $pRT66B_{LY}$ and $pRT66B_{LWY}$ as templates and the mutagenic primers shown in Table 5. Table 6 shows a list with all of the mutant RTs purified (derived from the HIV-1 group M subtype B BH-10 strain) in this work and their sequence differences in comparison to the wild-type HIV-1 (BH-10 strain) RT.

Mutagenesis reactions were carried out in 50 µl of 20 mM Tris-HCl pH 8.8 buffer, containing 10 mM KCl, 10 mM $(NH_4)_2SO_4$, 2 mM $MgSO_4$, 0.1% (w/v) Triton X-100, 0.1 mg/ml bovine serum albumin (BSA), 125 ng of each of the corresponding mutagenic primers, around 50 ng of the template plasmid, 500 µM of each of the four dNTPs and 2.5 U of Pfu Turbo DNA polymerase (Stratagene). The polymerase chain reaction (PCR) was started with an incubation of 2 min at 95ºC followed by 20 cycles each one including incubations of 30 s at 95ºC, 1 min at 55ºC and 12 min at 68ºC. The obtained product was treated with 10 U of DpnI (Stratagene) for 1 hour at 37ºC. DpnI is an endonuclease that specifically degrades the methylated or hemimethylated DNA, leaving undigested the newly synthesized DNA with the desired mutations. The template plasmids used in the reaction are methylated because they are amplified in an *E. coli dam*$^+$ strain.

Table 5. Primers used in mutagenesis reactions

Mutation(s)	Primer sequence
M41L	5´ GTAGAAATTTGTACAGAACTGGAAAAGGAAGGGAA 3´ 3´ CATCTTTAAACATGTCTTGACCTTTTCCTTCCCTT 5´
H208Y	5´ GGAGCTGAGACAATATCTGTTGAGGTGGGG 3´ 3´ CCTCGACTCTGTTATAGACAACTCCACCCC 5´
H208Y[a]	5´ GGAGCTGAGACAATATCTGTGGAGGTGGGG 3´ 3´ CCTCGACTCTGTTATAGACACCTCCACCCC 5´
L210W	5´ GCTGAGACAACATCTGTGGAGGTGGGGACTTACC 3´ 3´ CGACTCTGTTGTAGACACCTCCACCCCTGAATGG 5´
T215Y	5´ TGAGGTGGGGATTTTACACACCAGACAAA 3´ 3´ ACTCCACCCCTAAAATGTGTGGTCTGTTT 5´
P272A/R277K	5´ CAAGTCAGATTTACGCAGGGATTAAAGTAAAGCAATTATGTAAAC 3´ 3´ GTTCAGTCTAAATGCGTCCCTAATTTCATTTCGTTAATACATTTG 5´
R284K	5´ GTAAACTCCTTAAAGGAACCAAAGCACTAAC 3´ 3´ CATTTGAGGAATTTCCTTGGTTTCGTGATTG 5´
T286A	5´ CTCCTTAGAGGAGCCAAAGCACTAACAGA 3´ 3´ GAGGAATCTCCTCGGTTTCGTGATTGTCT 5´
N348I	5´ CAAGAGCCATTTAAAATTCTGAAAACAGGAAAATATGCAAGAATGAGG 3´ 3´ GTTCTCGGTAAATTTTAAGACTTTTGTCCTTTTATACGTTCTTACTCC 5´
M357T	5´ GGAAAATATGCAAGAACGAGGGGTGCCCAC 3´ 3´ CCTTTTATACGTTCTTGCTCCCCACGGGTG 5´
T369I	5´ CTAATGATGTAAAACAATTAATAGAGGCAGTGCAAAAAATAACCAC 3´ 3´ GATTACTACATTTTGTTAATTATCTCCGTCACGTTTTTTATTGGTG 5´
T369V	5´ CACTAATGATGTAAAACAATTAGTAGAGGCAGTGCAAAAAATAACCACAG 3´ 3´ GTGATTACTACATTTTGTTAATCATCTCCGTCACGTTTTTTATTGGTGTC 5´
T376S	5´ CAGAGGCAGTGCAAAAAATATCCACAGAAAGCATAGTAATATGGGG 3´ 3´ GTCTCCGTCACGTTTTTTATAGGTGTCTTTCGTATCATTATACCCC 5´

Left column indicates the mutation(s) introduced in the RT. Mutagenized codons are shown in red. The sequence of RTs obtained after the mutagenesis reactions were confirmed by DNA sequencing.

[a] H208Y mutation introduced in a M41L/L210W/T215Y background. Underlined sequence indicates the triplet encoding for the L210W mutation.

E. coli DH5α [*F-, φ80dlacZΔM15, Δ(lacZYAargF),U169, recA1, endA1, hsdR17 (rK- mK+), phoA, supE44, λ-, thi-1, gyrA96, relA1]* competent cells were then transformed with 3 µl of the product of the mutagenesis reaction, and ampicillin-resistant colonies were selected.

The integrity of the entire RT sequence, as well as the presence of the desired mutations, were confirmed by sequencing of the plasmidic DNA extracted with the "Wizard Plus SV Minipreps" kit (Promega). The sequencing reactions were carried out in Macrogen Korea (Seoul, South Korea). The sequences were analyzed using the Seqman 4.0 (DNAstar Inc.) software. Once the presence of the mutation was confirmed, the plasmids were used to transform the *E. coli* XL1-Blue PR strain. This strain derives from *E. coli* XL1-Blue, previously transformed with the pATPR plasmid (Fig 17), that contains the nucleotide sequence encoding the HIV-1 protease (Boretto *et al.*, 2001).

Table 6. Purified recombinant RTs

RT	41	62	69	70	208	210	215	272	277	284	286	348	357	369	376
WT (BH10)	**M**	**A**	**T**	**K**	**H**	**L**	**T**	**P**	**R**	**R**	**T**	**N**	**M**	**T**	**T**
M41L/H208Y/L210W/T215Y	L				Y	W	Y								
M41L/H208Y/T215Y	L				Y		Y								
M41L/L210W/T215Y	L					W	Y								
M41L/L210W/T215Y/R284K	L					W	Y			K					
M41L/L210W/T215Y/R284K/M357T	L					W	Y			K			T		
M41L/T215Y	L						Y								
M41L/T215Y/P272A/R277K/T286A	L						Y	A	K		A				
H208Y					Y										
P272A/R277K/T286A								A	K		A				
R284K										K					
N348I												I			
N348I/T369I												I		I	
T369I														I	
T369V														V	
T376S															S
MAK_SSSY	L	V	SSS	R			Y								

Left column indicates the name of the RT, while the amino acid substitution found in RT sequence of the different mutants are shown on the right. The second row on the top shows the amino acid sequence of the wild-type (BH10 strain) HIV-1 RT at relevant positions.

3.2 RT purification

RT purification relies on the coexpression of the large subunit of the RT (p66) and the HIV-1 protease in *E. coli*, previously transformed with plasmids pRT66B and pATPR (Fig 17) (Boretto *et al.*, 2001; Matamoros *et al.*, 2005).

3.2.1 RT expression

Twenty ml of LB medium containing ampicillim (100 µg/ml) and kanamicin (50 µg/ml) were inoculated with 5-10 µl of a glycerol-containing stock of *E. coli* XL1-Blue strain cells previously transformed with the pRT66B plasmid (which contains the sequence of the p66 subunit of the RT

with the desired mutations) and the pATPR plasmid (codifying the viral PR). This culture was grown overnight at 37ºC under constant stirring. Then, the obtained culture (20 ml) was added to 300 ml of the same medium and grown for another 4 hours under the same conditions. After this step, we prepared three flasks of one liter each with fresh LB medium containing ampicillin (100 μg/m) and kanamicin (50 μg/ml). To each flask we added 100 ml of the bacterial culture obtained in the previous step. These cultures were maintained under constant agitation at 37ºC until the optical density at 600 nm was around 0.7. Then, isopropyl β-D-1-thiogalactopyranoside (IPTG) was added to a final concentration of 0.6 mM to produce the p66 subunit of the RT and the PR encoded within the plasmids and the culture was left at 37ºC for another 24 hours. Then, the cells were harvested by centrifugation at 3000 rpm at 4ºC for 30 min using a rotor JLA 10.500 and an Avanti J-26 XP centrifuge (Beckman Coulter).

3.2.2 Lysis of bacteria

The bacterial pellet obtained (roughly 4 g) was resuspended in 20 ml of 40 mM Tris-HCl pH 8.0 buffer, containing 25 mM EDTA, 10% (w/v) sucrose, 1 mM phenylmethylsulfonyl fluoride (PMSF), 2 mM benzamidine, and 1 mg/ml lysozyme, and stirred at 4ºC for 15 min. Then, another 20 ml of a solution containing 0.8% (w/v) NP-40, 20 mM dithiothreitol, 1 mM PMSF and 2 mM benzamidine were added and again mixed at 4ºC for 15 min. Finally, we added NaCl to a final concentration of 0.5 M and the mixture was sonicated at an amplitude of 24 microns for 1 min using a Labsonic M sonifier (Sartorius). Then, the sample was centrifuged at 15000 g at 4ºC for 15 min using a rotor JA 25.50 and an Avanti J-26 XP centrifuge (Beckman Coulter). The supernatant obtained was diluted in 7 volumes of 50 mM sodium phosphate pH 6.8 buffer and stored at 4ºC.

3.2.3 Cation-exchange chromatography

First, a cellulose-phosphate column (P11 cellulose phosphate, Whatman) of around 5 ml was packed according to manufacturer's instructions in 50 mM sodium phosphate pH 6.8 buffer, leaving the column at the same pH. The sample was passed through the column and then washed with 10 volumes of the equilibrating buffer.

The bound enzyme was eluted from the column using a gradient prepared with 40 ml of 50 mM sodium phosphate pH 6.8 buffer, containing 30 mM NaCl, and 40 ml of the same buffer, containing 1 M NaCl. Fractions of 2 ml were collected and the presence of enzyme was checked by measuring the absorbance at 280 nm of all fractions. The enzyme-enriched fractions were pooled and subjected to affinity chromatography.

3.2.4 Affinity chromatography

The pooled sample collected after the cation-exchange chromatography step was loaded in a 2 ml-column of Ni^{2+}-nitriloacetic-agarose (ProBond™, Invitrogen), previously equilibrated in 50 mM sodium phosphate pH 6.8 buffer containing 30 mM NaCl. Then, the column was washed with 100 ml of 50 mM sodium phosphate pH 6.0 buffer containing 0.5 M NaCl.

The RT bound to the Ni^{2+} column was eluted with a gradient prepared with 20 ml of 50 mM sodium phosphate pH 6.0 buffer containing 0.5 M NaCl, and another 20 ml of the same buffer containing 0.5 M NaCl and 0.5 M imidazole. Fractions of 2 ml were collected and their absorbance at 280 nm was determined. The RT-enriched fractions were pooled and subjected to dialysis using Visking 20/32 dialysis bags of 16 mm diameter in a 50 mM Tris-HCl pH 7.0 buffer, containing 25 mM NaCl, 1 mM EDTA and 10% (w/v) glycerol. Pooled fractions (around 20 ml) were usually dialyzed against 250 ml of dialysis buffer each time, and four changes of the dialysis solution were made. Finally, the sample was concentrated to a final volume of 1-2 ml by ultracentrifugation using Centiprep-30 (Millipore) and following manufacturer's instructions. The concentrated RT aliquots obtained were stored at -20ºC.

The purity of the heterodimers obtained was determined by SDS-polyacrylamide gel electrophoresis. The enzyme concentration was determined by using the RT molar extinction coefficient at 280 nm (ε_{280} = 260450 M^{-1} cm^{-1}) (Kati *et al.*, 1992).

3.3 Nucleotides and Inhibitors

Stock solutions (100 mM) of dNTPs, ddATP and rNTPs were obtained from GE Healthcare. AZT triphosphate (AZTTP) was purchased from Moravek Biochemicals (Brea, CA) and TriLink Biotechnologies (San Diego, CA). Carbovir triphosphate (CBVTP) and tenofovir diphosphate (tenofovir-DP) were obtained from Moravek Biochemicals (Brea, CA). Stavudine triphosphate (d4TTP) was purchased from Sierra Bioresearch (Tucson, AZ).

The NNRTIs nevirapine (NVP), efavirenz (EFV), etravirine (ETR) and rilpivirine (RPV) were obtained through the AIDS Research and Reference Reagent Program, Division of AIDS, NIAID, NIH (Rockville, Maryland, USA). In the case of rilpivirine and etravirine, drugs were contributed to the Program by Tibotec Pharmaceuticals, Inc.

3.4 Preparation of template/primers

In this work, we used several DNA/DNA and RNA/DNA complexes. Their sequences are given in Table 7.

3.4.1 Heteropolymeric nucleic acid complexes

M13mp2 oligonucleotide ssDNA was available in the laboratory from previous studies and was obtained as decribed in Bebenek & Kunkel (1995). Synthetic PPT17r8d (composed of 17 deoxyribonucleotides and 8 ribonucleotides) was obtained from Sigma-Aldrich (MO, USA). All other RNA and DNA oligonucleotides used in this work were supplied by Invitrogen Life Technologies (CA, USA).

3.4.1.1 Labeling of RNA and DNA oligonucleotides

DNA oligonucleotides, including the PPT17r8d primer (2 pmol) and RNA oligonucleotides (3 pmol) were labeled at their 5´-end by using 1 μCi of [γ^{32}P]ATP (Perkin Elmer) and 5 U of T4 polynucleotide kinase (Promega). The labeling reaction included an incubation with [γ^{32}P]ATP, the oligonucleotide and the polynucleotide kinase at 37ºC during 45 min, in 70 mM Tris-HCl pH 7.5 buffer, containing 10 mM $MgCl_2$ and 5 mM dithiothreitol. Then, the polynucleotide kinase was heat-inactivated by incubating the reaction at 90ºC for 10 min. The correct incorporation of the radioactive phosphorous was confirmed by thin-layer chromatography in PEI-cellulose plates (TLC, 20x20 cm, Merck) and using 0.5 M disodium phosphate as mobile phase.

Before annealing, labeled RNA templates, as well as the PPT17r8d chimeric RNA-DNA primer were subjected to a purification step using mini Quick Spin 764 columns (Roche) by following the manufacturer's instructions. Since part of the RNA could be lost at this step, the RNA was chromatographed in PEI-cellulose plates (TLC, 20x20 cm, Merck) using 0.5 M disodium phosphate as mobile phase. The PEI-cellulose sheets were exposed to phosphoroimaging plates (Fujifilm BAS-MP 2040S) and the intensity of the RNA samples before and after the using the mini Quick Spin 764 column was determined by phosphoroimaging with a BAS 1500 scanner (Fujifilm), and using the software TINA 2.09 (Raytest Isotopenmessgerate GmbH, Staubenhardt, Germany). This method was used to estimate the final RNA concentration.

3.4.1.2 DNA/DNA and RNA/DNA duplexes annealing

The DNA/DNA and RNA/DNA duplexes containing a labeled DNA primer strand were obtained by heating a roughly 5-fold excess concentration of unlabeled template over the primer at 100ºC for 4 min in a solution containing 150 mM NaCl and 150 mM magnesium acetate (pH 7.0), followed by slowly cooling at room temperature. The obtained DNA/DNA and RNA/DNA complexes were then diluted to the desired concentration in 550 mM Hepes pH 7.0 buffer, containing 150 mM NaCl and 150 mM magnesium acetate.

The RNA/DNA complexes containing a labeled RNA template strand were obtained by heating a roughly 5-fold excess of the unlabeled DNA primer strand over the labeled-RNA template at 100ºC

for 4 min in 50 mM Tris-HCl pH 8.0 buffer containing 50 mM KCl, followed by slowly cooling at room temperature. Then, the RNA/DNA duplexes were diluted to a 200 nM final concentration in 50 mM Tris-HCl pH 8.0 buffer, containing 50 mM KCl and 2.5 U of rRNAsin® Plus (Promega).

Finally, the complex T57d/PPT17r8d was obtained by heating a roughly 5-fold excess of unlabeled T57d template over the primer at 100ºC for 4 min in 50 mM Tris-HCl pH 8.0 buffer containing 50 mM KCl, followed by slowly cooling at room temperature. Then, the RNA/DNA duplexes were diluted to a 200 nM final concentration in 50 mM Tris-HCl pH 8.0 buffer containing 50 mM KCl.

Table 7. Heteropolymeric template/primer complexes used

Name		Sequence
D38	3´	ACCATCCCGATATGTAAGAACGTCCATTCTTTCCTGGG 5´
25PGA	5´	TGGTAGGGCTATACATTCTTGCAGG 3´
D38C	3´	ACCATCCCGATATGTAAGAACGTCCCTTATTTCCTGGG 5´
25PGA	5´	TGGTAGGGCTATACATTCTTGCAGG 3´
D38T	3´	ACCATCCCGATATGTAAGAACGTCCTAACTTTCCTGGG 5´
25PGA	5´	TGGTAGGGCTATACATTCTTGCAGG 3´
ssM13mp2[a]	3´	--ACGACGTTCCGCTAATTCAACCCATTGCGGTCC-- 5´
ProLac110	5´	GCGATTAAGTTGGGT 3´
C120	3´	TACACCTTTTAGAGATCGTCA 5´
C220	5´	ATGTGGAAAATCTCTAGCAGT 3´
C120	3´	TACACCTTTTAGAGATCGTCA 5´
B2-1	5´	ATGTGGAAAATCTCTAGCA 3´
Dumbbell[b]	5´	TGCTAGTTCTAGCAGGCCCTTGGGCCGGCGCTGCGCC 3´
PPT30DNA	3´	AAATTTTCTTTTCCCCCCTGACCTTCCCGA 5´
PPT29RNA	5´	CUUUUUAAAAGAAAAGGGGGGACUGGAAG 3´
PPT29DNA	3´	AATTTTCTTTTCCCCCCTGACCTTCCCGA 5´
PPT29RNA	5´	CUUUUUAAAAGAAAAGGGGGGACUGGAAG 3´
PPT28DNA	3´	AATTTTCTTTTCCCCCCTGACCTTCCCGA 5´
PPT29RNA	5´	CUUUUUAAAAGAAAAGGGGGGACUGGAAG 3´
D38rna	5´	GGGUCCUUUCUUACCUGCAAGAAUGUAUAGCCCUACCA 3´
25PGA	3´	GGACGTTCTTACATATCGGGATGGT 5´
D38Crna	5´	GGGUCCUUUAUUCCCUGCAAGAAUGUAUAGCCCUACCA 3´
25PGA	3´	GGACGTTCTTACATATCGGGATGGT 5´
D38Trna	5´	GGGUCCUUUCAAUCCUGCAAGAAUGUAUAGCCCUACCA 3´
25PGA	3´	GGACGTTCTTACATATCGGGATGGT 5´
D31rna	5´	GGGUCCUUUCUUACCUGCAAGAAUGUAUAGC 3´
25PGA	3´	GGACGTTCTTACATATCGGGATGGT 5´
T57d	3´	AGAATCGGTGAAAATTTTCTTTTCCCCCCTGACCTTCCCGATTAAGTGAGGGTTGC 5´
PPT17r8d	5´	UUAAAAGAAAAGGGGGGACTGGAAG 3´
PPT29DNA	3´	AATTTTCTTTTCCCCCCTGACCTTCCCGA 5´
PPT17r	5´	UUAAAAGAAAAGGGGGG 3´
T35rna	5´	AGAAUGGAAAAUCUCUAGCAGUGGCGCCCGAACAG 3´
PR26	3´	TAGAGATCGTCACCGCGGGCTTGTCC 5´
31Trna	5´	UUUUUUUUUAGGAUACAUAUGGUUAAAGUAU 3´
21P	3´	CCTATGTATACCAATTTCATA 5´

[a] Dashes in the ssM13mp2 DNA strand indicate the sequence continues.

[b] The dumbbell strand is self-complementary.

3.4.2 Primers blocked with carbovir monophosphate (CBVMP) or d4T monophosphate (d4TMP)

Terminal transferase (Roche) was used to block 25PGA primers with CBVMP and d4TMP (the terminal transferase marketed by Roche is also known as terminal deoxynucleotidyl transferase, or TdT). These blocked oligonucleotides were used to determine the ATP-dependent excision of wild-type and mutant RTs. The reaction was initiated by incubating the 25PGA primer with a 2-fold excess concentration of d4TTP or CBVTP and 150 U of recombinant terminal transferase (Roche) in 25 mM Tris-HCl pH 6.6 buffer, containing 250 mM potassium cacodylate, 0.25 mg/ml BSA and 1 mM $MnCl_2$ at 37 ºC for 1 hour. Then, the enzyme was heat-inactivated by incubating the sample at 90ºC for 10 min. The blocked-primer obtained was precipitated with sodium acetate and 98% ethanol and diluted in 60 µl of water. However, the precipitation step does not eliminate all the free d4TTP and CBVTP present in the media. Therefore, the blocked-primer was subjected to a second purification step using mini Quick Spin 764 columns (Roche). The sample was passaged through the columns until the absorbance at 260 nm remained unchanged, indicating that all of the free triphosphorylated NRTI molecules had been eliminated.

Then, the purified primers were labeled using the same protocol described in section 3.4.1.1. Finally, the labeled $25PGA^{d4TMP}$ or $25PGA^{CBVMP}$ blocked-primers were annealed to their corresponding templates by incubating each one with a 2-fold excess of template strand in water at 100ºC for 4 min, followed by slowly cooling at room temperature.

3.4.3 Primers blocked with AZT monophosphate (AZTMP) or tenofovir

The terminal transferase is unable to incorporate AZTTP or tenofovir-DP at the 3´-end of a primer. Therefore, an alternative method was developed. This method is based on the production of template/primer (T/P) complexes containing a blocked primer, instead of the synthesis of a blocked primer that was later annealed to the corresponding template. The process initiates with the production of the corresponding nucleic acid duplex following the protocol described in section 3.4.1.2.

For AZTTP and tenofovir-DP incorporation reactions, the labeled T/P (4.6 µM) was preincubated with wild-type RT (4 µM) in 65 µl of 50 mM Hepes pH 7.0 buffer, containing 15 mM NaCl, 15 mM magnesium acetate, 130 mM potassium acetate, 1 mM dithiothreitol, and 5% (w/v) polyethyleneglycol 6000 for 10 min at 37°C. Then, 35 µl of 6 mM AZTTP or tenofovir-DP (diluted in the preincubation buffer) were added and incubated for another 30 min at 37°C to ensure that the primer was blocked completely. The RT was inactivated by heating the mixture for 10 min at 90°C. After slowly cooling the sample at room temperature, it was passaged several times through mini

Quick Spin columns (Roche) to eliminate the free inhibitor. Tests carried out previously in the laboratory demonstrated that complete elimination of free AZTTP or tenofovir-DP as well as salt traces was achieved after four successive passages through these columns. Finally, the blocked-T/P was precipitated with sodium acetate and 98% ethanol, and diluted in 50 µl of 550 mM Hepes pH 7.0 buffer, containing 150 mM NaCl and 150 mM magnesium aspartate.

The final T/P concentration was calculated after thin-layer chromatography in PEI-cellulose plates (TLC, 20x20 cm, Merck) using 0.5 M disodium phosphate as mobile phase, by comparing the intensity of the labeled-T/P before and after the purification process. For this purpose, the PEI-cellulose sheet used in the chromatography was exposed to phosphoroimaging plates (Fujifilm BAS-MP 2040S) and the intensity of each point was measured in the phosphoroimaging scanner BAS 1500 (Fujifilm) using the TINA 2.09 software (Raytest Isotopenmessgerate GmbH, Staubenhardt, Germany). This method yields approximately a 40-50% of the initial product.

3.5 Active enzyme titration

Active site titration of all RTs was carried out with the T/P D38/25PGA (prepared as described in section 3.4.1.2). The assay was performed in 20 µl of 100 mM Hepes pH 7.0 buffer, containing 30 mM NaCl, 30 mM magnesium acetate, 130 mM potassium acetate, 1 mM dithiothreitol, 5% (w/v) polyethyleneglycol 6000, 30 nM D38/25PGA, 500 µM dTTP and the corresponding RT at different concentrations.

Aliquots of 4 µl were removed 10, 20, 30 and 40 s after starting the reaction and mixed with 4 µl of stop solution (10 mM EDTA, 90% formamide, with 3 mg/ml xylene cyanol and 3 mg/ml bromophenol blue). Products were resolved on a denaturing 20% polyacrylamide/8 M urea gel, and primer elongation was quantified by phosphorimaging with a BAS 1500 scanner (Fuji), using the software TINA version 2.09 (Raytest Isotopenmessgerate Gmbh, Staubenhardt, Germany). Kinetic parameters were obtained by adjusting the total amount of primer elongated at each time point to the equation $y = ax + b$, where y is the percentage of elongated primer, x is the time and b represents the percentage of RT-T/P bound at time zero. This number, corrected with the T/P concentration used in the assay yields the active enzyme concentration of the sample (Kati et al., 1992).

3.6 Rescue assays

This assay has been developed to study the efficiency of the RT in removing NRTIs from blocked primers and resume DNA synthesis, using DNA/DNA and RNA/DNA complexes with a blocked 3´-end (rescue assay). A list of RTs and the inhibitors used in these assays is given in Table 8. All T/P duplexes were prepared as described in section 3.4.1.2.

Prior to their use, all dNTPs, rNTPs and NRTIs were subjected to treatment with pyrophosphatase (Roche) for 1 hour at 37ºC, in order to eliminate any trace of pyrophosphate (PPi) that could interfere with the assay. Then, pyrophosphatase was removed by centrifugation at 14000 rpm for 20 min at 4ºC using Amicon® Ultra-0.5 ml Ultracel® 10K centrifugal filters (Millipore), or by centrifugation at 7500g for 30 min at 4ºC using Amicon® Ultra Ultracel® 10K centrifugal filters (Millipore).

RT-catalyzed DNA/DNA rescue reactions were carried out in 55 mM Hepes pH 7.0 buffer, containing 15 mM NaCl, 15 mM magnesium acetate, 130 mM potassium acetate, 1 mM dithiothreitol and 5% (w/v) polyethyleneglycol 6000 (Fig 18). First, 25 µl of a mixture containing the phosphorylated T/Ps (75 nM) was preincubated with the RT (60 nM) for 10 minutes at 37°C. Then, 25 µl of the same preincubation buffer containing 50 µM AZTTP, d4TTP, ddATP, CBVTP or tenofovir-DP were added and incubated for another 10 min under the same conditions. Rescue reactions were triggered by adding 10 µl of a mixture of all dNTPs at final concentrations of 100 µM each and depending on the assay ATP, CTP, GTP or inosine triphosphate (ITP) at final concentrations ranging from 3.2 to 9.6 mM. The final concentration of the next complementary dNTP (dATP or dTTP under our assay conditions) was kept at 1 µM in order to minimize its inhibitory effect on the rescue reaction, due to the formation of a "dead-end" complexes (DEC).

Table 8. Nucleic acid substrates and NRTIs tested in rescue reactions with each RT

RT	DNA/DNA					RNA/DNA				
	AZT	d4T	ddA	CBV	Tenofovir	AZT	d4T	ddA	CBV	Tenofovir
WT	√	√	√	√	√	√	√	√	√	√
M41L/H208Y/L210W/T215Y	√	√	**x**	**x**	√	√	√	**x**	**x**	√
M41L/H208Y/T215Y	√	√	**x**	**x**	**x**	√	√	**x**	**x**	**x**
M41L/L210W/T215Y	√	√	**x**	**x**	√	√	√	**x**	**x**	√
M41L/L210W/T215Y/R284K	√	√	**x**	**x**	√	√	√	**x**	**x**	√
M41L/T215Y	√	√	√	√	**x**	√	√	√	√	**x**
M41L/T215Y/P272A/R277K/T286A	√	√	√	√	**x**	√	√	√	√	**x**
H208Y	√	√	**x**	**x**	√	√	√	**x**	**x**	√
P272A/R277K/T286A	√	√	√	√	**x**	√	√	√	√	**x**
R284K	√	√	**x**	**x**	√	√	√	**x**	**x**	√
MAK_SSSY	√	√	√	√	**x**	√	√	√	√	**x**

"√" is used to indicate that rescue assays under the specific conditions described have been carried out. If not, this is indicated with an "**x**".

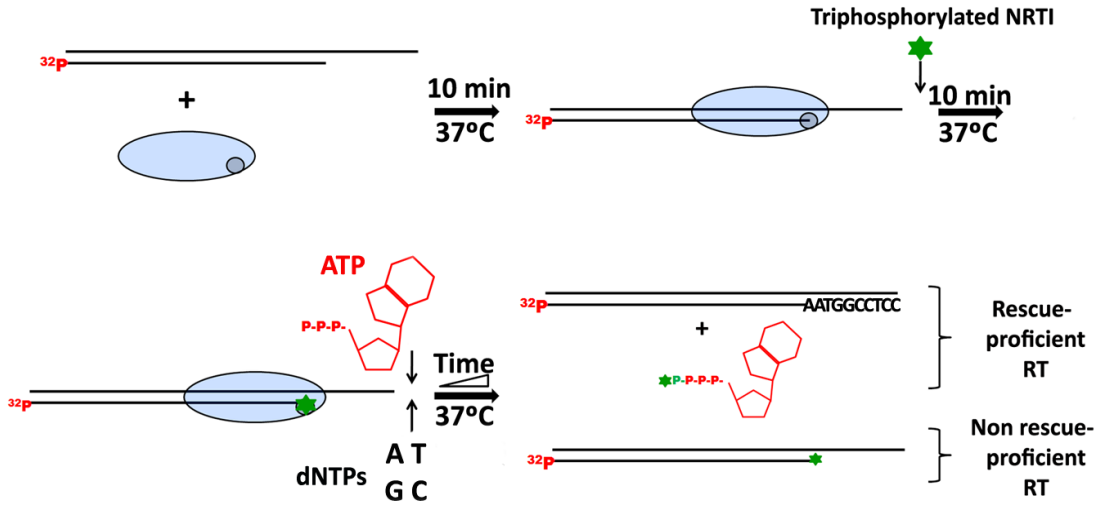

Fig 18. RT catalyzed rescue reactions. Schematic representation of the rescue reaction catalyzed by the RT. The template/primer is depicted in black lines, with a ^{32}P-labeled 5´-end, while the RT is represented by a blue oval with a grey circle inside, indicating the location of the DNA polymerase domain. RT and T/P preincubation at 37ºC allows the formation of the binary complex. Further addition of a triphosphorylated NRTI leads to the blockage of the nucleic acid. Incubation of the complex with ATP allows rescue-proficient enzymes to excise the inhibitor and resumes DNA elongation. On the contrary, enzymes lacking rescue activity are not able to remove the inhibitor and DNA synthesis remains blocked.

Assays with RNA/DNA complexes were carried out as above, but the primer was blocked with triphosphorylated nucleoside analogues at a 50 μM final concentration (2-fold more concentrated than in assays carried out with DNA/DNA complexes). The dNTP concentrations in the extension reactions were kept at 200 μM, except for the next complementary dNTP (dATP or dTTP under our assay conditions) that was supplied at 2 μM.

Rescue and extension reactions were incubated for 30 or 60 min (depending on the assay) at 37°C, with aliquots being removed at appropriate times. Reactions were stopped by adding an equal amount of stop solution. Products were analyzed by denaturing polyacrylamide gel electrophoresis and phosphoroimaging quantification as described in section 3.5.

This assay was modified in order to determine the inhibitory effect of the next corresponding nucleotide (dATP). For this purpose, dATP ranging from 0 to 200 μM was supplied to the rescue reaction and aliquots were removed at different times ranging from 15 to 40 min, depending on the RT used in the assay. In all cases, incubation times were within the linear range of the corresponding time course experiment. Reactions were stopped by adding an equal amount of stop solution. Products were resolved on 20% polyacrylamide/8 M urea gels, and data quantified as described above. The percentage of rescue reaction inhibition was plotted against the dATP concentration and the resulting slope was adjusted to a hyperbolic equation, to obtain the corresponding IC_{50} value.

The Michaelis-Menten constants for the PPi donors in rescue reactions were calculated by using a modified assay. For this purpose, rescue reactions were carried out in the presence of ATP, CTP,

GTP and ITP under steady-state conditions as described above. Rescue rates were determined with concentrations of NTP ranging from 0.4 to 12 mM and in the presence of 100 μM of each of four dNTPs (except dATP, the next complementary nucleotide, which was supplied at 1 μM). Reactions were stopped after 10 or 20 min, depending on the PPi-donor used, by adding an equal amount of stop solution. Products were resolved on 20% polyacrylamide/8 M urea gels, and data quantified as described above. The catalytic constants K_m and k_{cat} were obtained after fitting the rescue results to the Michaelis-Menten equation:

$$V_0 = V_{max} \frac{[NTP]}{K_m + [NTP]}$$

where V_{max} is the maximum NRTI-MP excision rate and K_m is the Michaelis-Menten constant for the PPi donor.

3.7 Chain terminator excision assays

Pre-steady-state kinetics of the ATP-dependent excision of AZTMP, d4TMP, CBVMP and tenofovir were determined using heteropolymeric T/Ps D38/25PGA^{d4TMP}, D38rna/25PGA^{d4TMP}, D38/25PGA^{AZTMP}, D38T/25PGA^{tenofovir} and D38Crna/25PGA^{CBVMP}. Complexes were prepared as described in sections 3.4.2 and 3.4.3. The wild-type and mutant RTs P272A/R277K/T286A, M41L/T215Y, M41L/T215Y/P272A/R277K/T286A, R284K, H208Y, M41L/L210W/T215Y, M41L/H208Y/L210W/T215Y, M41L/L210W/T215Y/R284K and MAK_SSSY, were tested in these assays.

Single-turnover conditions were used to study the excision of d4TMP, AZTMP, tenofovir and CBVMP. Solutions containing from 24 to 420 nM RT and 60 nM of the corresponding blocked-T/P in 110 mM Hepes pH 7.0 buffer, containing 30 mM NaCl, 30 mM magnesium acetate, 130 mM potassium acetate, 1 mM dithiothreitol, and 5% (w/v) polyethyleneglycol 6000 were preincubated at 37ºC for 10 min. Then, those samples were mixed with equal volumes of a solution containing 130 mM potassium acetate, 1 mM dithiothreitol, 5% (w/v) polyethyleneglycol 6000 and 6.4 mM ATP. Excision reactions were carried out for 0 to 60 min at 37°C. Aliquots were removed at different times, quenched with stop solution, heated at 90ºC for 10 min and then the products were analyzed by denaturing polyacrylamide gel electrophoresis and phosphoroimaging quantification as described in section 3.5

The formation of product (concentration of product [*P*]) over time was fitted to a single exponential decay equation:

$$[P] = A \times e^{-k_{obs} \times t}$$

where k_{obs} is the apparent kinetic constant of the excision reaction.

A linear regression was used to fit the data when the excision rates were low. In those cases, we assumed that the amount of active RT was identical to the T/P concentration in the assay, since these reactions were carried out with a large excess of RT relative to the RNA/DNA duplex.

A variation of this assay was used to determine the K_m and V_{max} values for M41L/L210W/T215Y and M41L/H208Y/L210W/T215Y RTs, for the excision reaction using the D38/25PGA^{AZTMP} T/P. For this purpose, assays were carried out as described above, maintaining a fixed RT concentration of 21 nM and using a T/P concentration ranging from 2.5 to 200 nM. Aliquots were removed at different times between 5 and 30 min and the reaction rates obtained at each T/P concentration were fitted to a Michaelis-Menten equation to obtain the K_m and V_{max} values.

3.8 Nucleotide incorporation assays

Two different types of kinetic constants can be calculated: the steady-state kinetic parameters K_m and k_{cat}, as well as the catalytic efficiency (k_{cat}/K_m), and the pre-steady-state kinetics constants k_{obs} and K_d. The difference between both types of determinations lies in that steady-state rates are dominated by the slowest step of the polymerization reaction (*i.e.*, dissociation of the RT-DNA complex), while pre-steady-state kinetics can monitor nucleotide incorporation directly.

3.8.1 Steady-state kinetics of nucleotide or nucleotide analogue incorporation

Nucleotide incorporation reactions under steady-state conditions were carried out for mutant RTs M41L/L210W/T215Y and M41L/L210W/T215Y/R284K as well as the wild-type enzyme. For this purpose D38/25PGA and D38T/25PGA heteropolymeric complexes were prepared as described in section 3.4.1.2. A mix of 10 µl containing the RT and the T/P in a preincubation solution of 110 mM Hepes pH 7.0 buffer, containing 30 mM NaCl, 30 mM magnesium acetate, 130 mM potassium acetate, 1 mM dithiothreitol, and 5% (w/v) polyethyleneglycol 6000 was preincubated at 37ºC for 10 min. Active RT and T/P were present at concentrations of 7‑20 nM and 60 nM, respectively. Then, an equal volume of a solution containing 130 mM potassium acetate, 1 mM dithiothreitol, 5% (w/v) polyethyleneglycol 6000 and dATP or dTTP at different concentrations was added. Aliquots of 4 µl were removed and the reaction was quenched after 20 s by adding the same amount of stop solution. Elongation rates were determined in the presence of dTTP concentrations ranging from 0.05 to 20 µM or with dATP concentrations ranging from 12 nM to 10 µM. Catalytic constants k_{cat} and K_m were determined after fitting the elongation data to the Michaelis‑Menten equation, as described in section 3.6.

A variation of this assay was used to determine the inhibition constants (K_i) for AZTTP and tenofovir-DP. Assays were carried out in the same conditions described above, but in the presence of 0, 2, 5 or 10 μM of the corresponding nucleotide analogue. To distinguish between the incorporation of the natural nucleotide or the nucleotide analogue, a concentration of 1 to 2 μM of the nucleotide corresponding to position +2 (dTTP or dATP under our assay conditions) was included in the reaction. Products were resolved on 20% polyacrylamide/8 M urea gels, and data quantified as described above. The percentage of +2 product formation was plotted against time for each NRTI concentration, fitting these data to a Michaelis-Menten equation, and the apparent K_m were then calculated. The K_m values obtained were fitted to the equation:

$$\textbf{Apparent } K_m = K_m \times \left(1 + \frac{[I]}{K_i}\right)$$

where apparent K_m is the K_m for the dNTP obtained in the presence of the analogue NRTI, K_m is the Michaelis-Menten constant obtained in the absence of the NRTI and K_i is the apparent inhibition constant.

3.8.2 Pre-steady-state kinetics of nucleotide incorporation

Pre-steady-state kinetics for dTTP incorporation were determined for M41L/L210W/T215Y and M41L/L210W/T215Y/R284K mutant enzymes using the heteropolymeric T/P D38/25PGA, prepared as described in section 3.4.1.2. Assays were carried out in a quench-flow instrument, model QFM-400 (Bio-Logic Science Instruments, France).

Reactions were carried out at high dTTP concentration (80 μM) with incubation times ranging from 25 to 6000 ms. Reactions were started by the addition of 12 μl of 160 μM dTTP diluted in a 50 mM Tris-HCl pH 8.0 buffer, containing 50 mM KCl and 25 mM $MgCl_2$ to 12 μl of a mix consisting in the same solution without $MgCl_2$, but containing 140 nM of active enzyme and 200 nM of D38/25PGA complex.

Reactions were stopped by the addition of 12 μl of 0.9 M EDTA. After mixing the product with the same volume of stop solution, samples were heated at 90ºC for 10 min and analyzed by denaturing polyacrylamide gel electrophoresis and phosphoroimaging as described in section 3.5

The appearance of product ([P]) over time (t) was adjusted to the following equation:

$$[P] = A \times \left(1 - e^{-k_{obs} \times t}\right) + k_{ss} \times t$$

where A is the amplitude, k_{obs} the apparent phosphodiester bond formation constant and k_{ss} is the enzyme turnover rate.

3.8.3 Determination of dissociation equilibrium constants (K_d) for DNA/DNA and RNA/DNA complexes

The determination of the affinity of wild-type and mutant enzymes for nucleic acid complexes was carried out using D38/25PGA DNA/DNA and D31rna/25PGA RNA/DNA complexes.

RTs were preincubated with increasing concentrations (2 to 60 nM) of the labeled D38/25PGA complex or D31rna/25PGA duplex (prepared as described in section 3.4.1.2) for 10 min at 37°C in 10 µl of 100 mM Hepes pH 7.0 buffer, containing 30 mM NaCl, 30 mM magnesium acetate, 130 mM potassium acetate, 1 mM dithiothreitol, and 5% (w/v) polyethyleneglycol 6000. Reactions were initiated by the addition of 10 µl of 1 mM dTTP to 10 µl of the solution indicated above, and incubated at 37°C. In these experiments, the active RT concentration was around 3 nM. Samples of 4 µl were then removed at 10, 20, 30, and 40 s and quenched with stop solution. Products were analyzed by denaturing polyacrylamide gel electrophoresis and phosphoroimaging quantification as described in section 3.5

The burst amplitudes (RT bound to T/P at time zero) were plotted as a function of the T/P concentration, and the data were fitted to the following quadratic equation:

$$[E \cdot T/P] = 0.5 \times [(K_d + E_T + T/P) - \sqrt{(K_d + E_T + T/P)^2 - (4 \times E_T \times T/P)}]$$

where E_T and T/P are the total active enzyme and T/P concentration, respectively, and K_d is the dissociation equilibrium constant for RT binding to T/P.

3.8.4 Determination of dissociation rate constants (k_{off})

Dissociation rate constants for T/Ps were determined using the D38/25PGA complex with M41L/L210W/T215Y and M41L/L210W/T215Y/R284K mutant RTs. Assays were carried out in Tris-HCl pH 8.0 buffer, containing 100 mM KCl, 2 mM dithiothreitol and 6 mM $MgCl_2$.

RTs (120 nM final concentration) were preincubated with the D38/25PGA substrate (at 8 nM final concentration) for 10 min at 37ºC. Then, 3 µl of sodium heparin (Serva 24590) trap (3 mg/ml final concentration) were added to 7 µl of the preincubated sample, and the incubation was continued for 0-60 s, before adding 10 µl of 200 µM dTTP. Elongation reactions were stopped after 7 s by addition of equal volume of stop solution. Products were resolved on a denaturing 20% polyacrylamide/8 M urea gel, and results were quantified by phosphorimaging with a BAS 1500 scanner (Fuji), using the software TINA version 2.09 (Raytest Isotopenmessgerate Gmbh, Staubenhardt, Germany).

The production of elongated primer ([P]) was fitted to the single exponential decay:

$$[P] = e^{(-k_{off} \times t)}$$

where k_{off} is the dissociation rate constant and t is the time of incubation with the trap (in seconds).

3.9 DNA polymerization assays

DNA polymerization assays were carried out to determine primer elongation efficiencies of wild-type and mutant enzymes using heteropolymeric T/Ps.

3.9.1 Primer extension assays

We determined the ability of M41L/T215Y and M41L/T215Y/P272A/R277K/T286A mutant RTs to extend the 25PGA primer in the D38rna/25PGA complex, as well as the efficiency of M41L/L210W/T215Y and M41L/L210W/T215Y/R284K RTs in extending the primer in D38/25PGA complexes. Labeled T/P was prepared as described in section 3.4.1.2.

First, 25 µl of a sample containing 3 or 20 nM of the appropriate T/P and 3 nM RT in 55 mM Hepes pH 7.0 buffer, containing 15 mM NaCl, 15 mM magnesium acetate, 130 mM potassium acetate, 1 mM dithiothreitol and 5% (w/v) polyethyleneglycol 6000 was incubated at 37ºC for 10 min. Then, 25 µl of a solution with the four dNTPs (200 µM each) diluted in the same buffer was added and aliquots of 4 µl were removed at different times (1 to 10 min). The reaction was then stopped by adding an equal volume of stop solution. Products were resolved on a denaturing 20% polyacrylamide/8 M urea gel, and the elongated primer quantified by phosphorimaging with a BAS 1500 scanner (Fuji), using the software TINA version 2.09 (Raytest Isotopenmessgerate Gmbh, Staubenhardt, Germany).

3.9.2 Processivity assays

The processivity of wild-type and M41L/L210W/T215Y, M41L/L210W/T215Y/R284K, and M41L/L210W/T215Y/R284K/M357T RTs was assessed with a complex made of M13mp2 single-stranded DNA as template and ProLac110 as primer, as well as with the 38/25-mer D38/25PGA.

RTs and T/P (both at 60 nM concentration) were preincubated at 37°C for 10 min in 12 µl of 50 mM Tris-HCl pH 8.0 buffer, containing 50 mM KCl. Reactions were initiated by adding 12 µl of preincubation buffer containing 12 mM $MgCl_2$ and a mixture of the four dNTPs (at 100 µM each) with or without 10 mg/ml sodium heparin. A control to confirm the validity of the trap was also introduced. In this control, the RT was preincubated with sodium heparin before the addition of the T/P and the dNTPs. Aliquots of 4 µl were removed after 5, 15, 30 and 45 min and quenched with an equal volume of sample loading buffer. Products were resolved on a denaturing 20%

polyacrylamide/8 M urea gel, and the elongated primer was quantified by phosphorimaging with a BAS 1500 scanner (Fuji), using the software TINA version 2.09 (Raytest Isotopenmessgerate Gmbh, Staubenhardt, Germany).

3.10 RNase H activity determination

The endonuclease activity of the RT (RNase H activity) was studied using different heteropolymeric RNA/DNA complexes with wild-type RT and mutant enzymes.

3.10.1 Cleavage of heteropolymeric T/Ps

The RNase H cleavage activity of the wild-type and mutant enzymes H208Y, R284K, N348I, T369I, T369V, T376S, N348I/T369I, M41L/T215Y/P272A/R277K/T286A, P272A/R277K/T286A, M41L/L210W/T215Y, M41L/T215Y, M41L/H208Y/L210W/T215Y and M41L/L210W/T215Y/R284K was determined with RNA/DNA complexes 31Trna/21P, D38rna/25PGA, D38Trna/25PGA, T35rna/PR26, T57d/PPT17r8d, PPT29RNA/PPT29DNA, PPT29RNA/PPT28DNA, PPT29RNA/PPT30DNA and PPT29DNA/PPT17r. In these assays, heteropolymeric complexes were prepared as described in section 3.4.1.2.

Assays were carried out in 50 mM Tris-HCl pH 8.0 buffer, containing 50 mM KCl (or 50 mM NaCl), 50 nM RT and 50 nM T/P (or 125 nM RT and 25 nM T/P in the case of the T57d/PPT17r8d complex). Reactions were initiated by adding $MgCl_2$ to a final concentration of 5 mM. Aliquots of 4 µl were removed at appropriate times (normally between 20 s and 5 min) and quenched with an equal volume of stop solution. Products were analyzed by denaturing polyacrylamide gel electrophoresis and quantified by phosphoroimaging as described in section 3.5. The amount of cleavage product generated over time was fitted to a single exponential decay as described in section 3.7 and the apparent kinetic constant of RNase H cleavage (k_{obs}) was determined.

3.10.2 Cleavage of AZTMP-blocked complexes

RNase H activity of wild-type RT and P272A/R277K/T286A, M41L/T215Y and M41L/T215Y/P272A/R277K/T286A mutant enzymes was measured using the T35rna/PR26 complex. After obtaining the labeled RNA/DNA duplex as described in section 3.4.1.2, a mutant HIV-1 group O RT containing the V75I/E478Q mutations (O_V75I/E478Q) was used to block the complex with AZTMP. Mutation E478Q completely inactivates the RNase H activity of the enzyme (Álvarez *et al.*, 2009), thus avoiding undesired cleavage events that would occur during the AZTTP incorporation step. The reaction was carried out for 1 hour at 37 ºC in Tris-HCl pH 8.0 buffer, containing 50 mM KCl, 10 mM $MgCl_2$, 80 nM of labeled T35rna/PR26 complex, 30 nM O_V75I/E478Q mutant enzyme and 60 µM AZTTP. The RT was inactivated by heating the sample

for 10 min at 90ºC, and the T35rna/PR26^{AZTMP} complex was then purified with mini Quick spin columns (Roche).

T35rna/PR26^{AZTMP} RNase H cleavage reactions were carried out at 37°C in 50 mM Tris-HCl pH 8.0 buffer, containing 50 mM KCl, 10 mM $MgCl_2$, 0.3 mM ATP, 20 nM labeled RNA/DNA complex and the corresponding RT at 200 nM active site concentration. Aliquots of 4 µl were removed at different times between 10 and 180 min and then quenched by using an equal volume of stop solution. Finally, samples were analyzed by denaturing polyacrylamide gel electrophoresis and quantified by phosphoroimaging as described in section 3.5.

3.11 RT inhibition by NNRTIs

The half maximal inhibitory concentration (IC_{50}) for NEV, EFV, ETR and RPV was determined using the D38/25PGA complex, prepared as described in section 3.4.1.2, with wild-type, and mutant RTs bearing amino acids substitutions N348I, T369I, T369V, T376S and N348I/T369I.

A preincubation mix (5 µl) of RT (from 14.4 to 36 nM) and T/P (72 nM) was maintained at 37ºC for 10 min in 120 mM Hepes pH 7.0 buffer, containing 24 mM NaCl, 24 nM $MgCl_2$ 208 mM potassium acetate, 1.6 mM dithiothreitol, and 8% (w/v) polyethyleneglycol 6000, and then mixed with 3 µl of the corresponding NNRTI at an appropriate concentration and diluted in 4% (w/v) dimethyl sulfoxide. Then the sample was incubated for 10 min at 37ºC. Four µl of a solution containing 100 µM dTTP, diluted in 130 mM potassium acetate, 1 mM dithiothreitol, and 5% (w/v) polyethyleneglycol 6000 was added and the reaction was then stopped after 20 s by mixing and aliquot of 4 µl with equal volume of stop solution and heating at 90ºC for 10 min. Samples were analyzed by denaturing polyacrylamide gel electrophoresis and quantified by phosphoroimaging as described in section 3.5.

NNRTI inhibition was determined as the percentage of dTTP-incorporation inhibited in the presence of a specific NNRTI concentration, when compared with dTTP incorporation in the absence of the drug. Data were fitted to a dose-response slope and the IC_{50} value determined.

3.12 Purification of HIV-1 integrase

A recombinant IN corresponding to the group M subtype B NL4-3 strain was purified. This recombinant enzyme had a polyhistidine tag at its N-terminus.

3.12.1 IN expression

One-hundred ml of LB medium containing ampicillim (80 μg/ml) and kanamicin (34 μg/ml) were inoculated with 5-10 μl of a glycerol stock of *E. coli* BL21 strain cells containing the pT7-7IN plasmid (which contains the sequence encoding for the full-length HIV-1 IN protein) (gift of Dr S.A. Chow, University of California, Los Angeles, USA). This culture was grown overnight at 37ºC under constant stirring. Next, 40 ml of this preculture were added to 1 liter of the same medium and grown at 32ºC until the optical density at 600 nm was around 0.8. Then, IPTG was added to a final concentration of 0.4 mM to trigger the expression of the sequence encoding the IN. After 3 hours at 32ºC, cells were harvested by centrifugation at 5100 rpm for 25 min at 4ºC using a centrifuge TJ-25 (Beckman-Coulter) and a swinging bucket rotor TS-5-1-500.

3.12.2 Lysis of bacteria

The bacterial pellet obtained was resuspended in 40 ml of 20 mM Hepes pH 7.5 buffer, containing 5 mM β-mercaptoethanol, 1 M NaCl, 10% (w/v) glycerol, 10 mM imidazole, 50 μM EDTA and 0.5% (w/v) NP-40. Just before using this lysis buffer, four pills of protease inhibitors (Completa®, Roche) were added, and once the pills had been diluted, we added lysozyme at a final concentration of 0.3 mg/ml. The bacterial solution was kept at 4ºC for one hour without agitation.

Cells were then sonicated using a Branson 450 sonifier at power level 5 and 45% duty cycle for one min, seven times each cycle. Then, the sample was centrifuged at 12000 rpm for one hour at 4ºC, using a rotor JA 25.50 and an Avanti J-26 XP centrifuge (Beckman Coulter). The supernatant obtained was stored at 4ºC.

3.12.3 Affinity chromatography

The supernatant collected in the bacterial lysis step was applied to a 5-ml Ni^{2+}-Sepharose-agarose medium column (His-trap HP columns, GE Healthcare) adapted to a BioRad BioLogic station (BioRad).

The IN bound to the Ni^{2+}-agarose column was eluted using 200 ml of 20 mM Hepes pH 7.5 buffer, containing 5 mM β-mercaptoethanol, 1 M NaCl and 0.1% (w/v) NP-40 and 50 ml of 20 mM Hepes pH 7.5 buffer, containing 5 mM β-mercaptoethanol 1 M NaCl, 0.1% (w/v) NP-40 and 500 mM imidazole, following the process described in Table 9. Fractions of 1 ml were collected and the presence of enzyme was monitored by measuring the absorbance at 280 nm. The purity of the samples was determined by SDS-polyacrylamide gel electrophoresis. The enzyme-enriched fractions were pooled in 1-ml fractions and subjected to overnight dialysis using SnakeSkin tubing (Thermo Scientific) dialysis bags, against 900 ml of 20 mM Hepes pH 7.5 buffer, containing 5 mM

β-mercaptoethanol, 0.5 M NaCl, 10 mM CHAPS and 20% (w/v) glycerol. Finally, the sample concentration was determined using a Bradford assay and BSA of known concentration as reference. The IN aliquots obtained were stored at -20ºC.

Table 9. HPLC program to purify HIV-1 IN

Step	Vol (ml)	Description	Parameters		
1	3	Isocratic Flow	Buffer A Buffer B	98% 2%	Volume: 3 ml Flow: 1 ml/min
2	10	Isocratic Flow	Buffer A Buffer B	90% 10%	Volume: 10 ml Flow: 1 ml/min
3	25	Linear Gradient	Buffer A Buffer B	90% - 0% 10% - 100%	Volume: 25 ml Flow: 1 ml/min
4	3	Isocratic Flow	Buffer A Buffer B	0% 100%	Volume: 3 ml Flow: 1 ml/min

Buffer A is composed of 20 mM Hepes pH 7.5, containing 5 mM β-mercaptoethanol, 1 M NaCl and 0.1% (w/v) NP-40 and buffer B of 20 mM Hepes pH 7.5, containing 5 mM β-mercaptoethanol, 1 M NaCl, 0.1% (w/v) NP-40 and 500 mM imidazole.

3.13 IN activity determination

The three different main activities that HIV-1 IN has (3´-end processing, strand transfer and disintegration) were measured biochemically using ^{32}P-labeled DNA complexes and recombinant HIV-1 IN proteins purified as described above (Chow, 1997).

3.13.1 Preparation of nucleic acid complexes

Three different DNA complexes were used in the characterization of IN activities: C220/C120, C120/B2-1 and the dumbbell single stranded DNA (Table 7, Fig 19). C220, B2-1 and dumbbell were labeled following a method similar to those described in section 3.4.1.1, but before annealing the ^{32}P-labeled DNA obtained (20 µl at 2.5 µM) was diluted in final volume of 97.5 µl of 10 mM Tris-HCl pH 7.5 buffer, containing 1 mM EDTA and 100 mM NaCl. The DNA/DNA duplexes C220/C120 and C120/B2-1 were prepared by the addition of a 3-fold excess (2.5 µl at 75 µM) of unlabeled template strand (C120 in both cases) followed by heating at 100ºC for 4 min and finally by slowly cooling at room temperature.

3.13.2 3´-end processing activity

Determination of the 3´-end processing activity of IN (Fig 19) was performed using the C220/C120 complex, prepared as described above.

The reaction was carried out in a final volume of 20 µl, and under two different conditions:

1) 5 nM C220/C120 and 200 nM IN in a 22 mM Hepes pH 7.5 buffer, containing 10 mM $MnCl_2$, 43.3 mM NaCl, 10.1 mM dithiothreitol, 1 mM Tris-HCl pH 7.5 and 0.11 mM EDTA.
2) 5 nM C220/C120 and 200 nM IN in a 50 mM Tris-HCl pH 8.0 buffer, containing 22 mM Hepes pH 7.5, 50 mM NaCl, 10 mM $MgCl_2$ and 1.8 mM dithiothreitol.

The 3´-end processing reactions were incubated for 1 hour at 37ºC. Aliquots of 4 µl were removed at appropriate times and reactions were stopped by adding 4 µl of stop solution and incubating the sample at 90ºC for 4 min. Products were resolved on denaturing 15% polyacrylamide/8 M urea gels, and DNA processing was quantified by phosphorimaging using a Typhoon scanner (Amershan Bioscience) and the software ImageQuant® version 5.0 (Molecular Dynamics).

3.13.3 Strand transfer activity

The determination of the strand transfer activity of IN (Fig 19) was carried out with the C120/B2-1 complex, prepared as described in section 3.13.1. Strand transfer reactions were carried out by incubating 5 nM C120/B2-1 with 200 nM IN, in 22 mM Hepes pH 7.5 buffer, containing 10 mM $MnCl_2$, 43.3 mM NaCl, 10.1 mM dithiothreitol, 1 mM Tris-HCl pH 7.5 and 0.11 mM EDTA at 37ºC. Aliquots of 4 µl were removed at 20, 40 and 60 min and quenched by mixing with equal volume of stop solution. Strand transfer events were analyzed by denaturing polyacrylamide gel electrophoresis and phosphoroimaging quantification as described in section 3.13.2.

3.13.4 Disintegration activity

The determination of the disintegration activity of IN (Fig 19) was performed using the dumbbell single stranded DNA, prepared as described in section 3.13.1. The dumbbell strand is able to associate with itself producing a double-stranded DNA region that is substrate for the disintegration activity of IN. Disintegration reaction was carried out at 37ºC in the presence of 5 nM dumbbell substrate and 200 IN, in 22 mM Hepes pH 7.5 buffer, containing 10 mM $MnCl_2$, 43.3 mM NaCl, 10.1 mM dithiothreitol, 1 mM Tris-HCl pH 7.5 and 0.11 mM EDTA at 37ºC. Aliquots of 4 µl were removed at 10, 20, 40 and 60 min and quenched by mixing with an equal volume of stop solution. Resulting products were analyzed by denaturing polyacrylamide gel electrophoresis and phosphoroimaging quantification as described in section 3.13.2.

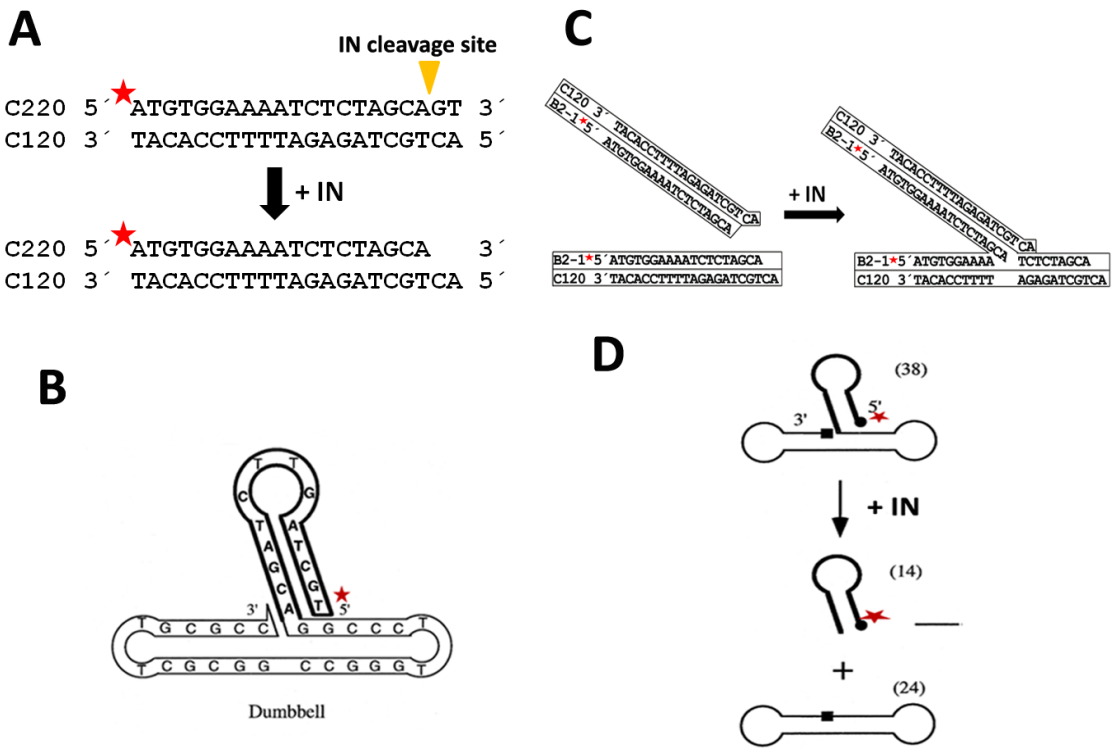

Fig 19. Integrase *in vitro* reactions. Schematic representation showing the substrates and reaction schemes of the 3´-end processing (A), strand transfer (B) and disintegration (C and D) activities carried out by HIV-1 integrase. The ^{32}P-labeled 5´-end is indicated by a red star. Figure adapted from Chow *et al* (1997). Sequence of the C120/B2-1 complex is given in Table 7.

3.14 RT RNase H activity in the presence of IN

The RNase H activity of the wild-type RT was determined in the presence of HIV-1 IN protein, obtained as described in section 3.12 and using the 31Trna/21P heteropolymeric complex and PPT29RNA/PPT29DNA and T57d/PPT17r8d heteroduplexes.

RT (50 nM) and IN (at different concentrations ranging from 50 nM to 1 µM), together with 31Trna/21P, PPT29RNA/PPT29DNA or T57d/PPT17r8d complex (50 nM) were preincubated in 50 mM Tris-HCl pH 8.0 buffer, containing 50 mM NaCl for 10 min at 37ºC. Cleavage activity was triggered by the addition of 5 mM $MgCl_2$. Aliquots of 4 µl were removed at 20 s, 40 s and 1, 2 and 4 min. Products were resolved on denaturing 15% polyacrylamide/8 M urea gels, and DNA processing was quantified by phosphorimaging with a Typhoon scanner (Amershan Bioscience), using the software ImageQuant® version 5.0 (Molecular Dynamics). The apparent kinetic constant of RNase H cleavage (k_{obs}) was determined as described in section 3.10.1.

4.Results

4.Results

4.1 Amino acid substitutions in the HIV-1 RT thumb subdomain associated with TAM-1 mutations and their role in resistance to NRTIs

4.1.1 Molecular mechanisms favoring the selection of RT thumb subdomain polymorphisms A272P/K277R/A286T associated with nucleoside analogue therapy failure

Extended use of RT inhibitors as well as the increased complexity of antiretroviral treatments facilitates the accumulation of resistance mutations. Classical HIV-1 genotypic assays do not provide RT sequence information beyond residues 250-300. Therefore, while mutations located in the palm-fingers subdomains are routinely detected, mutations outside these regions remain unidentified in most cases. However, recent reports have implicated thumb and connection subdomains, as well as the RNase H domain in drug resistance.

In an effort to identify mutations associated with antiretroviral therapy failure found outside the classical DNA polymerase region (residues 40-240), an epidemiological study was carried out previously, where thumb subdomain mutations were identified in patients failing antiretroviral therapy (Garriga *et al.*, 2009). In this study, thumb subdomain polymorphisms Pro-272, Arg-277 and Thr-286 were found to be selected under therapy with several combinations of two NRTIs: d4T/abacavir, d4T/ddI, ddI/abacavir, d4T/3TC and d4T/tenofovir. The largest levels of statistical significance were obtained for the d4T/abacavir and d4T/ddI combinations. Of note, correlated pairs of substitutions at positions 272 and 277 and at positions 272 and 286 were also reported in HIV-1 *pol* sequences from patients failing therapy with d4T and ddI. Interestingly, in most cases, polymorphisms were associated with TAMs, especially with the TAM-1 cluster, consisting of mutations M41L, L210W and T215Y. In order to determine the molecular mechanisms involved in the selection of these polymorphisms, we carried out a biochemical characterization of recombinant RTs bearing TAM-1 mutations M41L/T215Y with or without RT thumb subdomain polymorphisms.

4.1.1.1 Rescue of DNA/DNA complexes containing primers blocked with AZTMP, d4TMP, CBVMP and ddAMP

An association between TAM-1 pathway mutations and the presence of Pro-272, Arg-277 and Thr-286 was found in viruses from patients failing therapy (Garriga *et al.*, 2009). Therefore, we reasoned that thumb subdomain substitutions could be implicated in NRTI resistance through the excision mechanism, since TAMs have a major role in drug resistance acting as NRTI-excision enhancer mutations. To test this possibility, rescue assays using heteropolymeric template/primers

(T/P) blocked with AZT monophosphate (AZTMP), d4T monophosphate (d4TMP), ddA monophosphate (ddAMP) and carbovir monophosphate (CBVMP) were carried out.

A schematic representation of the standard rescue assay employed is shown in Fig 20. Rescue assays involve two different phases. After blocking the DNA primer with the corresponding NRTI, a PPi donor is supplied together with a mixture of dNTPs. If the RT has excision activity, the inhibitor can be removed from the 3´-end of the primer and the resulting DNA extended to obtain a full-length product.

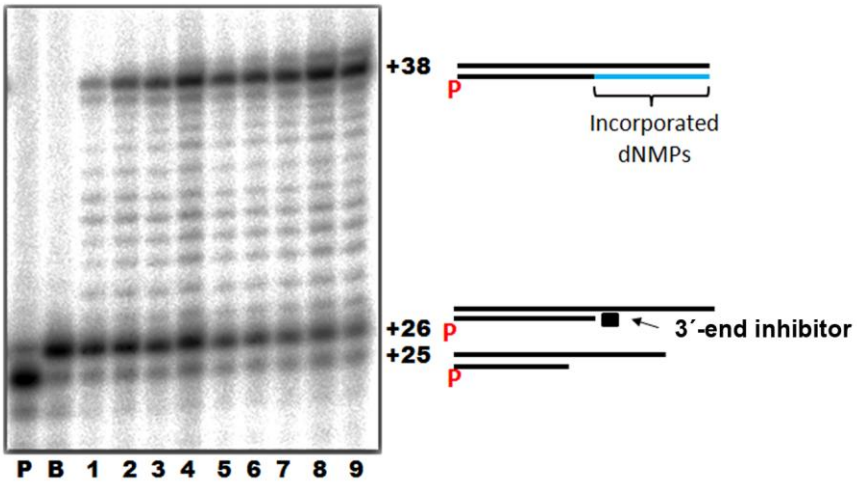

Fig 20. Schematic representation of the rescue reaction. A representative gel obtained in rescue assays together with a scheme of the T/P complexes formed during the assay are shown. The [^{32}P]-labeled-primer end is indicated by the presence of a red "p". First, the inhibitor was incorporated at position +1 (black box) of the 25-nucleotide primer (lane P) to generate a 26-nucleotide product (lane B). Excision of the inhibitor and further extension of the primer in the presence of a PPi donor and a mixture of dNTPs led to the formation of a fully extended 38-nucleotide product. A representative time course experiment of a primer rescue reaction is shown in lanes 1 to 9, which correspond to aliquots removed 2, 4, 6, 8, 10, 12, 15, 20, and 30 min after the addition of the PPi donor.

In our study the HIV-1 group M subtype B BH10 strain was used as wild-type (WT) reference. This strain has proline, arginine and threonine at positions 272, 277 and 286, respectively. Thumb subdomain polymorphisms P272A, R277K and T286A were introduced in the sequence context of the WT BH10 RT. The WT and P272A/R277K/T286A RTs were used, in addition to RTs with mutations M41L/T215Y/P272A/R277K/T286A and M41L/T215Y. As a control, a multidrug-resistant RT bearing M41L/A62V/T69SSS/K70R/T215Y mutations (MAK_SSSY) was used. This enzyme was used as positive control due to its high rescue activity (Matamoros *et al.*, 2004).

T/P complexes D38/25PGA^{AZTMP}, D38/25PGA^{d4TMP}, D38C/25PGA^{CBVMP} and D38T/25PGA^{ddAMP} were used (sequences shown in Fig 21). In the presence of 3.2 mM ATP, MAK_SSSY showed efficient rescue activity on primers blocked with AZTMP, d4TMP, CBVMP and in a lesser extend with primers terminated with ddAMP (Fig 21). In contrast, rescue activity of WT and P272A/R277K/T286A enzymes was almost negligible, independently of the inhibitor used in the assays. Mutant RTs M41L/T215Y and M41L/T215Y/P272A/R277K/T286A showed detectable

rescue activity on primers terminated with thymidine analogues or CBVMP, but were unable to excise ddAMP. Thumb subdomain mutations P272A, R277K and T286A had no effect when introduced in a WT sequence or in the presence of TAM-1 mutations. When 200 µM PPi was used, all RTs showed very high rescue efficiency with all tested NRTIs (Fig 22). It is important to note that unlike the ATP-dependent excision reaction, pyrophosphorolysis (PPi-mediated) is the polymerization reaction run in reverse. Therefore, it was not surprising to find out that the WT enzyme was very efficient in excising NRTIs in the presence of PPi.

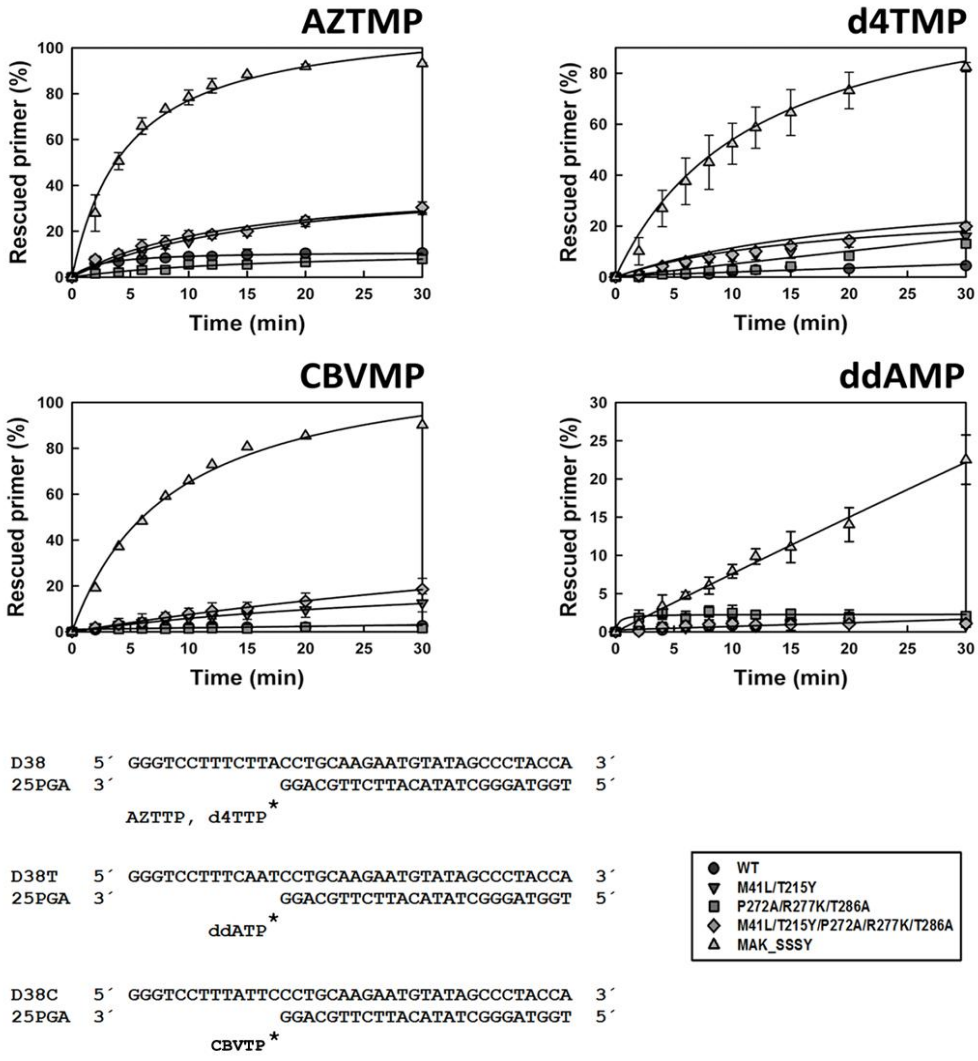

Fig 21. Rescue DNA polymerization initiated from AZTMP-, d4TMP-, ddAMP- and CBVMP-terminated primers annealed to a DNA template. Reactions were carried out with D38/25PGA, D38C/25PGA or D38T/25PGA complexes (sequences given below). First the inhibitor was incorporated at the 3´-end of the primer. Then, excision of the inhibitor, followed by extension of the primer was achieved after adding a mixture containing 3.2 mM ATP and the four dNTPs. Time course experiments of primer rescue reactions initiated from inhibitor-terminated primers are shown. All dNTPs in the assays were supplied at 100 µM, except for dATP or dTTP (depending on the reaction) whose concentration was 1 µM. T/P and active RT concentrations in these assays were 30 and 24 nM, respectively. The values (mean ± standard deviations [error bars]) were obtained from three independent experiments.

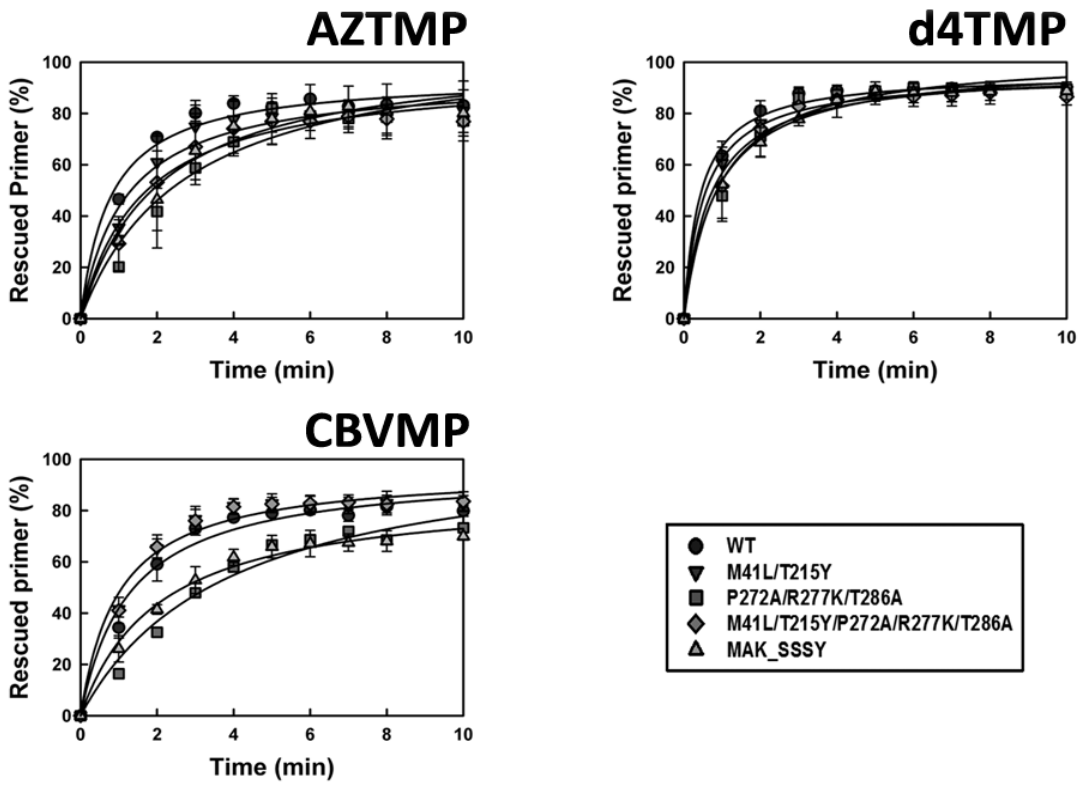

Fig 22. Rescue DNA polymerization in the presence of 200 μM PPi. AZTMP and d4TMP rescue assays were carried out by using the D38/25PGA heteroduplex, while the D38C/25PGA complex was used in CBVMP rescue assays. Reaction conditions were the same described for ATP-dependent rescue assays, but were carried out in the presence of 200 μM PPi. Time points were taken at 1, 2, 3, 4, 5, 6, 7, 8 and 10 min. The values (mean ± standard deviations [error bars]) were obtained from three independent experiments.

4.1.1.2 Rescue of RNA/DNA complexes blocked with AZTMP, d4TMP, CBVMP and ddAMP

As described for DNA/DNA complexes, rescue activity of MAK_SSSY was much higher than for the other RTs when assayed on T/Ps D38rna/25PGA^{AZTMP}, D38rna/25PGA^{d4TMP} and D38Crna/25PGA^{CBVMP} (Fig 23). In addition, AZTMP and d4TMP were more efficiently rescued than CBVMP. Interestingly, mutant RTs M41L/T215Y and M41L/T215Y/P272A/R277K/T286A showed higher rescue activity on RNA/DNA complexes than on DNA/DNA duplexes. While this behavior was also observed with the WT enzyme, mutant P272A/R277K/T286A showed negligible rescue activity on RNA/DNA complexes (Fig 23). Interestingly, the M41L/T215Y RT showed higher rescue activity on primers terminated with AZTMP than the M41L/T215Y/P272A/R277K/T286A RT (Fig 23). In addition, none of the enzymes were able to rescue T/P complexes blocked with ddAMP (data not shown). Also, as in the case of DNA/DNA complexes, PPi-dependent rescue activity on d4TMP-blocked complexes was similar for all tested RTs (data not shown).

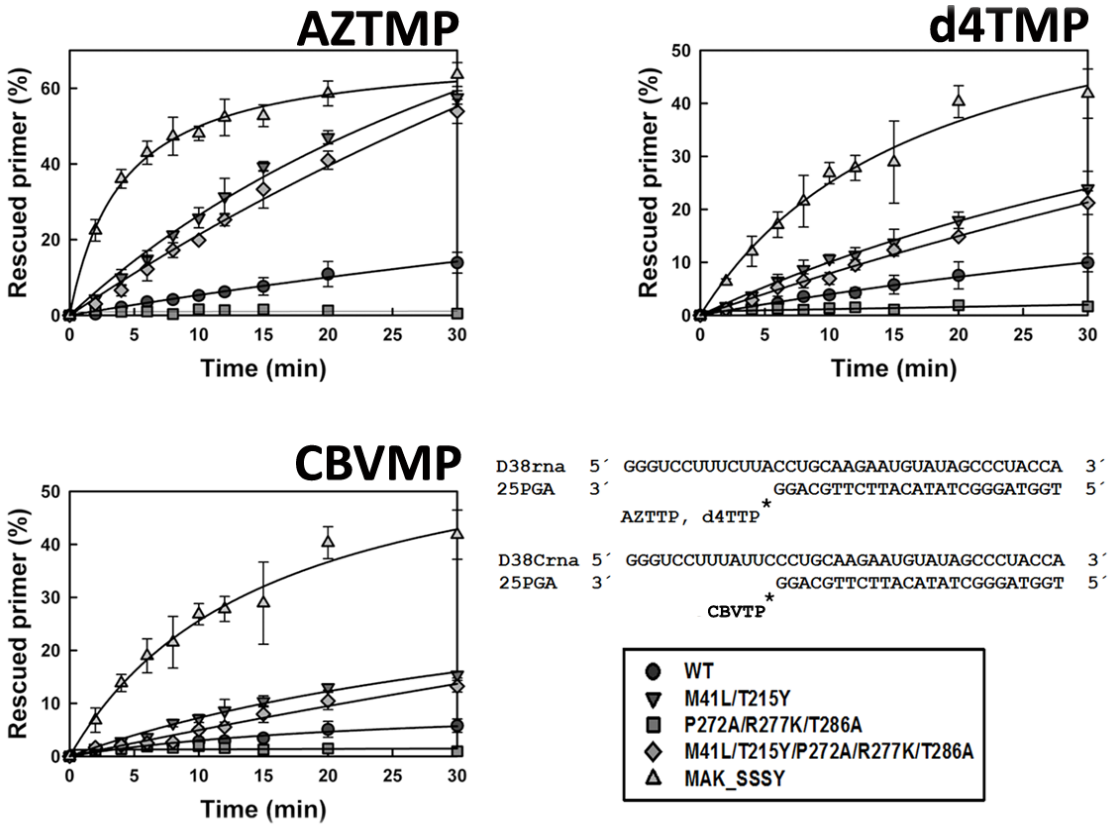

Fig 23. Rescue DNA polymerization initiated from AZTMP-, d4TMP-, and CBVMP-terminated primers annealed to an RNA template. Time course experiments of rescue reactions were carried out in the presence of 3.2 mM ATP. The nucleotide sequences of T/Ps used are given on the right lower panel. All dNTPs in the assays were supplied at 200 μM, except for dATP whose concentration was 2 μM. T/P and active RT concentrations in these assays were 10 and 30 nM, respectively. Represented values (mean ± standard deviation [error bars]) were obtained from three independent experiments.

4.1.1.3 RNase H activity of WT and mutant RTs

The RNase H activity of the RT produces the degradation of the RNA strand of RNA/DNA duplexes. Two different types of substrates were used in RNase H activity measurements.

RNase H activity and primary cleavage

D38rna/25PGA and 31Trna/21P complexes were used to determine the RNase H activity of WT and mutant RTs (Fig 24). Cleavage rates were similar for WT and mutant RTs when using 31Trna/21P as substrate. Primary cleavage products correspond to a fragment of 26 nucleotides (Fig 24). This cleavage occurred after RT polymerase active site bound the 3´-end of the 21P primer, with the RNase H active site located 16 nucleotides upstream of the dNTP binding site. No secondary cleavages were observed with this T/P under our assay conditions. As a control, an RNase H-deficient mutant (RNase H(-) RT) was used. This enzyme is an HIV-1 group O RT with mutations V75I/E478Q (Álvarez *et al.*, 2009).

The T/P complex D38rna/25PGA was used to assay the RNase H activity of the RTs in the same sequence context used in rescue assays. As in the case of 31Trna/21P, the kinetics of the reactions were essentially the same for all tested enzymes (Fig 24). A single processed product of 31 nucleotides was detected. This product corresponds to a 3´-end DNA-directed cleavage of the template strand at position -18. However, catalytic rate constants were higher for D38rna cleavage than for 31Trna cleavage (Fig 24). Student´s *t* tests carried out using the obtained k_{obs} values showed that differences between WT and P272A/R277K/T286A RTs and between M41L/T215Y/P272A/R277K/T286A and M41L/T215Y RTs were not significant ($p > 0.05$)

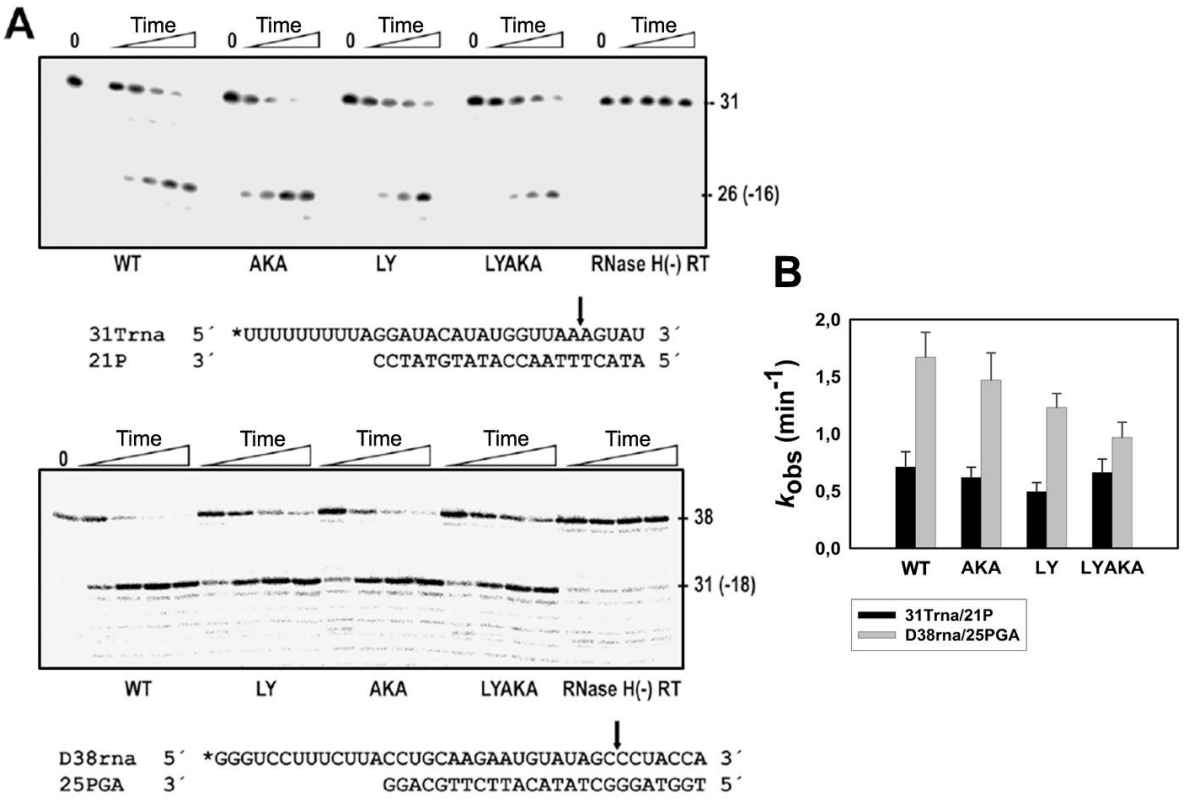

Fig 24. RNase H activity of WT and mutants RTs M41L/L210W/T215Y and M41L/L210W/T215Y/R284K. (A) [^{32}P]RNA/DNA substrates (50 nM) were cleaved at 37°C in the presence of the corresponding RT at 100 nM concentration. T/P sequences are shown below the corresponding gels. Arrows in the template sequences indicate the cleavage sites. For D38rna/25PGA, the time points were taken after incubating the samples for 10, 20, 30 and 40 s, while for 31Trna/21P time points correspond to 1-, 2-, 4- and 8-min incubations. (B) Apparent rate constants for the cleavage of D38rna and 31Trna were obtained from 3 or 4 independent experiments. RTs LY, AKA, LYAKA and RNase H(-) RT correspond to mutant enzymes M41L/T215Y, P272A/R277K/T286A, M41L/T215Y/P272A/R277K/T286A and HIV-1 group O RT with mutations V75I/E478Q, respectively.

RNase H secondary cleavages

RNase H secondary cleavages generated by WT and mutant RTs in excision-competent complexes were determined by using the T35rna/PR26^{AZTMP} complex in the presence of 0.3 mM ATP (Fig 25). As shown in Fig 25, all tested enzymes were able to degrade the RNA to produce RNA fragments resulting from cleavages at positions -15, -12 and -10. However, while

M41L/T215Y/P272A/R277K/T286A, P272A/R277K/T286A and M41L/T215Y RTs had similar kinetics of formation of the -10 cleavage product (Fig 25), the WT RT was 1.6-fold faster than the others. Interestingly, a slightly higher amount of -10 cleavage product was obtained for all RTs in the absence of ATP in comparison with reactions carried out in the presence of 0.3 mM ATP (Fig 25).

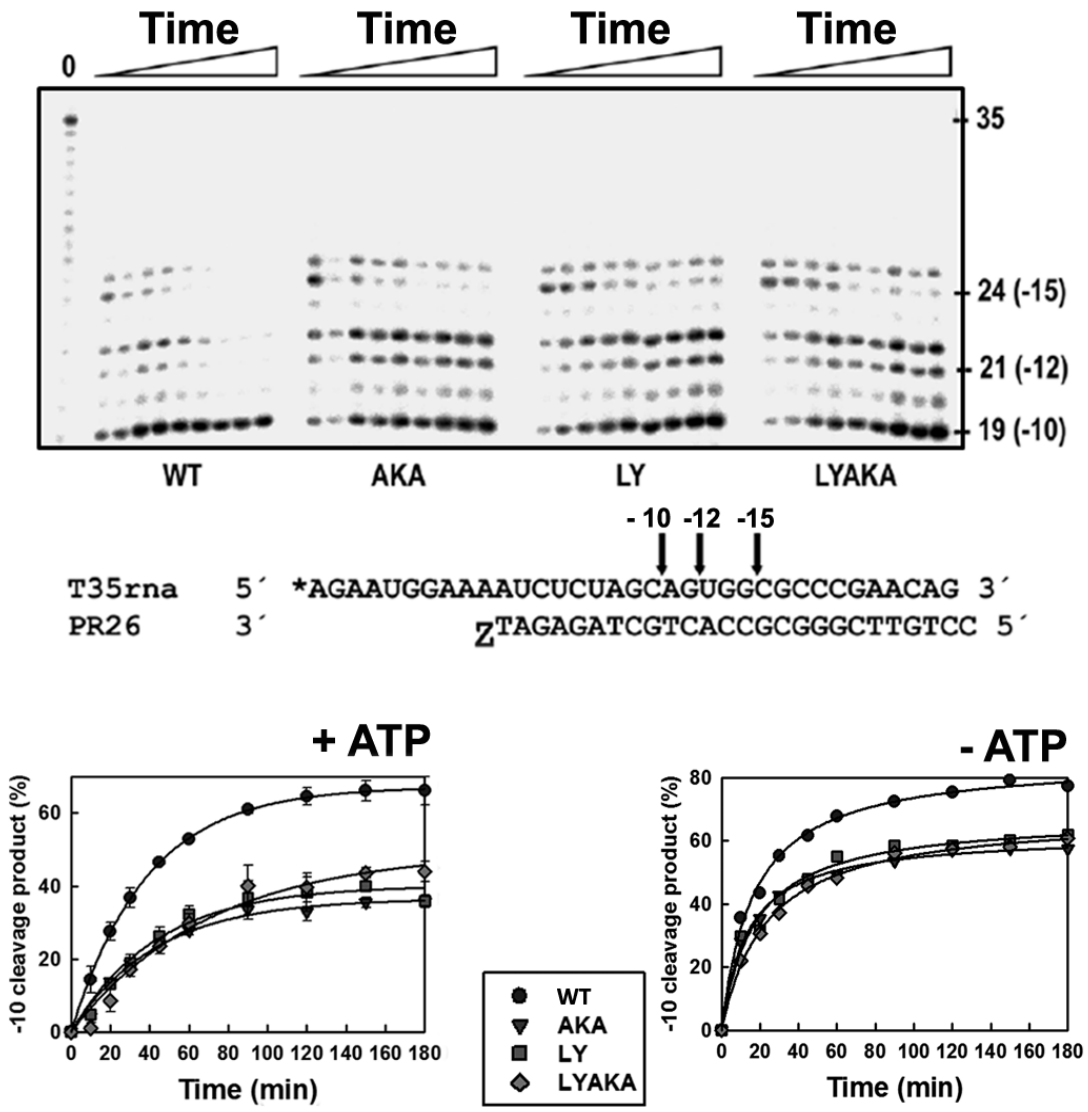

Fig 25. RNase H cleavage activity of WT and mutant RTs during ATP-mediated AZTMP excision. Assays were performed with the T/P shown below the gel (at 20 nM) in the presence of 200 nM RT. Aliquots were removed at 10, 20, 30, 45, 60, 90, 120, 150, and 180 min. Cleavage sites are indicated above the template sequence. The labeled 5´-ends of the templates are marked with asterisks. Time courses of RNase H cleavage reactions carried out in the presence (left) or absence (right) of 0.3 mM ATP are shown below. RTs LY, AKA and LYAKA, correspond to mutants M41L/T215Y, P272A/R277K/T286A and M41L/T215Y/P272A/R277K/T286A, respectively. The gel shown is a representative example of kinetics carried out in the presence of 0.3 mM ATP.

4.1.1.4 Pre-steady-state kinetics of the ATP-dependent excision reaction

As described above, rescue assays involve different steps. One of them is the excision of the inhibitor from the blocked DNA primer. Direct measurements of this reaction can be obtained by using pre-blocked T/P complexes and incubating them in the presence of a PPi donor and RT. For this purpose, 25PGA primers were blocked with d4TMP or CBVMP by using the recombinant terminal transferase enzyme as described in Material and Methods, and annealed to D38rna or D38Crna templates, respectively. Assays performed in the presence of 3.2 mM ATP showed that d4TMP was removed most efficiently by MAK_SSSY, but also by the other RTs containing TAM-1 mutations (Fig 26). Interestingly, while the excision rates were similar for both M41L/T215Y and M41L/T215Y/P272A/R277K/T286A RTs (k_{obs} around 0.08 min^{-1}), the presence of P272A/R277K/T286A in a WT sequence background reduced d4TMP excision by 2.3-fold (k_{obs} of 0.0032 min^{-1} and 0.0014 min^{-1}, respectively). These results were consistent with those obtained in RNA/DNA dependent rescue assays that revealed differences in rescue efficiencies between the WT RT and the mutant P272A/R277K/T286A RT (Fig 23). As observed in rescue assays, CBVMP was a poor substrate of the excision reaction, and only the excision-proficient MAK_SSSY RT was able to remove it efficiently (Fig 26). The excision activities of M41L/T215Y/P272A/R277K/T286A and M41L/T215Y RTs were relatively low (k_{obs} around 0.0036 min^{-1}). On the other hand, WT and P272A/R277K/T286A enzymes were devoid of excision on CBVMP-terminated primers.

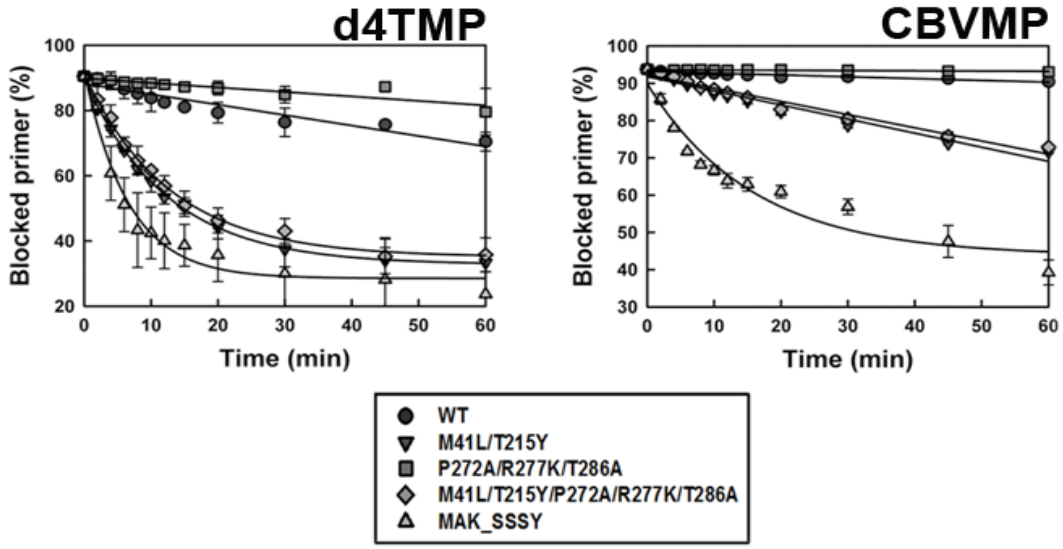

Fig 26. Kinetics of the ATP-dependent excision of d4TMP and CBVMP from RNA/DNA T/Ps. Time course experiments for the excision reaction of d4TMP- or CBVMP-terminated primers (26-mers) annealed to their corresponding 38-nucleotide RNA templates (30 nM) were determined in the presence of 3.2 mM ATP. The excision reaction was catalyzed by WT and mutant RTs (250 nM). The calculated k_{obs} values for the d4TMP excision reaction were 0.0032 ± 0.0003 min^{-1} for WT RT, 0.0014 ± 0.0002 min^{-1} for mutant P272A/R277K/T286A RT, 0.0810 ± 0.0025 min^{-1} for mutant M41L/T215Y RT, 0.0782 ± 0.0044 min^{-1} for mutant M41L/T215Y/P272A/R277K/T286A RT, and 0.153 ± 0.018 min^{-1} for the MAK_SSSY RT. For the excision of CBVMP, the k_{obs} values for mutants M41L/T215Y, M41L/T215Y/P272A/R277K/T286A, and MAK_SSSY RTs were 0.0038 ± 0.0003 min^{-1}, 0.0035 ± 0.0002 min^{-1}, and 0.0629 ± 0.0138 min^{-1}, respectively.

4.1.1.5 Determination of the half maximal inhibitory concentration (IC_{50}) of the excision reaction by the next complementary dNTP

The incorporation of an NRTI to the 3´-end of the primer and its translocation to the priming (P) site leaves the nucleotide binding (N) site free for binding an incoming nucleotide. If this occurs, and a dNTP complementary to template position +1 binds the N-site of the RT, a "dead-end-complex" (DEC) constituted by the RT, the T/P and the complementary dNTP is formed. DECs are not substrates of the excision reaction, but inhibit NRTI excision (Fig 10). In order to gain further insights on the contribution of this mechanism to the effects produced by P272A/R277K/T286A in rescue reaction efficiency, we determined the 50% inhibitory concentration (IC_{50}) by the next complementary nucleotide. As shown in Table 10, M41L/T215Y and M41L/T215Y/P272A/R277K/T286A RTs were equally susceptible to dATP, in rescue reactions carried out with D38rna/25PGA^{d4TMP} complexes, showing IC_{50} values around 4 μM. IC_{50} values obtained for MAK_SSSY were about two-fold higher (Table 10). When the reactions were carried out with heteropolymeric DNA duplexes such as D38/25PGA^{d4TMP}, we obtained essentially the same values than with RNA/DNA complexes, thereby suggesting a minimal impact of the type of template (*i.e.*, RNA *vs* DNA) on the inhibition by the next complementary dNTP.

Table 10. Ability of the next complementary dNTP to inhibit ATP-dependent rescue of primers terminated with d4TMP in RNA/DNA duplexes by mutant RTs.

RT	IC_{50} (μM)
M41L/T215Y	4.4 ± 1.6
M41L/T215Y/P272A/R277K/T286A	3.9 ± 1.0
MAK_SSSY	10.6 ± 4.8 (7.8 ± 0.3)[a]

Assays were carried out in the presence of 3.2 mM ATP. All dNTPs in these assays were supplied at 100 μM, except dATP that was supplied from 1 to 200 μM depending on the assay. Active enzyme concentrations in these assays were in the range of 10-20 nM, and the concentration of D38rna/25PGA T/P was 30 nM. Samples were incubated for 0-15 min depending on the assay. In all cases, incubation times were within the linear range of the corresponding time course. The percent inhibition was plotted against the concentration of dATP, and the data were fitted to a hyperbola to obtain the IC_{50} for each enzyme. Reported values were obtained from 2-3 experiments and are given as mean values ± standard deviations.

[a] Value obtained under the same conditions, but with the heteropolymeric DNA/DNA substrate D38/25PGA.

4.1.1.6 Determination of T/P binding affinity of WT and mutant enzymes.

The effects on T/P binding of substituting Ala-272, Lys-277 and Ala-286 for Pro-272, Arg-277 and Thr-286, respectively, were determined from the dissociation equilibrium constants (K_d) for DNA/DNA and RNA/DNA duplexes. D38/25PGA T/P was selected to determine DNA/DNA binding affinity as this was the complex used in rescue assays. However, 31rna/25PGA was chosen instead of D38rna/25PGA to measure RNA/DNA binding affinity (Table 11). The 31rna/25PGA complex results from primary RNase H cleavage using the T/P D38rna/25PGA, and represents the

predominant T/P form present in the rescue assays, since almost all template strands in the D38rna/25PGA complex are expected to be cleaved after only 30 s in the presence of RT (Fig 24). As shown in Table 11, thumb subdomain polymorphisms did not affect the DNA/DNA binding affinity. All K_d values were around 2-3 nM. In contrast, WT and M41L/T215Y RTs showed around two-fold higher binding affinity for 31rna/25PGA complexes in comparison to RTs bearing the P272A/R277K/T286A substitutions (Table 11). Thus, WT and M41L/T215Y RTs have K_d values of 1.23 ± 0.33 nM and 1.14 ± 0.30 nM, respectively, while mutants P272A/R277K/T286A and M41L/T215Y/P272A/R277K/T286A showed K_d values in the range of 2.09 to 2.76 nM.

Table 11. Dissociation equilibrium constants for WT and mutant HIV-1 RTs and DNA/DNA and RNA/DNA T/Ps.

RT	Apparent K_d (nM)	
	D38/25PGA	31rna/25PGA
WT	2.19 ± 0.34	1.23 ± 0.33
P272A/R277K/T286A	1.75 ± 0.44	2.76 ± 0.45
M41L/T215Y	3.13 ± 0.04	1.14 ± 0.30
M41L/T215Y/P272A/R277K/T286A	2.77 ± 0.31	2.09 ± 0.46

Sequences of D38/25PGA and 31rna/25PGA are:

```
D38     5´ GGGTCCTTTCTTACCTGCAAGAATGTATAGCCCTACCA  3´
25PGA   3´               GGACGTTCTTACATATCGGGATGGT  5´

31rna   5´ GGGUCCUUUCUUACCUGCAAGAAUGUAUAGC         3´
25PGA   3´               GGACGTTCTTACATATCGGGATGGT  5´
```

Data reported are mean values ± standard deviations obtained from three independent experiments.

4.1.1.7 DNA polymerization and RNase H activity of WT and mutant RTs in the presence of low concentrations of T/P

The differences in the K_d values for RNA/DNA *versus* DNA/DNA could have a significant impact in the DNA polymerase and RNase H activities of the RT. We have carried out assays with WT and mutant RTs in the presence of limiting concentrations of T/P to evaluate their efficiencies in these conditions.

RNase H activity at limiting T/P concentration

RNase H reactions were carried out in the presence of 1.5 nM D38rna/25PGA. This concentration was chosen because it was intermediate between the K_d for RNA/DNA of WT and M41L/T215Y RTs (K_d around 1.2 nM) and those of P272A/R277K/T286A and M41L/T215Y/P272A/R277K/T286A RTs (K_d around 2.4 nM). RT concentration was maintained at 3 nM in these assays. We found that thumb subdomain polymorphisms had a minor influence on the RNase H cleavage rates (Fig 27). In general, differences were not significant between WT and M41L/T215Y RTs and their homologs bearing thumb subdomain mutations. However, the mutant

M41L/T215Y/P272A/R277K/T286A RT showed slightly reduced RNase H activity in comparison with the M41L/T215Y RT suggesting that thumb subdomain polymorphisms could impair usage of T/P at low concentrations.

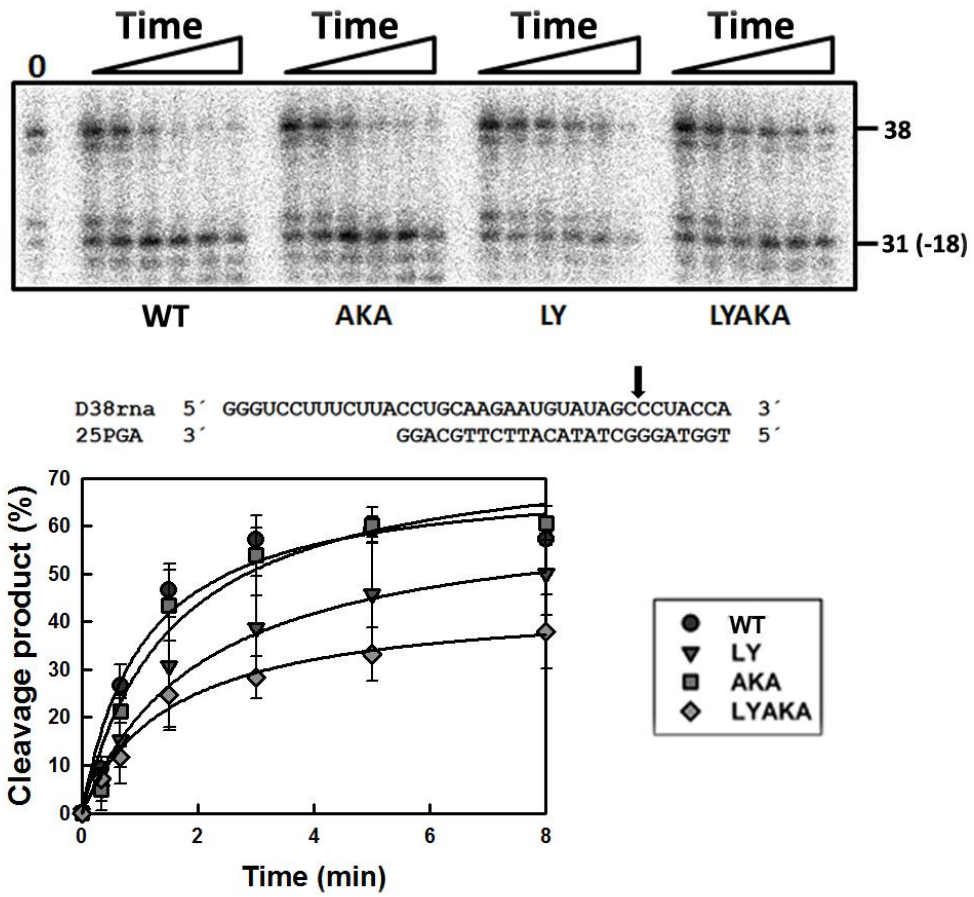

Fig 27. RNase H activity of WT and mutant RTs determined under limiting concentration of T/P. The labeled-RNA/DNA substrate D38rna/25PGA (1.5 nM) was cleaved at 37ºC in the presence of the corresponding RT at 3 nM (active enzyme concentration). Time points were obtained after incubating the samples for 20 s, 40 s, 1.5, 3, 5 and 8 min, respectively. A representative autoradiogram of the RNase H cleavage activity of WT and mutant RTs is shown, as well as the time courses of the RNase H cleavage reactions carried out with WT and mutant RTs. Represented values (mean values ± standard deviations [error bars]) were obtained from three independent experiments. RTs AKA, LYAKA and LY, correspond to mutant enzymes P272A/R277K/T286A, M41L/T215Y/P272A/R277K/T286A and M41L/T215Y, respectively.

Primer extension ability of WT and mutant RTs at limiting T/P concentration

Primer extension reactions were carried out in the presence of 3 nM active RT, with an excess of dNTPs (200 μM), with the exception of dATP which was supplied at 2 μM. In these assays, the 31rna/25PGA complex was added at a limiting concentration (1 nM) and also at 10 nM to directly compare RT DNA polymerization under different conditions. Interestingly, while at 10 nM T/P differences were not significant, at 1 nM concentration there was an approximately two-fold increase in the rate of formation of 38-nucleotide product by the M41L/T215Y mutant in comparison with the

M41L/T215Y/P272A/R277K/T286A RT (Fig 28). Notably, these differences are consistent with the higher RNA/DNA affinity reported for the M41L/T215Y enzyme (Table 11).

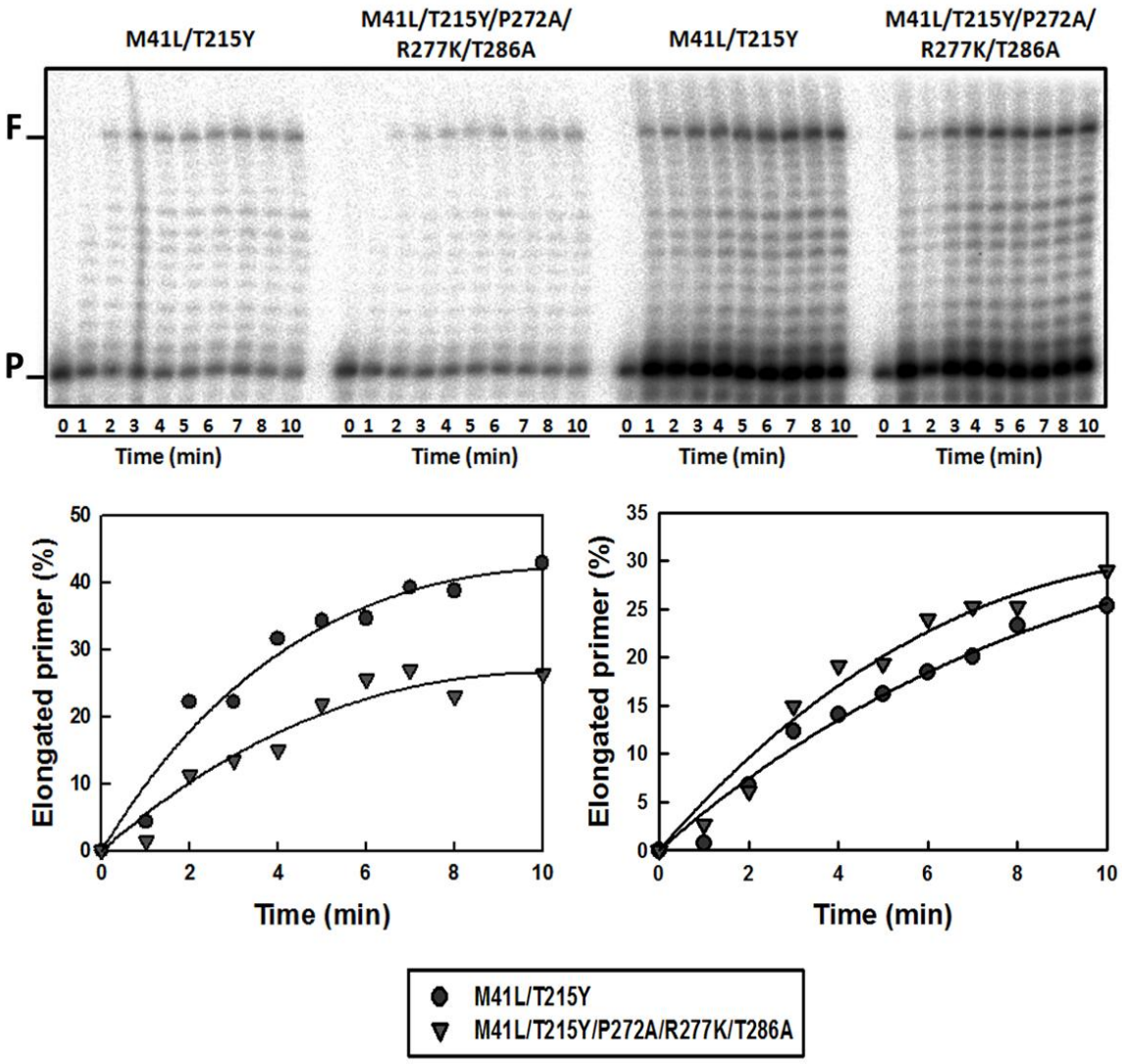

Fig 28. Extension of unblocked DNA primer 25PGA by WT and mutant RTs in the presence of an RNA template. Reactions were carried out with 31rna/25PGA concentrations of 1.5 and 10 nM, in the presence of 3 nM RT and 100 μM of each dNTP. P, primer; F, full length product.

4.1.2 Mechanistic insights into the association of the amino acid substitution R284K in the RT thumb subdomain and the TAM-1 pathway mutations M41L, L210W and T215Y

RT thumb subdomain mutation R284K has been identified in several studies associated with NRTI treatment (Cane *et al.*, 2007; Waters *et al.*, 2009; Von Wyl *et al.*, 2010). To further characterize the role of thumb subdomain substitutions on NRTI resistance and based on published evidence, we decided to study the molecular mechanism involved in the selection of R284K mutation under antiretroviral treatment. RT sequence analysis of viral isolates obtained from patients failing treatment with NRTIs showed a significant correlation between the presence of R284K and TAM-1 mutations M41L, L210W and T215Y (Cane *et al.*, 2007). Therefore, we characterized the WT (BH10 strain) RT, and mutant RTs R284K, M41L/L210W/T215Y and M41L/L210W/T215Y/R284K.

4.1.2.1 Rescue of DNA/DNA complexes blocked with AZTMP, d4TMP and tenofovir

The rescue ability of WT and mutant RTs was tested using DNA/DNA complexes blocked with AZTMP, d4TMP or tenofovir (Fig 29). After incorporation of the corresponding NRTI, we added a mixture of the four dNTPs and 3.2 mM ATP to facilitate excision and resume DNA polymerization. The mutant M41L/L210W/T215Y/R284K RT was able to rescue a significantly larger amount of blocked DNA than the M41L/L210W/T215Y RT with all three studied NRTIs (Fig 29). These differences were higher for primers blocked with thymidine-analogues than for primers blocked with tenofovir. However, R284K alone had no effect on the rescue activity of the WT enzyme (Fig 29).

Unlike in the case of reactions carried out in the presence of ATP, D38/25PGA^{AZTMP} rescue assays carried out in the presence of 9.6 mM GTP showed relatively minor differences between M41L/L210W/T215Y and M41L/L210W/T215Y/R284K RTs. This was due to the increase in rescue efficiency observed in reactions catalyzed by M41L/L210W/T215Y RT, relative to those carried out with M41L/L210W/T215Y/R284K RT (Fig 30). In the presence of 200 μM PPi, differences between M41L/L210W/T215Y and M41L/L210W/T215Y/R284K RTs were not significant (Fig 30). Under these conditions both mutant enzymes were less efficient than the WT in rescuing primers terminated with AZTMP.

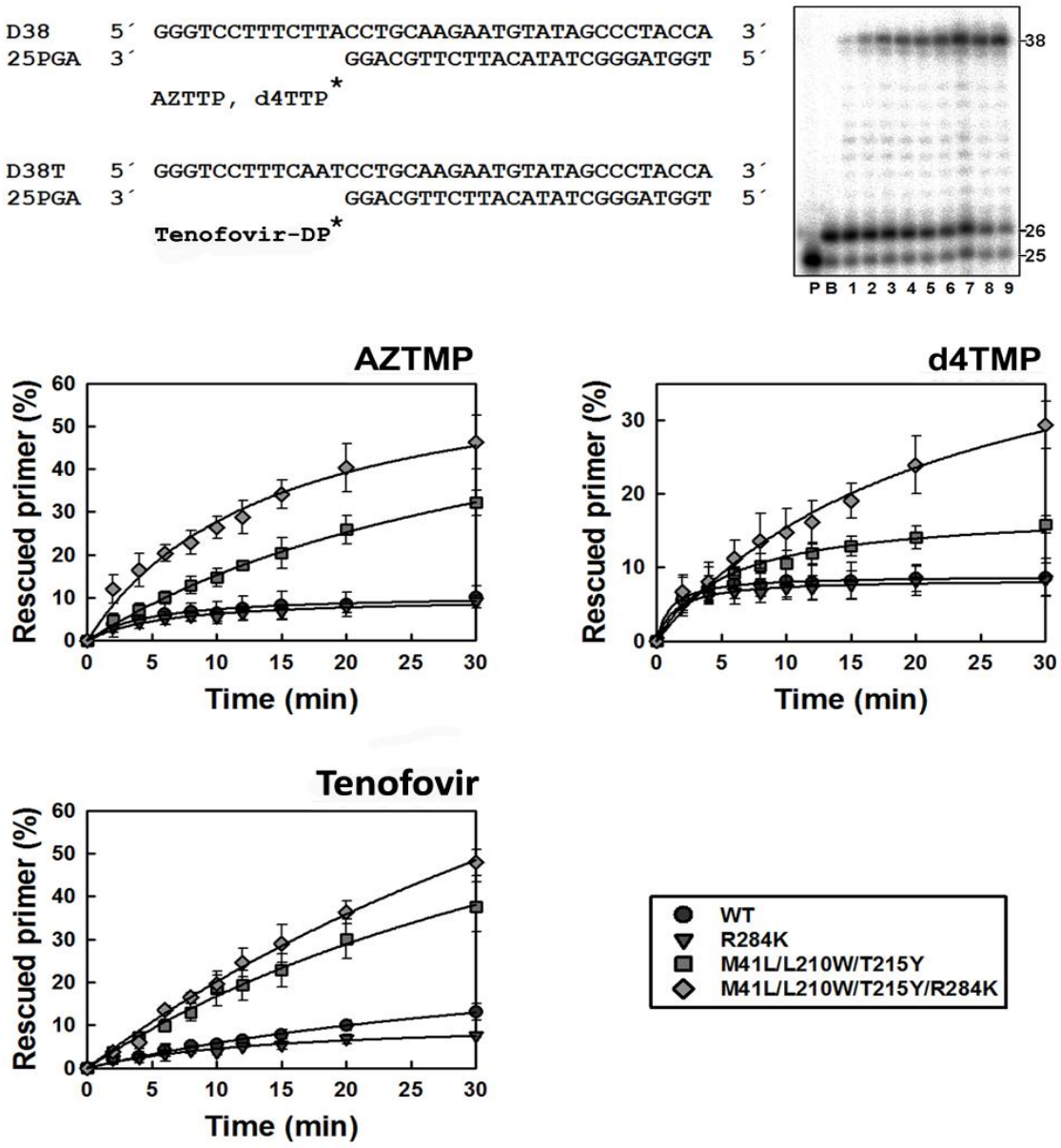

Fig 29. ATP-mediated excision of AZTMP-, d4TMP-, and tenofovir-terminated DNA/DNA T/Ps by WT and mutant RTs. Reactions were carried out with 38/25-mer DNA/DNA heteropolymeric complexes (sequences shown in the upper part of the figure). First, the inhibitor was incorporated at position +1 (indicated with an asterisk) of the 25-nucleotide primer (lane P) to generate a 26-nucleotide product (lane B). Excision of the inhibitor and further extension of the primer in the presence of 3.2 mM ATP and a mixture of dNTPs led to the formation of a fully extended 38-nucleotide product. A representative time course experiment of a primer rescue reaction is shown in lanes 1 to 9, which correspond to aliquots removed 2, 4, 6, 8, 10, 12, 15, 20, and 30 min after the addition of 3.2 mM ATP (gel on the right in the top panel). Graphs of time course experiments of primer rescue reactions initiated from inhibitor-terminated primers are given below. All dNTPs in the assays were supplied at 100 μM, except for dATP or dTTP (depending on the assay) whose concentration was 1 μM. T/P and active RT concentrations in these assays were 30 and 24 nM, respectively. Mean values ± standard deviations [error bars] were obtained from three independent experiments.

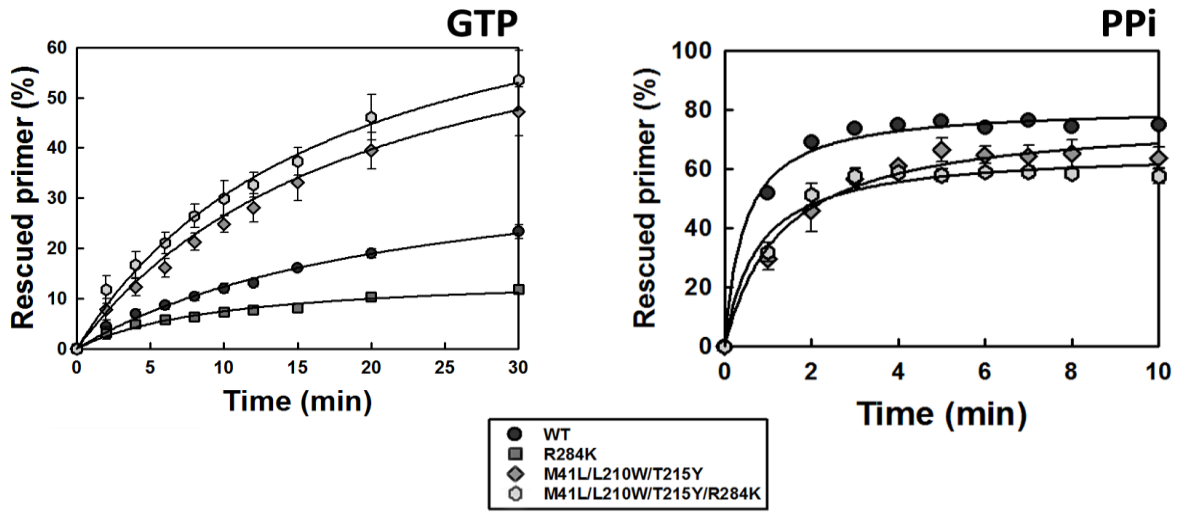

Fig 30. Rescue of AZTMP-blocked complexes in the presence of GTP or PPi. AZTMP rescue assays were carried out with the D38/25PGA DNA/DNA complex. Reaction conditions were the same described for ATP-dependent rescue assays, but using 9.6 mM GTP (left) or 200 μM PPi (right). Time points were taken at 2, 4, 6, 8, 10, 12, 15, 20, and 30 min after the addition of GTP or at 1, 2, 3, 4, 5, 6, 7, 8 and 10 min, after the addition of PPi. Mean values ± standard deviations [error bars] were obtained from three independent experiments.

4.1.2.2 Rescue of RNA/DNA complexes blocked with AZTMP, d4TMP and tenofovir

D38rna/25PGA and D38Trna/25PGA RNA/DNA complexes were used to measure AZTMP-, d4TMP- and tenofovir-terminated primer rescue efficiencies (Fig 31). In contrast with the results obtained with DNA/DNA complexes, we did not detect any significant differences between M41L/L210W/T215Y and M41L/L210W/T215Y/R284K RTs (Fig 31). Although both enzymes had remarkable ATP-dependent phosphorolytic activity, slightly higher than on DNA/DNA T/Ps, the presence of R284K had a minimal impact on rescue efficiency. The R284K mutant and the WT RT also showed higher NRTI-excision activity than on DNA/DNA, especially in the case of tenofovir (Fig 31).

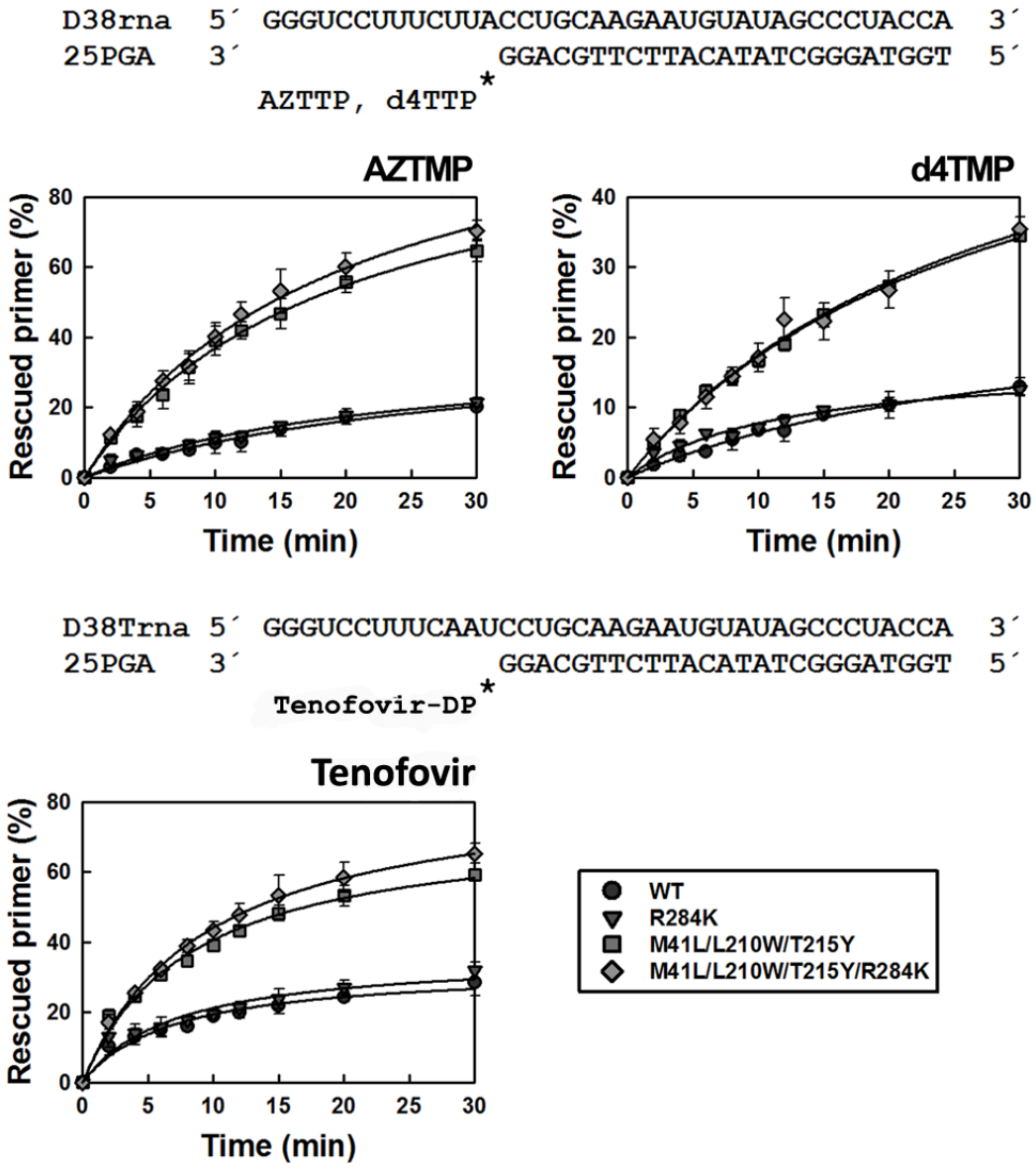

Fig 31. ATP-mediated rescue of AZTMP-, d4TMP-, and tenofovir-terminated primers in RNA/DNA duplexes by WT and mutant RTs. Time course experiments of excision reactions were carried out in the presence of 3.2 mM ATP. T/Ps used are indicated above corresponding graphs. All dNTPs in the assays were supplied at 200 μM, except dATP or dTTP (depending on the assay) whose concentration was 2 μM. T/P and active RT concentrations in these assays were 30 and 24 nM, respectively. Mean values ± standard deviations [error bars] were obtained from three independent experiments.

4.1.2.3 RNase H activity of WT and mutant RTs

The endonucleolytic activity of WT and mutant RTs was determined by using the heteropolymeric complexes 31Trna/21P and D38Trna/25PGA. D38Trna/25PGA was one of the T/Ps used in rescue assays with RNA/DNA complexes. We found no differences between the endonucleolytic activities of the M41L/L210W/T215Y RT and the WT enzyme, independently of the substrate used (Fig 32). Interestingly, RNase H kinetics obtained with these enzymes showed similar

cleavage rates between them on both tested T/Ps (catalytic rate constants around 0.35 min^{-1}). The M41L/L210W/T215Y/R284K RT showed higher endonucleolytic activity than the WT and the M41L/L210W/T215Y enzymes. Thus, when 31Trna/21P was used as substrate, mutant M41L/L210W/T215Y/R284K showed a 2.5-fold increased catalytic rate in comparison with the WT RT (Fig 32). A similar increase was observed with D38Trna/25PGA that showed a catalytic rate constant that was roughly 3.3 times higher for the M41L/L210W/T215Y/R284K RT than for the WT and M41L/L210W/T215Y RTs (Fig 32). Thus, while approximately 35% of the 31Trna/21P remains uncleaved after 3 min of incubation in the presence of WT and M41L/L210W/T215Y RTs, this value was < 8% in the presence of M41L/L210W/T215Y/R284K RT.

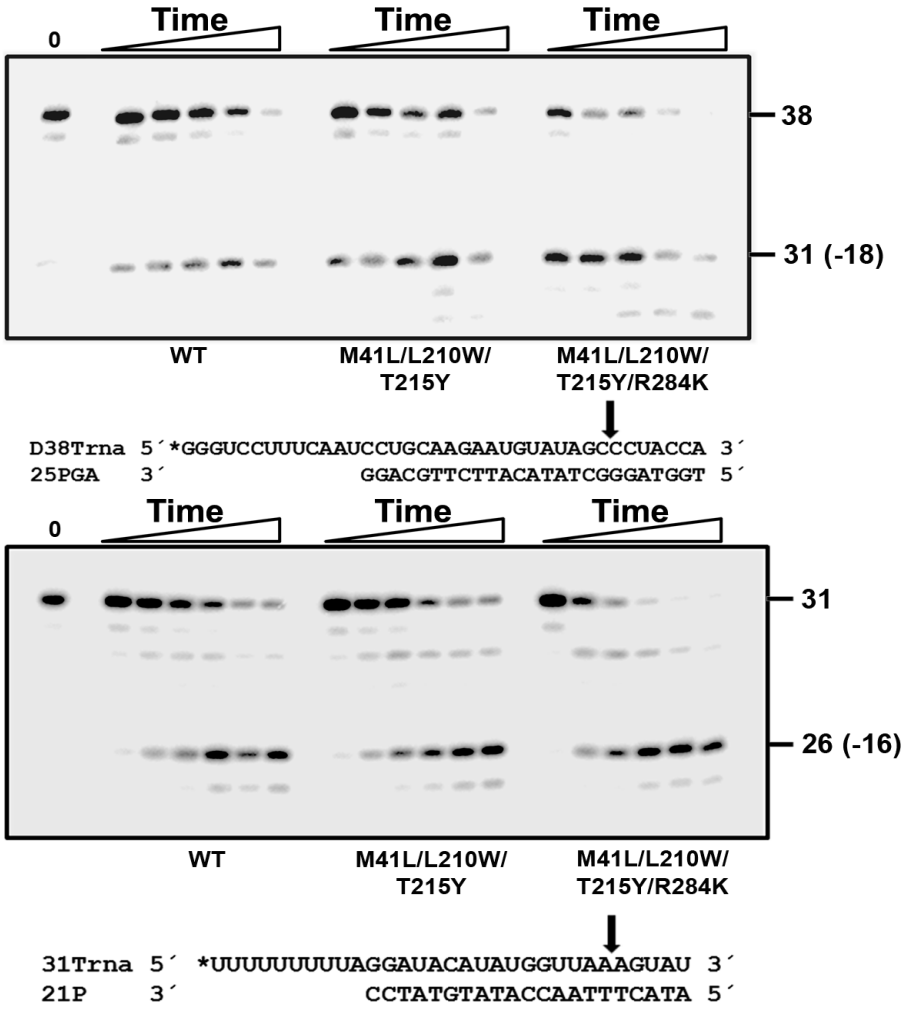

Fig 32. RNase H activity of WT and mutant RTs. [^{32}P]RNA/DNA substrates (50 nM) were cleaved at 37°C in the presence of the corresponding RT at 50 nM (active enzyme concentration). The T/P sequences used are shown below the corresponding gel. For D38Trna/25PGA, the time points were obtained after incubating the samples for 20 s, 40 s and 1, 2 and 4 min. For 31Trna/21P, aliquots were removed at 20 s, 40 s and 1, 2, 3 and 4 min. Catalytic rate constants for the cleavage of D38Trna were 0.34 ± 0.15 min^{-1}, 0.39 ± 0.18 min^{-1} and 1.16 ± 0.54 min^{-1} for WT, and mutant RTs M41L/L210W/T215Y and M41L/L210W/T215Y/R284K, respectively. For 31Trna the catalytic rate constant of the WT enzyme was 0.33 ± 0.05 min^{-1}. Rate constants for mutants M41L/L210W/T215Y and M41L/L210W/T215Y/R284K were 0.35 ± 0.03 min^{-1} and 0.87 ± 0.12 min^{-1}, respectively.

Interestingly, an increased frequency of RNase H secondary cleavages was also detected with the D38Trna/25PGA complex in reactions carried out with the M41L/L210W/T215Y/R284K RT (data not shown). However, this cleavage, corresponding to position -16 of the template strand, could not be measured accurately. Taken together, those results suggest that the reduced stability of the RNA template in reactions catalyzed by the M41L/L210W/T215Y/R284K RT could affect the elongation efficiency of unblocked DNA primers on rescue assays.

4.1.2.4 Kinetics of ATP-dependent excision of AZTMP and d4TMP from DNA/DNA blocked-complexes

In order to determine whether the improved DNA/DNA rescue efficiency displayed by the M41L/L210W/T215Y/R284K RT could be attributed to an increased chain-terminator excision activity, excision rates for WT and mutant RTs were determined under single-turnover conditions.

Preparation of NRTI-blocked DNA primers annealed to DNA templates

For the determination of the ATP-dependent excision activity of WT and mutant RTs, we obtained DNA/DNA complexes blocked with d4TMP, AZTMP and tenofovir. Primers terminated with d4TMP were obtained by using the terminal transferase enzyme (see section 4.1.1.4 and Material and Methods). It was known that AZTTP was a poor substrate of the terminal transferase (Mas *et al.*, 2002). However, it was not known whether tenofovir-DP could be used as substrate by the terminal transferase enzyme. Our assays revealed some incorporation of tenofovir by the terminal transferase on 25PGA (Fig 33A). However, catalytic incorporation rates calculated for d4TTP and tenofovir-DP showed that d4TTP incorporation was around 18 times faster than tenofovir-DP incorporation (Fig 33B). Use of $CoCl_2$ instead of $MnCl_2$ did not improve AZTTP or tenofovir-DP incorporation. In order to obtain complexes with primers blocked with AZTMP or tenofovir, we used the WT RT to incorporate AZTTP and tenofovir-DP on preformed D38/25PGA or D38T/25PGA complexes, respectively (Fig 33C). Once the NRTI was incorporated, the WT RT was heat-inactivated and the sample slowly cooled down at room temperature to allow T/P re-association. Finally the T/P was purified by gel-filtration chromatography and alcohol precipitation. This method yielded 40-50% of final purified product.

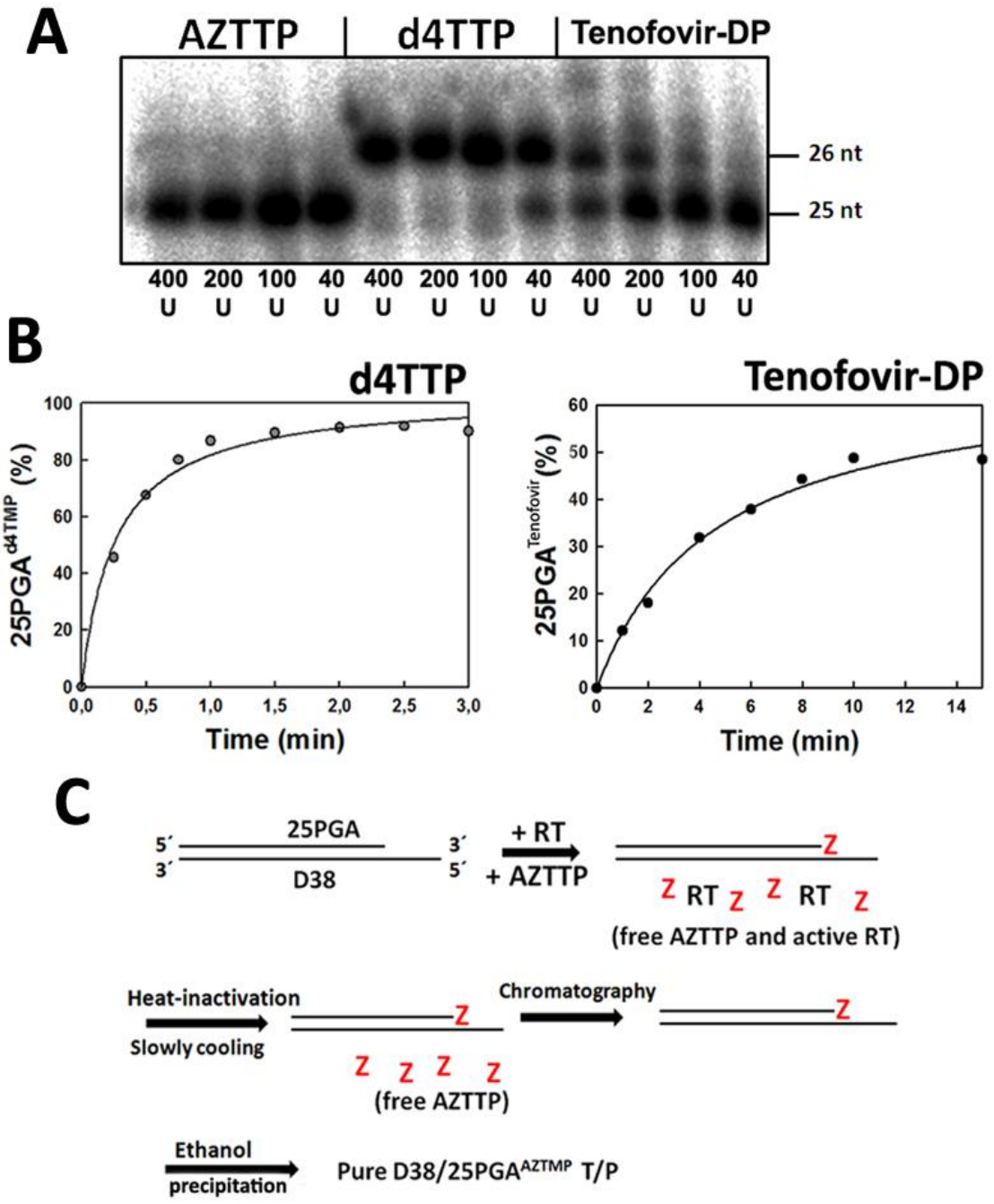

Fig 33. AZTTP, d4TTP and tenofovir-DP incorporation to the 3´-end of 25PGA and formation of T/Ps containing blocked DNA primers. (A) AZTTP, d4TTP and tenofovir-DP incorporation in 25PGA primers using the terminal transferase enzyme. The amount of enzyme used (in activity units) is shown below the gel. (B) Time courses of d4TTP and tenofovir-DP incorporation reactions carried out with the terminal transferase enzyme. Catalytic rate constants for the incorporation of d4TTP and tenofovir-DP were 4.59 ± 0.74 min^{-1} and 0.26 ± 0.03 min^{-1}, respectively. (C) Schematic representation of the methodology employed in the production of D38/25PGA^{AZTMP} complexes. First, the primer was blocked in the presence of template, WT RT and a large excess of AZTTP (represented as a red Z). The RT was heat-inactivated (10 min, 90ºC) and the T/P re-associated by slowly cooling to room temperature. Free AZTTP molecules were eliminated by gel-filtration chromatography and finally the T/P further purified and concentrated by ethanol precipitation.

ATP-dependent excision of d4TMP- and AZTMP-terminated primers

WT and mutant RTs R284K, M41L/L210W/T215Y and M41L/L210W/T215Y/R284K were incubated with D38/25PGA^{d4TMP} and D38/25PGA^{AZTMP} complexes in the presence of 3.2 mM ATP and the kinetics of the excision reaction were monitored by measuring the formation of free 25PGA. Two groups of mutations could be easily identified based on their excision activity. While WT and R284K RTs showed low-level activity on primers terminated with AZTMP or d4TMP, M41L/L210W/T215Y and M41L/L210W/T215Y/R284K RTs showed measurable levels of excision activity (Fig 34). Addition of R284K mutation to a M41L/L210W/T215Y background did not improve excision ability of the enzyme containing TAM-1 mutations. Notably, excision rate constants were roughly similar for both NRTIs (Fig 34).

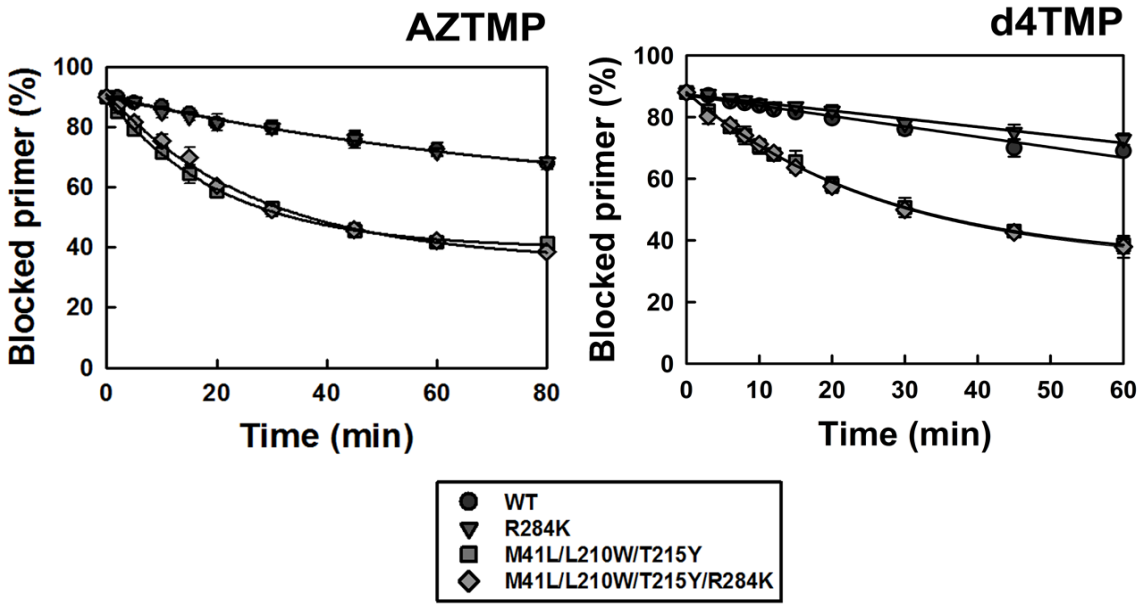

Fig 34. Kinetics of ATP-dependent excision of AZTMP and d4TMP from NRTI-terminated DNA/DNA T/Ps. Excision reactions of AZTMP- and d4TMP-terminated primers (26-mers) annealed to their corresponding 38-nucleotide DNA templates (30 nM) were initiated by the addition of 3.2 mM ATP. The active RT was 210 nM. The calculated k_{obs} values for the AZTMP were 2.82 ± 0.15 x 10^{-3} min^{-1}, 2.42 ± 0.12 x 10^{-3} min^{-1}, 4.69 ± 0.17 x 10^{-2} min^{-1} and 3.64 ± 0.31 x 10^{-2} min^{-1} for WT, R284K, M41L/L210W/T215Y and M41L/L210W/T215Y/R284K RTs, respectively. For d4TMP excision, catalytic rate of the WT enzyme was 3.37 ± 0.19 x 10^{-3} min^{-1}, while k_{obs} for mutants R284K, M41L/L210W/T215Y and M41L/L210W/T215Y/R284K were 2.62 ± 0.14 x 10^{-3} min^{-1}, 3.72 ± 0.16 x 10^{-2} min^{-1} and 3.70 ± 0.23 x 10^{-2} min^{-1}, respectively.

4.1.2.5 DNA/DNA binding affinity of WT and mutant RTs

We determined the DNA/DNA dissociation equilibrium constant (K_d) of WT and mutant RTs for the D38/25PGA complex used in rescue assays. The obtained K_d values were essentially the same (around 2 nM) for all tested RTs (Table 12), and similar to DNA/DNA binding affinities reported for

RTs M41L/T215Y, M41L/T215Y/P272A/R277K/T286A and P272A/R277K/T286A (Table 12). These results suggest a negligible impact of the DNA/DNA binding affinity on the higher rescue efficiency shown by the M41L/L210W/T215Y/R284K RT.

Table 12. Dissociation equilibrium constants for WT and mutant HIV-1 RTs and DNA/DNA T/Ps.

RT	K_d (nM)
WT	1.65 ± 0.48
R284K	1.94 ± 0.42
M41L/L210W/T215Y	2.37 ± 0.65
M41L/L210W/T215Y/R284K	1.71 ± 0.21

The nucleotide sequence of the T/P was:

```
D38     5´ GGGTCCTTTCTTACCTGCAAGAATGTATAGCCCTACCA  3´
25PGA   3´                GGACGTTCTTACATATCGGGATGGT  5´
```

Reported data are mean values ± standard deviations obtained from three independent experiments.

4.1.2.6 AZTTP and tenofovir-DP inhibition constants (K_i) for WT and mutant RTs

As described previously, the addition of the R284K substitution did not improve the excision activity of the M41L/L210W/T215Y RT. Following primer unblocking, the RT has to extend the primer strand to generate the full length product of the rescue reaction. However, the free triphosphorylated inhibitor present in the sample (or even the polyphosphate product resulting from the ATP-mediated excision) could be incorporated at the same position instead of the corresponding dNTP and block the primer again. In order to check if the presence of R284K could affect the ability of M41L/L210W/T215Y RT to incorporate AZTTP or tenofovir-DP, inhibition constants for both inhibitors were determined. As shown in Table 13, AZTTP and tenofovir-DP K_i values for WT, M41L/L210W/T215Y and M41L/L210W/T215Y/R284K RTs were broadly similar and around 2.5 µM in all cases. The only exception was the WT RT, which showed a 1.7-fold increase in K_i for tenofovir-DP in comparison with AZTTP. Taken together, these results suggest a minimal effect of amino acid substitutions of the TAM-1 cluster or R284K in AZTTP or tenofovir-DP discrimination.

Table 13. Inhibition constants for AZTTP and tenofovir-DP incorporation.

RT	K_i (µM)	
	AZTTP	Tenofovir-DP
WT	2.10 ± 0.38	3.59 ± 0.26
M41L/L210W/T215Y	2.18 ± 0.17	2.63 ± 0.64
M41L/L210W/T215Y/R284K	2.32 ± 0.74	2.54 ± 0.55

D38/25PGA and D38T/25PGA were used as substrates for AZTTP and tenofovir-DP incorporation, respectively. Reported values are the mean values ± standard deviations, obtained from at least three independent experiments.

4.1.2.7 Steady-state kinetic parameters of nucleotide incorporation of WT and mutant RTs

As discussed above, efficient DNA elongation after primer unblocking is important to complete the rescue reaction. Therefore, the ability of M41L/L210W/T215Y/R284K and M41L/L210W/T215Y/ RTs to incorporate nucleotides in the growing DNA chain was determined. For this purpose, D38/25PGA and D38T/25PGA complexes were obtained and the incorporation of dTTP or dATP was monitored. Kinetic parameters such as the catalytic rate of nucleotide incorporation (k_{cat}), the Michaelis-Menten constant (K_m) and the catalytic efficiency (k_{cat}/K_m) for each nucleotide are given in Table 14. The k_{cat} values for dTTP and dATP incorporation by the M41L/L210W/T215Y/R284K RT were around 1.7- and 3-fold higher, respectively, than those obtained with the WT and the M41L/L210W/T215Y RTs, respectively. However, the higher k_{cat} of dNTP incorporation obtained with RTs bearing the R284K mutation resulted in a higher catalytic efficiency only in the case of dATP, since the K_m value for dTTP incorporation shown by the M41L/L210W/T215Y/R284K RT was also 1.6-fold higher than the corresponding values obtained with the WT and M41L/L210W/T215Y enzymes (Table 14).

Table 14. Steady-state kinetic parameters of nucleotide incorporation catalyzed by WT and mutant RTs.

Nucleotide	RT	k_{cat} (min^{-1})	K_m (nM)	k_{cat}/K_m (μM^{-1} min^{-1})
dTTP	WT	3.14 ± 0.55	108.3 ± 12.9	30.9 ± 4.7
	M41L/L210W/T215Y	3.53 ± 0.09	117.4 ± 21.9	30.8 ± 6.0
	M41L/L210W/T215Y/R284K	5.66 ± 0.23	184.5 ± 6.1	30.7 ± 2.3
dATP	WT	3.87 ± 0.99	25.8 ± 6.7	172.0 ± 27.7
	M41L/L210W/T215Y	5.70 ± 0.87	32.1 ± 9.6	243.9 ± 51.1
	M41L/L210W/T215Y/R284K	10.09 ± 1.47	15.9 ± 2.5	639.6 ± 101.2

D38/25PGA and D38T/25PGA were used as T/Ps for dTTP and dATP incorporation, respectively. Reported data are the mean values ± standard deviations, obtained from at least three independent experiments.

4.1.2.8 Pre-steady-state kinetics of dTTP incorporation

Although the M41L/L210W/T215Y/R284K RT showed increased steady-state rates of nucleotide incorporation, it should be noted that these rates are dominated by the slowest step of the polymerization reaction (*i.e.*, dissociation of the RT-DNA complex). Therefore, differences in dissociation rate constants (k_{off}) could have a large influence on the k_{cat} values obtained. However, this does not seem to affect the comparison of M41L/L210W/T215Y and M41L/L210W/T215Y/R284K RTs, since both RTs showed similar k_{off}s in assays carried out with the D38/25PGA complex (0.215 ± 0.030 s^{-1} and 0.201 ± 0.033 s^{-1} for M41L/L210W/T215Y and M41L/L210W/T215Y/R284K RTs, respectively). Further evidence in support of these results was obtained by determining the pre-steady-state kinetics of single-nucleotide incorporation with the D38/25PGA T/P (Fig 35). These assays were performed in the presence of high dTTP concentrations (80 μM) to ensure optimal binding of dNTP. Under these conditions, the M41L/L210W/T215Y RT showed a nucleotide incorporation rate (k_{obs}) of 21.5 ± 4.4 s^{-1} while the k_{obs} value of the M41L/L210W/T215Y/R284K RT was 38.8 ± 9.4 s^{-1}. These results gave additional support to the role

of the R284K mutation as an enhancer of nucleotide incorporation efficiency when added to M41L/L210W/T215Y RT.

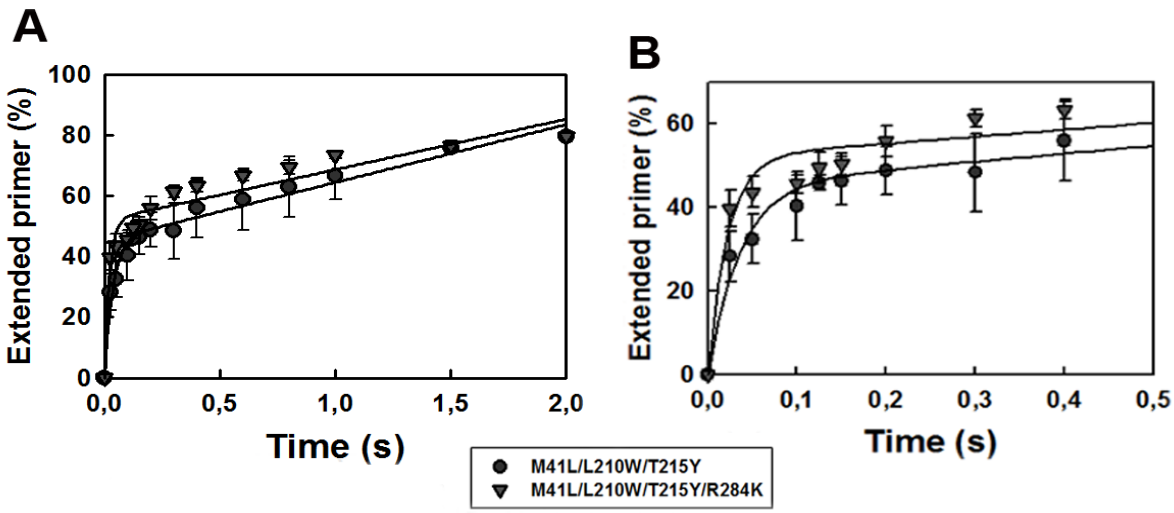

Fig 35. Pre-steady-state kinetics of single-nucleotide incorporation by RTs in the presence of high concentrations of dNTP. (A) Graphic representation of a complete time course reaction. Assays were carried in the presence of high dTTP concentration (80 μM), RT (70 nM) and D38/25PGA T/P (100 nM). Mean values ± standard deviations [error bars] were obtained from three independent experiments. (B) Close-up of nucleotide incorporation kinetics covering the first 500 ms of the reaction.

4.1.2.9 Polymerization ability of WT and mutant RTs

DNA primer extension assays as well as processivity measurements were also carried out with WT and mutant RTs.

Primer extension assays

Ability of WT and mutant RTs to extend the unblocked D38/25PGA DNA/DNA complex was determined in the presence of excess dNTPs (*i.e.* 100 μM each) and at 1, 5 and 10 nM T/P. In assays carried out with 10 nM D38/25PGA, the mutant RT M41L/L210W/T215Y/R284K showed increased ability to extend the DNA primer, in comparison with the WT and M41L/L210W/T215Y RTs (Fig 36). This increase in primer extension was mitigated at lower T/P concentrations. Interestingly, when the R284K mutation was introduced in a WT background also produced an increase on primer elongation (Fig 36). Consistent with the results obtained with the M41L/L210W/T215Y/R284K RT, this effect was clearly observed at the highest T/P concentration (*i.e.*, 10 nM).

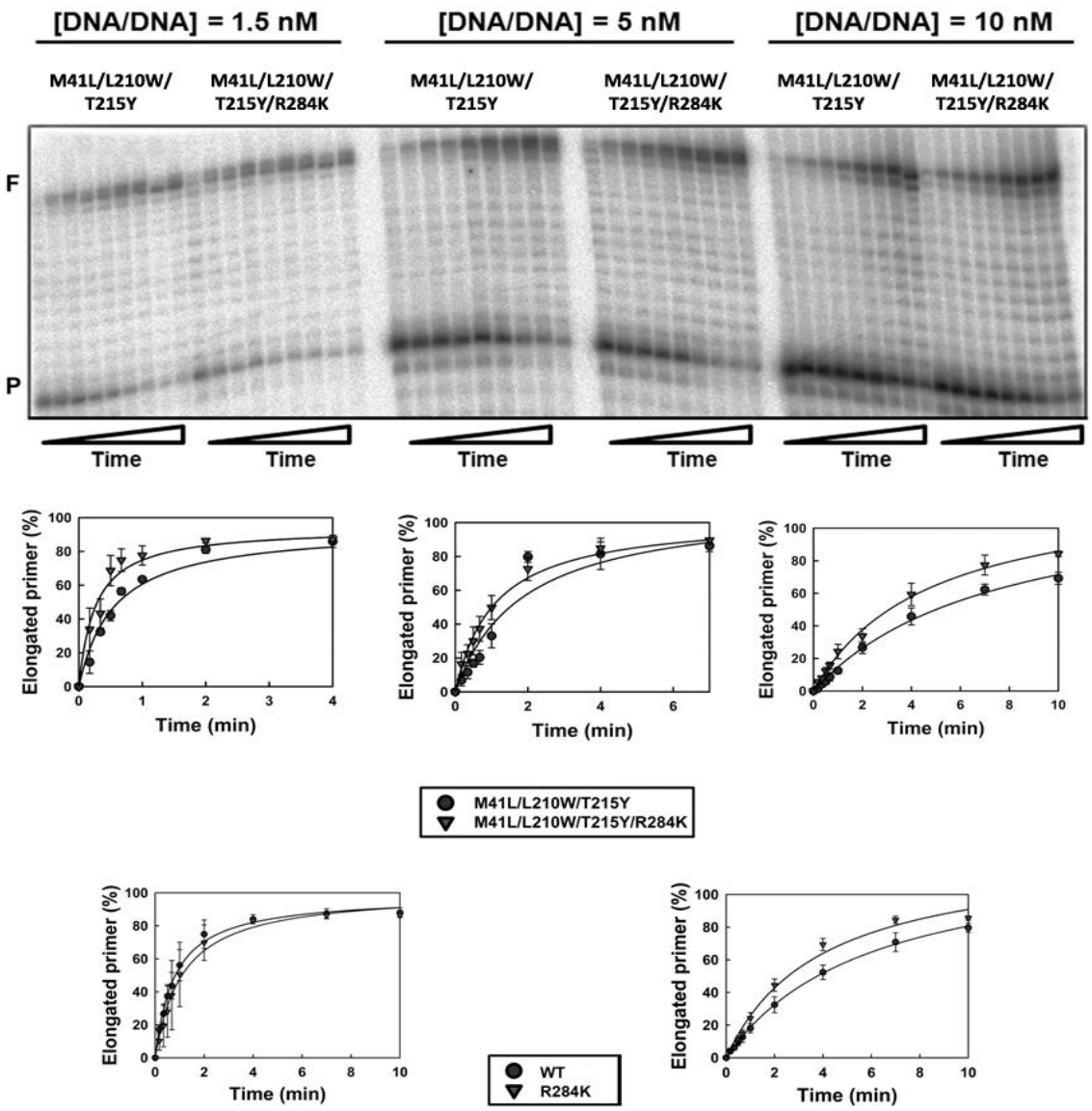

Fig 36. Extension of unblocked primers in heteropolymeric DNA/DNA D38/25PGA complex by WT and mutant RTs. Reactions were carried out in the presence of 1.5, 5 and 10 nM T/P concentrations, 3 nM RT and 100 μM of each dNTP. Represented values shown in the plots below were mean values ± standard deviations [error bars], obtained from three independent experiments.

Processivity assays

Processivity is defined as the number of nucleotides that the RT is able to incorporate in a growing DNA chain before dissociation (*i.e.*, the number of nucleotides incorporated in a single cycle of DNA synthesis). To ensure that only one synthesis cycle is taking place, the presence of an RT trap is essential. One of the most common traps used in RT biochemical assays is sodium heparin. Heparin acts by sequestering all free RT present in the media. Therefore, as soon as the RT dissociates from the preformed RT-T/P binary complex, the heparin will bind the enzyme, thus avoiding further polymerization events. Although processivity assays are usually carried out with large templates, we first assessed WT and mutants RTs processivity with the D38/25PGA complex

used in rescue assays. In the presence of 5 mg/ml heparin, M41L/L210W/T215Y/R284K RT showed higher processivity than the M41L/L210W/T215Y enzyme (Fig 37A, B). These results were highly consistent with data obtained in primer extension and nucleotide incorporation assays, further supporting the role of R284K in DNA polymerization efficiency when this amino acid substitution was accompanying the M41L/L210W/T215Y set of mutations. In additional experiments, processive synthesis of WT and mutant RTs were evaluated using a long template, corresponding to the M13mp2 single-stranded DNA in complex with the 15-mer ProLac110 in the presence of 5 mg/ml heparin. Under these conditions accurate measurements of primer extension were limited by high frequency of bands corresponding with primers whose elongation was not completed (Fig 37C). However, there was a clear tendency to produce longer extension products in reactions catalyzed by RTs bearing R284K compared with their counterparts without this mutation. This is particularly evident for WT and R284K enzymes (as indicated with asterisks in Fig 37C).

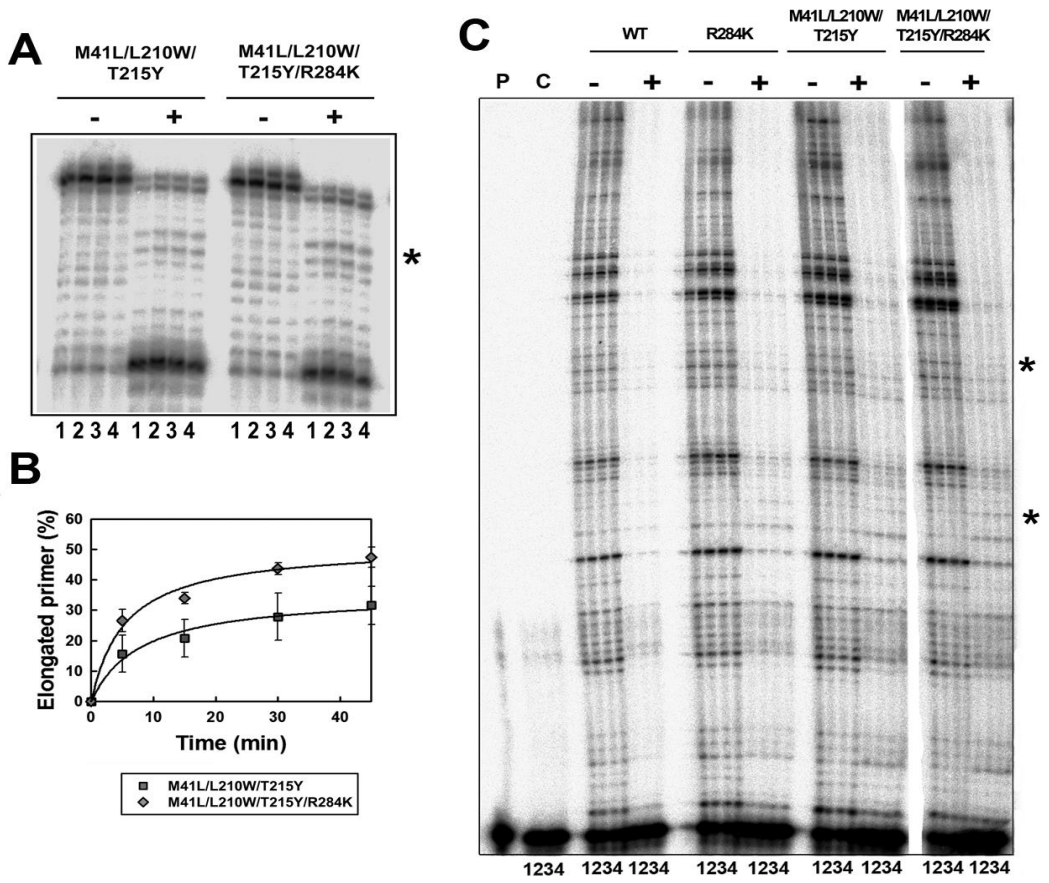

Fig 37. Processivity of WT and mutant RTs. (A) Processivity assays carried out with M41L/L210W/T215Y and M41L/L210W/T215Y/R284K RTs and the heteropolymeric T/P D38/25PGA. Elongation reactions were carried out in the presence of heparin (5 mg/ml) as an enzyme trap. After formation of the binary complex of RT and T/P (D38/25PGA), reactions were initiated by adding a mixture of all four dNTPs (50 μM final concentration), with or without heparin (indicated above the gel with plus and minus signs, respectively). Lanes 1 to 4 represent samples taken 5, 15, 30 and 45 min after initiating the polymerization reaction. Asterisks in panels (A) and (C) indicate bands that are significantly more intense in the reactions catalyzed by the M41L/L210W/T215Y/R284K RT. (B) Shows the amount of extended primer in reactions carried out with D38/25PGA in the presence of trap. (C) Processivity assays using the M13mp2 single-stranded DNA as template. Assays were carried out in the same conditions described above for D38/25PGA. P stands for primer, and C represents control reactions where the heparin trap was added before the enzyme. The oligonucleotide ProLac110 (5'- GCGATTAAGTTGGGT-3') is complementary to positions 105-119 of the *lacZα* coding sequence.

4.1.2.10 Connection subdomain substitution M357T: a possible R284K associated mutation

In order to identify possible partners of the R284K mutation, a rational search of new mutations was carried out. Firstly, the RT-DNA/DNA-dNTP ternary complex (Huang *et al.*, 1998) was analyzed to identify residues in the vicinity of Arg-284. Structural data revealed that connection subdomain residues 355-357 as well as the side-chain of Arg-284 interact with the same template region (nucleotides -12 and -13 of template strand). Therefore an extensive search on the Stanford University HIV drug resistance database (http://hivdb.stanford.edu/) was performed in order to identify possible associations between R284K and mutations at positions 355, 356 and 357. Sequences from HIV-1 group M subtype B HIV-1 isolates bearing R284K, M41L/L210W/T215Y or M41L/L210W/T215Y/R284K mutations, as well as the WT strain were identified. While Ala-355 is highly conserved in all sequence contexts (around 97% of HIV-1 isolates), the residue at position 356 is polymorphic, with Arg-356 being the most frequently found amino acid. The R356K substitution had the same frequency (around 10%) in all sequence contexts bearing the R284K mutation. Interestingly, in genotypes lacking the R284K mutation (*i.e.*, in the WT and the M41L/L210W/T215Y backgrounds) the substitution R356K was found around 2 times more frequently (Table 15). Notably, the M357T substitution was found in 34% and 42.7% of viruses bearing the R284K and M41L/L210W/T215Y/R284K mutations, respectively. On the other hand, M357T was found in 25.8% of the viruses bearing the M41L/L210W/T215Y set of mutations, and in 23% of the WT viruses (Table 15). Therefore, the frequency of M357T was about two-thirds higher in virus having M41L/L210W/T215Y/R284K than in virus having only the TAM-1 cluster of mutations. Furthermore, if we extend the analysis of other mutations at position 357 (*e.g.*, M357I and M357V), the observed increase is even larger (Table 15). These results suggested that polymorphisms at position 357 could be related with mutations M41L/L210W/T215Y only when the R284K mutation was present.

Table 15. Frequency of connection subdomain mutations R356K and M357T found in different sequence backgrounds.

Sequence background	R356K (%)	M357T (%)
WT	18.0	23.6
R284K	9.7	34.0
M41L/L210W/T215Y	24.6	25.8 (31.1)[a]
M41L/L210W/T215Y/R284K	10.7	42.7 (60.0)[a]

[a] Frequency of mutations M357I/T/V

Data obtained from the Stanford University HIV drug resistance database (http://hivdb.stanford.edu/).

Effects of M357T on rescue activity and processivity in the presence of TAMs and R284K

Based on the evidence described above, we purified a mutant RT with the combination of amino acid substitutions M41L/L210W/T215Y/R284K/M357T. Rescue assays with DNA/DNA and

RNA/DNA complexes containing an AZTMP-blocked primer, carried out in the presence of 3.2 mM ATP, showed that mutant M41L/L210W/T215Y/R284K/M357T had significant ATP-dependent phosphorolytic activity, but similar to the M41L/L210W/T215Y/R284K RT (Fig 38A).

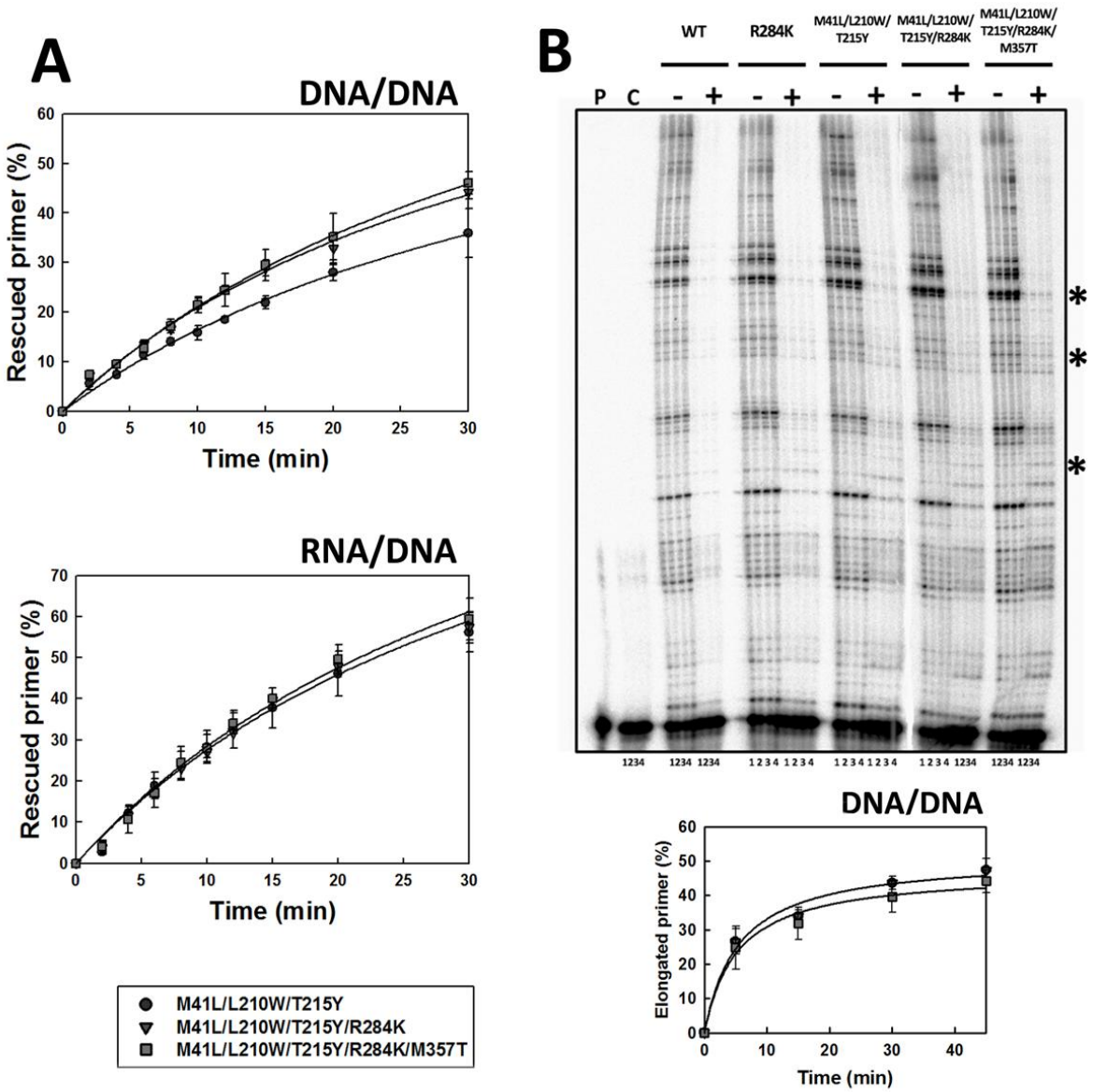

Fig 38. Effect of M357T in the presence of the mutational complex M41L/L210W/T215Y/R284K ATP-dependent rescue activity and processivity. (A) Time course experiments with D38/25PGA^{AZTMP} (up) and D38rna/25PGA^{AZTMP} (down) were carried out in the presence of 3.2 mM ATP. T/P concentration was 30 nM, while RT was present at 24 nM. All dNTPs were supplied at 100 μM (DNA/DNA) or 200 μM (RNA/DNA), except for dATP, whose concentration was 1 μM (DNA/DNA) or 2 μM (RNA/DNA). (B) Processivity assays carried out with M13mp2 single-stranded DNA as template. Elongation reactions were monitored in the presence of heparin (5 mg/ml) as an enzyme trap. After formation of the binary complex of RT and T/P (M13mp2 single-stranded DNA/ProLac110), reactions were initiated by adding a mixture of all four dNTPs (50 μM final concentration), with or without heparin (indicated above the gel with plus and minus signs, respectively). Lanes 1 to 4 represent samples taken 5, 15, 30 and 45 min after initiating the polymerization reaction. P stands for primer, and C represents control reactions where the heparin trap was added before the enzyme. Asterisks indicate bands that are significantly more intense in the reactions catalyzed by the M41L/L210W/T215Y/R284K/M357T RT. Time course experiments carried out with the D38/25PGA complex did not show significant differences between M41L/L210W/T215Y/R284K and M41L/L210W/T215Y/R284K/M357T RTs (see panel below).

In addition, the processivity of M41L/L210W/T215Y/R284K/M357T RT was also evaluated on M13mp2ssDNA/ProLac110 and D38/25PGA complexes. While on D38/25PGA duplexes RTs with and without the M357T substitution showed similar processivities (Fig 38B), we found some differences with the M13mp2ssDNA/ProLac110 complex. Thus, when using this T/P, mutant M41L/L210W/T215Y/R284K/M357T RT produced longer products than the M41L/L210W/T215Y/R284K enzyme (Fig 38B). However, as discussed above, accurate quantification of processive polymerization was not possible and therefore the significance of these results remains unclear.

4.2 Mechanistic insights into the association of H208Y and the TAM-1 pathway mutations M41L, L210W and T215Y

RT thumb subdomain mutations described so far are away from the DNA polymerase active site as well as from the ATP binding site. Results described above show that their impact on ATP-dependent excision activity is not relevant.

Another secondary mutation usually found associated with TAMs in treated HIV-1 infected patients is H208Y. Residue 208 is located at the palm subdomain, very close to the ATP binding site created by TAMs. However, its hypothetical role on excision is unknown, although H208Y has been associated with antiretroviral treatment failure and with the presence of TAM-1 mutations M41L, L210W and T215Y (Svicher *et al.*, 2006; Nebbia *et al.*, 2007; von Wyl *et al.*, 2010). For these studies, in addition to the WT and mutant M41L/L210W/T215Y RTs, we purified two additional mutant enzymes containing the amino acid substitution H208Y: M41L/H208Y/L210W/T215Y and H208Y RTs.

4.2.1 ATP-dependent rescue activity of WT and mutant RTs

The ability of WT and mutant enzymes to rescue primers blocked with different NRTIs in the presence of 3.2 mM ATP was first analyzed using DNA/DNA duplexes (*i.e.*, the D38/25PGA complex in the case of AZTMP and d4TMP, and D38T/25PGA in the case of tenofovir). Results obtained are shown in Fig 39. As expected, the single-mutant enzyme H208Y showed very low or negligible rescue activity, with final extension product levels similar to those obtained with the WT RT. These levels of rescue activity displayed by both enzymes were similar for all tested NRTIs. In contrast with the single-mutant, when H208Y was present in a background containing M41L/L210W/T215Y mutations, a measurable amount of fully-extended primer was obtained (Fig 39). The mutant M41L/L210W/T215Y RT also showed remarkable rescue activity, as described in section 4.1.2.1. However, the amount of fully-extended product was lower than in reactions carried out with the M41L/H208Y/L210W/T215Y RT. Differences between M41L/L210W/T215Y and M41L/H208Y/L210W/T215Y RTs were significant with tenofovir, as well with both thymidine

analogues. Tenofovir- and AZTMP-terminated primers were the best substrates of excision reactions carried out with both enzymes. In contrast, rescue of d4TMP-terminated primers was about two times less efficient.

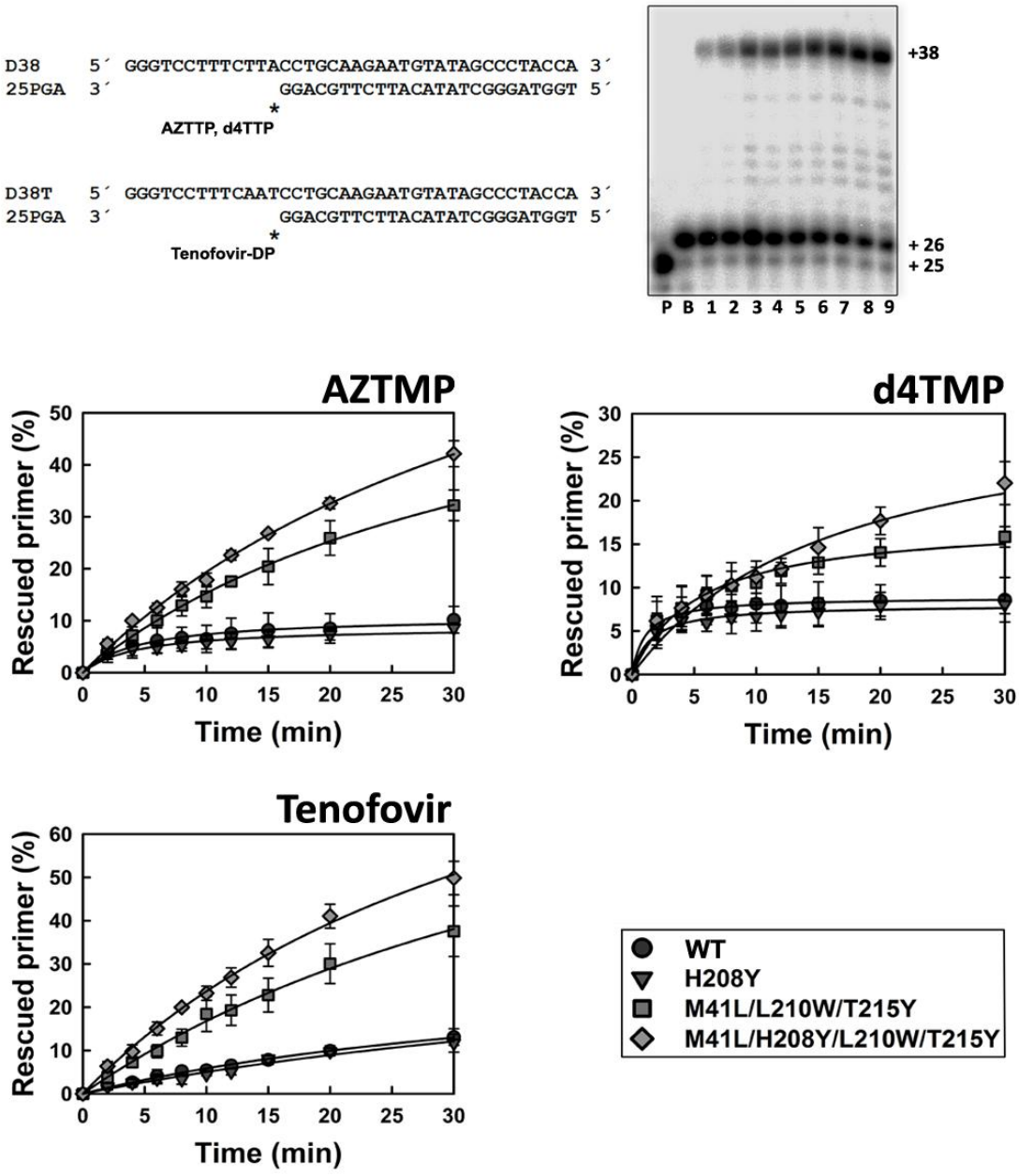

Fig 39. DNA rescue activity of WT and mutant RTs from AZTMP-, d4TMP- and tenofovir-terminated T/Ps. Reactions were carried out with D38/25PGA and D38T/25PGA complexes (sequences shown to the left of the gel). Primers (lane P) were blocked with a nucleot(s)ide analogue to generate a 26-nucleotide blocked primer (lane B). Excision of the inhibitor allows the extension of the primer to the final product of 38 nucleotides. Lanes 1 to 9 represent time points at 2, 4, 6, 8, 10, 12, 15, 20 and 30 min taken after adding a mixture containing all four dNTPs and ATP at a 3.2 mM concentration. Time course experiments of primer rescue reactions are shown below. T/P and active RT concentrations in these assays were 30 and 24 nM, respectively. Mean values ± standard deviations [error bars] were obtained from three independent experiments.

Interestingly, when rescue assays were carried out on AZTMP-, d4TMP- and tenofovir-terminated primers using the RNA/DNA complexes D38rna/25PGA and D38Trna/25PGA, we obtained different results than with DNA/DNA duplexes. Although the rescue activity of M41L/H208Y/L210W/T215Y RT was slightly higher than the activity of M41L/L210W/T215Y RT, differences were very small (Fig 40).

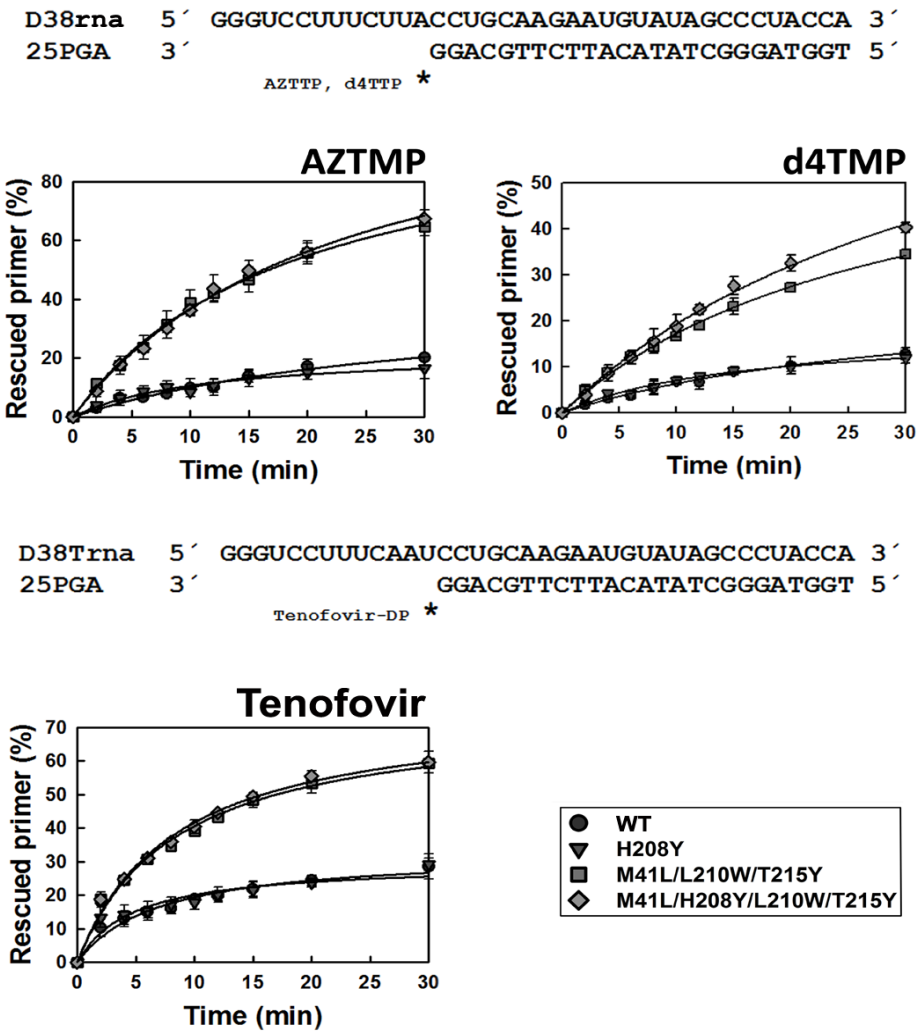

Fig 40. RNA-dependent rescue activity of primers blocked with AZTMP, d4TMP and tenofovir. Time course experiments of the excision reaction were carried out in the presence of 3.2 mM ATP. T/Ps used are indicated above their corresponding graphs. All dNTPs in the assays were supplied at 200 μM, except dATP or dTTP (depending on the assay) whose concentration was 2 μM. T/P and active RT concentrations in these assays were 30 and 24 nM, respectively. Mean values ± standard deviations [error bars] were obtained from three independent experiments.

4.2.2 Effect of H208Y in the RNase H activity of WT and mutant RTs

Reductions in the rescue efficiency of the M41L/L210W/T215Y/R284K RT compared with the M41L/L210W/T215Y RT in assays carried out with RNA/DNA complexes were attributed to its higher RNase H activity (see Fig 32). Therefore, we tested whether H208Y had a similar impact on RNase H cleavage with the 31Trna/21P complex (Fig 41). Interestingly, as in the case of R284K,

addition of H208Y to the M41L/L210W/T215Y complex produced an increase in RNase H cleavage rates. Thus, while M41L/L210W/T215Y RT showed a k_{obs} value of 0.41 ± 0.08 min^{-1}, addition of H208Y produced a two-fold increase in catalytic rate of the RNase H (k_{obs} 0.93 ± 0.013 min^{-1}). This observation could explain in part the reduced rescue efficiency of this enzyme on RNA/DNA complexes, due to the instability of the short RNA fragments rendered by the reaction. The WT RT displayed a catalytic rate of 0.62 ± 0.08 min^{-1}, a value intermediate between the M41L/L210W/T215Y and M41L/H208Y/L210W/T215Y enzymes.

In addition, secondary cleavages produced by the WT and mutant RTs were monitored by using the T35rna/PR26 RNA/DNA complex. Secondary cleavage events at positions -15, -12 and -10 of the template strand were observed. However, differences in cleavage efficiency between the two TAM-1-containing enzymes were undetectable (Fig 42).

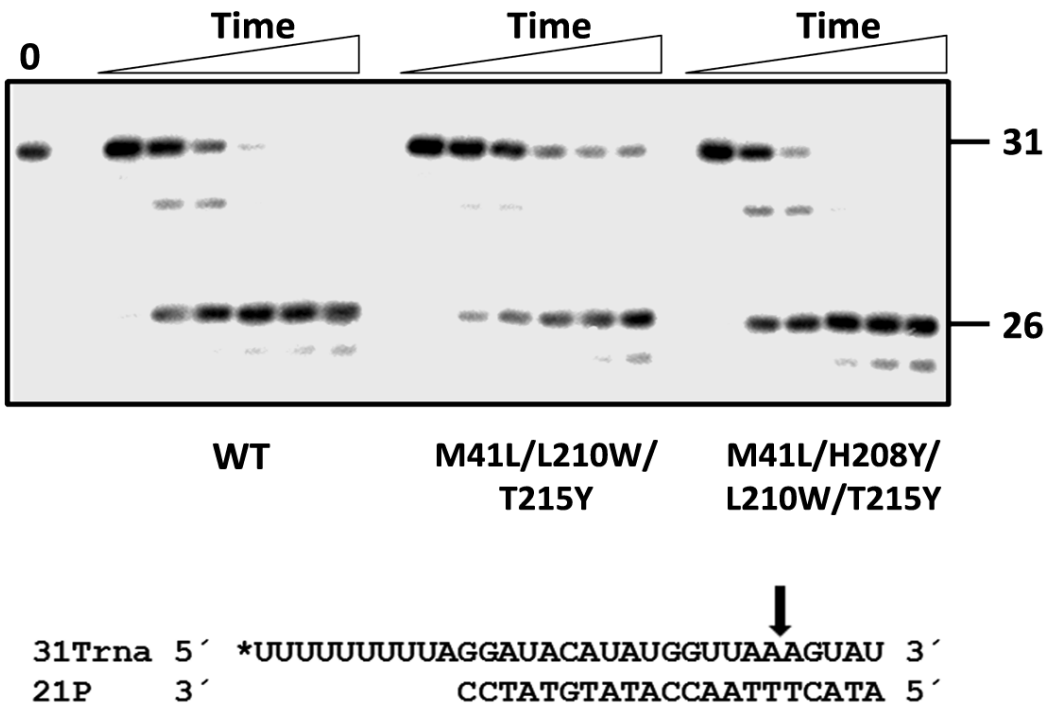

Fig 41. RNase H activity of WT and mutant RTs. [^{32}P]31Trna/21P (50 nM) cleavage was carried out in the presence of the corresponding RT at 50 nM (active enzyme concentration). Time points were taken after 20 s, 40 s, 1, 2, 3 and 4 min. Arrow in the RNA template sequence is used to indicate the cleavage site. Catalytic rate constants were 0.68 ± 0.04 min^{-1}, 0.41 ± 0.08 min^{-1} and 0.93 ± 0.13 min^{-1} for WT, M41L/L210W/T215Y and M41L/H208Y/L210W/T215Y RTs, respectively.

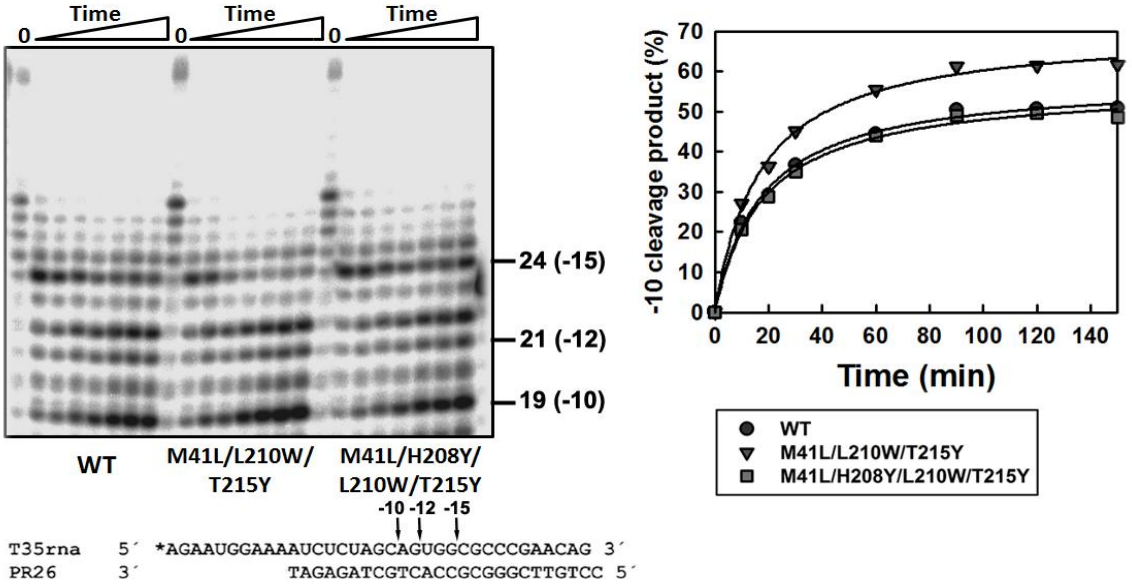

Fig 42. Secondary RNase H cleavage activity of WT and mutant RTs. The T35rna/PR26 complex (20 nM) was used to monitor the secondary cleavages displayed by WT and mutant RTs (200 nM). Aliquots were removed after 10, 20, 30, 60, 90, 120 and 150 min. Secondary cleavages occurring at -15, -12 and -10 are indicated in the T/P sequence, below the gel. Time course of the -10 cleavage event is shown on the right panel.

4.2.3 DNA binding affinity of WT and mutant RTs

D38/25PGA DNA/DNA complex binding affinity measurements of WT, H208Y, M41L/L210W/T215Y and M41L/H208Y/L210W/T215Y RTs showed no differences in K_d values between those RTs, with all of them showing K_d values around 2 nM (Table 16).

Table 16. Dissociation equilibrium constants for WT and mutant HIV-1 RTs and DNA/DNA T/Ps.

RT	K_d (nM)
WT	1,65 ± 0,48
H208Y	2,15 ± 0,59
M41L/L210W/T215Y	2,37 ± 0,65
M41L/H208Y/L210W/T215Y	2,65 ± 0,39

The sequence of the complex was:

```
D38    5´ GGGTCCTTTCTTACCTGCAAGAATGTATAGCCCTACCA 3´
25PGA  3´              GGACGTTCTTACATATCGGGATGGT 5´
```

Data reported are mean values ± standard deviations obtained from three independent experiments.

4.2.4 Rescue activity of WT and mutant RTs in the presence of different ribonucleotides

Previous studies have shown that GTP is a potent PPi donor, as least as potent as ATP (Meyer *et al.*, 1998). Rescue reactions with primers terminated with AZTMP were carried out in the presence of 9.6 mM GTP. Under these conditions, unlike in ATP-dependent excision reactions, there was a significant amount of rescued primer produced by the WT RT (Fig 43). The amounts of rescued

primer in reactions catalyzed by the M41L/L210W/T215Y RT were higher in the presence of 9.6 mM GTP than in the presence of 3.2 mM ATP. However, these differences were not observed with RTs having the H208Y substitution that showed similar rescue efficiencies with ATP than with GTP. Therefore, the rescue rates of AZTMP-terminated primers obtained in the presence of 9.6 mM GTP for the M41L/L210W/T215Y RT and the M41L/H208Y/L210W/T215Y RT showed only minor differences. Interestingly, the rescue activity of the WT RT under these conditions was slightly higher than the H208Y enzyme (Fig 43).

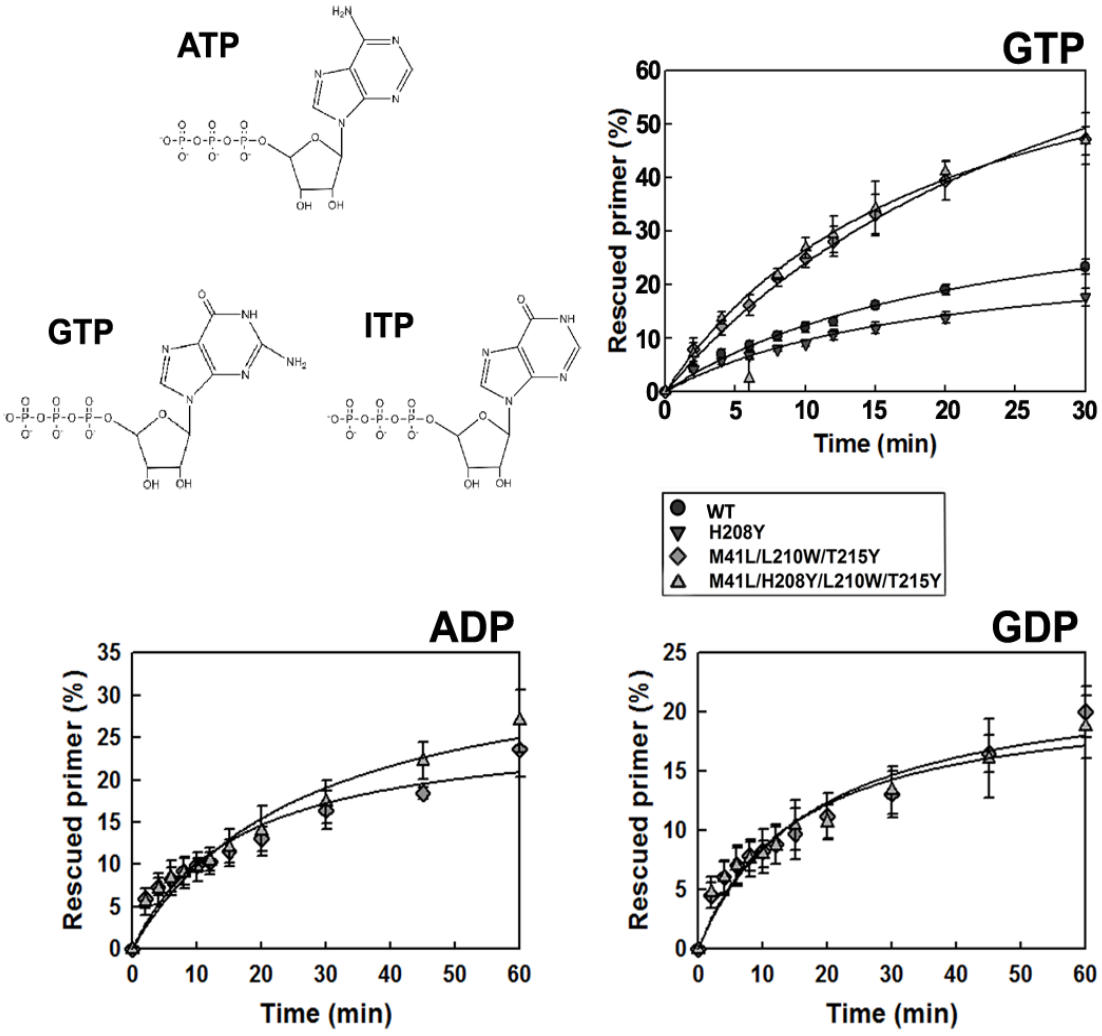

Fig 43. DNA rescue activity of WT and mutant RTs from AZTMP-terminated complexes in the presence of different ribonucleotides. Structures of ATP, GTP and ITP are illustrated in the top-left corner. Rescue assays with D38/25PGA^{AZTMP} T/Ps were carried out in the presence of 9.6 mM GTP, 9.6 mM GDP or 3.2 mM ADP. All assays were done in the presence of 30 nM T/P, 24 nM RT and 100 μM dNTPs, except for dATP, whose concentration was 1 μM.

Assuming that rescue efficiencies are dominated by the catalytic rate of the ribonucleotide-dependent excision reaction, we determined catalytic parameters (*i.e.*, k_{cat} and K_m) for ribonucleotides used as PPi donors in the unblocking reaction. Results are shown in Table 17. In reaction carried out

using ATP as a PPi donor, the catalytic rate (k_{cat}) of the excision reaction was significantly lower for mutant M41L/L210W/T215Y than for the M41L/H208Y/L210W/T215Y RT ($p < 0.05$, unpaired Student's *t* test). However these differences were not significant for GTP or ITP, suggesting that they could be related to the presence of an amino group at position 6´ of the purine ring, instead of an oxygen atom (as occurs in GTP or ITP).

Reactions carried out using ADP or GDP as PPi donors rendered lower amounts of rescued products than reactions carried out in the presence of nucleoside triphosphates (*i.e.*, ATP or GTP). No differences between the M41L/H208Y/L210W/T215Y RT and the M41L/L210W/T215Y enzyme were detected (Fig 43).

Table 17. Steady-state kinetics parameters of rescue reaction catalyzed by mutants M41L/L210W/T215Y and M41L/H208Y/L210W/T215Y.

RT	Pyrophosphate donor					
	K_m (mM)			k_{cat} (min^{-1})		
	ATP	GTP	ITP	ATP	GTP	ITP
M41L/L210W/T215Y	0.96 ± 0.12	2.26 ± 0.28	0.67 ± 0.08	1.77 ± 0.05	3.12 ± 0.17	0.95 ± 0.04
M41L/H208Y/L210W/T215Y	1.14 ± 0.12	1.92 ± 0.33	0.67 ± 0.1	2.14 + 0.06	2.79 ± 0.19	0.98 ± 0.03

Reported data are the mean values ± standard deviations, obtained from at least three independent experiments.

4.2.5 Pre-steady-state kinetics of ATP-dependent excision of primers terminated with AZTMP

We measured the ATP-dependent excision activity of WT and mutant RTs by using the D38/25PGA^{AZTMP} complex. Reactions were carried out at fixed 30 nM concentration of T/P in the presence of 3.2 mM ATP and with increasing concentration of RT ranging from 3.5 to 210 nM. In all cases, addition of H208Y produced an enhancement in the AZTMP excision efficiency of the M41L/L210W/T215Y RT (Fig 44). Additional support of these results was obtained from experiments carried out in the presence of 60 nM D38/25PGA^{AZTMP} and 21 nM RT, showing also an improved excision activity of the M41L/H208Y/L210W/T215Y RT (data not shown). Finally, as expected, experiments carried out using 21 nM RT and 3.2 mM GTP did not show significant differences between M41L/H208Y/L210W/T215Y and M41L/L210W/T215Y RTs (data not shown).

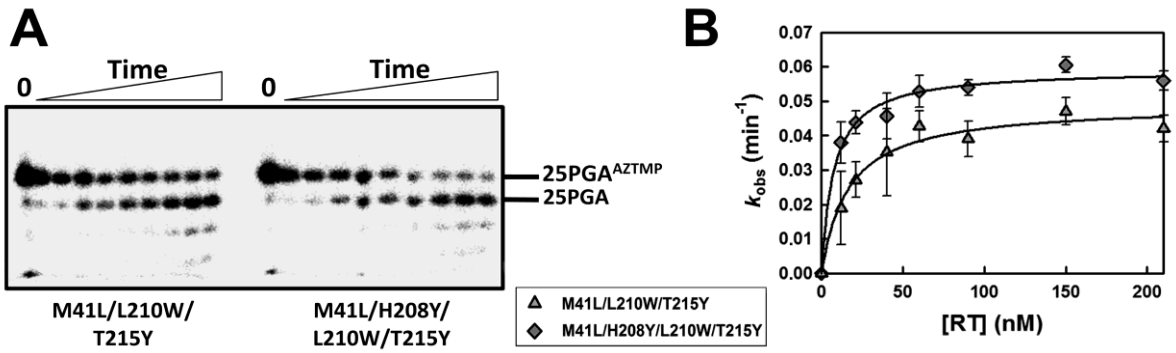

Fig 44. Kinetics of ATP-dependent excision of AZTMP from a blocked D38/25PGA^{AZTMP} T/P. (A) Representative gel showing the results of assays carried out in the presence of 3.2 mM ATP and mutant RTs (90 nM). (B) Dependence of the excision rate (k_{obs}) on the RT concentration was determined for mutants M41L/L210W/T215Y and M41L/H208Y/L210W/T215Y.

To further characterize the role of H208Y mutation in the excision reaction, kinetic parameters V_{max} (maximum velocity of the excision reaction) and K_m were determined by maintaining a fixed RT concentration of 21 nM and ranging D38/25PGA^{AZTMP} from 2.5 to 100 nM. As shown in Table 18, similar K_m values were obtained for M41L/H208Y/L210W/T215Y and M41L/L210W/T215Y RTs. However, the V_{max} of the M41L/H208Y/L210W/T215Y RT was significantly higher than V_{max} of the M41L/L210W/T215Y enzyme ($p < 0.05$, unpaired Student's *t* test).

Table 18. Steady-state kinetic parameters of the ATP-dependent excision reaction catalyzed by M41L/L210W/T215Y and M41L/H208Y/L210W/T215Y RTs.

RT	V_{max} (pM/min)	K_m (nM)
M41L/L210W/T215Y	648,1 ± 27,66	29,91 ± 2,81
M41L/H208Y/L210W/T215Y	713,8 ± 49,62	27,19 ± 4,3

Data shown are mean values ± standard deviations, obtained from at least three independent experiments.

4.2.6 Catalytic implications of the presence of the L210W mutation together with H208Y

To study the interaction between residues at positions 208 and 210 we decided to revert the L210W mutation to the wild-type amino acid Leu-210 and to check the rescue ability of the resulting M41L/H208Y/T215Y RT. As control, mutants M41L/T215Y, M41L/L210W/T215Y and M41L/H208Y/L210W/T215Y were incorporated in the assays. As expected, AZTMP rescue assays carried out in the presence of 9 mM GTP showed that all four mutant RTs were equally efficient in the rescue of AZTMP-terminated primers (Fig 45A). However, when 3.2 mM ATP was used as PPi donor, H208Y conferred increased rescue ability only when accompanied by L210W (Fig 45A). When D38rna/25PGA was used as T/P, all mutant RTs (*i.e.*, M41L/T215Y, M41L/H208Y/T215Y, M41L/L210W/T215Y and M41L/H208Y/L210W/T215Y) showed a similar efficiency in the rescue of AZTMP-blocked primers (Fig 45B).

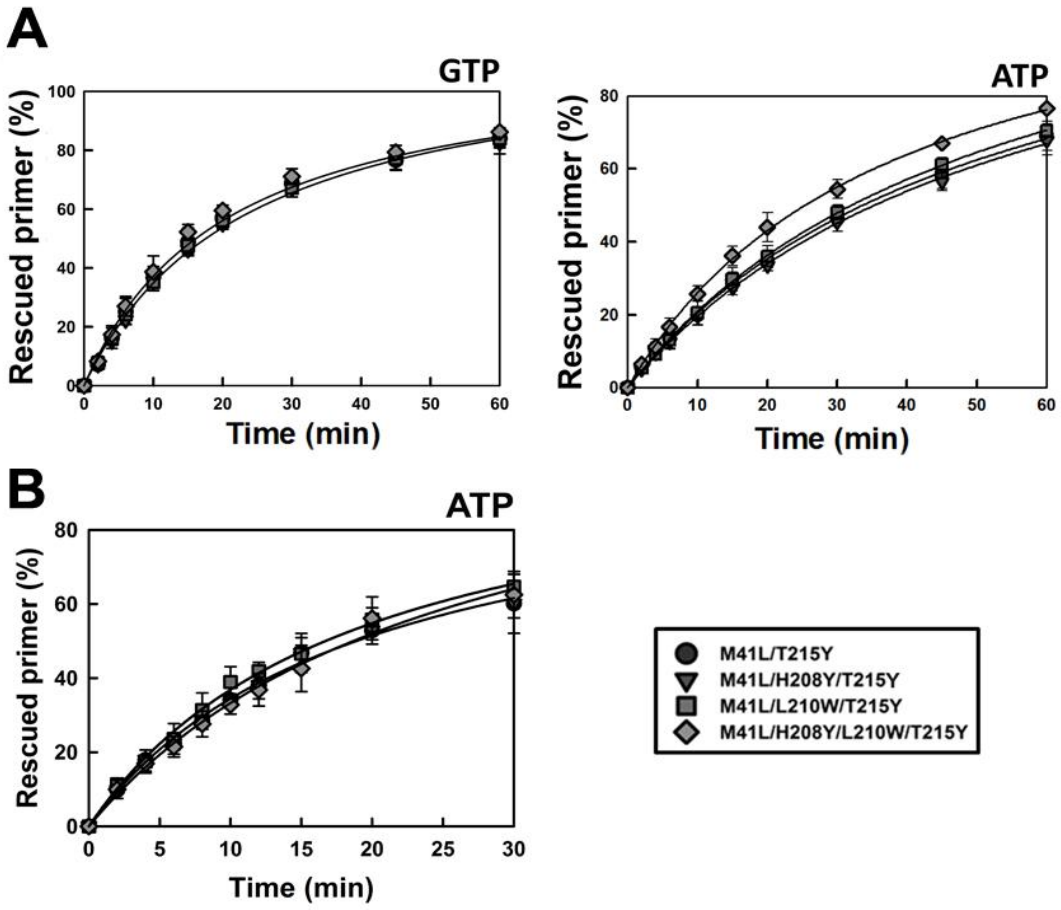

Fig 45. Contribution of L210W mutation on the DNA- and RNA-dependent rescue activity of the M41L/H208Y/L210W/T215Y RT. Rescue activity of M41L/T215Y, M41L/H208Y/T215Y, M41L/L210W/T215Y and M41L/L210W/H208Y/T215Y mutant RTs on AZTMP-terminated primers. (A) The D38/25PGA^{AZTMP} complex (30 nM) was mixed with 30 nM active RT concentration and the rescue activity reaction was then initiated by adding a mixture containing all four dNTPs, and 9 mM GTP (left) or 3.2 mM ATP (right). (B) RNA-dependent rescue activity of M41L/H208Y/T215Y, M41L/L210W/T215Y and M41L/H208Y/L210W/T215Y mutant enzymes was monitored by using D38rna/25PGA^{AZTMP}-blocked complexes in the presence of 3.2 mM ATP and the four dNTPs.

4.3 Role of connection subdomain mutations in resistance to non-nucleoside RT inhibitors

The increasing complexity of antiretroviral treatments and suboptimal therapies have lead to the accumulation of primary and accessory resistance mutations in the HIV genome. Since the mid-90s antiretroviral therapies were based on the combination of one or two NRTIs and one NNRTI and/or one protease inhibitor. Therefore, NNRTI resistance mutations have been frequently found in treated patients. Classical NNRTI resistance mutations locate around the NNRTI binding pocket. However, accumulating data obtained from viral sequences from treated patients have shown that mutations located far from this pocket could also play a role in drug resistance. For example, recent studies have demonstrated that certain mutations in the RT connection subdomain could increase the IC_{50} for certain NNRTIs (Gupta *et al.*, 2010, 2011). In order to determine the molecular mechanism/s

implicated in the selection of resistance mutations in the connection subdomain, HIV-1 RTs bearing mutations T369I, T369V, T376S and N348I/T369I were purified and characterized. In addition, mutant enzyme N348I was added to the study as control, since this mutation has been previously characterized as a substitution contributing to increasing nevirapine resistance (Biondi *et al.*, 2010; Schukman *et al.*, 2010; Radzio & Sluis-Cremer, 2011).

4.3.1 Determination of the half maximal inhibitory concentration (IC_{50}) for NVP, EFV and ETR

DNA polymerase activity of WT and mutant RTs was measured by determining single-nucleotide incorporation kinetics. None of the connection subdomain mutations produced an effect in the catalytic rate of nucleotide incorporation of the RT, since k_{cat} values for WT and mutant RTs N348I, T369I, T369V, T376S and N348I/T369I were in the range of 0.8 min^{-1} to 1.16 min^{-1} (data not shown).

Then, we determined the impact of N348I, T369I, T369V, T376S as well as the combination N348I/T369I in NNRTI resistance by measuring the IC_{50} for different NNRTIs in DNA polymerization assays. For this purpose, the heteropolymeric DNA/DNA complex D38/25PGA was incubated with WT and mutant RTs in the presence of increasing concentrations of NVP, EFV or ETV and dTTP, and the amount of extended 26-nucleotide long primer was determined. Data obtained are given in Table 19. IC_{50} values obtained with the WT enzyme were similar for all NNRTIs and were in the range of 2.7 to 5 µM. All mutant RTs showed similar susceptibilities to EFV and ETR in comparison with the WT enzyme, with IC_{50} values in the range of 3.2 to 6.2 µM. However, in the case of NVP, we observed significant differences in the IC_{50} values between WT and mutant RTs. Thus, mutants T369V and T376S displayed the lowest IC_{50} values of all mutant RTs, which were 2.8 and 3.5 times higher, respectively, compared with the IC_{50}s obtained with the WT RT. Mutants N348I and T369I showed an intermediate level (5.5- and 5.2-fold increase in resistance, respectively). Finally, the double-mutant N348I/T369I displayed the highest level of NVP resistance, showing an IC_{50} value 7.8 times higher than the IC_{50} obtained with WT RT (Table 19).

Table 19. Inhibition of WT and mutant RTs by NNRTIs.

	IC_{50} (µM)		
RT	**NVP**	**EFV**	**ETR**
WT	2.7 ± 1.1	5.0 ± 1.9	3.2 ± 0.4
N348I	14.8 ± 3.4	5.5 ± 2.1	4.6 ± 0.8
T369I	9.4 ± 2.0	5.4 ± 2.2	4.8 ± 1.2
T369V	14.2 ± 3.9	4.5 ± 1.8	3.4 ± 0.5
T376S	7.6 ± 2.6	5.9 ± 1. 8	4.3 ± 0.9
N348I/T369I	21.0 ± 6.8	6.2 ± 2.4	5.2 ± 0.9

Data shown are mean values ± standard deviations, from at least three independent experiments.

4.3.2 Role of connection subdomain mutations in NNRTI resistance during different steps of reverse transcription

Recent reports suggested a novel NVP resistance mechanism relevant during PPT extension in (+) strand DNA synthesis. This mechanism implies a role for NVP in modulating how RT binds the PPT primer; either in a polymerase-dependent binding mode or in the RNase H-dependent binding mode (Fig 46). According with the proposed mechanism, while the WT enzyme is pushed by the NVP to bind in an RNase H-dependent binding mode, triggering the cleavage of the RNA portion of the DNA-RNA primer, and consequently blocking (+) strand DNA synthesis, the N348I mutation would favour the DNA polymerase-dependent binding mode (Fig 46) (Biondi *et al*, 2010).

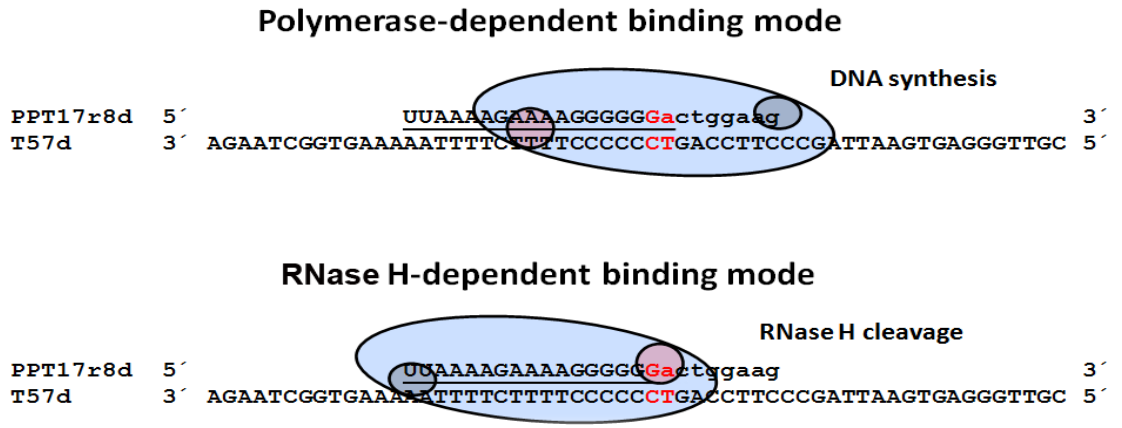

Fig 46. RT binding orientations on PPT-RNA/DNA complexes. Schematic representation of the two binding modes of the RT to an intermediate of the (+) strand DNA synthesis. The T/P (T57d/PPT17r8d) contains a large DNA template annealed to a chimeric RNA-DNA primer, with a 5´-RNA region (in uppercase and underlined), involving the PPT sequence, and a 3´-DNA region (lowercase) representing 8 nucleotides incorporated during the DNA synthesis. The PPT-U3 junction cleavage point is highlighted in red in the sequence. The RT is represented by a big blue oval and the polymerase and RNase H active sites as light blue and pink circles, respectively. Polymerase-dependent binding mode promotes primer elongation while RNase H-dependent binding mode produces the RNase H cleavage of the primer.

4.3.2.1 Determination of the RNase H activity using a physiological relevant intermediate of the (+) strand DNA synthesis

In order to check if the connection subdomain mutations studied could impact NNRTI resistance by using a similar mechanism, the endonucleolytic activity of WT and mutant RTs were determined with a series of PPT-RNA/DNA complexes mimicking the (+) strand DNA synthesis initiation complex (Fig 47). Incubation of the T57d/PPT17r8d complex with the WT and mutant RTs resulted in the production of RNase H cleavage products of 17, 16, and sometimes 15 nucleotides (Fig 47A). The product of 17 nucleotides is the physiologically relevant cleavage product, resulting from the cleavage at the PPT-U3 junction. Subsequent cleavage of this oligonucleotide renders bands representing oligonucleotides of 16 and 15 nucleotides. It is important to note that all cleavages generated from this T/P result from the RNase H-dependent binding mode of the RT. An alternative

binding orientation (*i.e.*, polymerase-dependent binding mode) implies that the RNase H active site would interact with the DNA template (Fig 46).

Interestingly, according with the obtained RNase H catalytic rates, tested enzymes could be classified in three groups. WT, T369V, T369I and T376S RTs showed high RNase H activity, with k_{obs} values between 0.72 and 1.25 min^{-1} (Fig 47A). The N348I RT, showed an intermediate RNase H activity with a k_{obs} of 0.36 min^{-1}. Finally, the double-mutant N348I/T369I showed the lowest RNase H cleavage rate, with a value of 0.07 min^{-1}. These results indicate that the reduced RNase H catalytic activity of the N348I mutant RT could be further decreased by the presence of T369I.

Further characterization of this important step in reverse transcription involved usage of a second T/P complex. This complex that contains a 17-nucleotide RNA primer (PPT29DNA/PPT17r) mimics the initiation of (+) strand DNA synthesis, where no dNTPs have been incorporated at the 3´-end of the primer (Fig 47B). WT, N348I and N348I/T369I RTs were incubated in the presence of this complex. Interestingly, unlike in the case of PPT17r8d none of the enzymes were able to cleave the RNA primer (Fig 47B).

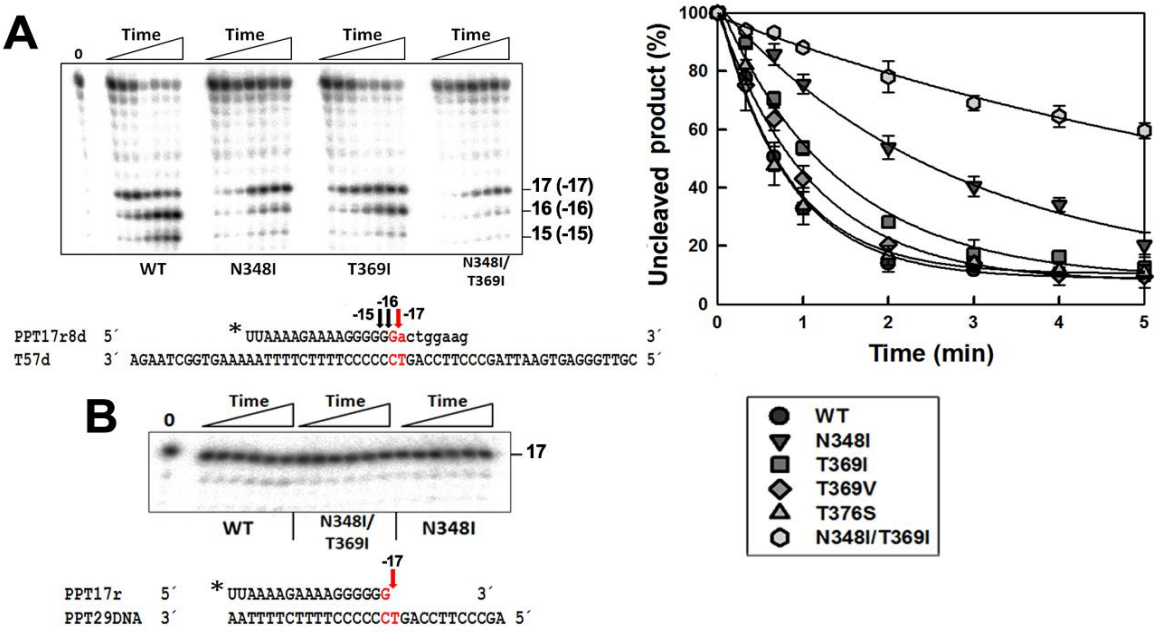

Fig 47. RNase H activity of WT and mutant enzymes during (+) strand DNA synthesis (A) Representative gel of RNase H kinetics obtained using the T57d/PPT17r8d complex. T/P complex T57d/PPT17r8d mimics a (+) strand DNA synthesis intermediate where 8 dNTPs have been added to the 17-nucleotide PPT-RNA primer. This complex (25 nM) was incubated with WT and mutant enzymes at 125 nM concentration. Aliquots were removed at 20 s, 40 s, and 1, 2, 3, 4 and 5 min. Cleavages at positions -16 and -15 in the PPT17r8d strand are indicated with black arrows, while the -17 cleavage at the PPT-U3 junction is marked with a red arrow. Likewise, bands produced by such cleavages are indicated in the gel. A graphic representation of the time course kinetics of the reaction is shown on the right (data were obtained from three independent experiments). (B) RNase H activity of WT, N348I/T369I and N348I mutant enzymes on a PPT29DNA/PPT17r complex. This complex represents the first step in the (+) strand DNA synthesis, where no dNTPs have been yet added. In the sequence, the last PPT ribonucleotide is highlighted in red, as well as the PPT-U3 cleavage point with a red arrow, for direct comparison with the PPT/17r8d complex.

Analysis of the integrity of the PPT17r8d primer.

The expected cleavage product resulting from the release of the DNA segment of the PPT17r8d primer should have 17 nucleotides. However, band-patterns obtained seemed to correspond with a cleavage product 7 nucleotides shorter. To verify than the 25-nucleotide long substrate had the right size, it was incubated in the presence of recombinant Exo I from *E. coli* (Affimetrix), and the 3´ to 5´ exonuclease reaction monitored over time. Results shown in Fig 48A indicate that the Exo I enzyme eliminated all dNMPs to produce a 17-nucleotide RNA oligonucleotide (PPT17r). Comparison of the digestion products with the PPT17r primer showed that bands corresponding to the 17-nucleotide product and those corresponding to the 17-nucleotide-RNA elongated after addition of one dNTP migrated very close to each other (Fig 48A).

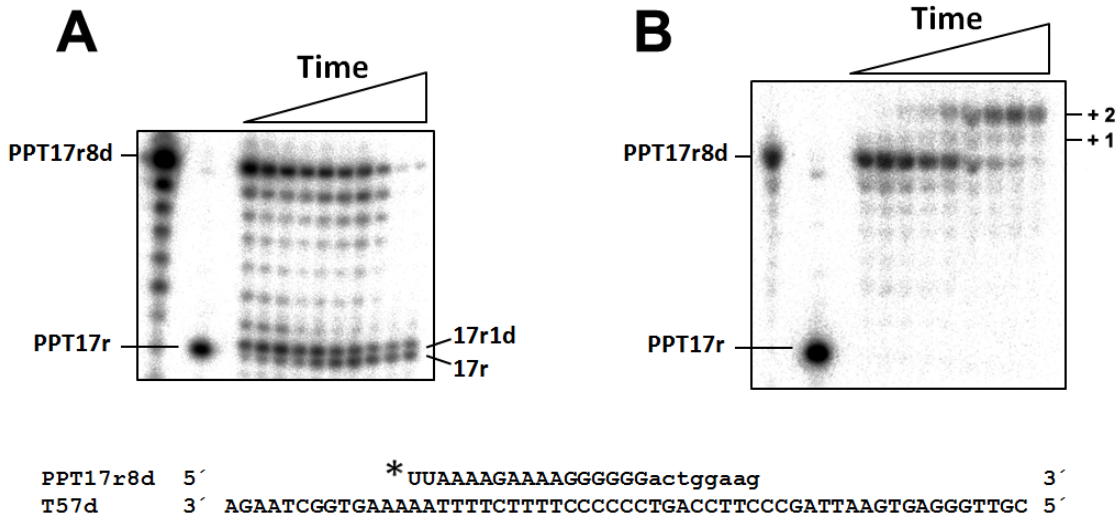

Fig 48. Sequence analysis of the PPT17r8d primer. (A) PPT17r8d primer was subjected to *E. coli* Exo I digestion and the resulting products revealed in a polyacrylamide gel. Bands corresponding to the intact PPT17r8d, PPT17r and PPT17r1d are indicated. (B) T57d/PPT17r8d (25 nM) was mixed with the RNase H-deficient HIV-1 group O mutant V75I/E478Q RT (100 nM active enzyme). Synthesis reactions were initiated by adding 100 μM dGTP and 50 μM CBVTP. Bands corresponding with the unextended primer and those corresponding to primers extended in one or two nucleotides indicated.

Further confirmation of the composition of the PPT17r8d primer was obtained by incubating the preformed T57d/PPT17r8d complex with the RNase H-deficient mutant HIV-1 group O RT V75I/E478Q in the presence of dGTP and CBVTP. A correct complex should be a good substrate for the incorporation of dGMP in the next two positions (Fig 48). Therefore if PPT17r8d had the right size, two incorporation events would be expected. As shown in Fig 48B, at the longest incubation times, a product of 27 nucleotides was obtained, thereby confirming the correct length of the primer.

4.3.2.2 Effects of NVP and EFV in RNase H activity during (+) strand DNA synthesis.

PPT17r8d cleavage by the RNase H activity of WT and mutant enzymes was monitored in the presence of increasing concentrations of NVP and EFV. As shown in Fig 49A, EFV was efficient in

promoting the cleavage of the PPT-containing strand. It should be noted that although total amount of RNase H-hydrolyzed product was highly variable among tested enzymes, enhancement of the RNase H activity by EFV occurred with all RTs.

A representative example of the experiments carried out in the presence of increasing concentrations of NVP is presented in Fig 49B. As observed with EFV, we detected different amounts of cleavage products represented by bands of 17, 16 and 15 nucleotides. Interestingly, under our assay conditions, NVP showed to be a more potent enhancer of the RNase H activity than EFV, since lower concentrations of the inhibitor led to large accumulations of cleavage products (Fig 49B). This effect was observed with all tested RTs, independently of their mutational background. Therefore, NVP and EFV promoted RNase H cleavage catalyzed by HIV-1 RTs (Fig 49C).

Kinetics of RNase H cleavage by WT and mutant RTs in the presence of NVP and EFV

Experiments shown in Fig 49 represented single aliquots taken at 20 s for each NNRTI concentration. However, more accurate determinations on the effect of the inhibitors in the RNase H function of the RT can be obtained from time course experiments. This was done by measuring PPT17r8d cleavage for each RT in the presence of NVP or EFV concentrations that would significantly enhance the RNase H activity of the enzymes (*e.g.*, 5 μM and 12.5 μM, respectively). Consistent with previous results, all tested RTs showed higher RNase H activity in the presence of both inhibitors (Fig 50). Similar results were obtained in RNase H cleavage determinations carried out in the presence of 15 μM ETR (data not shown). The amount of cleaved product observed in the presence of 12.5 μM EFV was somewhat higher than in the presence of 5 μM NVP, although differences were not significant. Interestingly, in the presence of drugs, RNase H activities of WT and mutant N348I/T369I RTs were rather similar, although in the absence of RT inhibitor the double-mutant showed very low activity (Fig 50). These results suggest that the RNase H activity of both enzymes was maximal at the tested NNRTI concentrations. Therefore, these results further confirm the ability of NVP and EFV to foster the cleavage of the PPT17r8d substrate of all tested RTs.

When the T/P complex PPT29DNA/PPT17r was used in the same type of experiments, different results were obtained. Thus, while in the absence of NNRTIs, the complex PPT29DNA/PPT17r was not a substrate for the RNase H activity of WT, N348I/T369I and N348I enzymes, addition of NVP and especially EFV produced a strong stimulation of cleavage of the PPT17r oligonucleotide to produce bands of 16 and 15 nucleotides. The WT RT showed the highest RNase H activity in the presence of the drugs (Fig 50). In contrast, mutant N348I/T369I was not affected by the addition of 5 μM NVP, while EFV had only a small stimulatory effect of its endonucleolytic activity (Fig 50).

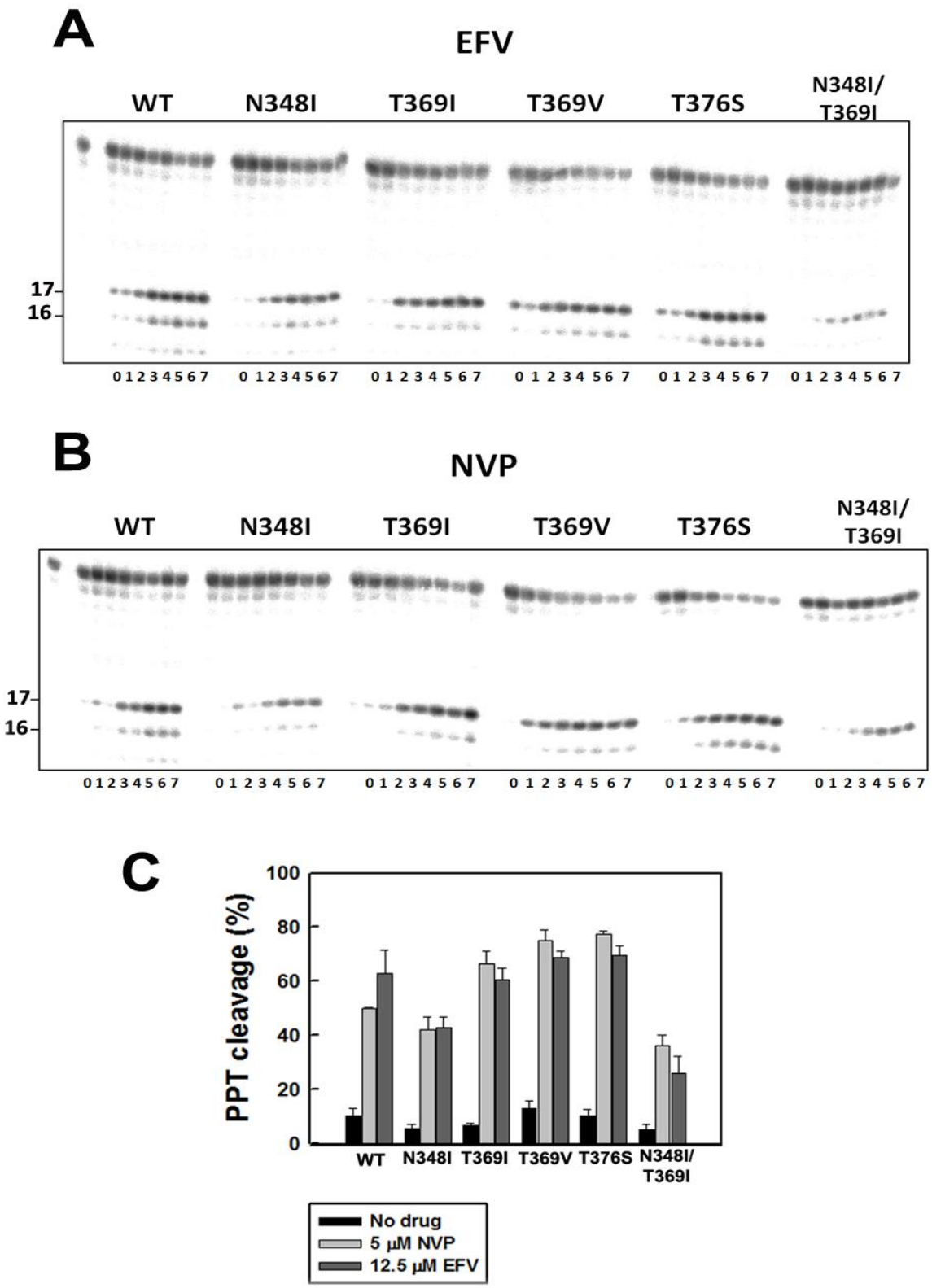

Fig 49. Effects of NVP and EFV in the RNase H activity of WT and mutant RTs. T57d/PPT17r8d concentration was 25 nM while RTs were supplied at 125 nM. (A) Lanes 0 to 7 below each enzyme reaction correspond to EFV concentrations 0, 0.63, 1.25, 2.5, 3.75, 5, 7.5 and 12.5 µM. (B) Same as (A) but NVP was supplied at 0, 0.08, 0.16, 0.32, 0.63, 1.25, 2.5 and 5 µM, corresponding with lines 0 to 7, respectively. (C) Graphical representation of the percentage of PPT17r8d primer cleavage by WT and mutant RTs in the absence of drug, or in the presence of 5 µM NVP or 12.5 µM EFV.

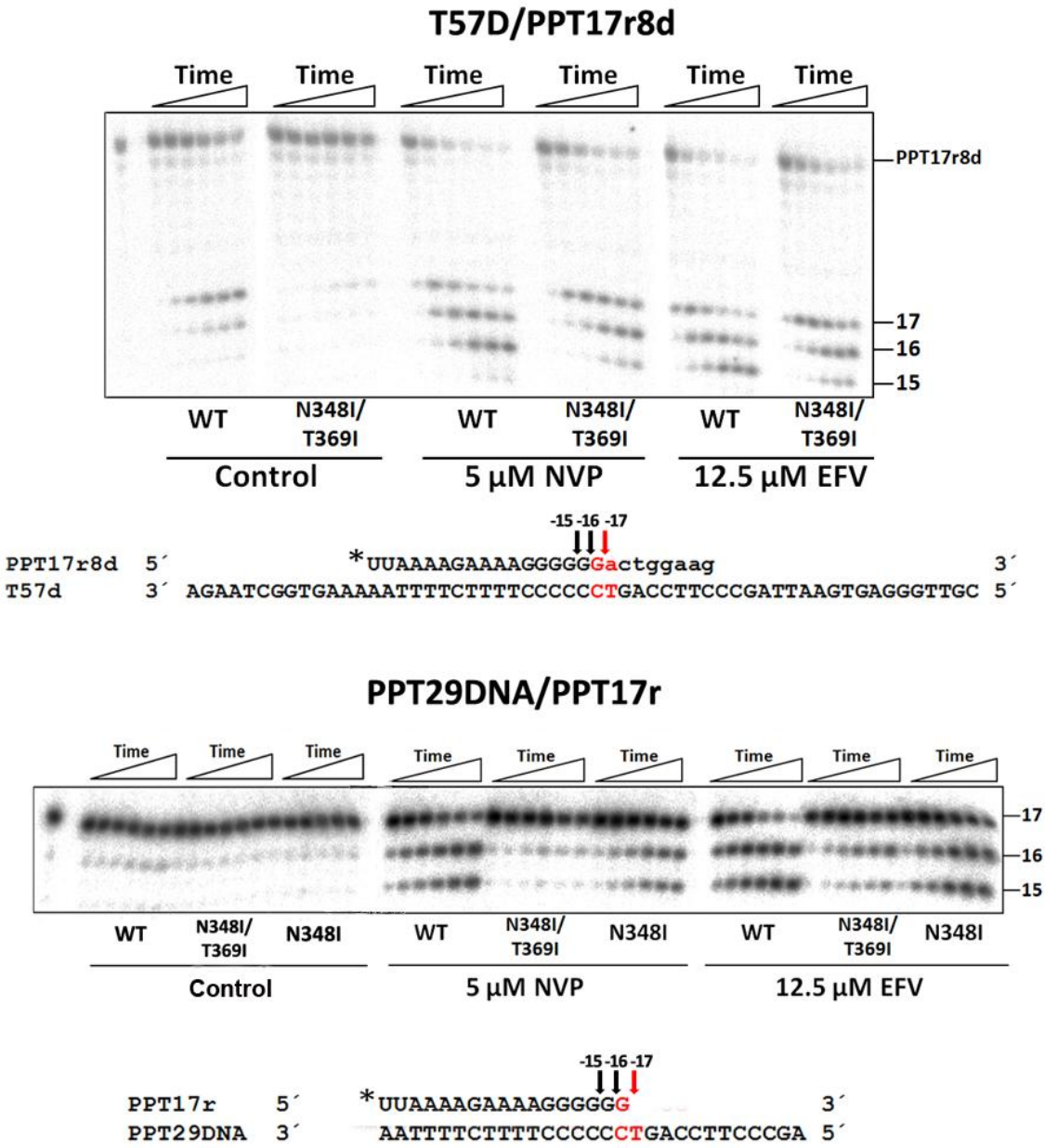

Fig 50. Kinetics of T57d/PPT17r8d and PPT29DNA/PPT17r cleavage in the presence of NVP and EFV. WT, N348I and/or N348I/T369I RTs (50 nM) were mixed with 25 nM of T57d/PPT17r8d or PPT29DNA/PPT17r complex and the cleavage of the RNA strand monitored in the presence of 5 µM NVP, 12.5 µM EFV, or in the absence of drug. Aliquots were removed at 20 s, 40 s, and 1, 2, 3, and 4 min. Cleavage products corresponding to bands of 17, 16 and 15 nucleotides are indicated in the gel.

4.3.2.3 Determination of the RNase H activity using different intermediates in which the PPT sequence acts as a template

PPT29RNA/PPT29DNA

PPT29RNA/PPT29DNA is a PPT-containing RNA template annealed to a DNA primer with a recessed 3´-OH end. This complex takes advantage of the preference of the RT to bind a recessed DNA 3´-end. Therefore, RT will bind the PPT29RNA/PPT29DNA complex in the DNA-polymerase binding mode. In this orientation the PPT-U3 junction between nucleotides G and A is positioned 17

nucleotides away from DNA 3´-end, exactly at the same location of the RNA-DNA junction in the T57d/PPT17r8d complex (Fig 51).

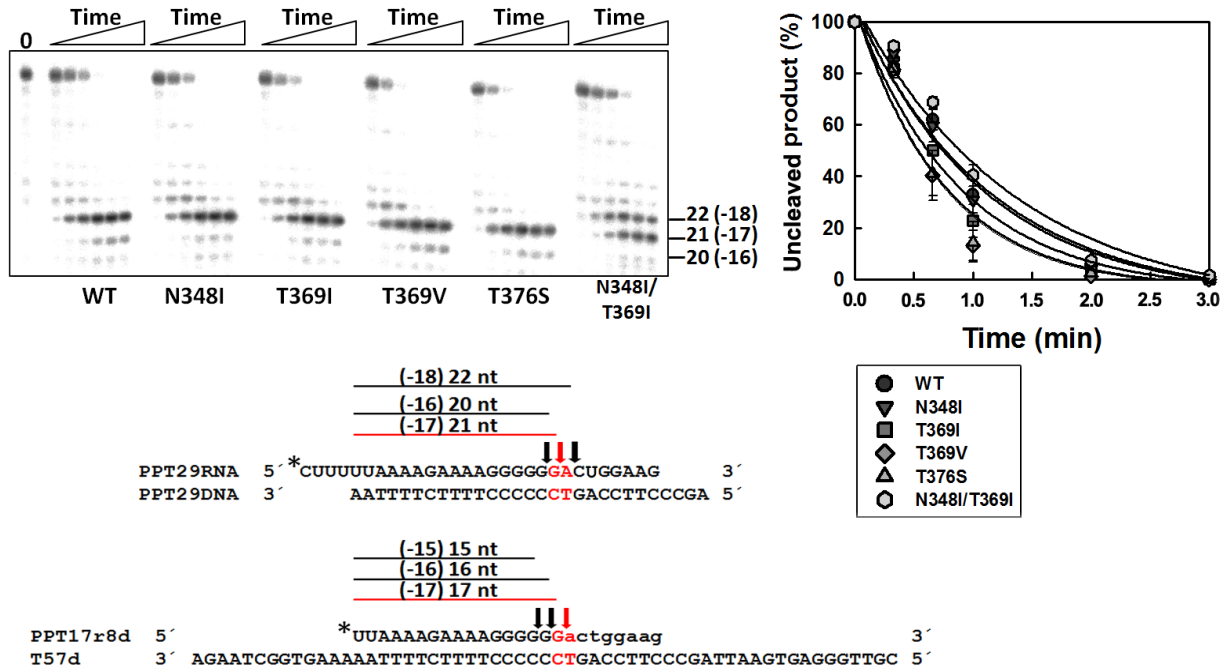

Fig 51. RNase H activity of WT and mutant RTs while using the PPT sequence as a template for DNA synthesis. T/P complex PPT29RNA/PPT29DNA mimics a (-) strand DNA synthesis intermediate where the PPT has not been yet cut to produce the PPT primer. In addition, this complex has a DNA 3´-end available for RT binding, therefore, RT binds this complex in a DNA polymerase-dependent binding mode. PPT29RNA/PPT29DNA (25 nM) was incubated with 50 nM of the corresponding RT and the RNase H cleavage products quantified. Aliquots were removed at 20 s, 40 s, and 1, 2, 3, and 4 min. PPT-U3 cleavage at position -17 renders a product of 21 nucleotides. Additional cleavages in its vicinity are indicated in the gel. To facilitate the comparison between PPT29RNA/PPT29DNA and T57d/PPT17r8d, their sequences are depicted below the gel, with the PPT-U3 cleavage site indicated with a red arrow and the neighboring cleavage sites by black arrows. Above each complex, a red (PPT-U3 cleavage) or black lines (no-specific cleavages) are shown to illustrate nucleotide cleavage distances and resulting products. On the right, a graphic representation of a time course kinetics obtained for each enzyme, determined from three independent experiments (means ± standard deviations [error bars]) are shown.

RNase H activity measurements using PPT29RNA/PPT29DNA T/P, and based on the disappearance of the 29 nucleotide band, showed that T369V and T376S were the RTs with the highest activity, followed by the T369I RT. The N348I RT and the WT enzyme showed similar kinetics, and the double-mutant N348I/T369I was the RT with the lowest activity (Fig 51). However, we also observed remarkable differences affecting the sizes of the reaction products. Thus, the WT RT and mutants T369V and T376S only rendered a product of 21 nucleotides, corresponding to the canonical cleavage event at position -17, also observed in T57d/PPT17r8d processing. However, all

the enzymes mutated in the 348 residue (and in a lesser extend the T369I mutant) produced the band of 21 nucleotides, but together with another one that was one nucleotide longer that corresponded to a cleavage at position -18 (Fig 51). This was particularly evident in the case of the double-mutant N348I/T369I RT, where the -18 band was the major product of the reaction, particularly at the earliest time points of the assay. Therefore, although RNase H cleavage kinetics were similar for all enzymes, resulting products showed a clearly distinct preference regarding the preferred cleavage sites.

One interesting conclusion drawn from the aforementioned results is that N348I/T369I RT preferred to cut the RNA 18 nucleotides away from the polymerase active site, while the preferred cleavage site of WT RT was one nucleotide closer, at the PPT-U3-conserved junction. In principle, these differences between WT and mutant N348I/T369I RT should not have a large impact in viral fitness, since products should be functional in both cases. However, the PPT17r8d primer annealed to the T57d template can be cleaved only at positions -17, since the -18 position falls within the DNA moiety of PPT17r8d. A reduced ability of the N348I/T369I enzyme to cut at position -17 could explain its reduced cleavage efficiency at the PPT-U3 junction in the T57D/PPT17r8d complex. However, as shown in Fig 50, the presence of NVP or EFV facilitates cleavage at -17 position by the N348I/T369I mutant RT, thereby generating a very similar band pattern in comparison with WT RT (Fig 50).

We tested whether NVP and EFV had similar effects on RNase H cleavage patterns produced by N348I/T369I and WT RTs on the T/P PPT29RNA/PPT29DNA. As shown in Fig 52, the 29-nucelotide band disappeared rapidly in the presence of both inhibitors, slightly faster with EFV than with NVP. Interestingly, new cleavage products, not present in the absence of NNRTIs, of 27 (-23 position), 26 (-22 position) and 24 (-20 position) nucleotides appeared upon NVP and EFV addition (Fig 52). While the WT RT yielded processed products corresponding to cleavages at positions -16 and -15, the N348I/T369I RT only produced a small amount of the -16 cleavage product at the largest time points (Fig 52). These results showed that NVP and EFV were able to accelerate the cleavage of the PPT29RNA/PPT29DNA complex as much as the T57d/PPT17r8d duplex in reactions catalyzed by both enzymes. However, the WT RT was able to produce further cleavages at -16 and -15, while the N348I/T369I RT was much less efficient in making these shorter cuts.

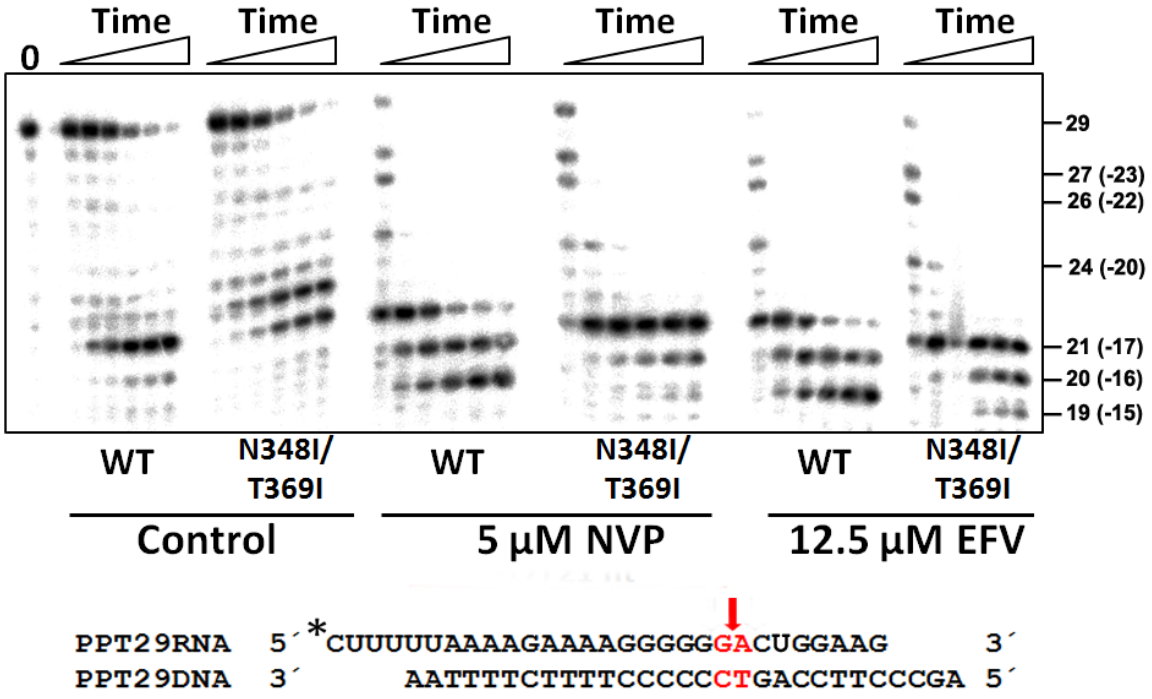

Fig 52. Time course of RNase H cleavage in the presence of NVP and EFV using T/P PPT29RNA/PPT29DNA. WT and N348I/T369I RTs (50 nM) were mixed with 25 nM of the PPT29RNA/PPT29DNA complex (sequence below the gel with the PPT-U3 cleavage site indicated with a red arrow) and the cleavage of the PPT29RNA template was then monitored in the absence of drug (control) or in the presence of 5 µM NVP or 12.5 µM EFV. Aliquots were removed at 20 s, 40 s, and 1, 2, 3, and 4 min. Cleavage products corresponding to the cut at the PPT-U3 junction (-17 position, product of 21 nucleotides) and those rendering one and two nucleotides shorter products (at positions -16 and -15) are indicated in the gel.

PPT29RNA/PPT28DNA

The presence of mutations N348I and T369I seem to impair the ability of the RT to carry out cleavages at positions closer to the DNA polymerase active site. This particular phenotype could be affecting the adequate processing of the PPT primer. In order to test this hypothesis, we used a T/P complex identical to PPT29RNA/PPT29DNA, but with a DNA primer one nucleotide shorter at its 3´-end. This new T/P (PPT29RNA/PPT28DNA) positions the scissile GA dinucleotide one nucleotide closer to the DNA 3´-end and therefore restricts cleavage to the -16 position (Fig 53). This restriction reduced the cleavage rate for all tested enzymes by half in comparison with those obtained with PPT29RNA/PPT29DNA (Fig 53). Interestingly, while all the RTs yielded the canonical 21-nucleotide band product (-16 cleavage), N348I/T369I RT and in a lesser extend the N348I mutant enzymes also produced bands of 23 and 24 nucleotides, corresponding to cleavages at positions -18 and -19, respectively (Fig 53). In the case of N348I/T369I RT, these products were more frequent than the 21-nucleotide product in all time points, further demonstrating the expanded cleavage window of this enzyme compared with the rest of the RTs.

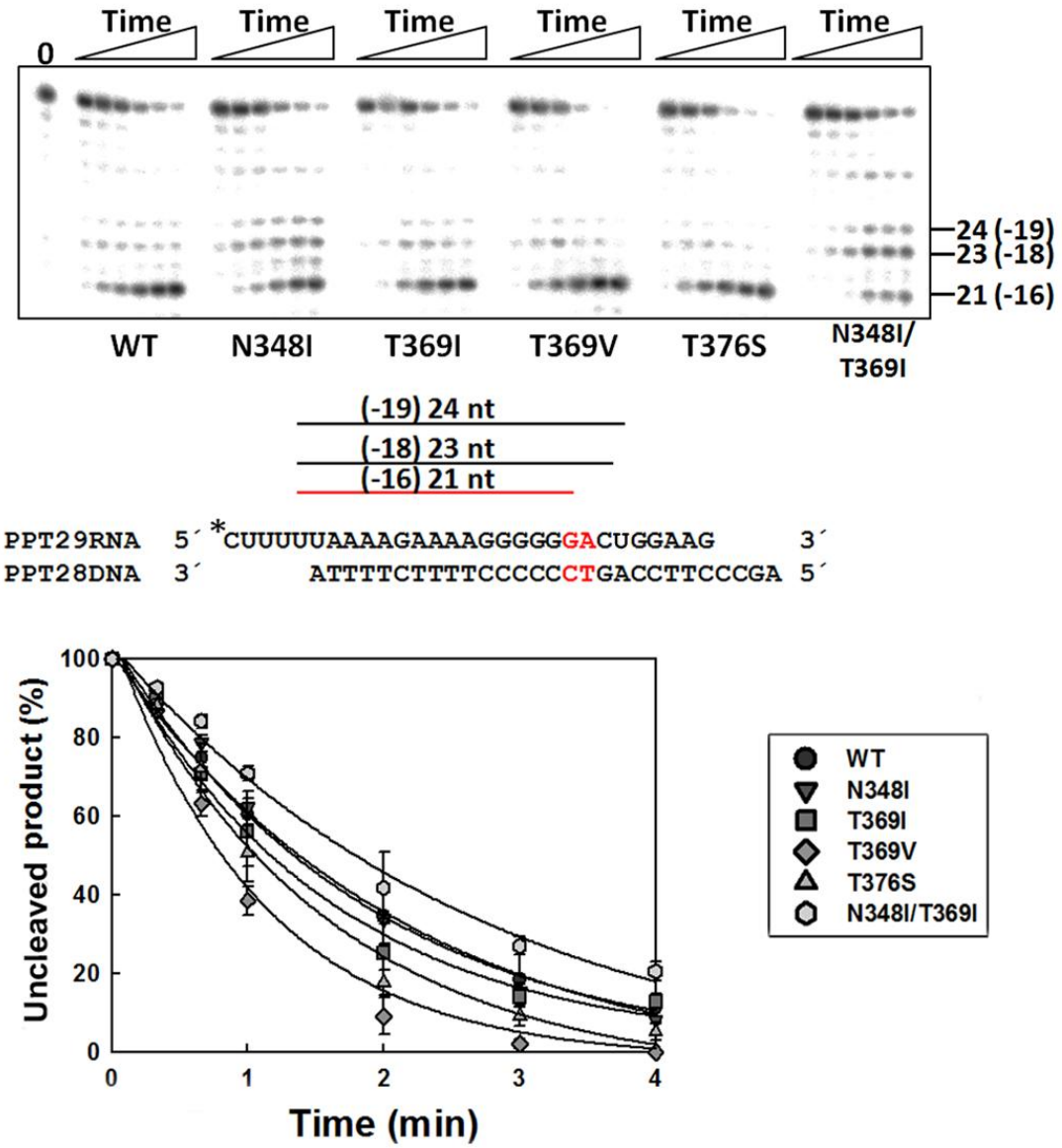

Fig 53. Effect of the cleavage window in the RNase H activity of WT and mutant RTs. PPT29RNA/PPT28DNA (25 nM) was incubated with the corresponding RT (50 nM) and the RNase H cleavage products quantified. Aliquots were removed at 20 s, 40 s, and 1, 2, 3, and 4 min. PPT-U3 cleavage at position -16 produces a product of 21 nucleotides. In addition, cleavages two and three positions downstream of the RNA template (at positions -18 and -19) are indicated in the gel. The T/P sequence of PPT29RNA/PPT28DNA is illustrated below the gel, with the PPT-U3 cleavage site highlighted in red. Above each complex, a red (PPT-U3 cleavage) or black lines (no-specific cleavages) are shown to illustrate nucleotide cleavage distances and resulting products. Below, a graphic representation of a time course kinetics obtained for each enzyme, determined from three independent experiments, (means ± standard deviations [error bars]) are shown.

As with T/P complexes described above, we tested the ability of WT, N348I and N348I/T369I RTs to cleave the RNA in the presence of 5 μM NVP and 12.5 μM EFV. As in the case of the PPT29RNA/PPT29DNA complex, a large increase on RNase H activity was observed with all enzymes (Fig 54), including the production of longer cleavage products undetectable in the absence of drugs. Interestingly, while with the PPT29RNA/PPT29DNA complex two cleavages yielding

products of 16 and 15 nucleotides (one and two nucleotides shorter than the product resulting from the cleavage at the PPT-U3 junction) were detected in reactions carried out by the WT RT, here only one band corresponding to a cleavage product one nucleotide shorter than the product resulting from the cleavage at the PPT-U3 junction could be observed (Fig 54). This cleavage corresponds to position -15 of the template strand, yielding a band of 20 nucleotides. Digested bands of 23 and 24 nucleotides detected in assays carried out with N348I and N348I/T369I RTs were rapidly processed to shorter products when NVP or EFV was added (Fig 54). However, while N348I was able to cleave at position -15, producing a band of 20 nucleotides (although in a lesser extend than the WT RT), N348I/T369I showed very little efficiency, even in the presence of 12.5 µM EFV (Fig 54).

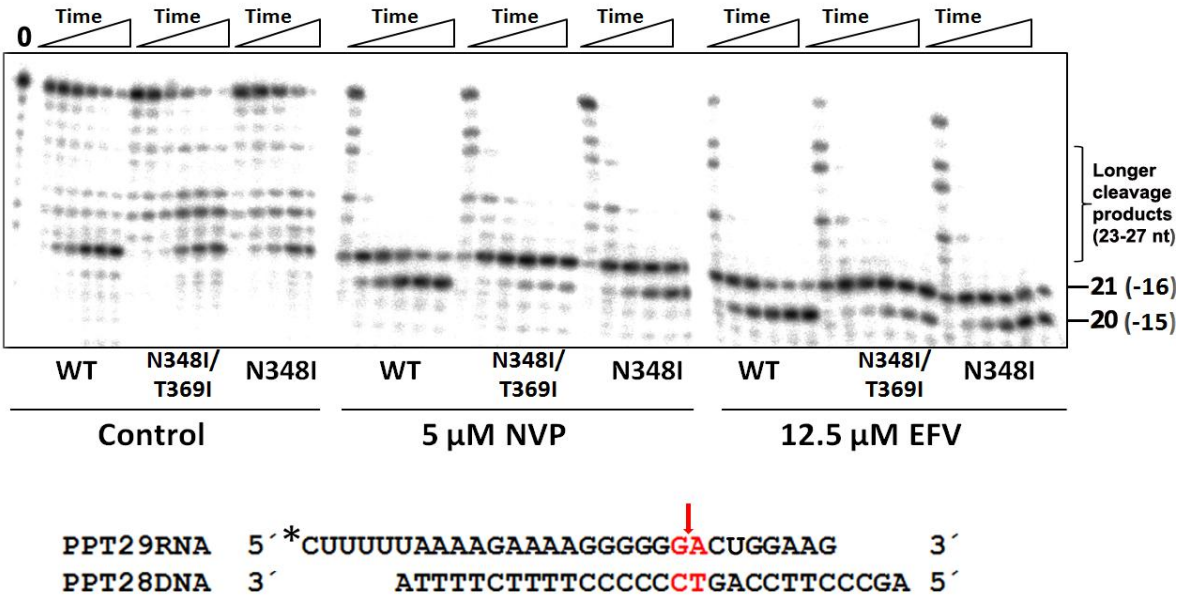

Fig 54. Time course of RNase H cleavage in the presence of NVP and EFV using T/P PPT29RNA/PPT28DNA. WT, N348I/T369I and N348I RTs (50 nM) were mixed with the PPT29RNA/PPT28DNA complex (25 nM) (below the gel with the PPT-U3 cleavage site indicated with a red arrow), and the cleavage of the PPT29RNA template was monitored in the absence of drug and in presence of 5 µM NVP or 12.5 µM EFV. Aliquots were removed at 20 s, 40 s, and 1, 2, 3, and 4 min. PPT-U3 cleavage takes place at position -16 and results in a product of 21 nucleotides, while further cleavages at position -15 lead to a product of 20 nucleotides. Both cleavage events are indicated in the gel.

PPT29RNA/PPT30DNA

So far, results obtained indicate that the presence of N348I, but especially N348I/T369I mutations impose restrictions in the ability of RT to cleave the RNA template at distances below 18 nucleotides from the DNA polymerase active site. To further test this possibility, a new T/P complex (PPT29RNA/PPT30DNA) was used. This heteroduplex has the same RNA-PPT-containing sequence that the two previous ones, but it has one and two nucleotides more in the DNA 3´-end than the PPT29DNA and the PPT28DNA oligonucleotides, respectively (Fig 55). Therefore, in the

PPT29RNA/PPT30DNA complex the canonical PPT-U3 cleavage would take place 18 nucleotides away from the DNA 3´-end. Interestingly, all tested enzymes showed nearly identical RNase H activity, since all of them produced only a single cleavage at position -18 (yielding a band of 21 nucleotides) and with very similar catalytic rates, except for the T369V mutant that was slightly faster (Fig 55). As expected, when the cleavage at the DNA-RNA junction is further away from position -17, mutations N348I and N348I/T369I had a minor impact on the RNase H cleavage specificity of the RT.

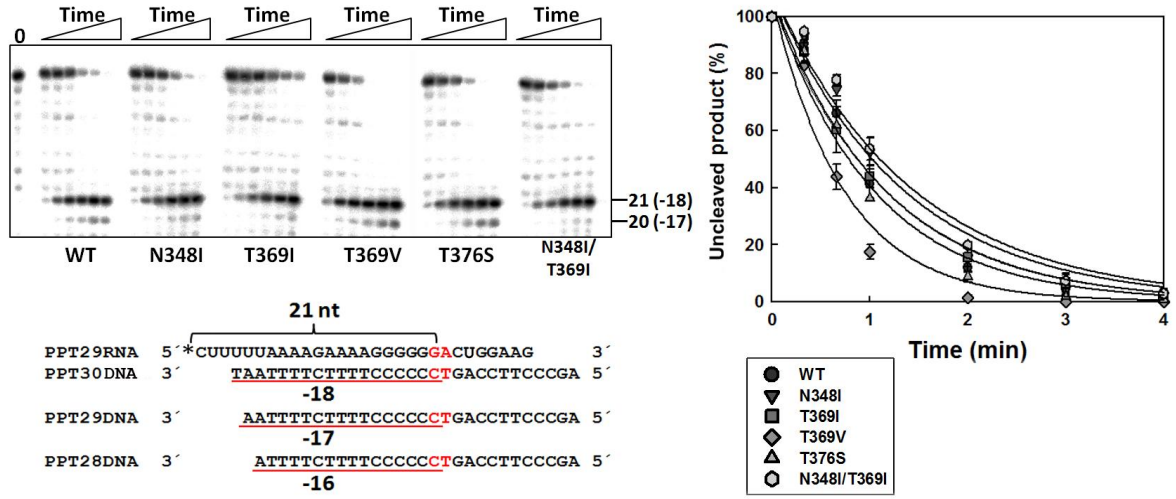

Fig 55. Kinetics of the RNase H cleavage activity of WT and mutant RTs using the PPT29RNA/PPT30DNA complex. PPT29RNA/PPT30DNA (25 nM) was incubated with the corresponding RT (50 nM) and the RNase H cleavage products quantified. Aliquots were removed at 20 s, 40 s, and 1, 2, 3, and 4 min. PPT-U3 cleavage at position -18 produces a product of 21 nucleotides. In addition, cleavage one nucleotide upstream of the RNA template (at position -17) is indicated in the gel. The T/P sequence of the PPT29RNA/PPT30DNA complex, as well as those of primers PPT29DNA and PPT28 DNA are illustrated below the gel, with the PPT-U3 cleavage site highlighted in red. Below each primer strand, a red line indicates the nucleotide cleavage length imposed to produce the cleavage at the PPT-U3 junction. On the right, a graphic representation of a time course kinetics obtained for each enzyme, determined from three independent experiments, (means ± standard deviations [error bars]) are shown.

4.3.3 RNase H activity of WT and mutant RTs in heteropolymeric RNA/DNA complexes

It is important to note that experiments carried out so far have been done using very specific substrates. The PPT is resistant to RNase H cleavage and cut at the PPT-U3 junction is highly favoured due to the unique structure of PPT-sequence. Therefore, to check if the results obtained with PPT-based substrates could be extended to heteropolymeric RNAs, the T/P 31Trna/21P was subjected to cleavage by WT, N348I and N348I/T369I RTs. As shown in Fig 56, primary cleavage produced by all enzymes yielded a band of 26 nucleotides, corresponding with a cut at position -16. However, two other cleavage events occurred at position -15 (in reactions carried out with WT and

N348I RTs) and at position -19 (in reactions carried out with N348I and N348I/T369I RTs). A higher amount of the 26-nucleotide band was produced by WT and N348I RTs in comparison with the double-mutant N348I/T369I, consistent with its expanded cleavage window. In contrast, N348I/T369I yielded a higher amount of the 29-nucleotide band product. N348I RT was efficient producing both cleavage products, but preferred to cleave at position -16 (Fig 56). Kinetics of the disappearance of the 31-nucleotide long substrate showed that N348I was as efficient as the WT enzyme (k_{obs} of 0.87 ± 0.08 min^{-1} and 0.85 ± 0.07 min^{-1}, respectively). However, the N348I/T369I RT cleaved the substrate at a slower rate, showing a k_{obs} of 0.53 ± 0.03 min^{-1}.

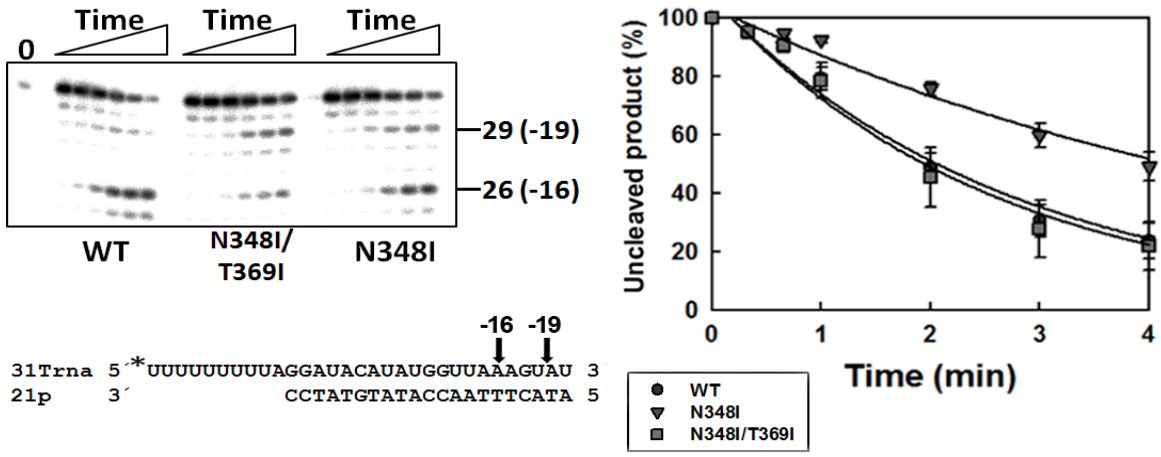

Fig 56. RNase H activity of WT and mutant RTs N348I/T369I and N348I on a heteropolymeric T/P. A mix containing WT, N348I/T369I or N348I RTs at 50 nM concentration and 31Trna/21P (25 nM) was incubated at 37ºC, and aliquots removed at 20 s, 40 s and 1, 2, 3 and 4 min. Cleavage products corresponding to bands of 26 and 29 nucleotides are indicated in the gel and in the T/P complex sequence shown below. A graph representing the time course reactions for all three enzymes is showed in the right part of the panel. Values representing average ± standard deviations [error bars] were extracted from four independent experiments.

As well as in all previous cases, the addition of NNRTIs produced a large increase in the RNase H activity of all three RTs, and the appearance of shorter cleavage products (Fig 57). Therefore, 5 μM NVP or 12.5 μM EFV promoted the RNase H activity of all tested RTs. Interestingly, a cleavage at position -13 producing a band of 23 nucleotides was clearly visible in reactions carried out with the WT RT. However, this 23-nucleotide band was less intense in reactions carried out with the N348I RT and absent in those carried out with the double-mutant N348I/T369I (Fig 57). Therefore, the enhancement of the RNase H activity showed by NNRTIs was not only restricted to PPT-containing complexes.

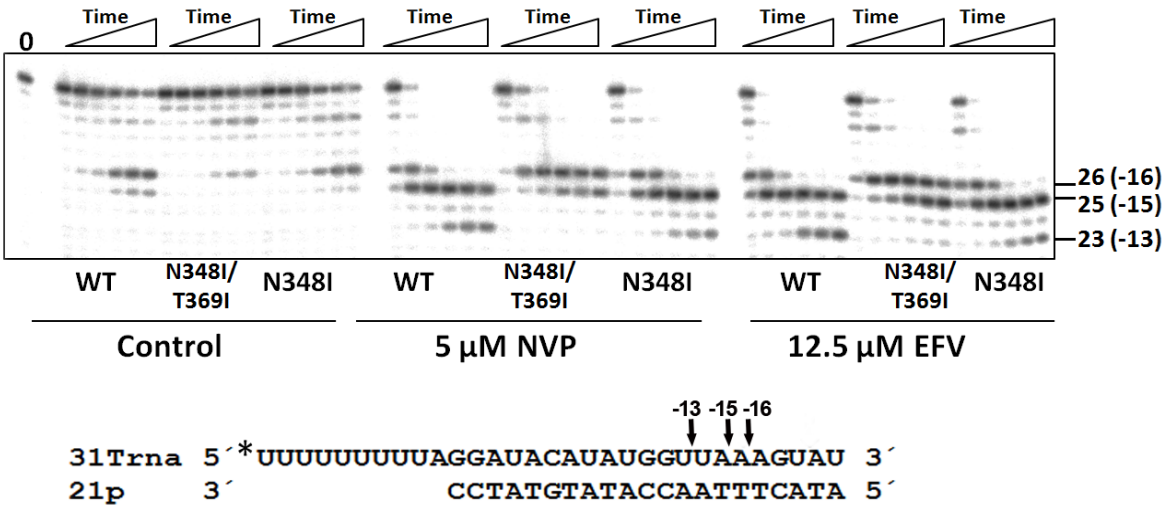

Fig 57. Time course of RNase H cleavage of the heteropolymeric complex 31Trna/21P carried out in the presence of NVP and EFV. WT, N348I/T369I and N348I RTs (50 nM) were mixed with 31Trna/21P complex (25 nM) (sequence below) and the cleavage of the RNA template monitored in the presence of 5 µM NVP, 12.5 µM EFV, or in the absence of drug. Aliquots were removed at 20 s, 40 s, and 1, 2, 3, and 4 min. Cleavage products of 26, 25 and 23 nucleotides occurring at positions -16, -15 and -13, respectively, are indicated in the gel.

4.4 HIV-1 IN activity and its effects in RT activity

The HIV-1 IN is the enzyme responsible of integrating the viral DNA into the host genome. As described in the Introduction, IN has two different activities to accomplish this task, a 3´-end processing activity that trims the viral ends, and a strand transfer activity, responsible for the covalent binding of the viral DNA to the host genome. In addition, IN has been described as a reverse transcription factor, promoting efficient production of RT products. Previous works have pointed out a role of IN in tRNA extension during (-) strand DNA synthesis, showing an enhancer effect of IN on RT-DNA polymerase activity (Dobard *et al.*, 2007).

Studies using PPT-containing complexes described above have shown that the use of PPT primers differs from those of heteropolymeric complexes, regarding their cleavage specificity. As PPT processing is a necessary step occurring during reverse transcription, the IN protein could be implicated in the removal of the PPT. In order to answer this question and to get insights into the possible role of IN as a modulator of RT RNase H activity, we decided to produce and characterize the HIV-1 IN enzyme, and then, test its impact on RT RNase H activity using PPT- and heteropolymeric-T/Ps.

4.4.1 Characterization of IN activities

As described, HIV-1 IN has two major physiological activities: 3´-end processing and strand transfer. However, disintegration has been described as a third activity that can be tested *in vitro*. We

check the catalytic integrity of purified IN (HIV-1 group M subtype B NL4-3 strain), by using appropriate assays for all three activities.

4.4.1.1 IN 3´-end processing

Through this reaction IN recognizes a conserved dinucleotide CA from both viral ends and removes the 2 nucleotides (GT pair) situated at 3´-end of this sequence. Therefore, at this stage the IN acts as an endonuclease, catalyzing a metal-dependent nucleophilic attack. Its 3´-end processing activity can be measured by using the C220/C120 complex, which resembles a viral end (Fig 58A). Assays carried out in the presence of a large excess of IN over T/P (200 nM and 5 nM, respectively), allowed the identification of cleavage products, of 19 nucleotides, lacking the GT dinucleotide of their 3´-end (Fig 58A). Conditions in these assays involve the use of Mn^{2+}, instead of Mg^{2+}. No activity was detected in the presence of Mg^{2+} at 3 mM or 10 mM concentration (Fig 58B).

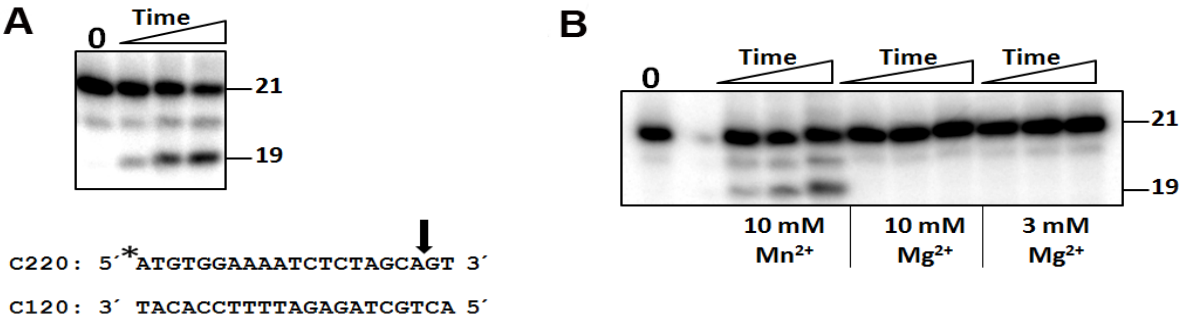

Fig 58. HIV-1 IN 3´-end processing activity. The T/P C220/C120 mimics a viral DNA end. (A) 200 nM IN was incubated with 5 nM C220/C120 and production of a band of 19 nucleotides resulting from IN cleavage was monitored. The sequence of the T/P complex is given below the gel, indicating the IN cleavage site with a black arrow. (B) Representative gel showing the lack of IN 3´-end processing activity in the presence of different $MgCl_2$ concentrations under our assay conditions.

4.4.1.2 Strand transfer activity

The strand transfer reaction uses the pre-processed 3´-ends of viral DNA for the nucleophilic attack of chromosomal DNA, creating the integrated product. Therefore, the pre-processed complex C120/B2-1, which contains a 2-nucleotides recessed 3´-end was used to measure the strand transfer activity of IN (Fig 59).

As shown in Fig 59, purified IN was efficient in strand transfer. The random nature of the integration process *in vitro* produced different integrated products of variable length, depending on the integration site.

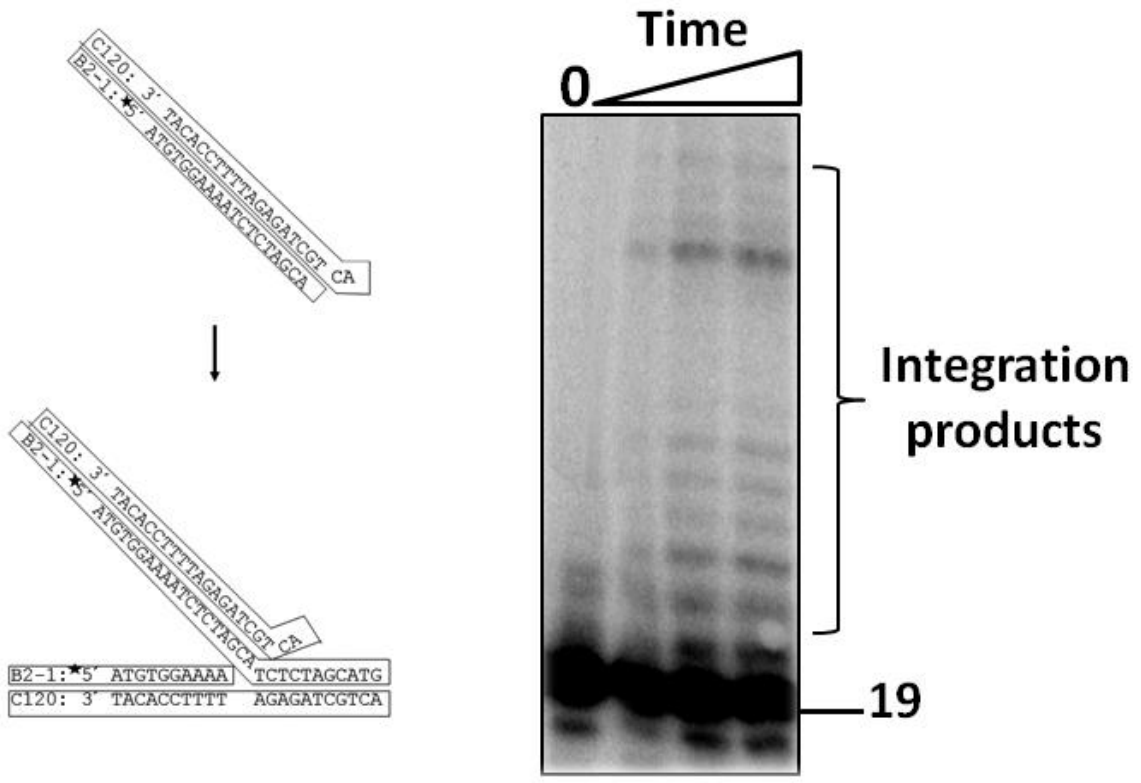

Fig 59. HIV-1 IN strand transfer activity. The left part of the figure shows the C120/B2-1 complex used in this assay, indicating the result of one possible integration event. 200 nM IN was incubated with 5 nM C120/B2-1 and production of integration products monitored. A representative gel showing a time course reaction is also illustrated, where the original B2-1 primer of 19 nucleotides and the strand transfer products obtained are indicated.

4.4.1.3 Disintegration

The disintegration activity has no apparent physiological role during HIV-1 life cycle *in vivo*. However, it can be tested by using the "dumbbell" strand as substrate. The dumbbell consists of a single oligonuleotide with self-complementation, resembling an integration intermediate (Fig 60). IN cleaves after the conserved CA dinucleotide, liberating a "disintegrated" product, in a reaction that is the strand transfer reaction run in reverse. As depicted in Fig 60, purified IN showed measurable activity in "dumbbell" cleavage, confirming the ability of the HIV-1 IN in processing integrated products *in vitro*.

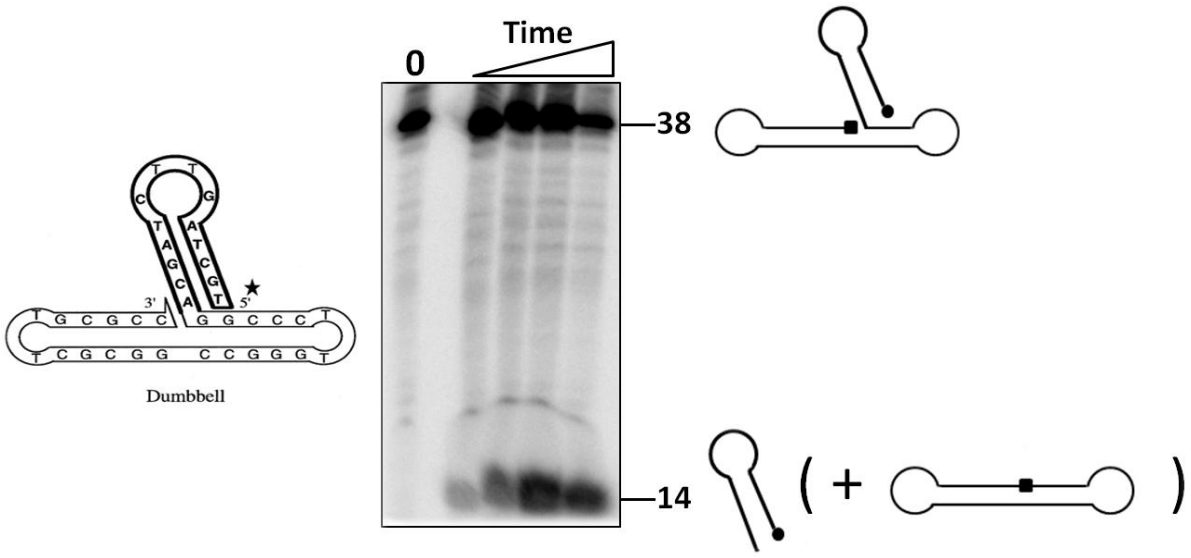

Fig 60. HIV-1 IN disintegration activity. The single-stranded "dumbbell" substrate sequence used in the disintegration activity measurements is shown in the left part of the figure, in its folded configuration. IN (200 nM) was incubated with 5 nM "dumbbell" substrate and production of the 14-nucleotide band resulting from IN cleavage was monitored. A gel containing the result of a disintegration assay is shown, together with the size of the obtained products.

4.4.2 Modulation of RT activity by IN

Available studies on the interactions between RT and IN have mainly focused on the impact of IN in the DNA polymerase activity of the RT (Oz *et al.*, 2002; Hehl *et al.*, 2004; Dobard *et al.*, 2007). Therefore, we decided to study the influence of IN in the RNase H activity of the RT, examining the cleavage of heteropolymeric complexes, as well as processing of PPT during (-) and (+) strand DNA synthesis, since both steps are physiologically relevant during reverse transcription.

4.4.2.1 Impact of IN on the RNase H activity of the RT over heteropolymeric complexes

We measured the endonucleolytic digestion of the heteropolymeric T/P 31Trna/21P by RT in the presence of 10-fold excess of IN. Although an increase in the RNase H catalytic rate of the WT RT was obtained in reactions carried out in the presence of small concentrations of CHAPS or NP-40 (around 60 μM and 0.0006%, respectively) (Fig 61), cleavage of the 31Trna template strand to produce the 26 nucleotides product occurred at similar rates in the presence of active IN or the heat-inactivated enzyme (Fig 62A). Similar results were obtained with the IN mutant V250E (provided by Shewit Tekeste; University of California, Los Angeles) that is unable to interact with the RT (Tom Wilkinson and Shewit Tekeste; University of California, Los Angeles, personal communication), produced a cleavage activity indistinguishable from that seen in the presence of the WT IN (Fig 62B). These results lead us to conclude that under our assay conditions, cleavage of the heteropolymeric 31Trna/21P was not enhanced by the presence of IN.

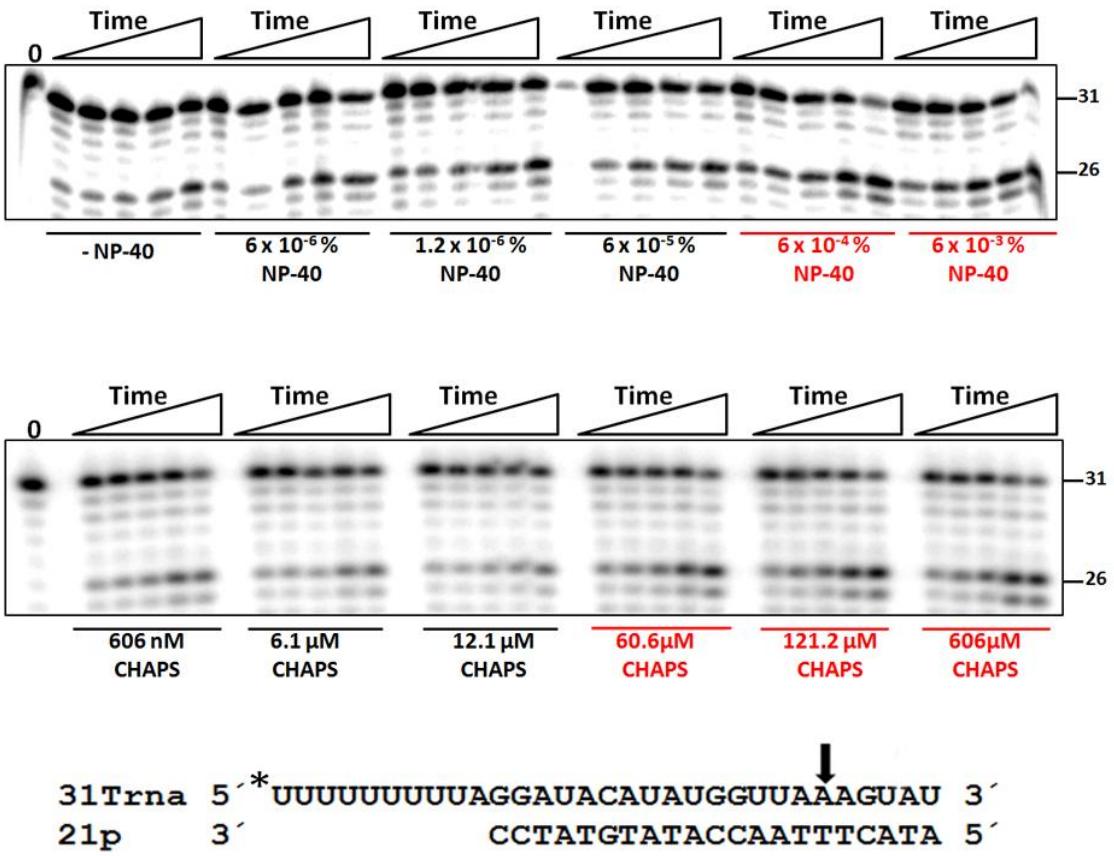

Fig 61. Effect of detergents NP-40 and CHAPS in the RNase H activity of the RT. Gels corresponding to RNase H digestion of the 31Trna/21P complex in the presence of increasing concentrations of NP-40 (up) or CHAPS (down). Below each RNase H reaction the detergent concentration used is indicated. Highlighted in red, significant increases in RNase H activity are shown. The T/P sequence is given in the lower part of the figure, indicating with an arrow the cleavage site producing the band of 26 nucleotides. RT and T/P were used at 50 nM concentration.

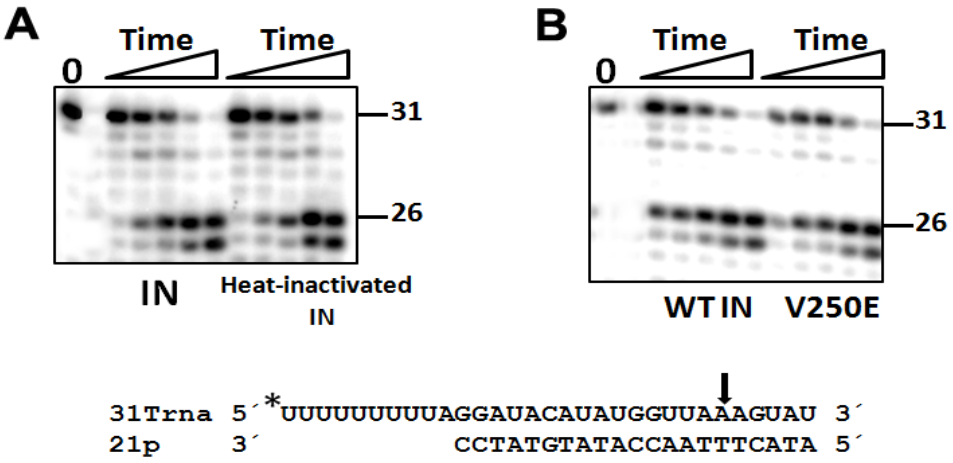

Fig 62. Effect of IN on the RT-mediated cleavage of heteropolymeric RNA/DNA complexes. The 31Trna/21P complex (50 nM) was mixed with equimolar WT RT concentration and a 10-fold excess of WT IN, heat-inactivated IN or the RT-interacting deficient mutant V250E. The T/P sequence is shown below the gels, indicating with an arrow the cleavage site producing the band of 26 nucleotides. Aliquots were removed 20 s, 40 s and 1, 2, and 4 min and the formation of the 26-nucleotide product was quantified.

4.4.2.2 PPT cleavage in the presence of IN during (-) and (+) strand DNA synthesis

The complex PPT29RNA/PPT29DNA (Fig 63) mimics a possible intermediate during (-) strand DNA synthesis. Thus, the RT has to cleave the RNA at the 3´-end of the PPT (*i.e.*, at the PPT-U3 junction) to leave the free 3´-OH of the PPT primer that will be used to initiate (+) strand DNA synthesis afterwards.

According with results shown in Fig 63, the presence of a large excess of IN over RT (100 nM and 10 nM, respectively), produced a substantial increase in the ability of the WT RT to cleavage at the PPT-U3 junction. However, heat-inactivated IN (heated at 90ºC for 10 min), did not produce such an effect (Fig 63). Therefore, a 10-fold excess of IN over the RT increased the apparent k_{obs} of RNase H cleavage from 0.62 min^{-1} to 1.29 min^{-1}. On the other hand, unlike in the presence of NNRTIs (see Fig 52), IN addition did not produce cleavages at new positions, but only the canonical PPT-U3 cut, rendering a product of 21 nucleotides (Fig 63).

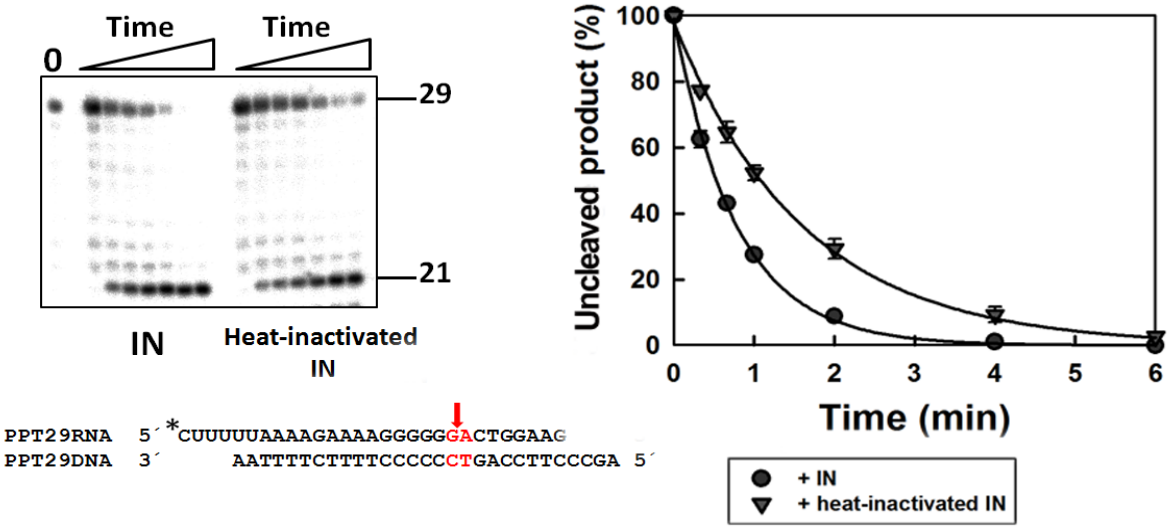

Fig 63. Effect of IN on the RT-mediated cleavage of PPT-containing RNA (DNA-dependent binding mode). Complex PPT29RNA/PPT29DNA (100 nM) was incubated with 10 nM WT RT and 100 nM IN. The T/P sequence is shown below the gel. The PPT-U3 cleavage site is highlighted in red. Aliquots were removed 20 s, 40 s and 1, 2, 4 and 6 min and the formation of the 21-nucleotide product was quantified. Time course experiments carried out in the presence of IN and heat-inactivated IN were performed in triplicate. Averages ± standard deviations [error bars] were extracted from three independent experiments and are represented in the graph shown on the right.

In addition, the ability of IN to modulate the RNase H activity of the RT using a complex mimicking the (+) strand DNA synthesis was tested. For this purpose, the aforementioned T57d/PPT17r8d (Fig 64) was incubated in the presence of the RT and a large excess of IN or heat-inactivated IN. The amount of cleaved product of 17 nucleotides was clearly increased when 10-fold

IN relative to RT was included in the reaction mixture, in comparison with the heat-inactivated IN (Fig 64). In fact, in the presence of IN, in addition to the expected cleavage at position -17, a one-nucleotide shorter product was also obtained, probably derived from the -17 product (Fig 64).

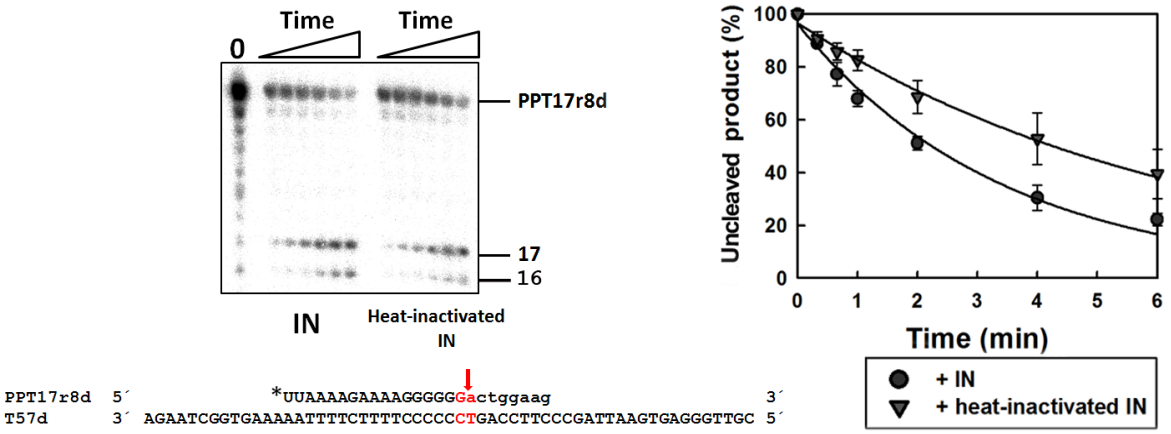

Fig 64. Effect of IN on the RT-mediated cleavage of PPT-containing RNA (RNase H-dependent binding mode). The T57d/PPT17r8d sequence is indicated, as well as the PPT-U3 cleavage site (red characters and red arrow). This complex represents a possible intermediate during (+) strand DNA synthesis. RT cleavage at the RNA-DNA junction of PPT17r8d produces a 17 nucleotide product, in a reaction that is enhanced by the presence of IN.

5.Discussion

5. Discussion

Suboptimal use of anti-HIV drugs facilitates the development of RT mutations and the selection of drug-resistant strains. Mutations conferring resistance to NRTIs can act by two different mechanisms: (i) by discriminating against the triphosphorylated form of the NRTI or (ii), by promoting the excision of the incorporated NRTI from the 3´-end of the primer. One of the most common sets of mutations selected during antiretroviral treatment that confer resistance to NRTIs through the excision mechanism are thymidine analogue resistance mutations (TAMs).

TAMs are classified in two different clusters: TAM-1 and TAM-2. TAM-2 cluster includes mutations D67N, K70R and K219Q or N, and sometimes T215F. The TAM-1 set of mutations includes M41L, L210W and T215Y. The TAM-1 pathway is more prevalent in clinical isolates, and in general it confers higher levels of resistance to NRTIs (reviewed in Menéndez-Arias, 2010). TAMs are frequently selected in therapies including thymidine analogues (*i.e.*, containing AZT or d4T). Combinations of TAMs can confer resistance to virtually all NRTIs except cytidine analogues (Meyer *et al.*, 1999; Mas *et al.*, 2000). However, in virus isolated from patients receiving therapy for a long time, it is common to identify additional mutations that appear associated with the TAM-1 and TAM-2 clusters (Cane *et al.*, 2007; Santoro *et al.*, 2013). In most cases, these associated mutations do not play a direct role in NRTI resistance, but they can facilitate the selection of TAM-containing strains during exposure to antiretroviral drugs. By virtue of their secondary role, TAM-associated mutations are also known as accessory mutations, and in this work we have shown different mechanisms of action that favor the selection of accessory mutations specifically associated with the TAM-1 cluster.

Many amino acid substitutions in the RT have been associated with TAMs in epidemiological studies. Examples are E40F, K43E or Q or N, E44A or D, K64H, V118I, K122E, I135T, E203D or K, H208Y, L214F, D218E, K223E or Q, L228H or R, the cluster A272P/K277R/A286T and R284K (Stürmer *et al.*, 2003; Lu *et al.*, 2005a; Svicher *et al.*, 2006; Cane *et al.*, 2007; Nebbia *et al.*, 2007; Garriga *et al.*, 2009; Puertas *et al.*, 2009; Melikian *et al.*, 2012). Phe-40, Glu-43, Asp-44, Ile-118, Tyr-208, the cluster Pro-272/Arg-277/Thr-286 and Lys-284 have been shown to associate with the TAM-1 pathway (Romano *et al.*, 2002; Gonzales *et al.*, 2003; Saracino *et al.*, 2006; Svicher *et al.*, 2006; Nebbia *et al.*, 2007; Huigen *et al.*, 2008; Garriga *et al.*, 2009; von Wyl *et al.*, 2010). However, there are very few studies estimating the impact of accessory mutations on resistance mediated by TAMs.

Mutations E40F (Huigen *et al.*, 2008) and Q207D (Lu *et al.*, 2005a) have been found to increase AZT resistance of viral strains bearing different subsets of TAMs, while substitution L214F was found to increase the replication capacity of viral strains bearing TAM-1 mutation T215Y in the presence of AZT (Puertas *et al.*, 2009). Interestingly, molecular models predict that the presence of Leu-214 together with Tyr-215 could interfere in the interaction between the RT and AZTMP-terminated T/P complexes, hampering the excision of the inhibitor (Puertas *et al.*, 2009). More detailed biochemical studies have been carried out only for mutations E44D and V118I (Hertogs *et al.*, 2000; Girouard *et al.*, 2003). Mutation E44D has been found associated with TAMs in HIV isolates obtained from

patients treated with various NRTIs (Ceccherini-Silberstein, *et al.*, 2005), and more specifically with d4T or ddI (Romano *et al.*, 2002), AZT (Stoeckli *et al.*, 2002), AZT and 3TC (Hertogs *et al.*, 2000) or with thymidine analogues (von Wyl *et al.*, 2010). In biochemical assays, E44D has been found to improve the ATP-dependent rescue activity of DNA/DNA complexes containing a 3TCMP-terminated primer (Girouard *et al.*, 2003). However, V118I confers AZT and 3TC resistance in the absence of TAMs, and therefore cannot be considered as an accessory mutation associated with TAMs (Hertogs *et al.*, 2000; Girouard *et al.*, 2003).

More recently, mutations in the connection subdomain and the RNase H domain of the RT have been also identified in RT sequences of HIV-1 isolates from treated patients. Thus, N348I, A360V and Q509L have been found associated with the exposure to treatments containing different NRTI combinations, as well as with the presence of TAMs (Nikolenko *et al.*, 2007; Yap *et al.*, 2007; Brehm *et al.*, 2008, 2012; Ehteshami *et al.*, 2008; Hachiya *et al.*, 2008; Radzio & Sluis-Cremer, 2008; von Wyl *et al.*, 2010; Lengruber *et al.*, 2011). These mutations act by altering the balance between NRTI excision from blocked-primers and RNA template degradation. Thus, a slower rate of cleavage of the RNA template strand, allows more time for the RT to be in the right location to excise the chain-terminator inhibitor, and then resume DNA synthesis (Nikolenko *et al.*, 2005; Acosta-Hoyos *et al.*, 2012; reviewed in Delviks-Frankenberry *et al.*, 2010; Menéndez-Arias, 2013) (Fig 65). Among all of the mutations that have been associated with the TAM-1 pathway, we have selected for our study the palm subdomain mutation H208Y, the thumb subdomain mutation R284K and the set of thumb subdomain polymorphisms Pro-272/Arg-277/Thr-286.

H208Y is relatively uncommon in virus isolated from naïve patients. In the Stanford HIV Drug Resistance Database (http://hivdb.stanford.edu/; accessed in October 2013), only 0.2% of HIV-1 group M subtype B isolates from untreated patients contained H208Y. However, the frequency of the H208Y substitution increases up to 9.1% in treated individuals. In agreement with these observations, several epidemiological studies have shown a relationship between the increased prevalence of H208Y and the exposure to antiretroviral drugs (Rhee *et al.*, 2005; Nebbia *et al.*, 2007; von Wyl *et al.*, 2010). H208Y has been associated with therapies consisting of combinations of several nucleoside analogues including excisable NRTIs (Gonzales *et al.*, 2003; Stürmer *et al.*, 2003; Rhee *et al.*, 2005; Saracino *et al.*, 2006; Svicher *et al.*, 2006; Nebbia *et al.*, 2007; Garriga *et al.*, 2009; Shahriar *et al.*, 2009). Interestingly, the cluster H208Y/R211K/L214F in virus containing several TAMs (*i.e.*, D67N, K70R, M41L, L210W, T215Y and K219E) was found to be more prevalent in isolates from patients who failed therapies containing AZT and 3TC (Stoeckli *et al.*, 2002; Stürmer *at al.*, 2003). Several studies have found a strong association between H208Y and the mutations of the TAM-1 pathway (Gonzales *et al.*, 2003; Saracino *et al.*, 2006; Svicher *et al.*, 2006; Nebbia *et al.*, 2007; von Wyl *et al.*, 2010). In a study including 223 samples, authors found that the presence of M41L and T215Y is required for the development of H208Y (Stürmer *et al.*, 2003).

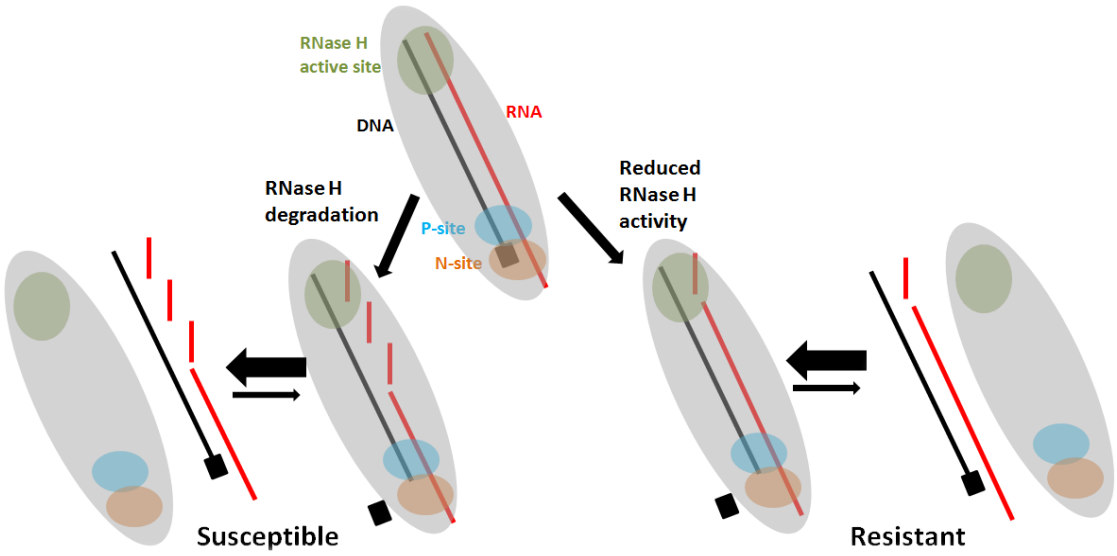

Fig 65. Model showing the potential effect of mutations in the connection subdomain and the RNase H domain of the RT in NRTI resistance. An RNA/DNA complex containing an inhibitor blocking the 3´-end of the primer (black box) is represented. The RT is represented by a gray oval, with an RNase H active site (green circle) and a DNA polymerase active site containing a priming (P) site and nucleotide binding (N) site, indicated with blue and brown circles, respectively. Reduced RNase H activity reduces degradation of the RNA template strand and increases the time available for the RT to excise the 3´-end inhibitor before RT-RNA/DNA dissociation.

Further support of the role of H208Y in drug resistance has been obtained from viral drug susceptibility measurements. The addition of the combination V118I/H208Y to a viral background bearing mutation T215Y increased phenotypic resistance to d4T (Clark *et al.*, 2006). In addition, studies carried out in the lab of Dr. M. A. Martínez (Fundació IrsiCaixa, Hospital Universitari Germans Trias i Pujol, Badalona, Spain) with recombinant HIV-1 carrying mutated RTs showed that viral strains bearing the combination M41L/H208Y/L210W/T215Y showed a higher level of resistance to AZT than viruses with the TAM-1 cluster of mutations alone (Table 20). However, both mutants were equally susceptible to d4T and tenofovir. It is well known that primers terminated with d4TMP or tenofovir are more susceptible than primers terminated with AZTMP to the inhibition by the next complementary nucleotide, and therefore have a stronger tendency to form "dead-end-complexes" (DEC) (Tong *et al.*, 1997; Meyer *et al.*, 2000). Since MT-4 cells used in viral IC_{50} determinations contain high dNTP concentrations, it is not surprising that the largest differences in drug susceptibility between WT and mutants were observed only with AZT.

Unlike the H208Y mutation, the amino acid substitution R284K and the cluster of polymorphisms Pro-272/Arg-277/Thr-286 are located in the thumb subdomain of the RT, far from the putative ATP binding site created by TAMs (see Fig 11). The thumb subdomain is essential in RT activity and alanine scanning mutagenesis studies affecting key residues in α-helices H and I have shown that mutations in this region produce large alterations in RT processivity, fidelity, T/P affinity and in the catalytic rate of DNA polymerization (Beard *et al.*, 1994, 1996; Bebenek *et al.*, 1995; Wang *et al.*, 2008).

Table 20. Susceptibility of HIV-1 constructs with and without H208Y to RT inhibitors

	IC_{50} (nM)		
RT	**AZT**	**d4T**	**Tenofovir[a]**
WT	2.3 ± 1.5	276 ± 90.5	6.7 ± 2.2
H208Y	2.3 ± 1.2 (1)	160.3 ± 53.5 (0.58)	7.4 ± 2.8 (1.1)
M41L/T215Y	17.7 ± 6.1 (7.6)	302.7 ± 69 (1.1)	15.9 ± 3.3 (2.4)
M41L/L210W/T215Y	11.7 ± 1.2 (5)	217 ± 75.5 (0.8)	11 ± 4.6 (1.6)
M41L/H208Y/L210W/T215Y	24.5 ± 1.5 (10.5)[b]	314 ± 56.3 (1.1)	20.6 ± 6.9 (3.1)

The IC_{50} values shown are the averages ± standard deviations of at least three independent determinations, each one performed six times. The fold-increase in IC_{50} relative to the wild-type HXB2 virus control carrying the RT sequence of BH10 is shown between parentheses. Unpublished data obtained by Drs. M. Nevot and M. A. Martínez (Fundació IrsiCaixa, Hospital Universitari Germans Trias i Pujol, Badalona, Spain).

[a] Experiments were carried out with the water soluble diester prodrug tenofovir disoproxil fumarate.

[b] Significant differences between M41L/L210W/T215Y and M41L/H208Y/L210W/T215Y RTs (Student *t* test $p < 0.05$).

Positions 272, 277 and 286 are highly polymorphic in group M subtype B HIV-1 isolated from untreated patients. According to the Stanford HIV Drug Resistance Database (http://hivdb.stanford.edu/; accessed in October 2013), in untreated patients residue 272 is a proline in 47.6% of the isolates, alanine in 44.6% of the cases, and serine in 5.6% of the isolates. Positions 277 and 286 are less polymorphic. At position 277, lysine is predominant (57.5%) while arginine is observed in 42.1% of the HIV-1 isolates. At position 286, most isolates contain threonine (68.0%), followed by alanine (29.5%). A cross-sectional study carried out with HIV-1 group M subtype B *pol* sequences from patients treated in Spanish hospitals revealed that Pro-272, Arg-277 and Thr-286 increased their prevalence in individuals failing therapy with abacavir/d4T and other NRTI combinations (Garriga *et al.*, 2009). In that study, Pro-272, Arg-277 and Thr-286 were found in 45.0%, 25.7% and 54.5% of the isolates obtained from untreated patients, respectively. However, their frequency increased up to 82.6%, 63.0% and 91.3%, respectively, in virus identified in patients who had failed abacavir/d4T therapy. In the same study, an association between TAMs, mainly Leu-41 and Tyr-215 and polymorphisms Pro-272, Arg-277 and Thr-286 was also detected. In addition, another study has also reported on the association of T286A with exposure to NRTIs during the antiretroviral treatment (Ceccherini-Silberstein *et al.*, 2005).

Addition of thumb subdomain polymorphisms Pro-272/Arg-277/Thr-286 to viral strains bearing RT mutations M41L/T215Y had no effect on viral susceptibility to NRTIs in MT4-cells (Table 21). As described for the H208Y mutants, recombinant HIV-1 susceptibility to NRTIs was measured using MT-4 cells, whose high dNTP concentrations could facilitate the production of "dead-end-complexes" (Smith & Scott, 2006).

Phenotypic drug susceptibility assays failed to detect differences between viruses that carry the three thumb subdomain polymorphisms in the presence of M41L/T215Y, and those that only contain the two TAM-1 mutations. Viral replication capacity assays carried out in the presence of AZT with peripheral blood mononuclear cells (PBMCs), characterized by their low dNTP concentration (Back *et al.*, 1996), showed an increased growth rate of the recombinant HIV-1 strains bearing Pro-272, Arg-277 and Thr-286 in the RT, compared with those that had Ala-272, Lys-277 and Ala-286 (Fig 66).

Table 21. Susceptibility of HIV-1 constructs with and without P272A/R277K/T286A to RT inhibitors

	IC_{50} (μM)					
RT[a]	AZT	d4T	Abacavir	ddI	Tenofovir	3TC
WT	5.1 ± 2.6 x 10^{-3}	0.32 ± 0.04	1.28 ± 0.24	2.21 ± 0.36	0.18 ± 0.04	1.01 ± 0.04
AKA	6.1 ± 2.3 x 10^{-3} (1.2)	0.29 ± 0.05 (0.9)	1.17 ± 0.11 (0.9)	2.50 ± 0.89 (1.1)	0.22 ± 0.03 (1.2)	1.52 ± 0.49 (1.5)
LY	1.45 ± 0.8 x 10^{-2} (2.8)	0.40 ± 0.05 (1.3)	1.53 ± 0.24 (1.2)	1.89 ± 0.60 (0.9)	0.26 ± 0.04 (1.5)	1.99 ± 0.63 (1.9)
LYAKA	1.07 ± 6.5 x 10^{-2} (2.1)	0.38 ± 0.09 (1.2)	1.77 ± 0.19 (1.4)	2.56 ± 0.71 (1.2)	0.26 ± 008 (1.4)	1.56 ± 0.85 (1.5)

The IC_{50} values shown are averages ± standard deviations of at least three independent determinations, each one performed six times. The fold-increase in IC_{50} relative to the wild-type HXB2 virus control carrying the RT sequence of BH10 is shown between parentheses. Values obtained by Drs. M. Nevot and M. A. Martínez (Fundació IrsiCaixa, Hospital Universitari Germans Trias i Pujol, Badalona, Spain).

[a] RTs LY, LYAKA and AKA correspond to mutant enzymes M41L/T215Y, M41L/T215Y/P272A/R277K/T286A and P272A/R277K/T286A, respectively.

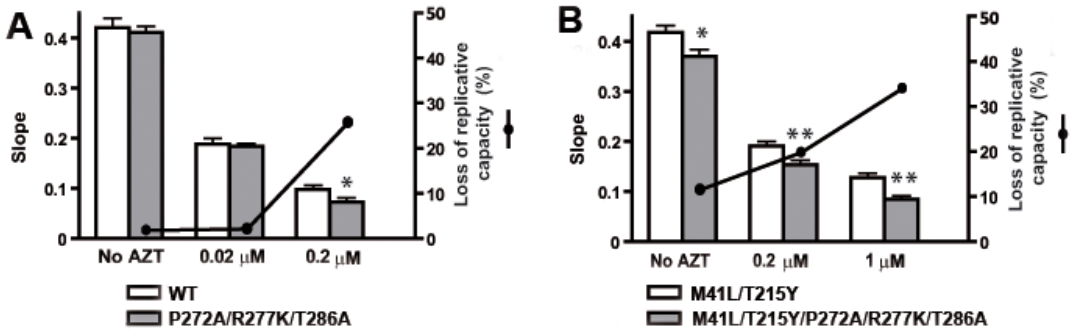

Fig 66. Replication kinetics assays carried out in the absence and in the presence of AZT. Histograms show the slope of p24 antigen production of each virus after infection of PBMCs (mixed from two donors). Comparisons of WT *versus* mutant P272A/R277K/T286A virus and mutant M41L/T215Y virus *versus* M41L/T215Y/P272A/R277K/T286A virus are shown in panels A and B, respectively. The significance of the differences between slopes was calculated using the GraphPrism v. 4 software (* $p < 0.05$; **, $p < 0.01$). Solid black circles represent the percentage loss of replication capacity of the recombinant HIV-1 variants containing the P272A, R277K, and T286A mutations in the absence (A) or presence (B) of M41L/T215Y, under different assay conditions. Figure provided by Drs. M. C. Puertas and J. Martínez-Picado (Fundació IrsiCaixa, Hospital Universitari Germans Trias i Pujol, Badalona, Spain).

Mutation R284K is rare in HIV-1 variants of therapy-naïve individuals. According to the Stanford HIV Drug Resistance Database (http://hivdb.stanford.edu/; accessed in October 2013), 1.9% of the group M subtype B HIV-1 isolates from untreated patients contained such a substitution. However, this number increases up to 4.2% for viruses isolated from patients who had been exposed to NRTIs in their treatment, consistent with published data showing the higher frequency of this mutation among isolates from treated individuals. Thus, in a study carried out with 100 naïve-patients and 248 treated individuals in the United States, authors found that the prevalence of this mutation was 7.3% in treated individuals, although it was not found in any of the untreated patients (Waters *et al.*, 2009). An increase in the frequency of R284K was also observed in patients who had been treated with a combination of thymidine analogues plus ddI (*i.e.*, from 1.1% in naïve individuals to 6.0% in patients treated with thymidine analogues plus ddI) (von Wyl *et al.*, 2010).

When *pol* sequences of virus isolated from patients treated in Spanish hospitals who had failed combination therapies including tenofovir and emtricitabine were examined, a 3.8-fold increase in the frequency of R284K was detected (from 2.5% in naïve patients to 9.6% in treated individuals) (C. Garriga and L. Menéndez-Arias, personal communication). Interestingly, in a principal factoring analysis, R284K associated with the cluster formed by TAM-1 mutations M41L, L210W and T215Y (Fig 67). The strongest correlation was found with T215Y. This result was consistent with data obtained in a study carried out in the U.K., where more than 3,000 HIV-1 *pol* sequences from treated patients were analyzed. In this study, authors reported a strong association between the presence of R284K and the number of TAMs found in the viral isolates (Cane *et al.*, 2007).

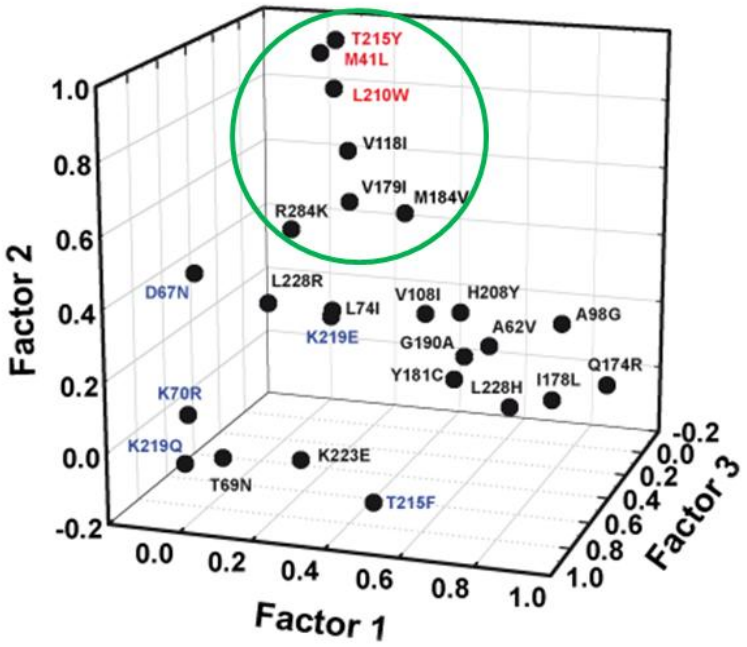

Fig 67. Principal axis factoring analysis of correlations between mutations associated with tenofovir/emtricitabine therapy failure. Amino acid changes with high coefficients of covariation are close together, while large distances separate those substitutions that show low or negative coefficients of association. Major mutations of the TAM-1 and TAM-2 complexes are indicated in red and blue, respectively. A cluster including the TAM-1 and R284K mutations is highlighted with a green circle. Figure and data provided by C. Garriga (Centro Nacional de Epidemiología, Instituto de Salud Carlos III, Madrid, Spain).

As in the case of thumb subdomain polymorphisms Pro-272/Arg-277/Thr-286, addition of R284K to viral strains bearing TAM-1 mutations (*i.e.*, M41L, L210W and T215Y) had no apparent effect on their susceptibility to AZT, d4T or tenofovir in assays carried out in MT-4 cells (Table 22). However, when viral replication assays were carried out in PBMCs, recombinant HIV-1 bearing RT mutations M41L/L210W/T215Y/R284K showed higher replication capacity in the presence of AZT and tenofovir than the virus carrying mutations M41L/L210W/T15Y (Fig 68).

Taken together, available virological data reveal an impact of H208Y on phenotypic drug susceptibility, while the thumb subdomain polymorphisms Pro-272/Arg-277/Thr-286 and R284K influence viral replication capacity in PBMCs, in the presence of excisable NRTIs such as AZT or tenofovir.

Table 22. Susceptibility of HIV-1 constructs with and without R284K to RT inhibitors

	IC_{50} (nM)			
RT	**AZT**	**d4T**	**Tenofovir[a]**	**FTC**
WT	2.3 ± 1.5	276.0 ± 90.5	6.7 ± 2.2	144.3 ± 69.9
R284K	1.7 ± 1.1 (0.7)	130.0 ± 24.8 (0.5)	12.1 ± 5.3 (1.8)	104.2 ± 81.5 (0.7)
M41L/L210W/T215Y	11.7±1.1(5.1)	217.0 ± 75.5 (0.8)	11.0 ± 4.6 (1.6)	226.9 ± 113.2 (1.6)
M41L/L210W/T215Y/R284K	13.3±1.5(5.8)	287.3 ± 84.5 (1.0)	18.1 ± 4.4 (2.7)	294.7 ± 93.7 (2.0)

The IC_{50} values represent averages ± standard deviations of at least three independent determinations, each one performed six times. The fold increase in IC_{50} relative to the wild-type HXB2 virus control carrying the RT sequence of BH10 is shown between parentheses. Values obtained by Drs. M. Nevot and M. A. Martínez (Fundació IrsiCaixa, Hospital Universitari Germans Trias i Pujol, Badalona, Spain).

[a] Experiments were carried out with the water soluble diester prodrug tenofovir disoproxil fumarate.

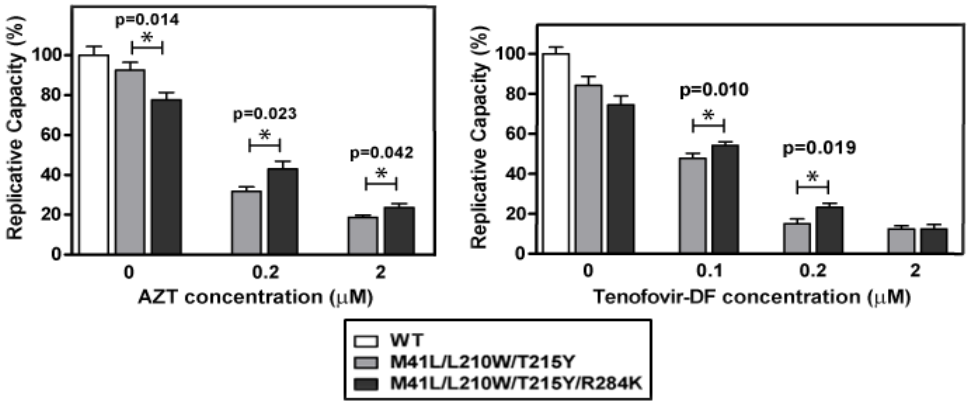

Figure 68. Replication kinetics of WT and mutant RTs in the absence and in the presence of AZT and tenofovir disoproxil fumarate (tenofovir-DF). In each case, histograms show the relative replication capacity (%), compared to the WT virus cultured in the absence of drug, based on the slopes of p24 antigen production of each recombinant virus after infection of stimulated PBMCs. The significance of the difference between slopes was calculated using the GraphPrism v. 4 software and significant *p* values are represented above the bars. Statistical analyses were performed by using a Student *t* test. Figure and data provided by Drs. M. C. Puertas and J. Martínez-Picado (Fundació IrsiCaixa, Hospital Universitari Germans Trias i Pujol, Badalona, Spain).

5.1 Role of mutations H208Y, R284K and the combination Pro-272/Arg-277/Thr-286 in resistance to NRTIs mediated by amino acid substitutions of the TAM-1 pathway

It is well known that TAM-1 mutations confer resistance to thymidine analogues and other NRTIs by improving the excision of inhibitors from the 3´-end of blocked primers (Meyer *et al.*, 1998, 1999). During this project, rescue assays have been used to simulate the events taking place during reverse transcription. Accordingly, primer termination due to the incorporation of an NRTI at the 3´-end of the growing DNA chain can be repaired by the RT through excision mediated by a PPi donor. DNA synthesis will then continue from the free 3´-end of the primer. Therefore, this assay can be divided in three different phases: (i) incorporation of the inhibitor in the 3´-end of the primer, (ii) excision of the inhibitor mediated by a PPi donor molecule (ATP, under physiological conditions), and (iii) extension of the free primer to the final product.

Different factors can be affecting the rate of the overall rescue reaction: the ability of the RT to bind nucleic acid complexes (*i.e.*, RNA/DNA and DNA/DNA T/Ps), the efficiency in the NRTI incorporation to the 3´-end of the primer (*i.e.*, the ability to discriminate against the NRTI), the capacity to excise the monophosphate form of the inhibitor from a terminated primer using a PPi donor molecule, and the catalytic rate of nucleotide incorporation and primer extension ability needed to elongate the primer to the final fully-extended product.

5.1.1 H208Y, a mutation contributing to NRTI excision

None of the studied RT thumb subdomain substitutions (*i.e.*, R284K and the set of polymorphisms Pro-272/Arg-277/Thr-286) showed a direct effect in the ability of TAM-containing RTs to excise chain-terminators from the 3´-end of blocked primers. On the other hand, excision of AZTMP from terminated DNA primers in T/P complexes was enhanced by the addition of the H208Y substitution to an RT containing the TAM-1 mutations M41L, L210W and T215Y. This effect was observed over a wide range of RT concentrations, suggesting that this mechanism of resistance could operate at many different multiplicities of infection. In addition, this result is in agreement with the lower susceptibility to AZT of viral strains bearing RT mutations M41L/H208Y/L210W/T215Y compared with those bearing the TAM-1 set of amino acid substitutions (*i.e.*, M41L/L210W/T215Y) (Table 20). The higher excision of AZTMP from blocked primers translates in a higher rescue rate of AZTMP-blocked DNA/DNA complexes. A similar mechanism is probably implicated in the higher rescue activity of d4TMP- and tenofovir-blocked DNA/DNA complexes shown by the M41L/H208Y/L210W/T215Y RT, compared with the enzyme containing only the TAM-1 mutations.

H208Y has been previously described as a foscarnet resistance-associated mutation (Mellors *et al.*, 1995). Previous studies have shown that foscarnet resistance mutations increase the AZT susceptibility of TAM-containing enzymes (Tachedjian *et al.*, 1996). Thus, introduction of H208Y and Q161L (another foscarnet resistance mutation) in an RT containing mutations D67N/K70R/T215F/K219Q produced a large reduction of the ATP-dependent excision of AZTMP from blocked complexes, although the individual effects of H208Y and Q161L were not elucidated (Meyer *et al.*, 2003). Studies carried out with WT and mutant RTs bearing H208Y, Q161L or the double-mutant Q161L/H208Y showed that Q161L was a major contributor to foscarnet resistance with IC_{50} values of 0.37, 0.52, 1.45 and 4.0 μM for WT RT and mutants H208Y, Q161L/H208Y and Q161L, respectively, in assays carried out with poly(rA)/oligo$(dT)_{10}$ (Tramontano *et al.*, 1998).

His-208 is situated in the vicinity of the ATP binding site created by TAMs, but not close enough to interact directly with the ribonucleotide needed for the excision reaction (Tu *et al.*, 2010). Molecular dynamics simulations of the structures of M41L/L210W/T215Y and M41L/H208Y/L210W/T215Y RTs carried out by Dr. J. Mendieta (Centro de Biología Molecular "Severo Ochoa", Madrid, Spain), and based on molecular models constructed by using as template the crystal structure of the ternary complex of M41L/D67N/K70R/T215Y/K219Q RT, dsDNA and $AZTp_4A$ revealed a potential role of the H208Y mutation in ATP-mediated excision. In the crystal

structure, the ATP moiety of the $AZTp_4A$ molecule is expected to locate at a position equivalent to that of the ATP molecule prior to the nucleophilic attack, resulting in the excision of the 3´-end inhibitor (Tu *et al.*, 2010).

Models generated by molecular dynamics predict that the relative position of the side-chain of Tyr-215 in the M41L/H208Y/L210W/T215Y RT is similar to that observed in the crystal structure of the M41L/D67N/K70R/T215Y/K219Q excision-proficient RT, with Tyr-215 making a stacking interaction with the adenine ring of the $AZTp_4A$ molecule (Fig 69A). However, in the RT containing Leu-41, Trp-210 and Tyr-215, the side-chain of Tyr-215 adopts a rather different conformation, away from the adenine ring of the $AZTp_4A$ molecule (Fig 69B). The phosphates of the $AZTp_4A$ molecule adopt a similar conformation in both RTs, compatible with the structural requirements of the excision reaction. It should be noted that in the crystal structure of the WT RT complexed with dsDNA and $AZTp_4A$ (Tu *et al.*, 2010), important hydrogen bonds are lost while the conformation of the ATP moiety would be incompatible with excision.

In the M41L/H208Y/L210W/T215Y RT model, the side-chains of Tyr-208 and Trp-212 make stacking interactions at the C-terminal end of α-helix F. These interactions affect the conformation of Arg-211 and indirectly the positioning of the side-chain of Trp-210, that shows a downwards location relative to the Tyr-215 ring (Fig 69A). This modified position eliminates the steric clash present in the M41L/L210W/T215Y model, created by the conformation of Trp-210 that pushes the side-chain of Tyr-215 towards the adenine ring of $AZTp_4A$. The presence of histidine at position 208 reduces its potential interaction with Trp-212, relaxing the packing of the C-terminal end of α-helix F, and ultimately affecting the interaction of Tyr-215 with the adenine moiety of $AZTp_4A$ (Fig 69B).

Hence, modeling studies reveal that a key factor that could explain the differences between the excision rates of M41L/H208Y/L210W/T215Y and M41L/L210W/T215Y RTs is the proper packaging of residues at the C-terminal end of α-helix F and their long-distance effect on the conformation of Tyr-215. This notion is consistent with results obtained in GTP- and ITP-dependent rescue assays. Thus, while ATP was more efficiently used by the M41L/H208Y/L210W/T215Y RT, no differences were detected between this RT and the M41L/L210W/T215Y mutant enzyme, when rescue assays were carried out in the presence of GTP or ITP. ATP differs from these two NTPs in the 6´-substituent of its nitrogen base, a position important for the proper interaction of the adenosine moiety with the side-chain of Tyr-215 (Fig 69).

In addition, results obtained in rescue assays carried out with the M41L/H208Y/T215Y RT provided further support for the modeling studies. Hence, when the interaction between the side-chains of Tyr-208 and Trp-210 was eliminated by reverting Trp-210 to Leu, the ability of the resulting M41L/H208Y/T215Y RT to rescue DNA synthesis from blocked-DNA/DNA complexes was indistinguishable from that of M41L/T215Y and M41L/L210W/T215Y RTs. According to the Stanford HIV Drug Resistance Database (http://hivdb.stanford.edu/; accessed in October 2013), only 6.4% of the 1,881 of all HIV-1 group M subtype B isolates bearing mutations M41L, H208Y and

T215Y contained Leu-210. In agreement with this observation, studies of phenotypic susceptibility to AZT have shown that viral strains bearing the H208Y/T215Y mutations are equally susceptible to those with only T215Y (Clark *et al.*, 2006), thereby indicating that the mutation H208Y alone is not enough to improve the resistance profile conferred by the T215Y substitution.

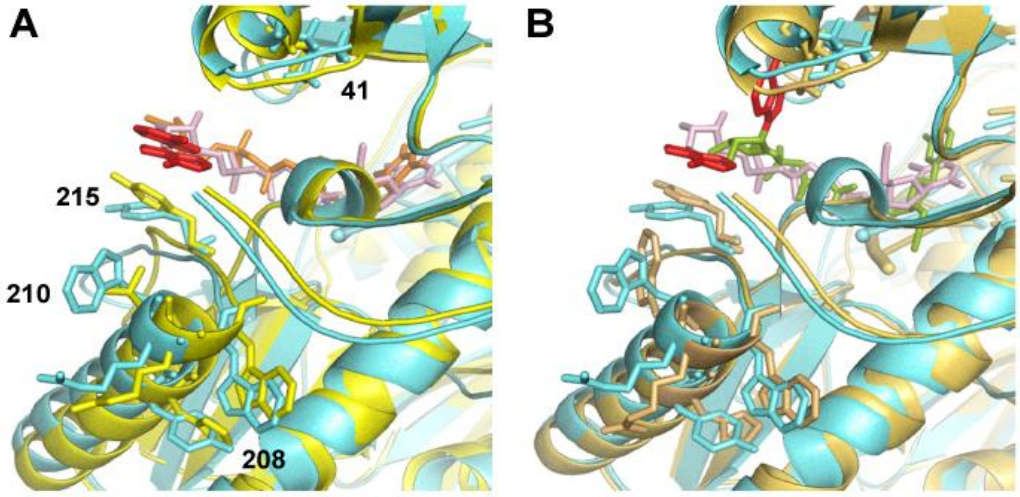

Fig 69. Comparison of the structural models of mutant M41L/L210W/T215Y and M41L/H208Y/L210W/T215Y RTs in complex with dsDNA and AZTp$_4$A. (A) Superposition of the refined crystal structure of M41L/D67N/K70R/T215Y/K219Q RT/dsDNA/AZTp$_4$A and the equivalent molecular model of the complex containing M41L/H208Y/L210W/T215Y RT. Cartoon representations of the polypeptide backbone of the M41L/D67N/K70R/T215Y/K219Q and M41L/H208Y/L210W/T215Y RTs are shown in yellow and cyan, respectively. Stick representations are used to indicate the location of relevant residues at positions 41, 208-212 and 215. The AZTp$_4$A molecule in the refined crystal structure is shown in orange, and in the molecular model containing the M41L/H208Y/L210W/T215Y RT is shown in purple. Adenine rings are shown in red. (B) Superposition of the refined molecular models of the ternary complexes containing M41L/H208Y/L210W/T215Y and M41L/L210W/T215Y RTs (cyan and wheat, respectively). Orange and green stick representations are used to show the AZTp$_4$A molecules in complexes containing M41L/H208Y/L210W/T215Y and M41L/L210W/T215Y RTs, respectively. In both cases, adenine moieties are shown in red. Molecular dynamics simulations were carried out by Dr. J. Mendieta (Centro de Biología Molecular "Severo Ochoa", Madrid, Spain). Structures were obtained with the PyMol molecular Graphics Systems (DeLano Scientific) software. Atom coordinates were taken from PDB file 3KLE.

5.1.2 R284K facilitates rescue of blocked DNA primers in DNA/DNA complexes by improving DNA polymerization efficiency of RTs containing TAM-1 mutations

The presence of the combination of TAMs M41L, L210W and T215Y confers relatively high rescue efficiency of primers terminated with AZTMP or tenofovir. This is a consequence of their high excision activity in the presence of ATP. R284K does not affect the ATP-mediated excision activity of mutant RTs bearing the combination M41L/L210W/T215Y. However, it improves the rescue efficiencies of these enzymes. This effect could not be attributed to an influence of the mutation on DNA binding affinity (K_d values for all tested RTs were around 2 nM for DNA/DNA complexes) or nucleotide discrimination, since AZTTP and tenofovir-DP inhibition constants (K_i) were essentially the same for M41L/L210W/T215Y and M41L/L210W/T215Y/R284K RTs.

However, the rescue advantage conferred by the presence of R284K in a TAM-1 background seems to be driven by its higher rates of nucleotide incorporation during DNA synthesis. The k_{cat} and k_{pol} values for nucleotide incorporation are 60-77% and 80% higher, respectively, for the mutant M41L/L210W/T215Y/R284K than for the M41L/L210W/T215Y RT. These significant increases translate in a higher efficiency of primer extension by the M41L/L210W/T215Y/R284K RT at different T/P concentrations. This effect was also observed when R284K was added to an otherwise WT background. Consistent with those results, a significant enhancement in the processivity of the M41L/L210W/T215Y/R284K RT was also observed.

The R284K mutation seems to affect the polymerase activity of the RT in a different way than other RT thumb subdomain substitutions as N255D, I257T, G262A, N265D or W266T, which have been reported to impair RT primer extension and processivity (Gao *et al.*, 1998; Fisher *et al.*, 2003). In addition, the higher catalytic rate of nucleotide incorporation provides a rational explanation for the higher fitness of the viral strain bearing mutations M41L/L210W/T215Y/R284K in its RT coding sequence when grown in the presence of AZT or tenofovir disoproxil fumarate (Fig 68).

Analysis of the structure of the ternary complex of RT, DNA/DNA and dTTP (Huang *et al.*, 1998) shows that in the p66 thumb subdomain the side-chain of Arg-284 is close to the template strand (Fig 70A). Amino groups of the side-chain of Arg-284 are situated 3.6 and 4.4 Å away from oxygen substituents of the phosphate group joining DNA template nucleotides -12 and -13 (Fig 70B).

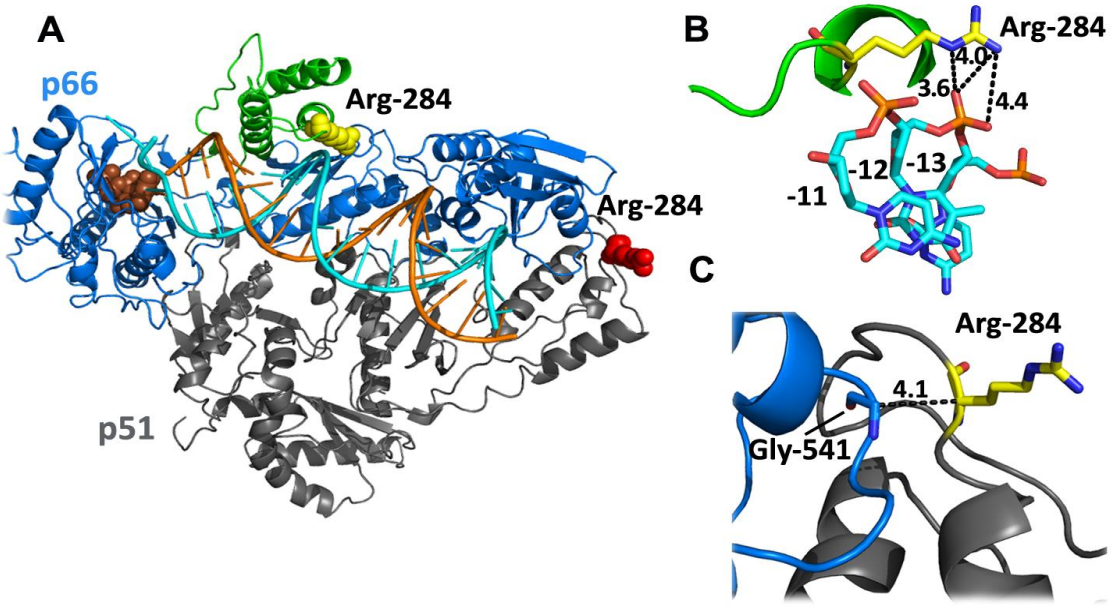

Fig 70. Structural role of Arg-284. (A) Structure of HIV-1 RT in complex with DNA/DNA and dTTP. The RT subunits are represented as ribbon diagrams (blue for p66, with the thumb subdomain in green, and grey for p51). The DNA primer is shown in orange, the template DNA in cyan and the dTTP molecule as brown spheres. The side-chains of Arg-284 in the p66 and p51 subunits are shown with a sphere representation in yellow and red, respectively. (B) Relevant distances (expressed in Å) between the side-chain of Arg-284 and the DNA template strand. The DNA backbone is shown in cyan with oxygen, nitrogen and sulfur atoms in red, blue and orange, respectively. (C) Relevant distances (expressed in Å) between main-chain of Arg-284 in the p51 subunit and Gly-541 in the p66 subunit. Structures were obtained with the PyMol molecular Graphics Systems (DeLano Scientific) software. Atom coordinates were taken from PDB file 1RTD.

Therefore, extensive contacts between the amino acid at position 284 and the template strand could be influencing T/P binding and probably its proper alignment at the DNA polymerase active site, thereby affecting nucleotide incorporation rates. In addition, residue 284 in the p51 thumb subdomain is also close to the p66 RNase H domain. The main-chain amino group of Arg-284 is located at 4.1 Å from p66 Gly-541 (Fig 70C). Hence, as proposed by others previously, the interaction of residue 284 in the p51 subunit with p66 could also contribute to the altered behavior of the RT (Hermann *et al.*, 1994; Waters *et al.*, 2009). The contribution of Lys-284 to the enhanced RNase H activity of the M41L/L210W/T215Y/R284K RT compared with the enzyme containing only the TAM-1 mutations could be due to the proximity of the p51 Lys-284 residue and the p66 RNase H domain.

5.1.3 The triad Pro-272/Arg-277/Thr-286 facilitates rescue of primers terminated with NRTIs annealed to an RNA template

As discussed above, in comparison with RTs having the TAM-1 cluster alone, mutant RTs M41L/H208Y/L210W/T215Y and M41L/L210W/T215Y/R284K showed enhanced rescue ability of primers terminated with NRTIs (d4TMP, AZTMP or tenofovir) annealed to DNA templates. However, these effects were not observed in rescue assays carried out with RNA/DNA-blocked complexes. A rational explanation for this behavior can be proposed from the results of RNase H measurements carried out with H208Y- and R284K-containing enzymes. Both RTs showed higher RNase H catalytic rates than their homologs having either only the TAM-1 mutations M41L, L210W and T215Y, or the WT sequence. Hence, enhanced template cleavage would be decreasing the excision of the inhibitor and the subsequent DNA primer elongation during the rescue reaction.

Many previous studies have shown that the higher the RNase H activity, the lower is the RNA/DNA-dependent rescue activity of the RT (Brehm *et al.*, 2008, 2012; Ehteshami *et al.*, 2008a; Radzio *et al.*, 2010; reviewed in Delviks-Frankenberry *et al.*, 2010), supporting our conclusion that the increased RNase H activity of the H208Y- and R284K-containing RTs is negatively affecting the rescue activity on RNA/DNA-blocked complexes.

RNase H activity assays carried out with three different complexes showed that thumb subdomain polymorphisms Pro-272, Arg-277 and Thr-286 had a minor impact on the generation of RNase H primary or secondary cleavage products by the RT. Thus, rescue assays with AZTMP-terminated DNA primers bound to RNA templates showed that the mutant M41L/T215Y RT (bearing Pro-272/Arg-277/Thr-286) produced a significantly higher amount of fully-extended product, compared with the M41L/T215Y/P272A/R277K/T286A mutant enzyme. Similar differences were also found in the case of d4TMP- and CBVMP-blocked complexes. In addition, we also observed that with all three inhibitors the rescue efficiency of the WT enzyme was higher than that of the P272A/R277K/T286A RT, when blocked primers were annealed to RNA templates.

The increased rescue activity of the M41L/T215Y RT cannot be attributed to a higher ATP-dependent excision rate, since mutant RTs bearing mutations M41L/T215Y with and without thumb

subdomain polymorphisms showed the same excision activity on d4TMP- and CBVMP-terminated primers annealed to RNA templates (Fig 26). However, our nucleic-acid binding affinity measurements showed that the presence of Pro-272, Arg-277 and Thr-286 increased the affinity of WT and M41L/T215Y RTs for RNA/DNA complexes, without affecting their interaction with DNA/DNA heteroduplexes. This result was consistent with data from primer extension assays carried out with RNA/DNA complexes under limiting T/P concentrations (1 nM). These experiments showed that the addition of Pro-272, Arg-277 and Thr-286 increased the amount of extended product in reactions catalyzed by the mutant M41L/T215Y RT. The enhanced ability to use RNA/DNA complexes at low concentrations conferred by polymorphisms Pro-272, Arg-277 and Thr-286 provides a rational explanation for the increased ability of the WT and M41L/T215Y RTs to rescue RNA/DNA^{AZTMP}-blocked complexes, as well as for the higher replication capacity of the viral clones bearing these RTs when grown in the presence of low concentrations of AZT (Fig. 66). Interestingly, the connection subdomain mutation G333D has also been found to improve rescue of DNA/DNA^{AZTMP} T/Ps by increasing the affinity of the M41L/M184V/L210W/T215Y RT for these blocked-complexes (Zelina *et al.*, 2008).

The increased affinity of RTs bearing Pro-272, Arg-277 and Thr-286 for binding RNA/DNA complexes can be analyzed from a structural point of view. Comparison of RT-DNA/DNA and RT-RNA/DNA crystal structures shows that Arg-277 and Thr-286 make more extensive contacts with the RNA template than with the DNA template (Ding *et al.*, 1998; Huang *et al.*, 1998; Sarafianos *et al.*, 2001) (Fig 71A). Thus, amino groups of Arg-277 are situated between 3.3 and 3.5 Å away from the oxygen substituent of the phosphate group linking RNA nucleotides -7 and -8, while in the DNA/DNA complex, Arg-277 is rotated away from the nucleic acid (Fig 71B, C). The hydroxyl group of the side-chain of Thr-286 is situated at 4.4 Å from the 2´-OH group of the ribose at position -8 of the template RNA, while the interaction with the template strand in the DNA/DNA complexes involves contacts with the sugar-phosphate backbone at positions -8 and -9 of the template, situated at around 3.7 to 5.5 Å (Fig 71B, C). Pro-272 lies in a region far from the template strand, independently of the nature of the nucleic acid, and could contribute to the proper folding of the thumb subdomain. However, Pro-272 has been found to reduce DNA/DNA binding affinity and RT processivity (Wang *et al.*, 2008). In the p51 subunit, studied thumb subdomain polymorphisms are located away from the T/P, except for Thr-286, which is situated near the p66 connection residue Asn-460 (Fig 71A). However, it is unlikely that Thr-286 could affect the interaction of the RT with the T/P complex.

In summary, our data show that there are at least three different mechanisms by which accessory mutations could facilitate the selection of HIV-1 variants carrying TAM-1 mutations under the selection pressure of drugs such as AZT or tenofovir. The palm subdomain mutation H208Y directly plays its role by increasing the excision ability of TAMs. The thumb subdomain substitution R284K and the polymorphisms Pro-272/Arg-277/Thr-286 enhance NRTI resistance by improving a natural property of the RT, not necessary related with the resistance mechanism *per se* (*i.e.*, not related to excision), that translates in an improved DNA synthesis in the presence of excisable NRTIs. RT thumb subdomain polymorphisms Pro-272/Arg-277/Thr-286 enhance the RT affinity for RNA/DNA

complexes, even in a WT background, while R284K improves the primer extension ability in WT and TAM-1-containing RTs. Although these mutations do not require the presence of TAMs to act, their impact in viral fitness in the absence of drug pressure seems to be negligible or very small, explaining why they are selected mainly during treatments containing NRTIs. Taken together, our results provide further evidence indicating that mutations far from the DNA polymerase active site or residues involved in TAMs could facilitate the selection of recombinant HIV-1 variants in the presence of drugs. In addition, our data highlight the plasticity of the RT, showing three different mechanisms by which amino acid substitutions in the DNA polymerase domain could modulate resistance to NRTIs.

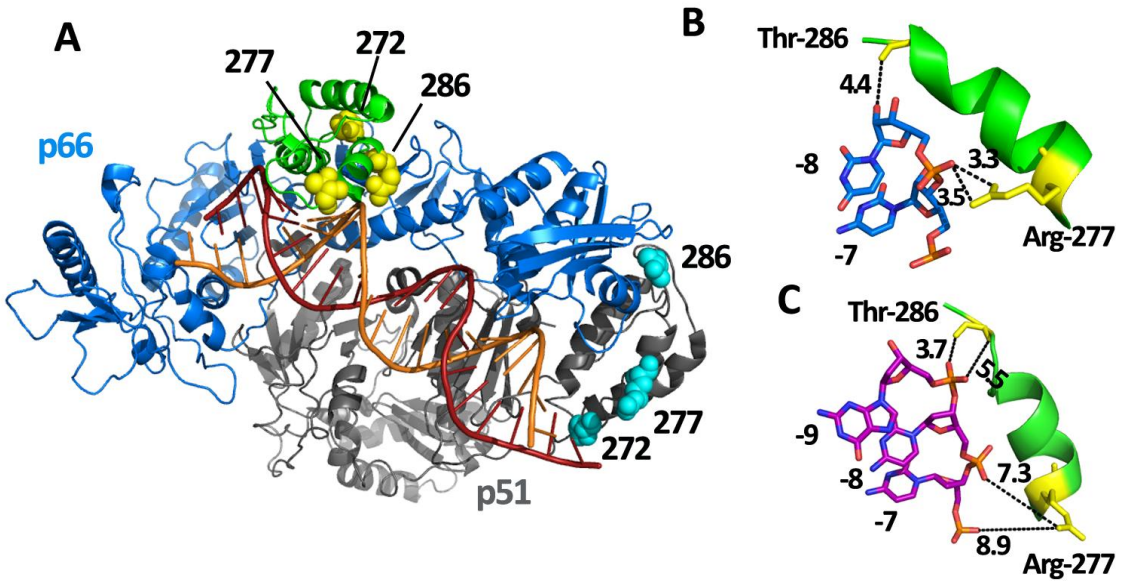

Fig 71. Interaction of RT thumb subdomain residues Pro-272, Arg-277 and Thr-286 with the template strand. (A) Structure of HIV-1 RT in complex with RNA/DNA. The RT subunits are represented as ribbon diagrams (blue for p66, with the thumb subdomain in green, and grey for p51). The DNA primer is shown in red and the template RNA in orange. The side-chains of residues Pro-272, Arg-277 and Thr-286 are shown using a sphere representation in yellow and cyan for p66 and p51 subunits, respectively. (B) Relevant interaction atomic distances (expressed in Å) between the side-chains of Arg-277 and Thr-286 and the RNA strand. The backbone of the RNA template is shown in blue, with oxygen, nitrogen and sulfur atoms in red, blue and orange, respectively. (C) Relevant interactions and distances (expressed in Å) between the side-chains of Arg-277 and Thr-286 and the template DNA strand in a binary complex of HIV-1 RT and a DNA/DNA T/P. The backbone of the DNA template is shown in purple, with oxygen, nitrogen and sulfur atoms in red, blue and orange, respectively. Atom coordinates of the RT bound to RNA/DNA and those of the RT bound to DNA/DNA were taken from PDB files 1HYS and 2HMI, respectively. Structures were obtained with the PyMol molecular Graphics Systems (DeLano Scientific) software.

5.2 Influence of RT connection subdomain mutations in NNRTI resistance and RNase H cleavage specificity

Very often, currently prescribed HAART regimens contain one NNRTI. Detailed sequence analysis of the whole RT-coding sequence in HIV-1 isolates has allowed the identification of residues far from the NNRTI binding-pocket implicated in drug resistance. Mutations N348I, T369I/V, and T376S have been related to exposure to NNRTIs, particularly NVP (Cane *et al.*, 2007; Hachiya *et al.*, 2009; Shariar *et al.*, 2009; Gupta *et al.*, 2010; Lengruber *et al.*, 2011; Paredes *et al.*, 2011). NVP

susceptibility data obtained in our study for mutant RTs N348I, T369I, T369V, T376S and N348I/T369I are consistent with those previous studies, since all RTs showed some degree of drug resistance. However, we did not detect a significant impact of those amino acid substitutions on the susceptibility to more potent inhibitors such as EFV and ETR. Previously, it has been shown that while mutant RTs N348I (Biondi *et al.*, 2010) and T376S (Paredes *et al.*, 2011) are resistant to NVP, both remain susceptible to EFV. Although some authors have reported low-level EFV resistance of viral strains carrying the T369I/V mutation or the combination N348I/T369I in phenotypic assays with mutant HIV-1 (Zhang *et al.*, 2007; Gupta *et al.*, 2010, 2011; Lengruber *et al.*, 2011), drug susceptibility assays carried out with recombinant viruses bearing our RT constructs failed to detect significant differences in resistance to EFV, ETR or RPV with any of the tested mutants and the WT RT (Table 23). Consistent with the NVP IC_{50} value obtained in our biochemical measurements, the viral strain carrying N348I/T369I showed the highest levels of NVP resistance in phenotypic assays.

Table 23. Susceptibility of HIV-1 constructs bearing mutations at the RT connection subdomain and the reference strain K103N[a]

	IC_{50} (nM)				
RT	**NVP**	**DLV**	**EFV**	**ETR**	**RPV**
WT	15.0 ± 1.70	1.8 ± 0.5	1.1 ± 0.2	1.0 ± 0.1	0.1 ± 0.01
T369I	28.0 ± 1.50 (1.9)	3.2 ± 0.6 (1.8)	1.1 ± 0.4 (1.0)	1.0 ± 0.1 (1.0)	0.1 ± 0.03 (1.1)
T369V	27.0 ± 12.0 (1.8)	2.9 ± 1.0 (1.6)	1.0 ± 0.1 (0.9)	1.1 ± 0.3 (1.1)	0.3 ± 0.03 (2.5)
T376S	26.0 ± 7.20 (1.7)	4.4 ± 0.8 (2.4)	1.5 ± 0.2 (1.4)	1.4 ± 0.2 (1.5)	0.2 ± 0.05 (1.7)
N348I	33.0 ± 4.60 (2.2)	4.1 ± 0.7 (2.3)	1.2 ± 0.3 (1.1)	1.2 ± 0.1 (1.2)	0.2 ± 0.10 (2.3)
N348I/T369I	102 ± 2.50 (6.8)	3.1 ± 0.6 (1.7)	1.4 ± 0.3 (1.3)	1.1 ± 0.1 (1.1)	0.1 ± 0.03 (0.7)
K103N	1830 ± 226 (122)	332 ± 39 (184)	44 ± 15 (38)	1.2 ± 0.4 (1.2)	0.1 ± 0.02 (1.2)

The IC_{50} values represent averages ± standard deviations of at least three independent determinations, each one performed six times. The fold-increase in IC_{50} relative to the wild-type HXB2 virus control carrying the RT sequence of BH10 is shown between parentheses. Values obtained by Drs. M. Nevot and M. A. Martínez (Fundació IrsiCaixa, Hospital Universitari Germans Trias i Pujol, Badalona, Spain).

[a] K103N is a well-characterized DLV, NVP and EFV resistance mutation.

It has been shown that viral strains bearing mutations N348I, T369I or N348I/T369I have a reduced replication capacity in the absence of drugs, especially the double-mutant, whose fitness was estimated around 11% relative to the WT virus (Gupta *et al.*, 2010). Our DNA polymerase activity determinations showed only minor differences in the nucleotide incorporation rates between N348I, T369I and N348I/T369I mutants and the WT RT. However, RNase H activity measurements have shown that the N348I/T369I RT had reduced RNase H activity on heteropolymeric RNA/DNA complexes. Its lower endonucleolytic activity could explain the reduced viral fitness observed in replication capacity assays.

Interestingly, RTs containing mutations N348I or T369I, but especially the double-mutant N348I/T369I also showed significant differences in cleavage specificity with PPT-containing oligonucleotides used either as templates (as in (-) strand DNA synthesis) or as primers (as in (+) strand DNA synthesis) (Fig 72). Our results indicate that the N348I/T369I RT has a different cleavage window specificity compared to the WT enzyme. Thus, when the highly conserved PPT-U3 cleavage site (Huber & Richardson, 1990; Powell *et al.*, 1999; Jones & Hughes, 2007) was situated less than 18

nucleotides away from the DNA 3´-end in systems mimicking (-) strand DNA synthesis (*i.e.*, in complexes with an RNA template containing the PPT sequence annealed to a DNA primer containing a recessed 3´-OH end), the N348I/T369I RT showed a stronger tendency than the WT enzyme to generate RNase H hydrolysis products longer than the PPT (Fig 72).

However, this change in cleavage specificity has more dramatic effects in PPT-processing when our system is mimicking the initiation of (+) strand DNA synthesis (*i.e.*, using the T57d/PPT17r8d complex). In this case, the change in cleavage specificity of the N348I/T369I mutant produced a large drop in its RNase H catalytic rate (Fig 72, lower left panel). This was due to the fact that the preferred cleavage site of this RT would locate in the DNA/DNA double-stranded region (Fig 72). These results provide additional support for impaired RNase H activity as the hypothetical main cause of the reduced fitness of the N348I/T369I viral strain.

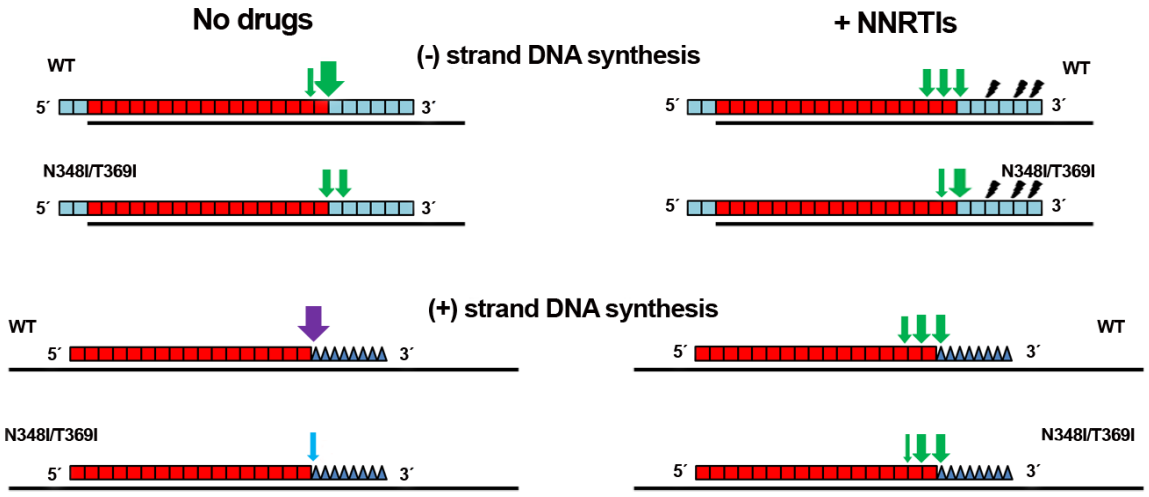

Fig 72. Schematic representation of the cleavage specificity of the WT RT and the double-mutant N348I/T369I. Upper part of the panel shows a scheme of a system mimicking the (-) strand DNA synthesis. The DNA primer (black line) is annealed to the viral RNA, with the PPT segment indicated by using 17 red boxes (equivalent to 17 ribonucleotides), with non-PPT RNA segments at both extremes (blue boxes). Cleavage specificity and substrate preference of WT and N348I/T369I RTs is indicated by using green arrows. The thickness of the arrow is equivalent to the preference of the enzyme to cut at that position. Longer-distance cleavages produced by the presence of NNRTIs are indicated with black bolts. The lower panel shows a system mimicking (+) strand DNA synthesis. The large template DNA (black line) is annealed to a primer containing the PPT segment, drawn as 17 red boxes (equivalent to 17 ribonucleotides) and with added dNTPs as blue triangles. Preferred cleavage sites of WT and N348I/T369I RTs in the absence of NNRTI are indicated with a purple and blue arrow, respectively, accounting for the overall higher RNase H rates of the WT RT. In the presence of NNRTIs RNase H cleavage sites are marked as in the upper panel.

Addition of NNRTIs produces a strong enhancement of the RNase H activity of all tested RTs. Although higher concentrations of EFV and ETR than of NVP were needed to promote the observed increase of RNase H activity, saturating concentrations of all NNRTIs had essentially the same effect. Interestingly, NNRTIs also changed the specificity of the RNase H-mediated cleavage, since unspecific long-distance cuts were detected in assays carried out using systems mimicking (-) strand DNA synthesis with WT, N348I and N348I/T369I RTs (Fig 72). Binding of NNRTIs has been

previously described to promote slippage of the RT along the T/P, and this could be the likely cause of the observed unspecific cleavage patterns (Palaniappan *et al*., 1995). These results are also consistent with previous work showing that NVP, EFV and other NNRTIs enhance the RT RNase H activity (Gopalakrishnan & Benkovic, 1994; Palanippan *et al.*, 1995; Shaw-Reid *et al.*, 2005; Hang *et al.*, 2007; Radzio & Sluis-Cremer, 2008). Although there is no clear explanation for such a phenomenon, several studies have shown that some NNRTIs, especially EFV, promote the dimerization of the RT subunits (Tachedjian *et al.*, 2001; Figuereido *et al.*, 2006; Braz *et al*., 2010a,b). However, enhanced RT dimerization does not completely explain the observed effect, since NVP does not promote RT subunit association, despite being a potent enhancer of RNase H activity.

Under our assay conditions, cleavage of the PPT17r8d by the WT RT and the N348I mutant enzyme was enhanced in the presence of NVP. However, Biondi and colleagues have previously reported that the N348I RT was not affected by NVP. According to these authors, in the presence of NVP this enzyme prefers to bind the T/P in the polymerase-dependent binding mode, thereby reducing the cleavage of the PPT17r8d strand (Biondi *et al.*, 2010). Although we do not have a clear explanation for this discrepancy, it is possible that differences in the RT background of the enzyme carrying the N348I mutation (*i.e.*, BH10 in our experiments and HXB2 in the assays of Biondi *et al.*) could be influencing the results. In agreement with this proposal, it has been shown that the presence of polymorphism R172K in the RT background (as is the case of our BH10 strain) could have a clear influence in the susceptibility to NVP of mutant N348I RT (Hachiya *et al.*, 2012).

PPT processing is a pivotal step in reverse transcription. Correct cleavage of this RNA sequence during (-) strand DNA synthesis yields primers of 15, 17 and 19 nucleotides (Huber & Richardson 1990; Julias *et al.*, 2002; Rausch & LeGrice, 2007). While the PPT 5´-end (A tract) accepts some variation, the tract of 6 Gs forming the 3´-end is highly conserved. Nucleotide substitutions or deletions at the polyguanosine segment produce a large reduction in the efficiency with which the RT uses the PPT during (+) strand DNA synthesis (Huber & Richardson 1990; Julias *et al.*, 2004; Jones & Hughes, 2007; Rausch & LeGrice, 2007). In addition, the correct cleavage at the PPT-U3 junction also determines the 5´-end of viral DNA, which should be conserved in order to be recognized by the IN to carry out the integration of the provirus. Results presented in this Thesis show that NNRTIs enhanced the RNase H activity of the RT to a level in which Gs situated at positions -1 and sometimes -2 of the PPT 3´-end were removed (Fig 73). Therefore, it seems likely that apart from inhibiting the DNA polymerase activity of the enzyme, NNRTIs could facilitate the formation of abortive PPT products. In agreement with these observations, it has been also shown that PPT-dependent synthesis is more susceptible to NVP and EFV inhibition than DNA-primed polymerization (Grobler *et al.*, 2007).

Recent structural and biochemical reports have found that residue 348 in the p51 subunit of the RT could be playing an important role in maintaining the stability of this subunit, affecting the interaction between both subunits and the correct positioning of the RNA strand in RNA/DNA T/Ps susceptible to cleavage by the viral RT (Chung *et al.*, 2013; Lapkouski *et al.*, 2013). Therefore, mutations affecting Asn-348 could distort the interaction between p66 and p51 and their spatial

organization. Residue 369 in p51 and p66 subunits is away from the T/P, the NNRTI binding pocket or the p66-p51 interface (Lapkouski *et al.*, 2013). Thr-369 has not been study thoroughly, but the similar phenotype of RTs N348I and T369I in RNase H cleavage measurements could be indicative of a similar role in affecting RT subunits interaction.

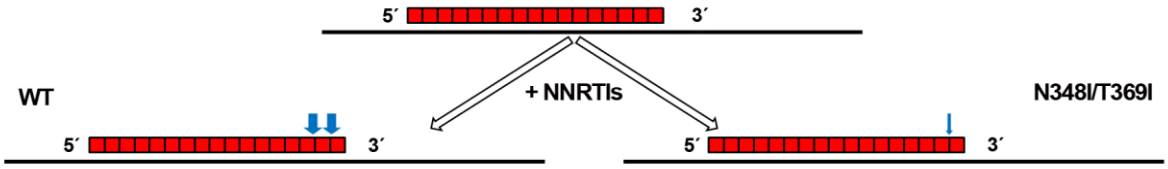

Fig 73. Schematic representation of RNase H cleavages displayed by the WT RT and the double-mutant N348I/T369I in a system mimicking the (+) strand DNA synthesis. The DNA template (black line) is annealed to a PPT primer of 17 ribonucleotides (represented by 17 red boxes). In the absence of NNRTIs none of the RTs is able to cut the PPT 3´-end. Addition of NNRTIs triggers the cleavage of the 3´-end of the PPT primer in the case of the WT RT, but it is much less effective in the case of the N348I/T369I RT. Cleavage sites are represented by blue arrows. Thickness of the arrow represents the cut preference at that position.

As discussed above, common PPTs produced during (-) strand DNA synthesis contain 17 nucleotides (Huber & Richardson, 1990). The length of the PPT-RNA primer is the factor that determines the distance between the DNA polymerase active site and the RNase H cleavage site, that is required to release the PPT sequence during (+) strand DNA synthesis (Götte *et al.*, 1999, 2001), Thus, PPTs of 17 nucleotides impose an RNase H cleavage window of 17 nucleotides. Our PPT29DNA/PPT17r system mimics the very first step during the (+) strand DNA synthesis when no dNTPs have been added. While in the absence of NNRTIs the 17-nucleotide RNA strand remains resistant to hydrolysis by all RTs (*i.e.*, the WT RT and mutants N348I and N348I/T369I), in the presence of NVP or EFV, WT and N348I RTs degrade the polyguanosine tract at the 3´-end of the PPT primer (Fig 73). These degraded PPTs are not expected to be used in (+) strand DNA synthesis. However, the double-mutant N348I/T369I RT was completely resistant to NVP and only partially susceptible to EFV. Under our assay conditions, this RT is able to maintain the intact PPT structure in the presence of NNRTIs, and therefore it would increase the amount of PPT primer available for initiation of (+) strand DNA synthesis (Fig 73). Although the combination of mutations N348I and T369I has a dramatic impact on viral fitness in the absence of drugs, probably due to an impaired RNase H activity, in the presence of NVP or EFV the different cleavage specificity of this mutant could prevent the degradation of the PPT primer prior to initiation of (+) strand DNA synthesis providing a selective advantage for the selection of these mutations in NNRTI-treated patients.

Reductions in viral fitness have also been observed in different studies carried out with viral strains lacking the IN, or carrying certain IN mutations (Wu *et al.*, 1999; Zhu *et al.*, 2004; Lu *et al.*, 2005b). In these studies, a severe impairment in the synthesis of reverse transcription products was detected. For example, Zhu and colleges showed that viral strains bearing an IN variant with the C130S mutation (that eliminates the interaction with the RT), were highly impaired for the production of early products of reverse transcription (Zhu *et al.*, 2004). Since a correct cleavage of the PPT is an

essential step in reverse transcription, it is possible that an impairment in this step would be the cause of the reduced fitness of IN mutant viruses.

Our studies show that although addition of IN to an RT preparation containing a heteropolymeric RNA/DNA complex did not increase the endonucleolytic activity of the RT, during PPT processing in (-) and (+) strand DNA synthesis the presence of IN increased the RNase H activity of the RT. Interestingly, this enhancement of PPT processing proceeded only with the production of PPTs of the correct length (*i.e.*, without degradation of the polyguanosine tract at the 3´-end of the PPT).

IN has been implicated in the promotion of RT polymerase activity during first steps of (-) strand DNA synthesis (Dobard *et al.*, 2007; Nishitsuji *et al.*, 2009). Our results are consistent with these studies, since the presence of IN seems to facilitate the correct cleavage of the PPT during both (-) and (+) strand DNA synthesis. The more efficient hydrolysis of the PPT could result in a higher viral fitness, thereby providing a plausible explanation for the reduced replication capacity of viral strains bearing IN mutations (Wu *et al.*, 1999; Zhu *et al.*, 2004).

However, the exact role of IN in reverse transcription seems to be more complicated. For example, an interaction between IN and the cellular protein Gemin2 has been described as a factor promoting reverse transcription (Hamamoto *et al.*, 2006; Nishitsuji *et al.*, 2009). In addition, other viral proteins have been described as components of the reverse transcription complex. Examples are Tat, Nef and NC (Fournier *et al.*, 2002; Apolloni *et al.*, 2007; Levin *et al.*, 2010).

In this Thesis we have shown that the interaction between RT and IN could be important in (-) and (+) strand DNA synthesis during reverse transcription. We have also shown the high adaptability of the RT to drug pressure. Thus, the potent NRTI-excision activity provided by TAM-1 mutations could be further potentiated by improving the usage of ATP molecules as PPi donors, by increasing the binding affinity of the enzyme to RNA/DNA complexes or by enhancing the RT DNA polymerization ability. In addition, structural features of the RT, such as the distance between the DNA polymerase and the RNase H active sites could be playing a role in drug resistance by impairing PPT degradation during reverse transcription in the presence of NNRTIs.

6.Conclusions

6. Conclusions

1. In the presence of M41L, L210W and T215Y (TAM-1 cluster of mutations), the amino acid substitution H208Y increases rescue efficiency of primers terminated with AZTMP, d4TMP or tenofovir by improving the ATP-dependent excision activity of the RT. These results are consistent with the decreased phenotypic susceptibility to AZT of recombinant HIV-1 strains bearing RT mutations M41L/H208Y/L210W/T215Y relative to those having only M41L, L210W and T215Y.
2. The amino acid substitution R284K improves the ATP-dependent rescue activity of the M41L/L210W/T215Y mutant RT on primers terminated with AZTMP, tenofovir and d4TMP annealed to DNA templates. However, R284K does not affect the rate of excision of NRTIs in the presence of ATP, but stimulates the nucleotide incorporation activity of the RT. In rescue assays, R284K promotes primer extension after excision of the corresponding NRTI. This result is in agreement with the observed fitness advantage of viral strains bearing the combination of R284K with TAM-1 mutations in the presence of AZT or tenofovir.
3. Substitutions R284K and H208Y increase the RNase H activity of the RT. As a consequence, when any of these mutations is added to an RT containing the substitutions M41L/L210W/T215Y, the resulting enzyme shows reduced rescue efficiency of RNA/DNA complexes containing blocked DNA primers.
4. RT thumb subdomain polymorphisms Pro-272, Arg-277 and Thr-286 have no effect in the ATP-dependent rescue activity of blocked-DNA/DNA complexes of RTs containing the amino acid substitutions M41L and T215Y. However, those thumb subdomain polymorphisms improve the ability of the M41L/T215Y RT to rescue RNA/DNA complexes blocked with thymidine analogues.
5. The Pro-272/Arg-277/Thr-286 triad increased the affinity of the RT for RNA/DNA complexes either in the absence of mutations or in the presence of TAMs M41L and T215Y. However, thumb polymorphisms do not affect the interaction of the RT with DNA/DNA template/primers. The increased affinity for RNA/DNA complexes facilitates rescue of blocked-DNA primers annealed to RNA templates, particularly at low concentrations of template/primer. These results are consistent with the observed fitness advantage of viral strains bearing RT polymorphisms Pro272/Arg-277/Thr-286 and TAM-1 mutations, in the presence of low concentrations of AZT.
6. RT connection subdomain mutations N348I, T369I, T369V, T376S, as well as the combination N348I/T369I confer nevirapine resistance without affecting the susceptibility to efavirenz or etravirine. All three NNRTIs enhance the RNase H activity of wild-type and mutant RTs as determined with heteropolymeric and PPT-containing RNA/DNA complexes.

7. N348I/T369I RT and in a lesser extent the mutant N348I show reduced RNase H activity, particularly when the distance between the DNA polymerase and the RNase H active sites is shorter than 18 nucleotides. This property has been demonstrated by measuring the susceptibility of the PPT primer to RNase H hydrolysis during (-) and (+) strand DNA synthesis, and is expected to modulate the inhibitory effect of NNRTIs during these steps of reverse transcription.
8. HIV-1 integrase also enhances RNase H activity while processing the PPT sequence, in (-) and (+) strand DNA synthesis, but it does not affect the RNase H catalytic rate during the hydrolysis of heteropolymeric RNA/DNA complexes. However, unlike the case of NNRTIs, the HIV-1 IN promotes specific cleavage at the PPT-U3 junction without generating PPT products degraded at their 3´-end.

6. Conclusiones

1. En presencia de M41L, L210W y T215Y (grupo de mutaciones TAM-1), el cambio de aminoácido H208Y aumenta la eficacia de rescate de iniciadores bloqueados con AZTMP, d4TMP o tenofovir, debido a que mejora la actividad de escisión dependiente de ATP de la RT. Estos resultados justifican la menor susceptibilidad fenotípica al AZT de cepas recombinantes del VIH-1 portadoras de la RT M41L/H208Y/L210W/T215Y en comparación con aquellas que sólo tienen las mutaciones M41L, L210W y T215Y.

2. El cambio de aminoácido R284K mejora la actividad de rescate dependiente de ATP de la RT mutante M41L/L210W/T215Y sobre iniciadores terminados con AZTMP, tenofovir y d4TMP, hibridados con moldes ADN. Sin embargo, R284K no afecta a la capacidad de escisión de NRTIs de la enzima en presencia de ATP, si bien aumenta su tasa de incorporación de nucleótidos en reacciones de síntesis de ADN. En ensayos de rescate de iniciadores bloqueados en su extremo 3´, R284K promueve su extensión tras la escisión del correspondiente NRTI. Este resultado es coherente con la mayor capacidad replicativa de las cepas virales portadoras de la combinación de R284K junto con las mutaciones TAM-1, observada en presencia de AZT o tenofovir.

3. Las sustituciones H208Y y R284K incrementan la actividad RNasa H de la RT. Como consecuencia de ello, cuando cualquiera de estas mutaciones se añade a una RT portadora de los cambios M41L/L210W/T215Y, la enzima resultante muestra menor eficacia en el rescate de complejos ARN/ADN que contienen un iniciador de ADN bloqueado con AZTMP, d4TMP o tenofovir.

4. Los polimorfismos del subdominio “thumb” Pro-272, Arg-277 y Thr-286 no tienen ningún efecto en la actividad de rescate dependiente de ATP sobre complejos ADN/ADN bloqueados de RTs portadoras de las sustituciones de aminoácidos M41L y T215Y. Sin embargo, los polimorfismos del subdominio “thumb” mejoran la capacidad de la RT M41L/T215Y para rescatar complejos de ARN/ADN bloqueados con análogos a timidina.

5. La triada Pro-272/Arg-277/Thr-286 aumenta la afinidad de la RT por complejos ARN/ADN tanto en ausencia como en presencia de las TAMs M41L y T215Y. Sin embargo, los polimorfismos del “thumb” no afectan a la interacción de la RT con complejos molde/iniciador de tipo ADN/ADN. La mayor afinidad por complejos ARN/ADN facilita el rescate de iniciadores de ADN bloqueados e hibridados con moldes de ARN. Estos resultados podrían explicar la mayor capacidad replicativa de las cepas virales portadoras de los polimorfismos Pro-272/Arg-277/Thr-286 y las mutaciones TAM-1 respecto a las que sólo llevan TAMs, observada en presencia de bajas concentraciones de AZT.

6. Las mutaciones del subdominio “connection” de la RT N348I, T369I, T369V, T376S, así como la combinación N348I/T369I confieren resistencia a nevirapina sin afectar a su susceptibilidad a efavirenz o etravirina. Los tres inhibidores de la RT no análogos a nucleósido (NNRTIs) aumentan la actividad RNasa H de las RTs de genotipo silvestre y mutantes, tal y como se ha determinado con complejos ARN/ADN heteropoliméricos y con complejos portadores de oligonucleótidos con la secuencia de polipurinas, PPT.

7. La RT N348I/T369I y en menor medida el mutante N348I muestran menor actividad RNasa H, especialmente cuando la distancia entre los centros activos de la actividad ADN polimerasa y

de la RNasa H es menor a 18 nucleótidos. Esta propiedad ha sido demostrada mediante medidas de la susceptibilidad del iniciador PPT a la hidrólisis por la actividad RNasa H de la RT durante la síntesis de las cadenas de ADN de polaridad negativa y positiva, propiedad que podría modular el efecto inhibidor de los NNRTIs durante dichas etapas de la retrotranscripción.

8. La integrasa (IN) del VIH-1 también aumenta la actividad RNasa H de la RT durante el procesamiento de la secuencia PPT en la síntesis de las cadenas de ADN de polaridad negativa y positiva. Sin embargo, la presencia de IN en la reacción no afecta a la tasa catalítica de la actividad RNasa H durante la hidrólisis de complejos ARN/ADN heteropoliméricos. Al contrario de lo que sucede en reacciones llevadas a cabo en presencia de NNRTIs, la IN del VIH-1 promueve los cortes específicos del molde ARN en el sitio PPT-U3, sin generar productos derivados de la secuencia del PPT con extremos 3´degradados.

7.References

7. References

Abbink, T. E. & Berkhout, B. (2008). HIV-1 reverse transcription initiation: a potential target for novel antivirals? *Virus Res* **134**, 4-18.

Abbondanzieri, E. A., Bokinsky, G., Rausch, J. W., Zhang, J. X., Le Grice, S. F. & Zhuang, X. (2008). Dynamic binding orientations direct activity of HIV reverse transcriptase. *Nature* **453**, 184-9.

Acosta-Hoyos, A. J., Matsuura, S. E., Meyer, P. R. & Scott, W. A. (2012). A role of template cleavage in reduced excision of chain-terminating nucleotides by human immunodeficiency virus type 1 reverse transcriptase containing the M184V mutation. *J Virol* **86**, 5122-33.

Acosta-Hoyos, A. J. & Scott, W. A. (2010). The Role of Nucleotide Excision by Reverse Transcriptase in HIV Drug Resistance. *Viruses* **2**, 372-394.

Adamson, C. S. & Freed, E. O. (2007). Human immunodeficiency virus type 1 assembly, release, and maturation. *Adv Pharmacol* **55**, 347-87.

Ahn, J., Byeon, I. J., Dharmasena, S., Huber, K., Concel, J., Gronenborn, A. M. & Sluis-Cremer, N. (2010). The RNA binding protein HuR does not interact directly with HIV-1 reverse transcriptase and does not affect reverse transcription in vitro. *Retrovirology* **7**, 40.

Akanbi, M. O., Scarci, K., Taiwo, B. & Murphy, R. L. (2012). Combination nucleoside/nucleotide reverse transcriptase inhibitors for treatment of HIV infection. *Expert Opin Pharmacother* **13**, 65-79.

Alcaro, S., Alteri, C., Artese, A., Ceccherini-Silberstein, F., Costa, G., Ortuso, F., Parrotta, L., Perno, C. F. & Svicher, V. (2011). Molecular and structural aspects of clinically relevant mutations related to the approved non-nucleoside inhibitors of HIV-1 reverse transcriptase. *Drug Resist Updat* **14**, 141-9.

Alvarez, M., Matamoros, T. & Menendez-Arias, L. (2009). Increased thermostability and fidelity of DNA synthesis of wild-type and mutant HIV-1 group O reverse transcriptases. *J Mol Biol* **392**, 872-84.

Ambrose, Z., Herman, B. D., Sheen, C. W., Zelina, S., Moore, K. L., Tachedjian, G., Nissley, D. V. & Sluis-Cremer, N. (2009). The human immunodeficiency virus type 1 nonnucleoside reverse transcriptase inhibitor resistance mutation I132M confers hypersensitivity to nucleoside analogs. *J Virol* **83**, 3826-33.

Anderson, K. S. (2010). A transient kinetic approach to investigate nucleoside inhibitors of mitochondrial DNA polymerase γ. *Methods* **51**, 392-8.

Apolloni, A., Meredith, L. W., Suhrbier, A., Kiernan, R. & Harrich, D. (2007). The HIV-1 Tat protein stimulates reverse transcription in vitro. *Curr HIV Res* **5**, 473-83.

Arion, D., Kaushik, N., McCormick, S., Borkow, G. & Parniak, M. A. (1998). Phenotypic mechanism of HIV-1 resistance to 3'-azido-3'-deoxythymidine (AZT): increased polymerization processivity and enhanced sensitivity to pyrophosphate of the mutant viral reverse transcriptase. *Biochemistry* **37**, 15908-17.

Arts, E. J. & Hazuda, D. J. (2012). HIV-1 antiretroviral drug therapy. *Cold Spring Harb Perspect Med* **2**, a007161.

Asahchop, E. L., Oliveira, M., Wainberg, M. A., Brenner, B. G., Moisi, D., Toni, T. & Tremblay, C. L. (2011). Characterization of the E138K resistance mutation in HIV-1 reverse transcriptase conferring susceptibility to etravirine in B and non-B HIV-1 subtypes. *Antimicrob Agents Chemother* **55**, 600-7.

Back, N. K., Nijhuis, M., Keulen, W., Boucher, C. A., Oude Essink, B. O., van Kuilenburg, A. B., van Gennip, A. H. & Berkhout, B. (1996). Reduced replication of 3TC-resistant HIV-1 variants in primary cells due to a processivity defect of the reverse transcriptase enzyme. *Embo J* **15**, 4040-9.

Barrè-Sinoussi, F., Chermann, J. C., Rey, F., Nugeyre, M. T., Chamaret, S., Gruest, J., Dauguet, C., Axler-Blin, C., Vezinet-Brun, F., Rouzioux, C., Rozenbaum, W. & Montagnier, L. (1983). Isolation of a T-lymphotropic retrovirus from a patient at risk for acquired immune deficiency syndrome (AIDS). *Science* **220**, 868-71.

Barshop, B. A., Adamson, D. T., Vellom, D. C., Rosen, F., Epstein, B. L. & Seegmiller, J. E. (1991). Luminescent immobilized enzyme test systems for inorganic pyrophosphate: assays using firefly luciferase and nicotinamide-mononucleotide adenylyl transferase or adenosine-5'-triphosphate sulfurylase. *Anal Biochem* **197**, 266-72.

Basavapathruni, A., Bailey, C. M. & Anderson, K. S. (2004). Defining a molecular mechanism of synergy between nucleoside and nonnucleoside AIDS drugs. *J Biol Chem* **279**, 6221-4.

Basavapathruni, A., Vingerhoets, J., de Bethune, M. P., Chung, R., Bailey, C. M., Kim, J. & Anderson, K. S. (2006). Modulation of human immunodeficiency virus type 1 synergistic inhibition by reverse transcriptase mutations. *Biochemistry* **45**, 7334-40.

Beard, W. A., Stahl, S. J., Kim, H. R., Bebenek, K., Kumar, A., Strub, M. P., Becerra, S. P., Kunkel, T. A. & Wilson, S. H. (1994). Structure/function studies of human immunodeficiency virus type 1 reverse transcriptase. Alanine scanning mutagenesis of an α-helix in the thumb subdomain. *J Biol Chem* **269**, 28091-7.

Beard, W. A., Minnick, D. T., Wade, C. L., Prasad, R., Won, R. L., Kumar, A., Kunkel, T. A. & Wilson, S. H. (1996). Role of the "helix clamp" in HIV-1 reverse transcriptase catalytic cycling as revealed by alanine-scanning mutagenesis. *J Biol Chem* **271**, 12213-20.

Bebenek, K., Beard, W. A., Casas-Finet, J. R., Kim, H. R., Darden, T. A., Wilson, S. H. & Kunkel, T. A. (1995). Reduced frameshift fidelity and processivity of HIV-1 reverse transcriptase mutants containing alanine substitutions in helix H of the thumb subdomain. *J Biol Chem* **270**, 19516-23.

Biondi, M. J., Beilhartz, G. L., McCormick, S. & Götte, M. (2010). N348I in HIV-1 reverse transcriptase can counteract the nevirapine-mediated bias toward RNase H cleavage during plus-strand initiation. *J Biol Chem* **285**, 26966-75.

Bishop, K. N., Verma, M., Kim, E. Y., Wolinsky, S. M. & Malim, M. H. (2008). APOBEC3G inhibits elongation of HIV-1 reverse transcripts. *PLoS Pathog* **4**, e1000231.

Blanca, G., Baldanti, F., Paolucci, S., Skoblov, A. Y., Victorova, L., Hubscher, U., Gerna, G., Spadari, S. & Maga, G. (2003). Nevirapine resistance mutation at codon 181 of the HIV-1 reverse transcriptase confers stavudine resistance by increasing nucleotide substrate discrimination and phosphorolytic activity. *J Biol Chem* **278**, 15469-72.

Boretto, J., Longhi, S., Navarro, J. M., Selmi, B., Sire, J. & Canard, B. (2001). An integrated system to study multiply substituted human immunodeficiency virus type 1 reverse transcriptase. *Anal Biochem* **292**, 139-47.

Boyer, P. L., Sarafianos, S. G., Arnold, E. & Hughes, S. H. (2001). Selective excision of AZTMP by drug-resistant human immunodeficiency virus reverse transcriptase. *J Virol* **75**, 4832-42.

Boyer, P. L., Sarafianos, S. G., Arnold, E. & Hughes, S. H. (2002a). The M184V mutation reduces the selective excision of zidovudine 5'-monophosphate (AZTMP) by the reverse transcriptase of human immunodeficiency virus type 1. *J Virol* **76**, 3248-56.

Boyer, P. L., Sarafianos, S. G., Arnold, E. & Hughes, S. H. (2002b). Nucleoside analog resistance caused by insertions in the fingers of human immunodeficiency virus type 1 reverse transcriptase involves ATP-mediated excision. *J Virol* **76**, 9143-51.

Boyer, P. L., Imamichi, T., Sarafianos, S. G., Arnold, E. & Hughes, S. H. (2004). Effects of the Delta67 complex of mutations in human immunodeficiency virus type 1 reverse transcriptase on nucleoside analog excision. *J Virol* **78**, 9987-97.

Boyer, P. L., Sarafianos, S. G., Clark, P. K., Arnold, E. & Hughes, S. H. (2006). Why do HIV-1 and HIV-2 use different pathways to develop AZT resistance? *PLoS Pathog* **2**, e10.

Brass, A. L., Dykxhoorn, D. M., Benita, Y., Yan, N., Engelman, A., Xavier, R. J., Lieberman, J. & Elledge, S. J. (2008). Identification of host proteins required for HIV infection through a functional genomic screen. *Science* **319**, 921-6.

Braz, V. A., Barkley, M. D., Jockusch, R. A. & Wintrode, P. L. (2010a). Efavirenz binding site in HIV-1 reverse transcriptase monomers. *Biochemistry* **49**, 10565-73.

Braz, V. A., Holladay, L. A. & Barkley, M. D. (2010b). Efavirenz binding to HIV-1 reverse transcriptase monomers and dimers. *Biochemistry* **49**, 601-10.

Brehm, J. H., Mellors, J. W. & Sluis-Cremer, N. (2008). Mechanism by which a glutamine to leucine substitution at residue 509 in the ribonuclease H domain of HIV-1 reverse transcriptase confers zidovudine resistance. *Biochemistry* **47**, 14020-7.

Brehm, J. H., Scott, Y., Koontz, D. L., Perry, S., Hammer, S., Katzenstein, D., Mellors, J. W. & Sluis-Cremer, N. (2012). Zidovudine (AZT) monotherapy selects for the A360V mutation in the connection domain of HIV-1 reverse transcriptase. *PLoS One* **7**, e31558.

Brenner, B. G., Oliveira, M., Doualla-Bell, F., Moisi, D. D., Ntemgwa, M., Frankel, F., Essex, M. & Wainberg, M. A. (2006). HIV-1 subtype C viruses rapidly develop K65R resistance to tenofovir in cell culture. *Aids* **20**, F9-13.

Brenner, B. G. & Coutsinos, D. (2009). The K65R mutation in HIV-1 reverse transcriptase: genetic barriers, resistance profile and clinical implications. *HIV Ther* **3**, 583-594.

Briggs, J. A. & Kraüsslich, H. G. (2011). The molecular architecture of HIV. *J Mol Biol* **410**, 491-500.

Caliendo, A. M., Savara, A., An, D., DeVore, K., Kaplan, J. C. & D'Aquila, R. T. (1996). Effects of zidovudine-selected human immunodeficiency virus type 1 reverse transcriptase amino acid substitutions on processive DNA synthesis and viral replication. *J Virol* **70**, 2146-53.

Canard, B., Sarfati, S. R. & Richardson, C. C. (1998). Enhanced binding of azidothymidine-resistant human immunodeficiency virus 1 reverse transcriptase to the 3'-azido-3'-deoxythymidine 5'-monophosphate-terminated primer. *J Biol Chem* **273**, 14596-604.

Cane, P. A., Green, H., Fearnhill, E. & Dunn, D. (2007). Identification of accessory mutations associated with high-level resistance in HIV-1 reverse transcriptase. *Aids* **21**, 447-55.

Carroll, S. S., Geib, J., Olsen, D. B., Stahlhut, M., Shafer, J. A. & Kuo, L. C. (1994). Sensitivity of HIV-1 reverse transcriptase and its mutants to inhibition by azidothymidine triphosphate. *Biochemistry* **33**, 2113-20.

Carter, C. A. & Ehrlich, L. S. (2008). Cell biology of HIV-1 infection of macrophages. *Annu Rev Microbiol* **62**, 425-43.

Cases-González, C. E., Gutiérrez-Rivas, M. & Menéndez-Arias, L. (2000). Coupling ribose selection to fidelity of DNA synthesis. The role of Tyr-115 of human immunodeficiency virus type 1 reverse transcriptase. *J Biol Chem* **275**, 19759-67.

Cases-González, C. E., Franco, S., Martínez, M. A. & Menéndez-Arias, L. (2007). Mutational patterns associated with the 69 insertion complex in multi-drug-resistant HIV-1 reverse transcriptase that confer increased excision activity and high-level resistance to zidovudine. *J Mol Biol* **365**, 298-309.

Ceccherini-Silberstein, F., Gago, F., Santoro, M., Gori, C., Svicher, V., Rodriguez-Barrios, F., d'Arrigo, R., Ciccozzi, M., Bertoli, A., d'Arminio Monforte, A., Balzarini, J., Antinori, A. & Perno, C. F. (2005). High sequence conservation of human immunodeficiency virus type 1 reverse transcriptase under drug pressure despite the continuous appearance of mutations. *J Virol* **79**, 10718-29.

Chamberlain, P. P., Ren, J., Nichols, C. E., Douglas, L., Lennerstrand, J., Larder, B. A., Stuart, D. I. & Stammers, D. K. (2002). Crystal structures of Zidovudine- or Lamivudine-resistant human immunodeficiency virus type 1 reverse transcriptases containing mutations at codons 41, 184, and 215. *J Virol* **76**, 10015-9.

Champoux, J. J. & Schultz, S. J. (2009). Ribonuclease H: properties, substrate specificity and roles in retroviral reverse transcription. *Febs J* **276**, 1506-16.

Chen, L., Perlina, A. & Lee, C. J. (2004). Positive selection detection in 40,000 human immunodeficiency

virus (HIV) type 1 sequences automatically identifies drug resistance and positive fitness mutations in HIV protease and reverse transcriptase. *J Virol* **78**, 3722-32.

Cherepanov, P., Maertens, G. N. & Hare, S. (2011). Structural insights into the retroviral DNA integration apparatus. *Curr Opin Struct Biol* **21**, 249-56.

Chiang, C. C., Wang, S. M., Tseng, Y. T., Huang, K. J. & Wang, C. T. (2009). Mutations at human immunodeficiency virus type 1 reverse transcriptase tryptophan repeat motif attenuate the inhibitory effect of efavirenz on virus production. *Virology* **383**, 261-70.

Chow, S. A. (1997). In vitro assays for activities of retroviral integrase. *Methods* **12**, 306-17.

Chow, S. A., Vincent, K. A., Ellison, V. & Brown, P. O. (1992). Reversal of integration and DNA splicing mediated by integrase of human immunodeficiency virus. *Science* **255**, 723-6.

Chung, S., Miller, J. T., Lapkouski, M., Tian, L., Yang, W. & Le Grice, S. F. (2013). Examining the role of the HIV-1 reverse transcriptase p51 subunit in positioning and hydrolysis of RNA/DNA hybrids. *J Biol Chem* **288**, 16177-84.

Cihlar, T. & Ray, A. S. (2010). Nucleoside and nucleotide HIV reverse transcriptase inhibitors: 25 years after zidovudine. *Antiviral Res* **85**, 39-58.

Clark, S. A., Shulman, N. S., Bosch, R. J. & Mellors, J. W. (2006). Reverse transcriptase mutations 118I, 208Y, and 215Y cause HIV-1 hypersusceptibility to non-nucleoside reverse transcriptase inhibitors. *Aids* **20**, 981-4.

Coakley, E. P., Gillis, J. M. & Hammer, S. M. (2000). Phenotypic and genotypic resistance patterns of HIV-1 isolates derived from individuals treated with didanosine and stavudine. *Aids* **14**, F9-15.

Cobrinik, D., Soskey, L. & Leis, J. (1988). A retroviral RNA secondary structure required for efficient initiation of reverse transcription. *J Virol* **62**, 3622-30.

Colin, L. & Van Lint, C. (2009). Molecular control of HIV-1 postintegration latency: implications for the development of new therapeutic strategies. *Retrovirology* **6**, 111.

Coutsinos, D., Invernizzi, C. F., Xu, H., Moisi, D., Oliveira, M., Brenner, B. G. & Wainberg, M. A. (2009). Template usage is responsible for the preferential acquisition of the K65R reverse transcriptase mutation in subtype C variants of human immunodeficiency virus type 1. *J Virol* **83**, 2029-33.

Cozzi-Lepri, A., Ruiz, L., Loveday, C., Phillips, A. N., Clotet, B., Reiss, P., Ledergerber, B., Holkmann, C., Staszewski, S. & Lundgren, J. D. (2005). Thymidine analogue mutation profiles: factors associated with acquiring specific profiles and their impact on the virological response to therapy. *Antivir Ther* **10**, 791-802.

Cozzi-Lepri, A., Phillips, A. N., Martínez-Picado, J., Monforte, A., Katlama, C., Eg Hansen, A. B., Horban, A., Bruun, J., Clotet, B. & Lundgren, J. D. (2009). Rate of accumulation of thymidine analogue mutations in patients continuing to receive virologically failing regimens containing zidovudine or stavudine: implications for antiretroviral therapy programs in resource-limited settings. *J Infect Dis* **200**, 687-97.

Das, K., Clark, A. D., Jr., Lewi, P. J., Heeres, J., De Jonge, M. R., Koymans, L. M., Vinkers, H. M., Daeyaert, F., Ludovici, D. W., Kukla, M. J., De Corte, B., Kavash, R. W., Ho, C. Y., Ye, H., Lichtenstein, M. A., Andries, K., Pauwels, R., De Bethune, M. P., Boyer, P. L., Clark, P., Hughes, S. H., Janssen, P. A. & Arnold, E. (2004). Roles of conformational and positional adaptability in structure-based design of TMC125-R165335 (etravirine) and related non-nucleoside reverse transcriptase inhibitors that are highly potent and effective against wild-type and drug-resistant HIV-1 variants. *J Med Chem* **47**, 2550-60.

Das, K., Sarafianos, S. G., Clark, A. D., Jr., Boyer, P. L., Hughes, S. H. & Arnold, E. (2007). Crystal structures of clinically relevant Lys103Asn/Tyr181Cys double mutant HIV-1 reverse transcriptase in complexes with ATP and non-nucleoside inhibitor HBY 097. *J Mol Biol* **365**, 77-89.

Das, K., Bauman, J. D., Clark, A. D., Jr., Frenkel, Y. V., Lewi, P. J., Shatkin, A. J., Hughes, S. H. & Arnold, E. (2008). High-resolution structures of HIV-1 reverse transcriptase/TMC278 complexes: strategic flexibility

explains potency against resistance mutations. *Proc Natl Acad Sci U S A* **105**, 1466-71.

Das, K., Bandwar, R. P., White, K. L., Feng, J. Y., Sarafianos, S. G., Tuske, S., Tu, X., Clark, A. D., Jr., Boyer, P. L., Hou, X., Gaffney, B. L., Jones, R. A., Miller, M. D., Hughes, S. H. & Arnold, E. (2009). Structural basis for the role of the K65R mutation in HIV-1 reverse transcriptase polymerization, excision antagonism, and tenofovir resistance. *J Biol Chem* **284**, 35092-100.

Das, K., Martínez, S. E., Bauman, J. D. & Arnold, E. (2012). HIV-1 reverse transcriptase complex with DNA and nevirapine reveals non-nucleoside inhibition mechanism. *Nat Struct Mol Biol* **19**, 253-9.

Das, K. & Arnold, E. (2013). HIV-1 reverse transcriptase and antiviral drug resistance. Part 2. *Curr Opin Virol* **3**, 119-28.

Dash, C., Yi-Brunozzi, H. Y. & Le Grice, S. F. (2004). Two modes of HIV-1 polypurine tract cleavage are affected by introducing locked nucleic acid analogs into the (-) DNA template. *J Biol Chem* **279**, 37095-102.

De Clercq, E. (2009a). Anti-HIV drugs: 25 compounds approved within 25 years after the discovery of HIV. *Int J Antimicrob Agents* **33**, 307-20.

De Clercq, E. (2009b). A new drug combination therapy for treatment-naive patients with HIV-1 infection, consisting of raltegravir, emtricitabine and tenofovir disoproxil fumarate. *Expert Opin Pharmacother* **10**, 2935-7.

De La Rosa, J., Kotb, M. & Kredich, N. M. (1991). Regulation of S-adenosylmethionine synthetase activity in cultured human lymphocytes. *Biochim Biophys Acta* **1077**, 225-32.

de Silva, T. I., Cotten, M. & Rowland-Jones, S. L. (2008). HIV-2: the forgotten AIDS virus. *Trends Microbiol* **16**, 588-95.

Delelis, O., Carayon, K., Saib, A., Deprez, E. & Mouscadet, J. F. (2008). Integrase and integration: biochemical activities of HIV-1 integrase. *Retrovirology* **5**, 114.

Delviks-Frankenberry, K. A., Nikolenko, G. N., Boyer, P. L., Hughes, S. H., Coffin, J. M., Jere, A. & Pathak, V. K. (2008). HIV-1 reverse transcriptase connection subdomain mutations reduce template RNA degradation and enhance AZT excision. *Proc Natl Acad Sci U S A* **105**, 10943-8.

Delviks-Frankenberry, K. A., Nikolenko, G. N., Maldarelli, F., Hase, S., Takebe, Y. & Pathak, V. K. (2009). Subtype-specific differences in the human immunodeficiency virus type 1 reverse transcriptase connection subdomain of CRF01_AE are associated with higher levels of resistance to 3'-azido-3'-deoxythymidine. *J Virol* **83**, 8502-13.

Delviks-Frankenberry, K. A., Nikolenko, G. N. & Pathak, V. K. (2010). The "Connection" Between HIV Drug Resistance and RNase H. *Viruses* **2**, 1476-1503.

Delviks-Frankenberry, K. A., Lengruber, R. B., Santos, A. F., Silveira, J. M., Soares, M. A., Kearney, M. F., Maldarelli, F. & Pathak, V. K. (2013). Connection subdomain mutations in HIV-1 subtype-C treatment-experienced patients enhance NRTI and NNRTI drug resistance. *Virology* **435**, 433-41.

Demeter, L. M., Shafer, R. W., Meehan, P. M., Holden-Wiltse, J., Fischl, M. A., Freimuth, W. W., Para, M. F. & Reichman, R. C. (2000). Delavirdine susceptibilities and associated reverse transcriptase mutations in human immunodeficiency virus type 1 isolates from patients in a phase I/II trial of delavirdine monotherapy (ACTG 260). *Antimicrob Agents Chemother* **44**, 794-7.

DeStefano, J. J., Bambara, R. A. & Fay, P. J. (1993a). Parameters that influence the binding of human immunodeficiency virus reverse transcriptase to nucleic acid structures. *Biochemistry* **32**, 6908-15.

DeStefano, J. J., Mallaber, L. M., Fay, P. J. & Bambara, R. A. (1993b). Determinants of the RNase H cleavage specificity of human immunodeficiency virus reverse transcriptase. *Nucleic Acids Res* **21**, 4330-8.

Deval, J., Selmi, B., Boretto, J., Egloff, M. P., Guerreiro, C., Sarfati, S. & Canard, B. (2002). The molecular mechanism of multidrug resistance by the Q151M human immunodeficiency virus type 1 reverse transcriptase and its suppression using α-boranophosphate nucleotide analogues. *J Biol Chem* **277**,

42097-104.

Deval, J., White, K. L., Miller, M. D., Parkin, N. T., Courcambeck, J., Halfon, P., Selmi, B., Boretto, J. & Canard, B. (2004). Mechanistic basis for reduced viral and enzymatic fitness of HIV-1 reverse transcriptase containing both K65R and M184V mutations. *J Biol Chem* **279**, 509-16.

Deval, J., Alvarez, K., Selmi, B., Bermond, M., Boretto, J., Guerreiro, C., Mulard, L. & Canard, B. (2005). Mechanistic insights into the suppression of drug resistance by human immunodeficiency virus type 1 reverse transcriptase using α-boranophosphate nucleoside analogs. *J Biol Chem* **280**, 3838-46.

Dharmasena, S., Pongracz, Z., Arnold, E., Sarafianos, S. G. & Parniak, M. A. (2007). 3'-Azido-3'-deoxythymidine-(5')-tetraphospho-(5')-adenosine, the product of ATP-mediated excision of chain-terminating AZTMP, is a potent chain-terminating substrate for HIV-1 reverse transcriptase. *Biochemistry* **46**, 828-36.

di Marzo Veronese, F., Copeland, T. D., DeVico, A. L., Rahman, R., Oroszlan, S., Gallo, R. C. & Sarngadharan, M. G. (1986). Characterization of highly immunogenic p66/p51 as the reverse transcriptase of HTLV-III/LAV. *Science* **231**, 1289-91.

Ding, J., Das, K., Hsiou, Y., Sarafianos, S. G., Clark, A. D., Jr., Jacobo-Molina, A., Tantillo, C., Hughes, S. H. & Arnold, E. (1998). Structure and functional implications of the polymerase active site region in a complex of HIV-1 RT with a double-stranded DNA template-primer and an antibody Fab fragment at 2.8 Å resolution. *J Mol Biol* **284**, 1095-111.

Dobard, C. W., Briones, M. S. & Chow, S. A. (2007). Molecular mechanisms by which human immunodeficiency virus type 1 integrase stimulates the early steps of reverse transcription. *J Virol* **81**, 10037-46.

Doualla-Bell, F., Avalos, A., Gaolathe, T., Mine, M., Gaseitsiwe, S., Ndwapi, N., Novitsky, V. A., Brenner, B., Oliveira, M., Moisi, D., Moffat, H., Thior, I., Essex, M. & Wainberg, M. A. (2006). Impact of human immunodeficiency virus type 1 subtype C on drug resistance mutations in patients from Botswana failing a nelfinavir-containing regimen. *Antimicrob Agents Chemother* **50**, 2210-3.

Ehteshami, M., Beilhartz, G. L., Scarth, B. J., Tchesnokov, E. P., McCormick, S., Wynhoven, B., Harrigan, P. R. & Götte, M. (2008). Connection domain mutations N348I and A360V in HIV-1 reverse transcriptase enhance resistance to 3'-azido-3'-deoxythymidine through both RNase H-dependent and -independent mechanisms. *J Biol Chem* **283**, 22222-32.

Ehteshami, M. & Götte, M. (2008). Effects of mutations in the connection and RNase H domains of HIV-1 reverse transcriptase on drug susceptibility. *AIDS Rev* **10**, 224-35.

Fassati, A. (2012). Multiple roles of the capsid protein in the early steps of HIV-1 infection. *Virus Res* **170**, 15-24.

Feng, J. Y., Murakami, E., Zorca, S. M., Johnson, A. A., Johnson, K. A., Schinazi, R. F., Furman, P. A. & Anderson, K. S. (2004). Relationship between antiviral activity and host toxicity: comparison of the incorporation efficiencies of 2',3'-dideoxy-5-fluoro-3'-thiacytidine-triphosphate analogs by human immunodeficiency virus type 1 reverse transcriptase and human mitochondrial DNA polymerase. *Antimicrob Agents Chemother* **48**, 1300-6.

Figueiredo, A., Moore, K. L., Mak, J., Sluis-Cremer, N., de Bethune, M. P. & Tachedjian, G. (2006). Potent nonnucleoside reverse transcriptase inhibitors target HIV-1 Gag-Pol. *PLoS Pathog* **2**, e119.

Fisher, T. S., Darden, T. & Prasad, V. R. (2003). Mutations proximal to the minor groove-binding track of human immunodeficiency virus type 1 reverse transcriptase differentially affect utilization of RNA versus DNA as template. *J Virol* **77**, 5837-45.

Fournier, C., Cortay, J. C., Carbonnelle, C., Ehresmann, C., Marquet, R. & Boulanger, P. (2002). The HIV-1 Nef protein enhances the affinity of reverse transcriptase for RNA in vitro. *Virus Genes* **25**, 255-69.

Frangeul, A., Bussetta, C., Deval, J., Barral, K., Alvarez, K. & Canard, B. (2008). Gln151 of HIV-1 reverse

transcriptase acts as a steric gate towards clinically relevant acyclic phosphonate nucleotide analogues. *Antivir Ther* **13**, 115-24.

Frankel, F. A., Marchand, B., Turner, D., Gotte, M. & Wainberg, M. A. (2005). Impaired rescue of chain-terminated DNA synthesis associated with the L74V mutation in human immunodeficiency virus type 1 reverse transcriptase. *Antimicrob Agents Chemother* **49**, 2657-64.

Friedrich, B. M., Dziuba, N., Li, G., Endsley, M. A., Murray, J. L. & Ferguson, M. R. (2011). Host factors mediating HIV-1 replication. *Virus Res* **161**, 101-14.

Fuentes, G. M., Rodríguez-Rodríguez, L., Fay, P. J. & Bambara, R. A. (1995). Use of an oligoribonucleotide containing the polypurine tract sequence as a primer by HIV reverse transcriptase. *J Biol Chem* **270**, 28169-76.

Furfine, E. S. & Reardon, J. E. (1991). Reverse transcriptase. RNase H from the human immunodeficiency virus. Relationship of the DNA polymerase and RNA hydrolysis activities. *J Biol Chem* **266**, 406-12.

Furman, P. A., Fyfe, J. A., St Clair, M. H., Weinhold, K., Rideout, J. L., Freeman, G. A., Lehrman, S. N., Bolognesi, D. P., Broder, S., Mitsuya, H. & Barry, D. W. (1986). Phosphorylation of 3'-azido-3'-deoxythymidine and selective interaction of the 5'-triphosphate with human immunodeficiency virus reverse transcriptase. *Proc Natl Acad Sci U S A* **83**, 8333-7.

Gallo, R., Wong-Staal, F., Montagnier, L., Haseltine, W. A. & Yoshida, M. (1988). HIV/HTLV gene nomenclature. *Nature* **333**, 504.

Gallo, R. C., Salahuddin, S. Z., Popovic, M., Shearer, G. M., Kaplan, M., Haynes, B. F., Palker, T. J., Redfield, R., Oleske, J., Safai, B., White, G., Foster, P. & Markham, P. D. (1984). Frequent detection and isolation of cytopathic retroviruses (HTLV-III) from patients with AIDS and at risk for AIDS. *Science* **224**, 500-3.

Ganser-Pornillos, B. K., Yeager, M. & Sundquist, W. I. (2008). The structural biology of HIV assembly. *Curr Opin Struct Biol* **18**, 203-17.

Ganser-Pornillos, B. K., Yeager, M. & Pornillos, O. (2012). Assembly and architecture of HIV. *Adv Exp Med Biol* **726**, 441-65.

Gao, H. Q., Boyer, P. L., Arnold, E. & Hughes, S. H. (1998). Effects of mutations in the polymerase domain on the polymerase, RNase H and strand transfer activities of human immunodeficiency virus type 1 reverse transcriptase. *J Mol Biol* **277**, 559-72.

Garriga, C., Pérez-Elías, M. J., Delgado, R., Ruiz, L., Pérez-Álvarez, L., Pumarola, T., López-Lirola, A., González-García, J. & Menéndez-Arias, L. (2009). HIV-1 reverse transcriptase thumb subdomain polymorphisms associated with virological failure to nucleoside drug combinations. *J Antimicrob Chemother* **64**, 251-8.

Ghosn, J., Chaix, M. L. & Delaugerre, C. (2009). HIV-1 resistance to first- and second-generation non-nucleoside reverse transcriptase inhibitors. *AIDS Rev* **11**, 165-73.

Girouard, M., Diallo, K., Marchand, B., McCormick, S. & Götte, M. (2003). Mutations E44D and V118I in the reverse transcriptase of HIV-1 play distinct mechanistic roles in dual resistance to AZT and 3TC. *J Biol Chem* **278**, 34403-10.

Goldschmidt, V. & Marquet, R. (2004). Primer unblocking by HIV-1 reverse transcriptase and resistance to nucleoside RT inhibitors (NRTIs). *Int J Biochem Cell Biol* **36**, 1687-705.

Goldschmidt, V., Didierjean, J., Ehresmann, B., Ehresmann, C., Isel, C. & Marquet, R. (2006). Mg2+ dependency of HIV-1 reverse transcription, inhibition by nucleoside analogues and resistance. *Nucleic Acids Res* **34**, 42-52.

Goldstone, D. C., Ennis-Adeniran, V., Hedden, J. J., Groom, H. C., Rice, G. I., Christodoulou, E., Walker, P. A., Kelly, G., Haire, L. F., Yap, M. W., de Carvalho, L. P., Stoye, J. P., Crow, Y. J., Taylor, I. A. & Webb,

M. (2011). HIV-1 restriction factor SAMHD1 is a deoxynucleoside triphosphate triphosphohydrolase. *Nature* **480**, 379-82.

Gomez, C. & Hope, T. J. (2005). The ins and outs of HIV replication. *Cell Microbiol* **7**, 621-6.

Gonzales, M. J., Wu, T. D., Taylor, J., Belitskaya, I., Kantor, R., Israelski, D., Chou, S., Zolopa, A. R., Fessel, W. J. & Shafer, R. W. (2003). Extended spectrum of HIV-1 reverse transcriptase mutations in patients receiving multiple nucleoside analog inhibitors. *Aids* **17**, 791-9.

Gopalakrishnan, V. & Benkovic, S. (1994). Effect of a thiobenzimidazolone derivative on DNA strand transfer catalyzed by HIV-1 reverse transcriptase. *J Biol Chem* **269**, 4110-5.

Götte, M., Maier, G., Onori, A. M., Cellai, L., Wainberg, M. A. & Heumann, H. (1999). Temporal coordination between initiation of HIV (+)-strand DNA synthesis and primer removal. *J Biol Chem* **274**, 11159-69.

Götte, M., Kameoka, M., McLellan, N., Cellai, L. & Wainberg, M. A. (2001). Analysis of efficiency and fidelity of HIV-1 (+)-strand DNA synthesis reveals a novel rate-limiting step during retroviral reverse transcription. *J Biol Chem* **276**, 6711-9.

Götte, M. (2007). Should we include connection domain mutations of HIV-1 reverse transcriptase in HIV resistance testing. *PLoS Med* **4**, e346.

Gribble, F. M., Loussouarn, G., Tucker, S. J., Zhao, C., Nichols, C. G. & Ashcroft, F. M. (2000). A novel method for measurement of submembrane ATP concentration. *J Biol Chem* **275**, 30046-9.

Grobler, J. A., Dornadula, G., Rice, M. R., Simcoe, A. L., Hazuda, D. J. & Miller, M. D. (2007). HIV-1 reverse transcriptase plus-strand initiation exhibits preferential sensitivity to non-nucleoside reverse transcriptase inhibitors in vitro. *J Biol Chem* **282**, 8005-10.

Gupta, S., Fransen, S., Paxinos, E. E., Stawiski, E., Huang, W. & Petropoulos, C. J. (2010). Combinations of mutations in the connection domain of human immunodeficiency virus type 1 reverse transcriptase: assessing the impact on nucleoside and nonnucleoside reverse transcriptase inhibitor resistance. *Antimicrob Agents Chemother* **54**, 1973-80.

Gupta, S., Vingerhoets, J., Fransen, S., Tambuyzer, L., Azijn, H., Frantzell, A., Paredes, R., Coakley, E., Nijs, S., Clotet, B., Petropoulos, C. J., Schapiro, J., Huang, W. & Picchio, G. (2011). Connection domain mutations in HIV-1 reverse transcriptase do not impact etravirine susceptibility and virologic responses to etravirine-containing regimens. *Antimicrob Agents Chemother* **55**, 2872-9.

Hachiya, A., Kodama, E. N., Sarafianos, S. G., Schuckmann, M. M., Sakagami, Y., Matsuoka, M., Takiguchi, M., Gatanaga, H. & Oka, S. (2008). Amino acid mutation N348I in the connection subdomain of human immunodeficiency virus type 1 reverse transcriptase confers multiclass resistance to nucleoside and nonnucleoside reverse transcriptase inhibitors. *J Virol* **82**, 3261-70.

Hachiya, A., Shimane, K., Sarafianos, S. G., Kodama, E. N., Sakagami, Y., Negishi, F., Koizumi, H., Gatanaga, H., Matsuoka, M., Takiguchi, M. & Oka, S. (2009). Clinical relevance of substitutions in the connection subdomain and RNase H domain of HIV-1 reverse transcriptase from a cohort of antiretroviral treatment-naive patients. *Antiviral Res* **82**, 115-21.

Hachiya, A., Kodama, E. N., Schuckmann, M. M., Kirby, K. A., Michailidis, E., Sakagami, Y., Oka, S., Singh, K. & Sarafianos, S. G. (2011). K70Q adds high-level tenofovir resistance to "Q151M complex" HIV reverse transcriptase through the enhanced discrimination mechanism. *PLoS One* **6**, e16242.

Hachiya, A., Marchand, B., Kirby, K. A., Michailidis, E., Tu, X., Palczewski, K., Ong, Y. T., Li, Z., Griffin, D. T., Schuckmann, M. M., Tanuma, J., Oka, S., Singh, K., Kodama, E. N. & Sarafianos, S. G. (2012). HIV-1 reverse transcriptase (RT) polymorphism 172K suppresses the effect of clinically relevant drug resistance mutations to both nucleoside and non-nucleoside RT inhibitors. *J Biol Chem* **287**, 29988-99.

Hamamoto, S., Nishitsuji, H., Amagasa, T., Kannagi, M. & Masuda, T. (2006). Identification of a novel human immunodeficiency virus type 1 integrase interactor, Gemin2, that facilitates efficient viral cDNA

synthesis in vivo. *J Virol* **80**, 5670-7.

Han, Y., Lassen, K., Monie, D., Sedaghat, A. R., Shimoji, S., Liu, X., Pierson, T. C., Margolick, J. B., Siliciano, R. F. & Siliciano, J. D. (2004). Resting CD4+ T cells from human immunodeficiency virus type 1 (HIV-1)-infected individuals carry integrated HIV-1 genomes within actively transcribed host genes. *J Virol* **78**, 6122-33.

Hang, J. Q., Li, Y., Yang, Y., Cammack, N., Mirzadegan, T. & Klumpp, K. (2007). Substrate-dependent inhibition or stimulation of HIV RNase H activity by non-nucleoside reverse transcriptase inhibitors (NNRTIs). *Biochem Biophys Res Commun* **352**, 341-50.

Hare, S., Gupta, S. S., Valkov, E., Engelman, A. & Cherepanov, P. (2010a). Retroviral intasome assembly and inhibition of DNA strand transfer. *Nature* **464**, 232-6.

Hare, S., Vos, A. M., Clayton, R. F., Thuring, J. W., Cummings, M. D. & Cherepanov, P. (2010b). Molecular mechanisms of retroviral integrase inhibition and the evolution of viral resistance. *Proc Natl Acad Sci U S A* **107**, 20057-62.

Hare, S., Maertens, G. N. & Cherepanov, P. (2012). 3'-processing and strand transfer catalysed by retroviral integrase in crystallo. *Embo J* **31**, 3020-8.

Harrigan, P. R., Kinghorn, I., Bloor, S., Kemp, S. D., Najera, I., Kohli, A. & Larder, B. A. (1996). Significance of amino acid variation at human immunodeficiency virus type 1 reverse transcriptase residue 210 for zidovudine susceptibility. *J Virol* **70**, 5930-4.

Harrigan, P. R., Salim, M., Stammers, D. K., Wynhoven, B., Brumme, Z. L., McKenna, P., Larder, B. & Kemp, S. D. (2002). A mutation in the 3' region of the human immunodeficiency virus type 1 reverse transcriptase (Y318F) associated with nonnucleoside reverse transcriptase inhibitor resistance. *J Virol* **76**, 6836-40.

Harris, R. S., Hultquist, J. F. & Evans, D. T. (2012). The restriction factors of human immunodeficiency virus. *J Biol Chem* **287**, 40875-83.

Hehl, E. A., Joshi, P., Kalpana, G. V. & Prasad, V. R. (2004). Interaction between human immunodeficiency virus type 1 reverse transcriptase and integrase proteins. *J Virol* **78**, 5056-67.

Hemelaar, J. (2012). The origin and diversity of the HIV-1 pandemic. *Trends Mol Med* **18**, 182-92.

Hermann, T., Meier, T., Gotte, M. & Heumann, H. (1994). The 'helix clamp' in HIV-1 reverse transcriptase: a new nucleic acid binding motif common in nucleic acid polymerases. *Nucleic Acids Res* **22**, 4625-33.

Herschhorn, A. & Hizi, A. (2010). Retroviral reverse transcriptases. *Cell Mol Life Sci* **67**, 2717-47.

Hertogs, K., Bloor, S., De Vroey, V., van Den Eynde, C., Dehertogh, P., van Cauwenberge, A., Sturmer, M., Alcorn, T., Wegner, S., van Houtte, M., Miller, V. & Larder, B. A. (2000). A novel human immunodeficiency virus type 1 reverse transcriptase mutational pattern confers phenotypic lamivudine resistance in the absence of mutation 184V. *Antimicrob Agents Chemother* **44**, 568-73.

Hooker, D. J., Tachedjian, G., Solomon, A. E., Gurusinghe, A. D., Land, S., Birch, C., Anderson, J. L., Roy, B. M., Arnold, E. & Deacon, N. J. (1996). An in vivo mutation from leucine to tryptophan at position 210 in human immunodeficiency virus type 1 reverse transcriptase contributes to high-level resistance to 3'-azido-3'-deoxythymidine. *J Virol* **70**, 8010-8.

Hottiger, M., Gramatikoff, K., Georgiev, O., Chaponnier, C., Schaffner, W. & Hubscher, U. (1995). The large subunit of HIV-1 reverse transcriptase interacts with β-actin. *Nucleic Acids Res* **23**, 736-41.

Hrecka, K., Hao, C., Gierszewska, M., Swanson, S. K., Kesik-Brodacka, M., Srivastava, S., Florens, L., Washburn, M. P. & Skowronski, J. (2011). Vpx relieves inhibition of HIV-1 infection of macrophages mediated by the SAMHD1 protein. *Nature* **474**, 658-61.

Hsiou, Y., Ding, J., Das, K., Clark, A. D., Jr., Hughes, S. H. & Arnold, E. (1996). Structure of unliganded HIV-1 reverse transcriptase at 2.7 Å resolution: implications of conformational changes for polymerization

and inhibition mechanisms. *Structure* **4**, 853-60.

Hsiou, Y., Das, K., Ding, J., Clark, A. D., Jr., Kleim, J. P., Rosner, M., Winkler, I., Riess, G., Hughes, S. H. & Arnold, E. (1998). Structures of Tyr188Leu mutant and wild-type HIV-1 reverse transcriptase complexed with the non-nucleoside inhibitor HBY 097: inhibitor flexibility is a useful design feature for reducing drug resistance. *J Mol Biol* **284**, 313-23.

Hsiou, Y., Ding, J., Das, K., Clark, A. D., Jr., Boyer, P. L., Lewi, P., Janssen, P. A., Kleim, J. P., Rosner, M., Hughes, S. H. & Arnold, E. (2001). The Lys103Asn mutation of HIV-1 RT: a novel mechanism of drug resistance. *J Mol Biol* **309**, 437-45.

Hu, Z. & Kuritzkes, D. R. (2011). Interaction of reverse transcriptase (RT) mutations conferring resistance to lamivudine and etravirine: effects on fitness and RT activity of human immunodeficiency virus type 1. *J Virol* **85**, 11309-14.

Hu, W. S. & Hughes, S. H. (2012). HIV-1 reverse transcription. *Cold Spring Harb Perspect Med* **2**, a006882.

Huang, H., Chopra, R., Verdine, G. L. & Harrison, S. C. (1998). Structure of a covalently trapped catalytic complex of HIV-1 reverse transcriptase: implications for drug resistance. *Science* **282**, 1669-75.

Huber, H. E. & Richardson, C. C. (1990). Processing of the primer for plus strand DNA synthesis by human immunodeficiency virus 1 reverse transcriptase. *J Biol Chem* **265**, 10565-73.

Huigen, M. C., van Ham, P. M., de Graaf, L., Kagan, R. M., Boucher, C. A. & Nijhuis, M. (2008). Identification of a novel resistance (E40F) and compensatory (K43E) substitution in HIV-1 reverse transcriptase. *Retrovirology* **5**, 20.

Invernizzi, C. F., Coutsinos, D., Oliveira, M., Moisi, D., Brenner, B. G. & Wainberg, M. A. (2009). Signature nucleotide polymorphisms at positions 64 and 65 in reverse transcriptase favor the selection of the K65R resistance mutation in HIV-1 subtype C. *J Infect Dis* **200**, 1202-6.

Isel, C., Ehresmann, C., Walter, P., Ehresmann, B. & Marquet, R. (2001). The emergence of different resistance mechanisms toward nucleoside inhibitors is explained by the properties of the wild type HIV-1 reverse transcriptase. *J Biol Chem* **276**, 48725-32.

Iversen, A. K., Shafer, R. W., Wehrly, K., Winters, M. A., Mullins, J. I., Chesebro, B. & Merigan, T. C. (1996). Multidrug-resistant human immunodeficiency virus type 1 strains resulting from combination antiretroviral therapy. *J Virol* **70**, 1086-90.

Iyidogan, P. & Anderson, K. S. (2012). Understanding the molecular mechanism of sequence dependent tenofovir removal by HIV-1 reverse transcriptase: differences in primer binding site versus polypurine tract. *Antiviral Res* **95**, 93-103.

Jacobo-Molina, A., Ding, J., Nanni, R. G., Clark, A. D., Jr., Lu, X., Tantillo, C., Williams, R. L., Kamer, G., Ferris, A. L., Clark, P., Hizi, A., Hughes, S. H. & Arnold, E. (1993). Crystal structure of human immunodeficiency virus type 1 reverse transcriptase complexed with double-stranded DNA at 3.0 Å resolution shows bent DNA. *Proc Natl Acad Sci U S A* **90**, 6320-4.

Jaju, M., Beard, W. A. & Wilson, S. H. (1995). Human immunodeficiency virus type 1 reverse transcriptase. 3'-Azidodeoxythymidine 5'-triphosphate inhibition indicates two-step binding for template-primer. *J Biol Chem* **270**, 9740-7.

Japour, A. J., Welles, S., D'Aquila, R. T., Johnson, V. A., Richman, D. D., Coombs, R. W., Reichelderfer, P. S., Kahn, J. O., Crumpacker, C. S. & Kuritzkes, D. R. (1995). Prevalence and clinical significance of zidovudine resistance mutations in human immunodeficiency virus isolated from patients after long-term zidovudine treatment. AIDS Clinical Trials Group 116B/117 Study Team and the Virology Committee Resistance Working Group. *J Infect Dis* **171**, 1172-9.

Jones, F. D. & Hughes, S. H. (2007). In vitro analysis of the effects of mutations in the G-tract of the human immunodeficiency virus type 1 polypurine tract on RNase H cleavage specificity. *Virology* **360**, 341-9.

Julias, J. G., McWilliams, M. J., Sarafianos, S. G., Arnold, E. & Hughes, S. H. (2002). Mutations in the RNase H domain of HIV-1 reverse transcriptase affect the initiation of DNA synthesis and the specificity of RNase H cleavage in vivo. *Proc Natl Acad Sci U S A* **99**, 9515-20.

Julias, J. G., McWilliams, M. J., Sarafianos, S. G., Alvord, W. G., Arnold, E. & Hughes, S. H. (2003). Mutation of amino acids in the connection domain of human immunodeficiency virus type 1 reverse transcriptase that contact the template-primer affects RNase H activity. *J Virol* **77**, 8548-54.

Julias, J. G., McWilliams, M. J., Sarafianos, S. G., Alvord, W. G., Arnold, E. & Hughes, S. H. (2004). Effects of mutations in the G tract of the human immunodeficiency virus type 1 polypurine tract on virus replication and RNase H cleavage. *J Virol* **78**, 13315-24.

Kati, W. M., Johnson, K. A., Jerva, L. F. & Anderson, K. S. (1992). Mechanism and fidelity of HIV reverse transcriptase. *J Biol Chem* **267**, 25988-97.

Keele, B. F., Van Heuverswyn, F., Li, Y., Bailes, E., Takehisa, J., Santiago, M. L., Bibollet-Ruche, F., Chen, Y., Wain, L. V., Liegeois, F., Loul, S., Ngole, E. M., Bienvenue, Y., Delaporte, E., Brookfield, J. F., Sharp, P. M., Shaw, G. M., Peeters, M. & Hahn, B. H. (2006). Chimpanzee reservoirs of pandemic and nonpandemic HIV-1. *Science* **313**, 523-6.

Kellam, P., Boucher, C. A. & Larder, B. A. (1992). Fifth mutation in human immunodeficiency virus type 1 reverse transcriptase contributes to the development of high-level resistance to zidovudine. *Proc Natl Acad Sci U S A* **89**, 1934-8.

Kemp, S. D., Shi, C., Bloor, S., Harrigan, P. R., Mellors, J. W. & Larder, B. A. (1998). A novel polymorphism at codon 333 of human immunodeficiency virus type 1 reverse transcriptase can facilitate dual resistance to zidovudine and L-2',3'-dideoxy-3'-thiacytidine. *J Virol* **72**, 5093-8.

Kessl, J. J., Li, M., Ignatov, M., Shkriabai, N., Eidahl, J. O., Feng, L., Musier-Forsyth, K., Craigie, R. & Kvaratskhelia, M. (2011). FRET analysis reveals distinct conformations of IN tetramers in the presence of viral DNA or LEDGF/p75. *Nucleic Acids Res* **39**, 9009-22.

Kisic, M., Mendieta, J., Puertas, M. C., Parera, M., Martínez, M. A., Martínez-Picado, J. & Menéndez-Arias, L. (2008). Mechanistic basis of zidovudine hypersusceptibility and lamivudine resistance conferred by the deletion of codon 69 in the HIV-1 reverse transcriptase coding region. *J Mol Biol* **382**, 327-41.

Kisic, M., Matamoros, T., Nevot, M., Mendieta, J., Martínez-Picado, J., Martínez, M. A. & Menéndez-Arias, L. (2011). Thymidine analogue excision and discrimination modulated by mutational complexes including single amino acid deletions of Asp-67 or Thr-69 in HIV-1 reverse transcriptase. *J Biol Chem* **286**, 20615-24.

Kohlstaedt, L. A., Wang, J., Friedman, J. M., Rice, P. A. & Steitz, T. A. (1992). Crystal structure at 3.5 Å resolution of HIV-1 reverse transcriptase complexed with an inhibitor. *Science* **256**, 1783-90.

König, R., Zhou, Y., Elleder, D., Diamond, T. L., Bonamy, G. M., Irelan, J. T., Chiang, C. Y., Tu, B. P., De Jesus, P. D., Lilley, C. E., Seidel, S., Opaluch, A. M., Caldwell, J. S., Weitzman, M. D., Kuhen, K. L., Bandyopadhyay, S., Ideker, T., Orth, A. P., Miraglia, L. J., Bushman, F. D., Young, J. A. & Chanda, S. K. (2008). Global analysis of host-pathogen interactions that regulate early-stage HIV-1 replication. *Cell* **135**, 49-60.

Koppensteiner, H., Brack-Werner, R. & Schindler, M. (2012). Macrophages and their relevance in Human Immunodeficiency Virus Type I infection. *Retrovirology* **9**, 82.

Korber, B., Muldoon, M., Theiler, J., Gao, F., Gupta, R., Lapedes, A., Hahn, B. H., Wolinsky, S. & Bhattacharya, T. (2000). Timing the ancestor of the HIV-1 pandemic strains. *Science* **288**, 1789-96.

Kosalaraksa, P., Kavlick, M. F., Maroun, V., Le, R. & Mitsuya, H. (1999). Comparative fitness of multi-dideoxynucleoside-resistant human immunodeficiency virus type 1 (HIV-1) in an In vitro competitive HIV-1 replication assay. *J Virol* **73**, 5356-63.

Krishnan, L. & Engelman, A. (2012). Retroviral integrase proteins and HIV-1 DNA integration. *J Biol Chem* **287**, 40858-66.

Krogstad, P. (2003). Molecular biology of the human immunodeficiency virus: current and future targets for intervention. *Semin Pediatr Infect Dis* **14**, 258-68.

Lacey, S. F., Reardon, J. E., Furfine, E. S., Kunkel, T. A., Bebenek, K., Eckert, K. A., Kemp, S. D. & Larder, B. A. (1992). Biochemical studies on the reverse transcriptase and RNase H activities from human immunodeficiency virus strains resistant to 3'-azido-3'-deoxythymidine. *J Biol Chem* **267**, 15789-94.

Lacey, S. F. & Larder, B. A. (1994). Mutagenic study of codons 74 and 215 of the human immunodeficiency virus type 1 reverse transcriptase, which are significant in nucleoside analog resistance. *J Virol* **68**, 3421-4.

Laguette, N., Sobhian, B., Casartelli, N., Ringeard, M., Chable-Bessia, C., Segeral, E., Yatim, A., Emiliani, S., Schwartz, O. & Benkirane, M. (2011). SAMHD1 is the dendritic- and myeloid-cell-specific HIV-1 restriction factor counteracted by Vpx. *Nature* **474**, 654-7.

Laguette, N. & Benkirane, M. (2012). How SAMHD1 changes our view of viral restriction. *Trends Immunol* **33**, 26-33.

Lahouassa, H., Daddacha, W., Hofmann, H., Ayinde, D., Logue, E. C., Dragin, L., Bloch, N., Maudet, C., Bertrand, M., Gramberg, T., Pancino, G., Priet, S., Canard, B., Laguette, N., Benkirane, M., Transy, C., Landau, N. R., Kim, B. & Margottin-Goguet, F. (2012). SAMHD1 restricts the replication of human immunodeficiency virus type 1 by depleting the intracellular pool of deoxynucleoside triphosphates. *Nat Immunol* **13**, 223-8.

Lansdon, E. B., Brendza, K. M., Hung, M., Wang, R., Mukund, S., Jin, D., Birkus, G., Kutty, N. & Liu, X. (2010). Crystal structures of HIV-1 reverse transcriptase with etravirine (TMC125) and rilpivirine (TMC278): implications for drug design. *J Med Chem* **53**, 4295-9.

Lapkouski, M., Tian, L., Miller, J. T., Le Grice, S. F. & Yang, W. (2013). Complexes of HIV-1 RT, NNRTI and RNA/DNA hybrid reveal a structure compatible with RNA degradation. *Nat Struct Mol Biol* **20**, 230-6.

Larder, B. A., Darby, G. & Richman, D. D. (1989). HIV with reduced sensitivity to zidovudine (AZT) isolated during prolonged therapy. *Science* **243**, 1731-4.

Larder, B. A. (1992). 3'-Azido-3'-deoxythymidine resistance suppressed by a mutation conferring human immunodeficiency virus type 1 resistance to nonnucleoside reverse transcriptase inhibitors. *Antimicrob Agents Chemother* **36**, 2664-9.

Le Grice, S. F. (2012). Human immunodeficiency virus reverse transcriptase: 25 years of research, drug discovery, and promise. *J Biol Chem* **287**, 40850-7.

Lee, S. K., Potempa, M. & Swanstrom, R. (2012). The choreography of HIV-1 proteolytic processing and virion assembly. *J Biol Chem* **287**, 40867-74.

Lemay, J., Maidou-Peindara, P., Bader, T., Ennifar, E., Rain, J. C., Benarous, R. & Liu, L. X. (2008a). HuR interacts with human immunodeficiency virus type 1 reverse transcriptase, and modulates reverse transcription in infected cells. *Retrovirology* **5**, 47.

Lemay, J., Maidou-Peindara, P., Cancio, R., Ennifar, E., Coadou, G., Maga, G., Rain, J. C., Benarous, R. & Liu, L. X. (2008b). AKAP149 binds to HIV-1 reverse transcriptase and is involved in the reverse transcription. *J Mol Biol* **383**, 783-96.

Lengruber, R. B., Delviks-Frankenberry, K. A., Nikolenko, G. N., Baumann, J., Santos, A. F., Pathak, V. K. & Soares, M. A. (2011). Phenotypic characterization of drug resistance-associated mutations in HIV-1 RT connection and RNase H domains and their correlation with thymidine analogue mutations. *J Antimicrob Chemother* **66**, 702-8.

Levin, J. G., Mitra, M., Mascarenhas, A. & Musier-Forsyth, K. (2010). Role of HIV-1 nucleocapsid protein in HIV-1 reverse transcription. *RNA Biol* **7**, 754-74.

Lewis, W., Day, B. J. & Copeland, W. C. (2003). Mitochondrial toxicity of NRTI antiviral drugs: an integrated cellular perspective. *Nat Rev Drug Discov* **2**, 812-22.

Lin, P. F., Samanta, H., Rose, R. E., Patick, A. K., Trimble, J., Bechtold, C. M., Revie, D. R., Khan, N. C., Federici, M. E., Li, H., Lee, A., Anderson, R. E. & Colonno, R. J. (1994). Genotypic and phenotypic analysis of human immunodeficiency virus type 1 isolates from patients on prolonged stavudine therapy. *J Infect Dis* **170**, 1157-64.

Liu, S., Abbondanzieri, E. A., Rausch, J. W., Le Grice, S. F. & Zhuang, X. (2008). Slide into action: dynamic shuttling of HIV reverse transcriptase on nucleic acid substrates. *Science* **322**, 1092-7.

Liu, S., Harada, B. T., Miller, J. T., Le Grice, S. F. & Zhuang, X. (2010). Initiation complex dynamics direct the transitions between distinct phases of early HIV reverse transcription. *Nat Struct Mol Biol* **17**, 1453-60.

Lu, J., Whitcomb, J. & Kuritzkes, D. R. (2005a). Effect of the Q207D mutation in HIV type 1 reverse transcriptase on zidovudine susceptibility and replicative fitness. *J Acquir Immune Defic Syndr* **40**, 20-3.

Lu, R., Ghory, H. Z. & Engelman, A. (2005b). Genetic analyses of conserved residues in the carboxyl-terminal domain of human immunodeficiency virus type 1 integrase. *J Virol* **79**, 10356-68.

Ly, J. K., Margot, N. A., MacArthur, H. L., Hung, M., Miller, M. D. & White, K. L. (2007). The balance between NRTI discrimination and excision drives the susceptibility of HIV-1 RT mutants K65R, M184V and K65r+M184V. *Antivir Chem Chemother* **18**, 307-16.

Maertens, G. N., Hare, S. & Cherepanov, P. (2010). The mechanism of retroviral integration from X-ray structures of its key intermediates. *Nature* **468**, 326-9.

Maga, G., Amacker, M., Ruel, N., Hubscher, U. & Spadari, S. (1997). Resistance to nevirapine of HIV-1 reverse transcriptase mutants: loss of stabilizing interactions and thermodynamic or steric barriers are induced by different single amino acid substitutions. *J Mol Biol* **274**, 738-47.

Malim, M. H. & Emerman, M. (2008). HIV-1 accessory proteins-ensuring viral survival in a hostile environment. *Cell Host Microbe* **3**, 388-98.

Malim, M. H. & Bieniasz, P. D. (2012). HIV Restriction Factors and Mechanisms of Evasion. *Cold Spring Harb Perspect Med* **2**, a006940.

Marchand, B. & Götte, M. (2003). Site-specific footprinting reveals differences in the translocation status of HIV-1 reverse transcriptase. Implications for polymerase translocation and drug resistance. *J Biol Chem* **278**, 35362-72.

Marchand, B., White, K. L., Ly, J. K., Margot, N. A., Wang, R., McDermott, M., Miller, M. D. & Götte, M. (2007). Effects of the translocation status of human immunodeficiency virus type 1 reverse transcriptase on the efficiency of excision of tenofovir. *Antimicrob Agents Chemother* **51**, 2911-9.

Margot, N. A., Waters, J. M. & Miller, M. D. (2006). In vitro human immunodeficiency virus type 1 resistance selections with combinations of tenofovir and emtricitabine or abacavir and lamivudine. *Antimicrob Agents Chemother* **50**, 4087-95.

Martin, J. L., Wilson, J. E., Haynes, R. L. & Furman, P. A. (1993). Mechanism of resistance of human immunodeficiency virus type 1 to 2',3'-dideoxyinosine. *Proc Natl Acad Sci U S A* **90**, 6135-9.

Martín-Hernández, A. M., Domingo, E. & Menéndez-Arias, L. (1996). Human immunodeficiency virus type 1 reverse transcriptase: role of Tyr115 in deoxynucleotide binding and misinsertion fidelity of DNA synthesis. *Embo J* **15**, 4434-42.

Mas, A., Parera, M., Briones, C., Soriano, V., Martínez, M. A., Domingo, E. & Menéndez-Arias, L. (2000). Role of a dipeptide insertion between codons 69 and 70 of HIV-1 reverse transcriptase in the mechanism of AZT resistance. *Embo J* **19**, 5752-61.

Mas, A., Vázquez-Álvarez, B. M., Domingo, E. & Menéndez-Arias, L. (2002). Multidrug-resistant HIV-1 reverse transcriptase: involvement of ribonucleotide-dependent phosphorolysis in cross-resistance to nucleoside analogue inhibitors. *J Mol Biol* **323**, 181-97.

Masquelier, B., Tamalet, C., Montes, B., Descamps, D., Peytavin, G., Bocket, L., Wirden, M., Izopet, J.,

Schneider, V., Ferre, V., Ruffault, A., Palmer, P., Trylesinski, A., Miller, M., Brun-Vezinet, F. & Costagliola, D. (2004). Genotypic determinants of the virological response to tenofovir disoproxil fumarate in nucleoside reverse transcriptase inhibitor-experienced patients. *Antivir Ther* **9**, 315-23.

Matamoros, T., Franco, S., Vázquez-Álvarez, B. M., Mas, A., Martínez, M. A. & Menéndez-Arias, L. (2004). Molecular determinants of multi-nucleoside analogue resistance in HIV-1 reverse transcriptases containing a dipeptide insertion in the fingers subdomain: effect of mutations D67N and T215Y on removal of thymidine nucleotide analogues from blocked DNA primers. *J Biol Chem* **279**, 24569-77.

Matamoros, T., Deval, J., Guerreiro, C., Mulard, L., Canard, B. & Menéndez-Arias, L. (2005). Suppression of multidrug-resistant HIV-1 reverse transcriptase primer unblocking activity by α-phosphate-modified thymidine analogues. *J Mol Biol* **349**, 451-63.

Matamoros, T., Nevot, M., Martinez, M. A. & Menéndez-Arias, L. (2009). Thymidine analogue resistance suppression by V75I of HIV-1 reverse transcriptase: effects of substituting valine 75 on stavudine excision and discrimination. *J Biol Chem* **284**, 32792-802.

Matamoros, T., Álvarez, M., Barrioluengo, V., Betancor, G. & Menéndez-Arias L. (2011). Reverse transcriptase and retroviral replication. In *DNA replication and related cellular processes* (Kusic-Tisma J., ed), pp. 111-142, InTech, Rijeka, Croatia.

McCormick, A. L., Parry, C. M., Crombe, A., Goodall, R. L., Gupta, R. K., Kaleebu, P., Kityo, C., Chirara, M., Towers, G. J. & Pillay, D. (2011). Impact of the N348I mutation in HIV-1 reverse transcriptase on nonnucleoside reverse transcriptase inhibitor resistance in non-subtype B HIV-1. *Antimicrob Agents Chemother* **55**, 1806-9.

McWilliams, M. J., Julias, J. G. & Hughes, S. H. (2008). Mutations in the human immunodeficiency virus type 1 polypurine tract (PPT) reduce the rate of PPT cleavage and plus-strand DNA synthesis. *J Virol* **82**, 5104-8.

McWilliams, M. J., Julias, J. G., Sarafianos, S. G., Alvord, W. G., Arnold, E. & Hughes, S. H. (2003). Mutations in the 5' end of the human immunodeficiency virus type 1 polypurine tract affect RNase H cleavage specificity and virus titer. *J Virol* **77**, 11150-7.

McWilliams, M. J., Julias, J. G., Sarafianos, S. G., Alvord, W. G., Arnold, E. & Hughes, S. H. (2006). Combining mutations in HIV-1 reverse transcriptase with mutations in the HIV-1 polypurine tract affects RNase H cleavages involved in PPT utilization. *Virology* **348**, 378-88.

Melikian, G. L., Rhee, S. Y., Taylor, J., Fessel, W. J., Kaufman, D., Towner, W., Troia-Cancio, P. V., Zolopa, A., Robbins, G. K., Kagan, R., Israelski, D. & Shafer, R. W. (2012). Standardized comparison of the relative impacts of HIV-1 reverse transcriptase (RT) mutations on nucleoside RT inhibitor susceptibility. *Antimicrob Agents Chemother* **56**, 2305-13.

Mellors, J. W., Bazmi, H. Z., Schinazi, R. F., Roy, B. M., Hsiou, Y., Arnold, E., Weir, J. & Mayers, D. L. (1995). Novel mutations in reverse transcriptase of human immunodeficiency virus type 1 reduce susceptibility to foscarnet in laboratory and clinical isolates. *Antimicrob Agents Chemother* **39**, 1087-92.

Mendieta, J., Cases-Gonzalez, C. E., Matamoros, T., Ramirez, G. & Menendez-Arias, L. (2008). A Mg^{2+}-induced conformational switch rendering a competent DNA polymerase catalytic complex. *Proteins* **71**, 565-74.

Menéndez-Arias, L. (2002). Molecular basis of fidelity of DNA synthesis and nucleotide specificity of retroviral reverse transcriptases. *Prog Nucleic Acid Res Mol Biol* **71**, 91-147.

Menéndez-Arias, L., Martínez, M. A., Quinones-Mateu, M. E. & Martínez-Picado, J. (2003). Fitness variations and their impact on the evolution of antiretroviral drug resistance. *Curr Drug Targets Infect Disord* **3**, 355-71.

Menéndez-Arias, L., Matamoros, T. & Cases-González, C. E. (2006). Insertions and deletions in HIV-1 reverse transcriptase: consequences for drug resistance and viral fitness. *Curr Pharm Des* **12**, 1811-25.

Menéndez-Arias, L. (2008). Mechanisms of resistance to nucleoside analogue inhibitors of HIV-1 reverse transcriptase. *Virus Res* **134**, 124-46.

Menéndez-Arias, L. (2009). Mutation rates and intrinsic fidelity of retroviral reverse transcriptases. *Viruses* **1**, 1137-65.

Menéndez-Arias, L. (2010). Molecular basis of human immunodeficiency virus drug resistance: an update. *Antiviral Res* **85**, 210-31.

Menéndez-Arias, L., Betancor, G. & Matamoros, T. (2011). HIV-1 reverse transcriptase connection subdomain mutations involved in resistance to approved non-nucleoside inhibitors. *Antiviral Res* **92**, 139-49.

Menéndez-Arias, L. (2013). Molecular basis of human immunodeficiency virus drug resistance: an update. *Antiviral Res* **85**, 210-31.

Meteer, J. D., Koontz, D., Asif, G., Zhang, H. W., Detorio, M., Solomon, S., Coats, S. J., Sluis-Cremer, N., Schinazi, R. F. & Mellors, J. W. (2011). The base component of 3'-azido-2',3'-dideoxynucleosides influences resistance mutations selected in HIV-1 reverse transcriptase. *Antimicrob Agents Chemother* **55**, 3758-64.

Meyer, P. R., Matsuura, S. E., So, A. G. & Scott, W. A. (1998). Unblocking of chain-terminated primer by HIV-1 reverse transcriptase through a nucleotide-dependent mechanism. *Proc Natl Acad Sci U S A* **95**, 13471-6.

Meyer, P. R., Matsuura, S. E., Mian, A. M., So, A. G. & Scott, W. A. (1999). A mechanism of AZT resistance: an increase in nucleotide-dependent primer unblocking by mutant HIV-1 reverse transcriptase. *Mol Cell* **4**, 35-43.

Meyer, P. R., Matsuura, S. E., Schinazi, R. F., So, A. G. & Scott, W. A. (2000). Differential removal of thymidine nucleotide analogues from blocked DNA chains by human immunodeficiency virus reverse transcriptase in the presence of physiological concentrations of 2'-deoxynucleoside triphosphates. *Antimicrob Agents Chemother* **44**, 3465-72.

Meyer, P. R., Matsuura, S. E., Zonarich, D., Chopra, R. R., Pendarvis, E., Bazmi, H. Z., Mellors, J. W. & Scott, W. A. (2003a). Relationship between 3'-azido-3'-deoxythymidine resistance and primer unblocking activity in foscarnet-resistant mutants of human immunodeficiency virus type 1 reverse transcriptase. *J Virol* **77**, 6127-37.

Meyer, P. R., Lennerstrand, J., Matsuura, S. E., Larder, B. A. & Scott, W. A. (2003b). Effects of dipeptide insertions between codons 69 and 70 of human immunodeficiency virus type 1 reverse transcriptase on primer unblocking, deoxynucleoside triphosphate inhibition, and DNA chain elongation. *J Virol* **77**, 3871-7.

Meyer, P. R., Smith, A. J., Matsuura, S. E. & Scott, W. A. (2004). Effects of primer-template sequence on ATP-dependent removal of chain-terminating nucleotide analogues by HIV-1 reverse transcriptase. *J Biol Chem* **279**, 45389-98.

Meyer, P. R., Smith, A. J., Matsuura, S. E. & Scott, W. A. (2006). Chain-terminating dinucleoside tetraphosphates are substrates for DNA polymerization by human immunodeficiency virus type 1 reverse transcriptase with increased activity against thymidine analogue-resistant mutants. *Antimicrob Agents Chemother* **50**, 3607-14.

Miller, M. D., Margot, N., Lu, B., Zhong, L., Chen, S. S., Cheng, A. & Wulfsohn, M. (2004). Genotypic and phenotypic predictors of the magnitude of response to tenofovir disoproxil fumarate treatment in antiretroviral-experienced patients. *J Infect Dis* **189**, 837-46.

Miranda, L. R., Götte, M., Liang, F. & Kuritzkes, D. R. (2005). The L74V mutation in human immunodeficiency virus type 1 reverse transcriptase counteracts enhanced excision of zidovudine monophosphate associated with thymidine analog resistance mutations. *Antimicrob Agents Chemother* **49**, 2648-56.

Murray, R. J., Lewis, F. I., Miller, M. D. & Brown, A. J. (2008). Genetic basis of variation in tenofovir drug susceptibility in HIV-1. *Aids* **22**, 1113-23.

Naeger, L. K., Margot, N. A. & Miller, M. D. (2002). ATP-dependent removal of nucleoside reverse transcriptase inhibitors by human immunodeficiency virus type 1 reverse transcriptase. *Antimicrob Agents Chemother* **46**, 2179-84.

Nebbia, G., Sabin, C. A., Dunn, D. T. & Geretti, A. M. (2007). Emergence of the H208Y mutation in the reverse transcriptase (RT) of HIV-1 in association with nucleoside RT inhibitor therapy. *J Antimicrob Chemother* **59**, 1013-6.

Nielsen, M. H., Pedersen, F. S. & Kjems, J. (2005). Molecular strategies to inhibit HIV-1 replication. *Retrovirology* **2**, 10.

Nikolenko, G. N., Palmer, S., Maldarelli, F., Mellors, J. W., Coffin, J. M. & Pathak, V. K. (2005). Mechanism for nucleoside analog-mediated abrogation of HIV-1 replication: balance between RNase H activity and nucleotide excision. *Proc Natl Acad Sci U S A* **102**, 2093-8.

Nikolenko, G. N., Delviks-Frankenberry, K. A., Palmer, S., Maldarelli, F., Fivash, M. J., Jr., Coffin, J. M. & Pathak, V. K. (2007). Mutations in the connection domain of HIV-1 reverse transcriptase increase 3'-azido-3'-deoxythymidine resistance. *Proc Natl Acad Sci U S A* **104**, 317-22.

Nikolenko, G. N., Delviks-Frankenberry, K. A. & Pathak, V. K. (2010). A novel molecular mechanism of dual resistance to nucleoside and nonnucleoside reverse transcriptase inhibitors. *J Virol* **84**, 5238-49.

Nishitsuji, H., Hayashi, T., Takahashi, T., Miyano, M., Kannagi, M. & Masuda, T. (2009). Augmentation of reverse transcription by integrase through an interaction with host factor, SIP1/Gemin2 is critical for HIV-1 infection. *PLoS One* **4**, e7825.

Nisole, S. & Saïb, A. (2004). Early steps of retrovirus replicative cycle. *Retrovirology* **1**, 9.

Nissley, D. V., Radzio, J., Ambrose, Z., Sheen, C. W., Hamamouch, N., Moore, K. L., Tachedjian, G. & Sluis-Cremer, N. (2007). Characterization of novel non-nucleoside reverse transcriptase (RT) inhibitor resistance mutations at residues 132 and 135 in the 51 kDa subunit of HIV-1 RT. *Biochem J* **404**, 151-7.

Nowotny, M., Gaidamakov, S. A., Ghirlando, R., Cerritelli, S. M., Crouch, R. J. & Yang, W. (2007). Structure of human RNase H1 complexed with an RNA/DNA hybrid: insight into HIV reverse transcription. *Mol Cell* **28**, 264-76.

Ott, M., Geyer, M. & Zhou, Q. (2011). The control of HIV transcription: keeping RNA polymerase II on track. *Cell Host Microbe* **10**, 426-35.

Oz, I., Avidan, O. & Hizi, A. (2002). Inhibition of the integrases of human immunodeficiency viruses type 1 and type 2 by reverse transcriptases. *Biochem J* **361**, 557-66.

Palaniappan, C., Fay, P. J. & Bambara, R. A. (1995). Nevirapine alters the cleavage specificity of ribonuclease H of human immunodeficiency virus 1 reverse transcriptase. *J Biol Chem* **270**, 4861-9.

Paredes, R., Puertas, M. C., Bannister, W., Kisic, M., Cozzi-Lepri, A., Pou, C., Bellido, R., Betancor, G., Bogner, J., Gargalianos, P., Banhegyi, D., Clotet, B., Lundgren, J., Menéndez-Arias, L. & Martínez-Picado, J. (2011). A376S in the connection subdomain of HIV-1 reverse transcriptase confers increased risk of virological failure to nevirapine therapy. *J Infect Dis* **204**, 741-52.

Parikh, U. M., Barnas, D. C., Faruki, H. & Mellors, J. W. (2006). Antagonism between the HIV-1 reverse-transcriptase mutation K65R and thymidine-analogue mutations at the genomic level. *J Infect Dis* **194**, 651-60.

Parikh, U. M., Zelina, S., Sluis-Cremer, N. & Mellors, J. W. (2007). Molecular mechanisms of bidirectional antagonism between K65R and thymidine analog mutations in HIV-1 reverse transcriptase. *Aids* **21**, 1405-14.

Patel, S. S., Wong, I. & Johnson, K. A. (1991). Pre-steady-state kinetic analysis of processive DNA replication including complete characterization of an exonuclease-deficient mutant. *Biochemistry* **30**, 511-25.

Pelemans, H., Esnouf, R. M., Jonckheere, H., De Clercq, E. & Balzarini, J. (1998). Mutational analysis of

Tyr-318 within the non-nucleoside reverse transcriptase inhibitor binding pocket of human immunodeficiency virus type I reverse transcriptase. *J Biol Chem* **273**, 34234-9.

Poeschla, E. M. (2008). Integrase, LEDGF/p75 and HIV replication. *Cell Mol Life Sci* **65**, 1403-24.

Popovic, M., Sarngadharan, M. G., Read, E. & Gallo, R. C. (1984). Detection, isolation, and continuous production of cytopathic retroviruses (HTLV-III) from patients with AIDS and pre-AIDS. *Science* **224**, 497-500.

Powell, M. D. & Levin, J. G. (1996). Sequence and structural determinants required for priming of plus-strand DNA synthesis by the human immunodeficiency virus type 1 polypurine tract. *J Virol* **70**, 5288-96.

Powell, M. D., Beard, W. A., Bebenek, K., Howard, K. J., Le Grice, S. F., Darden, T. A., Kunkel, T. A., Wilson, S. H. & Levin, J. G. (1999). Residues in the αH and αI helices of the HIV-1 reverse transcriptase thumb subdomain required for the specificity of RNase H-catalyzed removal of the polypurine tract primer. *J Biol Chem* **274**, 19885-93.

Powell, R. D., Holland, P. J., Hollis, T. & Perrino, F. W. (2011). Aicardi-Goutières syndrome gene and HIV-1 restriction factor SAMHD1 is a dGTP-regulated deoxynucleotide triphosphohydrolase. *J Biol Chem* **286**, 43596-600.

Puertas, M. C., Buzón, M. J., Artese, A., Alcaro, S., Menéndez-Arias, L., Perno, C. F., Clotet, B., Ceccherini-Silberstein, F. & Martínez-Picado, J. (2009). Effect of the human immunodeficiency virus type 1 reverse transcriptase polymorphism Leu-214 on replication capacity and drug susceptibility. *J Virol* **83**, 7434-9.

Radzio, J. & Sluis-Cremer, N. (2008). Efavirenz accelerates HIV-1 reverse transcriptase ribonuclease H cleavage, leading to diminished zidovudine excision. *Mol Pharmacol* **73**, 601-6.

Radzio, J., Yap, S. H., Tachedjian, G. & Sluis-Cremer, N. (2010). N348I in reverse transcriptase provides a genetic pathway for HIV-1 to select thymidine analogue mutations and mutations antagonistic to thymidine analogue mutations. *Aids* **24**, 659-67.

Radzio, J. & Sluis-Cremer, N. (2011). Subunit-specific mutational analysis of residue N348 in HIV-1 reverse transcriptase. *Retrovirology* **8**, 69.

Rausch, J. W. & Le Grice, S. F. (2004). 'Binding, bending and bonding': polypurine tract-primed initiation of plus-strand DNA synthesis in human immunodeficiency virus. *Int J Biochem Cell Biol* **36**, 1752-66.

Rausch, J. W. & Le Grice, S. F. (2007). Purine analog substitution of the HIV-1 polypurine tract primer defines regions controlling initiation of plus-strand DNA synthesis. *Nucleic Acids Res* **35**, 256-68.

Ray, A. S., Basavapathruni, A. & Anderson, K. S. (2002). Mechanistic studies to understand the progressive development of resistance in human immunodeficiency virus type 1 reverse transcriptase to abacavir. *J Biol Chem* **277**, 40479-90.

Ray, A. S., Murakami, E., Basavapathruni, A., Vaccaro, J. A., Ulrich, D., Chu, C. K., Schinazi, R. F. & Anderson, K. S. (2003). Probing the molecular mechanisms of AZT drug resistance mediated by HIV-1 reverse transcriptase using a transient kinetic analysis. *Biochemistry* **42**, 8831-41.

Reardon, J. E. & Miller, W. H. (1990). Human immunodeficiency virus reverse transcriptase. Substrate and inhibitor kinetics with thymidine 5'-triphosphate and 3'-azido-3'-deoxythymidine 5'-triphosphate. *J Biol Chem* **265**, 20302-7.

Reardon, J. E. (1992). Human immunodeficiency virus reverse transcriptase: steady-state and pre-steady-state kinetics of nucleotide incorporation. *Biochemistry* **31**, 4473-9.

Reid, P., MacInnes, H., Cong, M. E., Heneine, W. & Garcia-Lerma, J. G. (2005). Natural resistance of human immunodeficiency virus type 2 to zidovudine. *Virology* **336**, 251-64.

Ren, J., Esnouf, R. M., Hopkins, A. L., Jones, E. Y., Kirby, I., Keeling, J., Ross, C. K., Larder, B. A., Stuart,

D. I. & Stammers, D. K. (1998). 3'-Azido-3'-deoxythymidine drug resistance mutations in HIV-1 reverse transcriptase can induce long range conformational changes. *Proc Natl Acad Sci U S A* **95**, 9518-23.

Ren, J., Milton, J., Weaver, K. L., Short, S. A., Stuart, D. I. & Stammers, D. K. (2000). Structural basis for the resilience of efavirenz (DMP-266) to drug resistance mutations in HIV-1 reverse transcriptase. *Structure* **8**, 1089-94.

Ren, J., Nichols, C., Bird, L., Chamberlain, P., Weaver, K., Short, S., Stuart, D. I. & Stammers, D. K. (2001). Structural mechanisms of drug resistance for mutations at codons 181 and 188 in HIV-1 reverse transcriptase and the improved resilience of second generation non-nucleoside inhibitors. *J Mol Biol* **312**, 795-805.

Ren, J., Nichols, C. E., Chamberlain, P. P., Weaver, K. L., Short, S. A. & Stammers, D. K. (2004). Crystal structures of HIV-1 reverse transcriptases mutated at codons 100, 106 and 108 and mechanisms of resistance to non-nucleoside inhibitors. *J Mol Biol* **336**, 569-78.

Ren, J., Nichols, C. E., Stamp, A., Chamberlain, P. P., Ferris, R., Weaver, K. L., Short, S. A. & Stammers, D. K. (2006). Structural insights into mechanisms of non-nucleoside drug resistance for HIV-1 reverse transcriptases mutated at codons 101 or 138. *Febs J* **273**, 3850-60.

Ren, J. & Stammers, D. K. (2008). Structural basis for drug resistance mechanisms for non-nucleoside inhibitors of HIV reverse transcriptase. *Virus Res* **134**, 157-70.

Rhee, S. Y., Fessel, W. J., Zolopa, A. R., Hurley, L., Liu, T., Taylor, J., Nguyen, D. P., Slome, S., Klein, D., Horberg, M., Flamm, J., Follansbee, S., Schapiro, J. M. & Shafer, R. W. (2005). HIV-1 Protease and reverse-transcriptase mutations: correlations with antiretroviral therapy in subtype B isolates and implications for drug-resistance surveillance. *J Infect Dis* **192**, 456-65.

Rigourd, M., Ehresmann, C., Parniak, M. A., Ehresmann, B. & Marquet, R. (2002). Primer unblocking and rescue of DNA synthesis by azidothymidine (AZT)-resistant HIV-1 reverse transcriptase: comparison between initiation and elongation of reverse transcription and between (-) and (+) strand DNA synthesis. *J Biol Chem* **277**, 18611-8.

Rodgers, D. W., Gamblin, S. J., Harris, B. A., Ray, S., Culp, J. S., Hellmig, B., Woolf, D. J., Debouck, C. & Harrison, S. C. (1995). The structure of unliganded reverse transcriptase from the human immunodeficiency virus type 1. *Proc Natl Acad Sci U S A* **92**, 1222-6.

Romano, L., Venturi, G., Bloor, S., Harrigan, R., Larder, B. A., Major, J. C. & Zazzi, M. (2002). Broad nucleoside-analogue resistance implications for human immunodeficiency virus type 1 reverse-transcriptase mutations at codons 44 and 118. *J Infect Dis* **185**, 898-904.

Santoro, M., Sabin, C., Forbici, F., Bansi, L., Dunn, D., Fearnhill, E., Boumis, E., Nicastri, E., Antinori, A., Palamara, G., Callegaro, A., Francisci, D., Zoncada, A., Maggiolo, F., Zazzi, M., Perno, C., Ceccherini-Silberstein, F. & Mussini, C. (2013). Drug-resistance development differs between HIV-1-infected patients failing first-line antiretroviral therapy containing nonnucleoside reverse transcriptase inhibitors with and without thymidine analogues. *HIV Med* **14**, 571-7.

Saracino, A., Monno, L., Scudeller, L., Cibelli, D. C., Tartaglia, A., Punzi, G., Torti, C., Lo Caputo, S., Mazzotta, F., Scotto, G., Carosi, G. & Angarano, G. (2006). Impact of unreported HIV-1 reverse transcriptase mutations on phenotypic resistance to nucleoside and non-nucleoside inhibitors. *J Med Virol* **78**, 9-17.

Sarafianos, S. G., Das, K., Clark, A. D., Jr., Ding, J., Boyer, P. L., Hughes, S. H. & Arnold, E. (1999). Lamivudine (3TC) resistance in HIV-1 reverse transcriptase involves steric hindrance with β-branched amino acids. *Proc Natl Acad Sci U S A* **96**, 10027-32.

Sarafianos, S. G., Das, K., Tantillo, C., Clark, A. D., Jr., Ding, J., Whitcomb, J. M., Boyer, P. L., Hughes, S. H. & Arnold, E. (2001). Crystal structure of HIV-1 reverse transcriptase in complex with a polypurine tract RNA:DNA. *Embo J* **20**, 1449-61.

Sarafianos, S. G., Clark, A. D., Jr., Das, K., Tuske, S., Birktoft, J. J., Ilankumaran, P., Ramesha, A. R., Sayer, J. M., Jerina, D. M., Boyer, P. L., Hughes, S. H. & Arnold, E. (2002). Structures of HIV-1 reverse transcriptase with pre- and post-translocation AZTMP-terminated DNA. *Embo J* **21**, 6614-24.

Sarafianos, S. G., Marchand, B., Das, K., Himmel, D. M., Parniak, M. A., Hughes, S. H. & Arnold, E. (2009). Structure and function of HIV-1 reverse transcriptase: molecular mechanisms of polymerization and inhibition. *J Mol Biol* **385**, 693-713.

Schatz, O., Cromme, F. V., Gruninger-Leitch, F. & Le Grice, S. F. (1989). Point mutations in conserved amino acid residues within the C-terminal domain of HIV-1 reverse transcriptase specifically repress RNase H function. *FEBS Lett* **257**, 311-4.

Schroder, A. R., Shinn, P., Chen, H., Berry, C., Ecker, J. R. & Bushman, F. (2002). HIV-1 integration in the human genome favors active genes and local hotspots. *Cell* **110**, 521-9.

Schuckmann, M. M., Marchand, B., Hachiya, A., Kodama, E. N., Kirby, K. A., Singh, K. & Sarafianos, S. G. (2010). The N348I mutation at the connection subdomain of HIV-1 reverse transcriptase decreases binding to nevirapine. *J Biol Chem* **285**, 38700-9.

Schultz, S. J., Zhang, M. & Champoux, J. J. (2003). Specific cleavages by RNase H facilitate initiation of plus-strand RNA synthesis by Moloney murine leukemia virus. *J Virol* **77**, 5275-85.

Schultz, S. J., Zhang, M. & Champoux, J. J. (2004). Recognition of internal cleavage sites by retroviral RNases H. *J Mol Biol* **344**, 635-52.

Schultz, S. J. & Champoux, J. J. (2008). RNase H activity: structure, specificity, and function in reverse transcription. *Virus Res* **134**, 86-103.

Schultz, S. J., Zhang, M. & Champoux, J. J. (2009). Preferred sequences within a defined cleavage window specify DNA 3' end-directed cleavages by retroviral RNases H. *J Biol Chem* **284**, 32225-38.

Selmi, B., Boretto, J., Navarro, J. M., Sire, J., Longhi, S., Guerreiro, C., Mulard, L., Sarfati, S. & Canard, B. (2001). The valine-to-threonine 75 substitution in human immunodeficiency virus type 1 reverse transcriptase and its relation with stavudine resistance. *J Biol Chem* **276**, 13965-74.

Selmi, B., Deval, J., Alvarez, K., Boretto, J., Sarfati, S., Guerreiro, C. & Canard, B. (2003). The Y181C substitution in 3'-azido-3'-deoxythymidine-resistant human immunodeficiency virus, type 1, reverse transcriptase suppresses the ATP-mediated repair of the 3'-azido-3'-deoxythymidine 5'-monophosphate-terminated primer. *J Biol Chem* **278**, 40464-72.

Sevilya, Z., Loya, S., Hughes, S. H. & Hizi, A. (2001). The ribonuclease H activity of the reverse transcriptases of human immunodeficiency viruses type 1 and type 2 is affected by the thumb subdomain of the small protein subunits. *J Mol Biol* **311**, 957-71.

Sevilya, Z., Loya, S., Adir, N. & Hizi, A. (2003). The ribonuclease H activity of the reverse transcriptases of human immunodeficiency viruses type 1 and type 2 is modulated by residue 294 of the small subunit. *Nucleic Acids Res* **31**, 1481-7.

Shafer, R. W., Kozal, M. J., Winters, M. A., Iversen, A. K., Katzenstein, D. A., Ragni, M. V., Meyer, W. A., 3rd, Gupta, P., Rasheed, S., Coombs, R., Katzman, M., Fiscus, S. & Merigan, T. C. (1994). Combination therapy with zidovudine and didanosine selects for drug-resistant human immunodeficiency virus type 1 strains with unique patterns of *pol* gene mutations. *J Infect Dis* **169**, 722-9.

Shahriar, R., Rhee, S. Y., Liu, T. F., Fessel, W. J., Scarsella, A., Towner, W., Holmes, S. P., Zolopa, A. R. & Shafer, R. W. (2009). Nonpolymorphic human immunodeficiency virus type 1 protease and reverse transcriptase treatment-selected mutations. *Antimicrob Agents Chemother* **53**, 4869-78.

Sharp, P. M. & Hahn, B. H. (2011). Origins of HIV and the AIDS pandemic. *Cold Spring Harb Perspect Med* **1**, a006841.

Shaw-Reid, C. A., Feuston, B., Munshi, V., Getty, K., Krueger, J., Hazuda, D. J., Parniak, M. A., Miller, M.

D. & Lewis, D. (2005). Dissecting the effects of DNA polymerase and ribonuclease H inhibitor combinations on HIV-1 reverse-transcriptase activities. *Biochemistry* **44**, 1595-606.

Shirasaka, T., Yarchoan, R., O'Brien, M. C., Husson, R. N., Anderson, B. D., Kojima, E., Shimada, T., Broder, S. & Mitsuya, H. (1993). Changes in drug sensitivity of human immunodeficiency virus type 1 during therapy with azidothymidine, dideoxycytidine, and dideoxyinosine: an in vitro comparative study. *Proc Natl Acad Sci U S A* **90**, 562-6.

Shirasaka, T., Kavlick, M. F., Ueno, T., Gao, W. Y., Kojima, E., Alcaide, M. L., Chokekijchai, S., Roy, B. M., Arnold, E., Yarchoan, R. & Mitsuya, H. (1995). Emergence of human immunodeficiency virus type 1 variants with resistance to multiple dideoxynucleosides in patients receiving therapy with dideoxynucleosides. *Proc Natl Acad Sci U S A* **92**, 2398-402.

Shulman, N. S., Bosch, R. J., Mellors, J. W., Albrecht, M. A. & Katzenstein, D. A. (2004). Genetic correlates of efavirenz hypersusceptibility. *Aids* **18**, 1781-5.

Siliciano, R. F. & Greene, W. C. (2011). HIV latency. *Cold Spring Harb Perspect Med* **1**, a007096.

Singh, K., Marchand, B., Kirby, K. A., Michailidis, E. & Sarafianos, S. G. (2010). Structural Aspects of Drug Resistance and Inhibition of HIV-1 Reverse Transcriptase. *Viruses* **2**, 606-638.

Singh, K., Marchand, B., Rai, D. K., Sharma, B., Michailidis, E., Ryan, E. M., Matzek, K. B., Leslie, M. D., Hagedorn, A. N., Li, Z., Norden, P. R., Hachiya, A., Parniak, M. A., Xu, H. T., Wainberg, M. A. & Sarafianos, S. G. (2012). Biochemical mechanism of HIV-1 resistance to rilpivirine. *J Biol Chem* **287**, 38110-23.

Skalka, A. M. & Katz, R. A. (2005). Retroviral DNA integration and the DNA damage response. *Cell Death Differ* **12 Suppl 1**, 971-8.

Sluis-Cremer, N., Arion, D. & Parniak, M. A. (2000). Molecular mechanisms of HIV-1 resistance to nucleoside reverse transcriptase inhibitors (NRTIs). *Cell Mol Life Sci* **57**, 1408-22.

Sluis-Cremer, N., Arion, D., Parikh, U., Koontz, D., Schinazi, R. F., Mellors, J. W. & Parniak, M. A. (2005). The 3'-azido group is not the primary determinant of 3'-azido-3'-deoxythymidine (AZT) responsible for the excision phenotype of AZT-resistant HIV-1. *J Biol Chem* **280**, 29047-52.

Sluis-Cremer, N., Sheen, C. W., Zelina, S., Torres, P. S., Parikh, U. M. & Mellors, J. W. (2007). Molecular mechanism by which the K70E mutation in human immunodeficiency virus type 1 reverse transcriptase confers resistance to nucleoside reverse transcriptase inhibitors. *Antimicrob Agents Chemother* **51**, 48-53.

Sluis-Cremer, N. & Tachedjian, G. (2008). Mechanisms of inhibition of HIV replication by non-nucleoside reverse transcriptase inhibitors. *Virus Res* **134**, 147-56.

Sluis-Cremer, N., Moore, K., Radzio, J., Sonza, S. & Tachedjian, G. (2010). N348I in HIV-1 reverse transcriptase decreases susceptibility to tenofovir and etravirine in combination with other resistance mutations. *Aids* **24**, 317-9.

Smerdon, S. J., Jager, J., Wang, J., Kohlstaedt, L. A., Chirino, A. J., Friedman, J. M., Rice, P. A. & Steitz, T. A. (1994). Structure of the binding site for nonnucleoside inhibitors of the reverse transcriptase of human immunodeficiency virus type 1. *Proc Natl Acad Sci U S A* **91**, 3911-5.

Smith, A. J., Meyer, P. R., Asthana, D., Ashman, M. R. & Scott, W. A. (2005). Intracellular substrates for the primer-unblocking reaction by human immunodeficiency virus type 1 reverse transcriptase: detection and quantitation in extracts from quiescent- and activated-lymphocyte subpopulations. *Antimicrob Agents Chemother* **49**, 1761-9.

Smith, A. J. & Scott, W. A. (2006). The influence of natural substrates and inhibitors on the nucleotide-dependent excision activity of HIV-1 reverse transcriptase in the infected cell. *Curr Pharm Des* **12**, 1827-41.

Spence, R. A., Kati, W. M., Anderson, K. S. & Johnson, K. A. (1995). Mechanism of inhibition of HIV-1

reverse transcriptase by nonnucleoside inhibitors. *Science* **267**, 988-93.

Spence, R. A., Anderson, K. S. & Johnson, K. A. (1996). HIV-1 reverse transcriptase resistance to nonnucleoside inhibitors. *Biochemistry* **35**, 1054-63.

Srinivas, R. V. & Fridland, A. (1998). Antiviral activities of 9-R-2-phosphonomethoxypropyl adenine (PMPA) and bis(isopropyloxymethylcarbonyl)PMPA against various drug-resistant human immunodeficiency virus strains. *Antimicrob Agents Chemother* **42**, 1484-7.

St Clair, M. H., Martin, J. L., Tudor-Williams, G., Bach, M. C., Vavro, C. L., King, D. M., Kellam, P., Kemp, S. D. & Larder, B. A. (1991). Resistance to ddI and sensitivity to AZT induced by a mutation in HIV-1 reverse transcriptase. *Science* **253**, 1557-9.

Stoeckli, T. C., MaWhinney, S., Uy, J., Duan, C., Lu, J., Shugarts, D. & Kuritzkes, D. R. (2002). Phenotypic and genotypic analysis of biologically cloned human immunodeficiency virus type 1 isolates from patients treated with zidovudine and lamivudine. *Antimicrob Agents Chemother* **46**, 4000-3.

Stone, C., Ait-Khaled, M., Craig, C., Griffin, P. & Tisdale, M. (2004). Human immunodeficiency virus type 1 reverse transcriptase mutation selection during in vitro exposure to tenofovir alone or combined with abacavir or lamivudine. *Antimicrob Agents Chemother* **48**, 1413-5.

Stürmer, M., Staszewski, S., Doerr, H. W., Larder, B., Bloor, S. & Hertogs, K. (2003). Correlation of phenotypic zidovudine resistance with mutational patterns in the reverse transcriptase of human immunodeficiency virus type 1: interpretation of established mutations and characterization of new polymorphisms at codons 208, 211, and 214. *Antimicrob Agents Chemother* **47**, 54-61.

Sudo, S., Haraguchi, H., Hirai, Y., Gatanaga, H., Sakuragi, J., Momose, F. & Morikawa, Y. (2013). Efavirenz enhances HIV-1 Gag processing at the plasma membrane through Gag-Pol dimerization. *J Virol* **87**, 3348-60.

Svicher, V., Sing, T., Santoro, M. M., Forbici, F., Rodriguez-Barrios, F., Bertoli, A., Beerenwinkel, N., Bellocchi, M. C., Gago, F., d'Arminio Monforte, A., Antinori, A., Lengauer, T., Ceccherini-Silberstein, F. & Perno, C. F. (2006). Involvement of novel human immunodeficiency virus type 1 reverse transcriptase mutations in the regulation of resistance to nucleoside inhibitors. *J Virol* **80**, 7186-98.

Tachedjian, G., Mellors, J., Bazmi, H., Birch, C. & Mills, J. (1996). Zidovudine resistance is suppressed by mutations conferring resistance of human immunodeficiency virus type 1 to foscarnet. *J Virol* **70**, 7171-81.

Tachedjian, G., Orlova, M., Sarafianos, S. G., Arnold, E. & Goff, S. P. (2001). Nonnucleoside reverse transcriptase inhibitors are chemical enhancers of dimerization of the HIV type 1 reverse transcriptase. *Proc Natl Acad Sci U S A* **98**, 7188-93.

Tambuyzer, L., Azijn, H., Rimsky, L. T., Vingerhoets, J., Lecocq, P., Kraus, G., Picchio, G. & de Bethune, M. P. (2009). Compilation and prevalence of mutations associated with resistance to non-nucleoside reverse transcriptase inhibitors. *Antivir Ther* **14**, 103-9.

Tasara, T., Maga, G., Hottiger, M. O. & Hubscher, U. (2001). HIV-1 reverse transcriptase and integrase enzymes physically interact and inhibit each other. *FEBS Lett* **507**, 39-44.

Tong, W., Lu, C. D., Sharma, S. K., Matsuura, S., So, A. G. & Scott, W. A. (1997). Nucleotide-induced stable complex formation by HIV-1 reverse transcriptase. *Biochemistry* **36**, 5749-57.

Tramontano, E., Piras, G., Mellors, J. W., Putzolu, M., Bazmi, H. Z. & La Colla, P. (1998). Biochemical characterization of HIV-1 reverse transcriptases encoding mutations at amino acid residues 161 and 208 involved in resistance to phosphonoformate. *Biochem Pharmacol* **56**, 1583-9.

Tu, X., Das, K., Han, Q., Bauman, J. D., Clark, A. D., Jr., Hou, X., Frenkel, Y. V., Gaffney, B. L., Jones, R. A., Boyer, P. L., Hughes, S. H., Sarafianos, S. G. & Arnold, E. (2010). Structural basis of HIV-1 resistance to AZT by excision. *Nat Struct Mol Biol* **17**, 1202-9.

Turner, B. G. & Summers, M. F. (1999). Structural biology of HIV. *J Mol Biol* **285**, 1-32.

Tuske, S., Sarafianos, S. G., Clark, A. D., Jr., Ding, J., Naeger, L. K., White, K. L., Miller, M. D., Gibbs, C. S., Boyer, P. L., Clark, P., Wang, G., Gaffney, B. L., Jones, R. A., Jerina, D. M., Hughes, S. H. & Arnold, E. (2004). Structures of HIV-1 RT-DNA complexes before and after incorporation of the anti-AIDS drug tenofovir. *Nat Struct Mol Biol* **11**, 469-74.

Ueno, T., Shirasaka, T. & Mitsuya, H. (1995). Enzymatic characterization of human immunodeficiency virus type 1 reverse transcriptase resistant to multiple 2',3'-dideoxynucleoside 5'-triphosphates. *J Biol Chem* **270**, 23605-11.

Ueno, T. & Mitsuya, H. (1997). Comparative enzymatic study of HIV-1 reverse transcriptase resistant to 2',3'-dideoxynucleotide analogs using the single-nucleotide incorporation assay. *Biochemistry* **36**, 1092-9.

Vingerhoets, J., Azijn, H., Fransen, E., De Baere, I., Smeulders, L., Jochmans, D., Andries, K., Pauwels, R. & de Bethune, M. P. (2005). TMC125 displays a high genetic barrier to the development of resistance: evidence from in vitro selection experiments. *J Virol* **79**, 12773-82.

von Wyl, V., Yerly, S., Boni, J., Burgisser, P., Klimkait, T., Battegay, M., Bernasconi, E., Cavassini, M., Furrer, H., Hirschel, B., Vernazza, P. L., Rickenbach, M., Ledergerber, B. & Gunthard, H. F. (2008). Factors associated with the emergence of K65R in patients with HIV-1 infection treated with combination antiretroviral therapy containing tenofovir. *Clin Infect Dis* **46**, 1299-309.

von Wyl, V., Ehteshami, M., Symons, J., Burgisser, P., Nijhuis, M., Demeter, L. M., Yerly, S., Boni, J., Klimkait, T., Schuurman, R., Ledergerber, B., Gotte, M. & Gunthard, H. F. (2010). Epidemiological and biological evidence for a compensatory effect of connection domain mutation N348I on M184V in HIV-1 reverse transcriptase. *J Infect Dis* **201**, 1054-62.

Wainberg, M. A., Lewis, L., Salomon, H., Gu, Z., Keller, A., Cammack, N., Goldsmith, J., Church, J., Spira, B., Wheeler, S. & Pizzo, P. (1996). Resistance to (-)-2',3'-dideoxy-3'-thiacytidine (3TC) in HIV-1 isolated from paediatric patients. *Antivir Ther* **1**, 98-104.

Wainberg, M. A., Miller, M. D., Quan, Y., Salomon, H., Mulato, A. S., Lamy, P. D., Margot, N. A., Anton, K. E. & Cherrington, J. M. (1999). In vitro selection and characterization of HIV-1 with reduced susceptibility to PMPA. *Antivir Ther* **4**, 87-94.

Wang, Y. X., Zhang, H. J., Xu, J., Zheng, B. J. & Wen, Y. M. (2008). Mutational analysis of the "turn" of helix clamp motif of HIV-1 reverse transcriptase. *Biochem Biophys Res Commun* **377**, 915-20.

Warren, K., Warrilow, D., Meredith, L. & Harrich, D. (2009). Reverse Transcriptase and Cellular Factors: Regulators of HIV-1 Reverse Transcription. *Viruses* **1**, 873-94.

Warrilow, D., Meredith, L., Davis, A., Burrell, C., Li, P. & Harrich, D. (2008). Cell factors stimulate human immunodeficiency virus type 1 reverse transcription in vitro. *J Virol* **82**, 1425-37.

Warrilow, D., Tachedjian, G. & Harrich, D. (2009). Maturation of the HIV reverse transcription complex: putting the jigsaw together. *Rev Med Virol* **19**, 324-37.

Warrilow, D., Warren, K. & Harrich, D. (2010). Strand transfer and elongation of HIV-1 reverse transcription is facilitated by cell factors in vitro. *PLoS One* **5**, e13229.

Waters, J. M., O'Neal, W., White, K. L., Wakeford, C., Lansdon, E. B., Harris, J., Svarovskaia, E. S., Miller, M. D. & Borroto-Esoda, K. (2009). Mutations in the thumb-connection and RNase H domain of HIV type-1 reverse transcriptase of antiretroviral treatment-experienced patients. *Antivir Ther* **14**, 231-9.

Weiss, E. R. & Göttlinger, H. (2011). The role of cellular factors in promoting HIV budding. *J Mol Biol* **410**, 525-33.

Wertheim, J. O. & Worobey, M. (2009). Dating the age of the SIV lineages that gave rise to HIV-1 and HIV-2. *PLoS Comput Biol* **5**, e1000377.

Whitcomb, J. M., Parkin, N. T., Chappey, C., Hellmann, N. S. & Petropoulos, C. J. (2003). Broad nucleoside reverse-transcriptase inhibitor cross-resistance in human immunodeficiency virus type 1 clinical isolates. *J*

Infect Dis **188**, 992-1000.

White, K. L., Margot, N. A., Wrin, T., Petropoulos, C. J., Miller, M. D. & Naeger, L. K. (2002). Molecular mechanisms of resistance to human immunodeficiency virus type 1 with reverse transcriptase mutations K65R and K65R+M184V and their effects on enzyme function and viral replication capacity. *Antimicrob Agents Chemother* **46**, 3437-46.

White, K. L., Chen, J. M., Margot, N. A., Wrin, T., Petropoulos, C. J., Naeger, L. K., Swaminathan, S. & Miller, M. D. (2004). Molecular mechanisms of tenofovir resistance conferred by human immunodeficiency virus type 1 reverse transcriptase containing a diserine insertion after residue 69 and multiple thymidine analog-associated mutations. *Antimicrob Agents Chemother* **48**, 992-1003.

White, K. L., Margot, N. A., Ly, J. K., Chen, J. M., Ray, A. S., Pavelko, M., Wang, R., McDermott, M., Swaminathan, S. & Miller, M. D. (2005). A combination of decreased NRTI incorporation and decreased excision determines the resistance profile of HIV-1 K65R RT. *Aids* **19**, 1751-60.

Wilkinson, T. A., Januszyk, K., Phillips, M. L., Tekeste, S. S., Zhang, M., Miller, J. T., Le Grice, S. F., Clubb, R. T. & Chow, S. A. (2009). Identifying and characterizing a functional HIV-1 reverse transcriptase-binding site on integrase. *J Biol Chem* **284**, 7931-9.

Wilson, J. E., Aulabaugh, A., Caligan, B., McPherson, S., Wakefield, J. K., Jablonski, S., Morrow, C. D., Reardon, J. E. & Furman, P. A. (1996). Human immunodeficiency virus type-1 reverse transcriptase. Contribution of Met-184 to binding of nucleoside 5'-triphosphate. *J Biol Chem* **271**, 13656-62.

Wirden, M., Marcelin, A. G., Simon, A., Kirstetter, M., Tubiana, R., Valantin, M. A., Paris, L., Bonmarchand, M., Conan, F., Kalkias, L., Katlama, C. & Calvez, V. (2005). Resistance mutations before and after tenofovir regimen failure in HIV-1 infected patients. *J Med Virol* **76**, 297-301.

Wöhrl, B. M., Krebs, R., Goody, R. S. & Restle, T. (1999). Refined model for primer/template binding by HIV-1 reverse transcriptase: pre-steady-state kinetic analyses of primer/template binding and nucleotide incorporation events distinguish between different binding modes depending on the nature of the nucleic acid substrate. *J Mol Biol* **292**, 333-44.

Wu, X., Liu, H., Xiao, H., Conway, J. A., Hehl, E., Kalpana, G. V., Prasad, V. & Kappes, J. C. (1999). Human immunodeficiency virus type 1 integrase protein promotes reverse transcription through specific interactions with the nucleoprotein reverse transcription complex. *J Virol* **73**, 2126-35.

Xia, Q., Radzio, J., Anderson, K. S. & Sluis-Cremer, N. (2007). Probing nonnucleoside inhibitor-induced active-site distortion in HIV-1 reverse transcriptase by transient kinetic analyses. *Protein Sci* **16**, 1728-37.

Xu, H. T., Martinez-Cajas, J. L., Ntemgwa, M. L., Coutsinos, D., Frankel, F. A., Brenner, B. G. & Wainberg, M. A. (2009). Effects of the K65R and K65R/M184V reverse transcriptase mutations in subtype C HIV on enzyme function and drug resistance. *Retrovirology* **6**, 14.

Xu, H. T., Asahchop, E. L., Oliveira, M., Quashie, P. K., Quan, Y., Brenner, B. G. & Wainberg, M. A. (2011). Compensation by the E138K mutation in HIV-1 reverse transcriptase for deficits in viral replication capacity and enzyme processivity associated with the M184I/V mutations. *J Virol* **85**, 11300-8.

Xu, H. T., Oliveira, M., Asahchop, E. L., McCallum, M., Quashie, P. K., Han, Y., Quan, Y. & Wainberg, M. A. (2012). Molecular mechanism of antagonism between the Y181C and E138K mutations in HIV-1 reverse transcriptase. *J Virol* **86**, 12983-90.

Xu, H. T., Colby-Germinario, S. P., Asahchop, E. L., Oliveira, M., McCallum, M., Schader, S. M., Han, Y., Quan, Y., Sarafianos, S. G. & Wainberg, M. A. (2013). Effect of mutations at position E138 in HIV-1 reverse transcriptase and their interactions with the M184I mutation on defining patterns of resistance to nonnucleoside reverse transcriptase inhibitors rilpivirine and etravirine. *Antimicrob Agents Chemother* **57**, 3100-9.

Yahi, N., Tamalet, C., Tourres, C., Tivoli, N., Ariasi, F., Volot, F., Gastaut, J. A., Gallais, H., Moreau, J. & Fantini, J. (1999). Mutation patterns of the reverse transcriptase and protease genes in human

immunodeficiency virus type 1-infected patients undergoing combination therapy: survey of 787 sequences. *J Clin Microbiol* **37**, 4099-106.

Yap, S. H., Sheen, C. W., Fahey, J., Zanin, M., Tyssen, D., Lima, V. D., Wynhoven, B., Kuiper, M., Sluis-Cremer, N., Harrigan, P. R. & Tachedjian, G. (2007). N348I in the connection domain of HIV-1 reverse transcriptase confers zidovudine and nevirapine resistance. *PLoS Med* **4**, e335.

Zelina, S., Sheen, C. W., Radzio, J., Mellors, J. W. & Sluis-Cremer, N. (2008). Mechanisms by which the G333D mutation in human immunodeficiency virus type 1 Reverse transcriptase facilitates dual resistance to zidovudine and lamivudine. *Antimicrob Agents Chemother* **52**, 157-63.

Zhang, Z., Xu, W., Koh, Y. H., Shim, J. H., Girardet, J. L., Yeh, L. T., Hamatake, R. K. & Hong, Z. (2007). A novel nonnucleoside analogue that inhibits human immunodeficiency virus type 1 isolates resistant to current nonnucleoside reverse transcriptase inhibitors. *Antimicrob Agents Chemother* **51**, 429-37.

Zhu, T., Korber, B. T., Nahmias, A. J., Hooper, E., Sharp, P. M. & Ho, D. D. (1998). An African HIV-1 sequence from 1959 and implications for the origin of the epidemic. *Nature* **391**, 594-7.

Zhu, K., Dobard, C. & Chow, S. A. (2004). Requirement for integrase during reverse transcription of human immunodeficiency virus type 1 and the effect of cysteine mutations of integrase on its interactions with reverse transcriptase. *J Virol* **78**, 5045-55.